Carter, R.M., McCave, I.N., Richter, C., Carter, L., et al., 1999
Proceedings of the Ocean Drilling Program, Initial Reports Volume 181

7. Site 1123: North Chatham Drift—a 20-Ma Record of the Pacific Deep Western Boundary Current[1]

Shipboard Scientific Party[2]

BACKGROUND AND OBJECTIVES

General Description

Site 1123 is located 410 km northeast of the Chatham Islands, on the deep northeastern slopes of Chatham Rise (Fig. **F1**). The site was drilled in a water depth of 3290 m. Site 1123 is located on National Institute of Water and Atmosphere seismic line NIWA 3034-7 (Fig. **F2**).

Four main seismic units occur above basement, which is not well imaged on this or nearby lines (seismic Units D–A; Table **T1**). In ascending order, these units consist of sediment with short, irregular reflectors that passes up into sediment with strong, irregular, and laterally discontinuous reflectors (Unit D; 5.70-ms two-way traveltime [TWT] thick). Next, Unit C comprises 205 ms TWT of irregularly reflecting sediment, with stronger, more continuous reflections concentrated toward the top. Unit B, similarly to Unit D, comprises a lower unit of acoustically homogeneous sediment with markedly discontinuous reflectors in short segments (120-ms TWT thick, Subunit B2), and an upper unit of stronger, more continuous reflectors (180-ms TWT thick, Subunit B1), many displaying diffraction hyperbolae. At the top, Unit A comprises 180 ms of more regular but sometimes discontinuous reflectors, which are subparallel to the seafloor. The reflectors chosen to separate these units and subunits (R1 through R4) are all composite, in the sense that individual segments of each "reflector" can only be traced laterally for short distances, their extended correlation depending upon the presence of another similar reflector at about the same level. The zones of harder reflectors in the upper parts of Units B and C are made up of

F1. Locality map of Site 1123, **p. 52.**

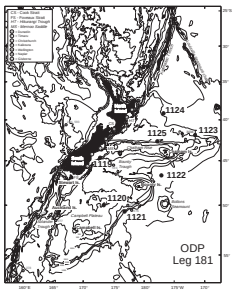

F2. Portion of seismic line NIWA 3034, **p. 53.**

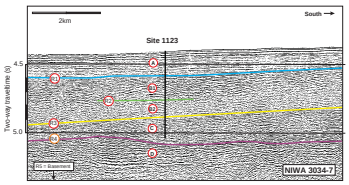

T1. Summary of main seismic units and reflectors, **p. 112.**

[1]**Examples of how to reference the whole or part of this volume.**
[2]**Shipboard Scientific Party addresses.**

large numbers of short, concave-downward segments, some of which represent refractions from hard zones lying within the sediments, possibly chert or carbonate concretions. These refractions obscure the precise relationships between Units A and B and B and C in particular, and, before drilling, were viewed as candidate unconformities.

The 3.5-kHz profiles through and near the site (Fig. F3) show the seafloor to be underlain by ~40 m of light, 2- to 6-m-spaced, semi-continuous reflectors at depths of ~3, 10, 23, 33, and 35 m. Reflector β (Carter and McCave, 1994) has a particularly hard acoustic response, and before drilling, was suspected of being either an unconformity or a sand unit.

F3. Portion of 3.5-kHz line NZOI 2050, p. 54.

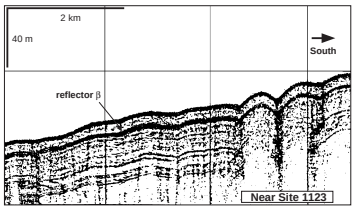

Little previous information exists to precisely correlate or date these seismic units. Although the geology of the Chatham Islands is now well described (Campbell et al., 1993), the thin, shallow water and the atypically volcanic-influenced nature of the Cenozoic stratigraphy there makes it difficult to extend into deep water. Regional interpretations of the offshore seismics have been attempted (Wood et al., 1989; Wood and Herzer, 1993) but are tenuous. Carter and McCave (1994) inferred an age of Pliocene–Pleistocene for regularly bedded Unit A, and correlated reflector R1 with regional Unconformity Y, of late Miocene age, with reference to the seismic stratigraphy of the outer Bounty Trough (Carter et al., 1994), which is itself an equivocal extension of that unconformity from Deep Sea Drilling Project (DSDP) Site 594 and petroleum exploration holes under the Canterbury shelf. Carter and McCave (1994) also suggested that Unit B represented Miocene, and perhaps older, sediment drifts deposited from the Pacific Deep Western Boundary Current (DWBC). The uppermost part of Unit A has also been sampled in a piston-coring transect some distance west of Site 1123 (Fenner et al., 1992) and in nearby core CHAT 1K at station S924 (Weaver et al., 1998; Lean and McCave, 1998). All cores have contained rhythmic glacial/interglacial hemipelagic/biopelagic couplets with an average sedimentation rate of ~2 cm/k.y.

Site Objectives

Site 1123 was drilled to document the stratigraphy of the northern slopes of the Chatham Rise and to establish the effects of the DWBC on Neogene sediment deposition. For parts of the column influenced by drift sedimentation, grain-size, geochemical and isotopic signals will be used to determine water-mass movement and DWBC velocity. Because the site is just north of the Subtropical Convergence (STC), information from Site 1123 will help indicate the position of the STC between glacial and interglacial times and test for associated variations in oceanic productivity (Fenner et al., 1992; Nelson et al., 1993; Weaver et al., 1997). It will also test the coherence of the paleoclimatic record with Milankovitch cycles.

OPERATIONS

Hole 1123A

The 384-nmi voyage to Site 1123 (proposed site SWPAC-5B) was accomplished at an average speed of 11.1 kt. The vessel proceeded directly to the Global Positioning System coordinates of the location. The positioning beacon was deployed at 1848 hr on 13 September. The

hydrophones and thrusters were lowered and the advanced hydraulic piston corer/extended core barrel (APC/XCB) bottom-hole assembly was assembled using a 9-⅞-in PDC bit and deployed. Hole 1123A was spudded with the APC at 0425 hr on 14 September. The recovery indicated that the water depth was 3290.1 meters below sea level (mbsl). APC coring advanced to refusal at 158.1 mbsf (Table T2, also in ASCII format). The bit cleared the seafloor at 2355 hr on 14 September.

T2. Site 1123 expanded coring summary, p. 113.

Hole 1123B

In order to obtain a stratigraphic overlap with the previous hole, the bit was raised up by 3 m from the spudding depth of Hole 1123A, and Hole 1123B was spudded with the APC at 0110 hr on 15 September. The recovery of the mudline core indicated a seafloor depth of 3289.8 mbsl. APC Cores 1H through 15H were recovered from 0 to 136.4 mbsf (Table T2). While attempting to retrieve Core 16H from a depth of 145.9 mbsf, the wireline parted at the sinker bar assembly socket. An eight-finger hard-formation core catcher was used as an overshot in order to latch onto the core barrel. The overshot was run in and engaged on the first attempt, and the core barrel was retrieved to the surface. Piston coring resumed in Hole 1123B with a full stroke of Core 17H. The core barrel could not be extracted from the sediment and had to be drilled over. The Adara heat-flow shoe was deployed with Cores 5H (41.4 mbsf), 6H (60.4 mbsf), 7H (79.4 mbsf), and 11H (98.4 mbsf). The data from these runs failed to provide heat-flow data because of the frictional heat that was generated by the vertical motion (heave) of the vessel. Coring was switched to the XCB and advanced without incident to 182.0 mbsf with >100% recovery. While retrieving Core 21X, the core winch operator noticed that the line on the drum was slack and that there was no line tension on the weight indicator. This was an obvious indication that the wireline and sinker bars were caught on an obstruction in the drill pipe. The obstruction turned out to be the core barrel, which had stuck in the pipe 124 m below the rig floor. As a result of running into the core barrel, the wireline on the drum backlashed. After respooling the line and after various attempts to free the stuck XCB barrel, the drill string had to be retrieved to the level of the stuck core barrel. There was nothing found on the inside of the drill pipe to suggest the cause of the jamming. The drill string was run back in to the bottom, and XCB operations recommenced at 0545 hr on 16 September. Coring advanced to 374.1 mbsf (Table T2). While pumping down the XCB core barrel to cut Core 41X, the barrel stopped at an obstruction in the hole of the drill pipe at 645 meters below rig floor (mbrf). On tagging the stuck barrel with the sinker assembly, a number of loose wraps were produced on the forward core winch drum, before the brakes could be applied. Approximately 50 m of wire was spooled from the drum to remove the loose wraps. A fishing assembly was deployed, and the core barrel was tagged at 645 mbrf. After the first hit of the wireline jars, the stuck core barrel was freed and recovered to the rig floor. XCB coring again resumed at 0900 hr on 17 September and advanced to 489 mbsf, which was the revised depth objective for this hole.

Logging Operations in Hole 1123B

In preparation for logging, an aluminum go-devil was dropped and the hole swept with 60 barrels of high-viscosity mud. The bit was pulled back in the hole to 520 mbsf and the hole was displaced with 175 bar-

rels of sepiolite mud. The bit was then positioned at the logging depth of 83 mbsf. Logging operations began at 1100 hr and lasted for 20 hr. Logging was conducted from the bottom of the hole at 489 mbsf to the bit at 84 mbsf. Three standard tool-string configurations were run: the triple combination, the FMS-sonic (two passes), and the GHMT (see "Downhole Measurements," p. 29, in the "Explanatory Notes" chapter). The NMRS (total field) tool on the GHMT failed to work. The condition of the borehole was good, and the quality of the data was excellent. After the logging equipment was disassembled, the bit was pulled out of the hole and cleared the seafloor at 0955 hr on 19 September, ending operations at Hole 1123B.

Hole 1123C

The vessel was offset by 30 m to the north and Hole 1123C was spudded with the APC at 1130 hr. Piston coring advanced to 151.5 mbsf (Table T2). A core barrel with a center bit was dropped, and the hole was deepened by drilling ahead to 230.0 mbsf. The center bit was retrieved and one XCB core (Core 17X) was obtained from 230.0 to 239.6 mbsf with 67% recovery to provide overlap with an interval of poor recovery in Hole 1123B. Following the recovery of the XCB core barrel, the center bit was dropped again and the hole was drilled ahead from 239.6 to 484.0 mbsf. After the center bit was recovered, XCB coring resumed and advanced from 484.0 mbsf to the modified depth objective of 632.8 mbsf (Cores 18X to 33X) with excellent recovery.

Logging Operations in Hole 1123C

In preparation for logging, an aluminum go-devil was dropped and the hole swept with 60 barrels of high-viscosity mud. The bit was pulled back in the hole to 629 mbsf and the hole was displaced with 213 barrels of sepiolite mud. The bit was then pulled back to logging depth of 68 mbsf. By the time the drill crew was preparing to rig up for logging, wind gusts of over 60 kt, seas of 3–4 m, and up to 12-m-high swells forced the decision to abandon logging plans. At 1050 hr on 22 September, the bit was pulled clear of the seafloor. The pipe was partially recovered, but by 1300 hr the maximum vessel pitch was over 9°. Pipe tripping was suspended because of the hazard to men and material, and operations were placed on weather standby. The storm abated by 0330 hr on 24 September, allowing the drill crew to recover the drill string and beacon. By 1000 hr, the drilling equipment was secured, and the thrusters and hydrophones retracted as the vessel began the 269-nmi transit to Site 1124.

LITHOSTRATIGRAPHY

Introduction

The presence of a DWBC off the eastern end of the Chatham Rise was first captured in the classic SCORPIO hydrographic transect of Warren (1973). He identified a major northward flow with a volume transport of up to 20 Sv in water depths greater than ~2000 m. Using more recent hydrographic data, together with seismic profiles, bottom sediments, and photographs, Carter and McCave (1994) and McCave and Carter (1997) showed that the DWBC swings around the eastern end of

Chatham Rise and travels northwest to the Kermadec Ridge where it alters course to the north. En route, the current has helped shape an extensive, fine-grained drift on the northern flank of the Rise. Termed the North Chatham drift by Carter and McCave (1994), this deposit appears on seismic profiles as a succession of acoustically laminated Pliocene–Pleistocene sediments above a more massive seismic unit that was interpreted to be Miocene in age. The base of this unit and the base of the proposed hole were considered to be an unconformity at the top of the Oligocene marked by seismic reflector X of Carter and McCave (1994). Profiles from a 3.5-kHz system reveal that much of the drift surface is covered by irregular, nonmigratory sediment waves, which were probably formed under the influence of the DWBC (Fig. F3). Thus, the sedimentary sequence at Site 1123 potentially offers a record of DWBC inflow to the Southwest Pacific under varying paleoclimatic conditions that influenced sediment input and possibly flow intensity.

Description of Lithostratigraphic Units

Cores from Site 1123 recovered a succession of clay-rich nannofossil ooze, chalk, and limestone. The sedimentary succession is divided into four basic lithologic units that are identified on the basis of changes in the calcareous biogenic and noncarbonate components, along with variations in bedding and color. The division of the lithologic units is supported by estimates of core composition from smear slides, together with shipboard measurements of calcium carbonate, physical properties, light reflectance, and bulk mineralogy using X-ray diffraction (XRD). The resulting lithologic logs, together with physical properties and biostratigraphic controls, are summarized in Figures F4 and F5.

Except in a few cases, calcium carbonate concentration is always >50% (the criterion for ooze designation), and on occasion reaches ~80%. The strength of the correlation between light reflectance at 550 nm and percentage calcium carbonate concentration (Fig. F6) suggests that reflectance is an accurate proxy for carbonate, and, thus, can provide detailed information on the carbonate contents (Mix et al., 1995a).

Unit I

Unit I extends from the present seafloor to 256.59 mbsf and represents an interglacial/glacial cyclic sedimentation pattern that can be divided into Subunits IA and IB on the basis of bedding style and lithology.

Subunit IA

Interval: Sections 181-1123A-1H-1 through 17H-CC; Sections 181-1123B-1H-1 through 20X-CC; Sections 181-1123C-1H-1 through 16H-CC
Depth: 0–158.1 mbsf (Hole 1123A); 0–181.9 mbsf (Hole 1123B); 0–151.5 mbsf (Hole 1123C)
Age: Pliocene to Pleistocene

Subunit IA corresponds to the Pliocene to Pleistocene drift sequence and extends from 0 to ~182 mbsf. Cores show Subunit IA to be a succession of alternating light greenish gray (5GY 7/1) to greenish gray (5GY 6/1) and white (5Y 8/1) clayey nannofossil oozes (i.e., the dominant biogenic component is nannofossils, with clay mostly as a subordinate constituent, although still occasionally rivaling nannofossil abundance).

F4. Site 1123 summary log synopsis, p. 55.

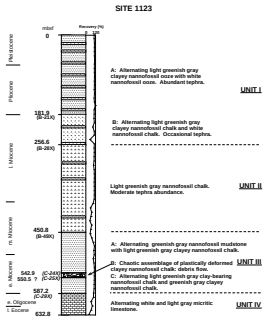

F5. Summary log for Site 1123, p. 56.

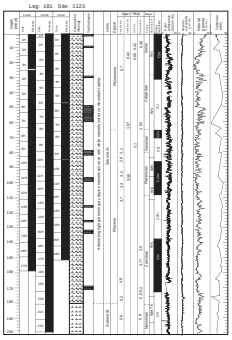

F6. Light reflectance vs. carbonate percentage, p. 60.

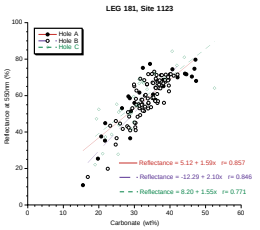

Beds are distinguished by color variations with layers typically between 1 and 1.5 m thick. Contacts are generally bioturbated and gradational. Accessory components include foraminifers, diatoms, sponge spicules, pyrite (found as smears or frequently as aureoles around and in-filling burrows), and trace amounts of mica. Compositional differences between beds are minimal, but smear-slide data suggest the greenish gray layers have a higher abundance of biogenic silica (within the "Present" category for both diatoms and sponge spicules) and possibly more mica and quartz as well. Beds tend to have faint color banding (particularly pale green laminae) and indistinct mottling associated with pervasive bioturbation. Identified ichnofauna include *Zoophycus, Chondrites, Planolites, Thalassinoides,* and *Terebellina*. Of note is the occasional presence of large (>5 cm long) pyritized *Teichichnus* burrows (e.g., Fig. **F7**) and centimeter-scale unidentified burrows filled mainly with foraminifers.

Numerous tephra layers are present in Subunit IA (Table **T3;** Fig. **F8**) and range in thickness from <1 cm to >20 cm. They typically have sharp bases, normal grading, and bioturbated upper contacts with the overlying ooze. Reworked tephra often occurs as burrow fill (mainly *Thalassinoides*) below a bed's basal contact (Fig. **F9**). Above ~90 m the tephra is typically pinkish gray (5YR 6/2), whereas, at deeper levels, the tephra layers are darkened by an increased presence of diagenetic pyrite. In the upper few cores of each hole a number of tephra-"blobs" and lenses are present that are unlikely to be in situ and may reflect drilling disturbance. Tephra layers commonly display dark green laminae at or close to their bases. These bands, of probable diagenetic origin, were used to determine orientation of the tephra layers, some of which were overturned by drilling.

Core disturbance is minimal through Subunit IA, with only a small amount of flow-in present in cores from Hole 1123A. The switch from APC to XCB coring and the coincident inception of drilling biscuits occur at around 155 mbsf (Core 181-1123B-18X), suggesting that the sediment is becoming lithified at that level through the formation of carbonate cement.

Subunit IB

Interval: Sections 181-1123B-21X-1 through 28X-5; Core 181-1123C-17X
Depth: 181.9–256.59 mbsf (Hole 1123B); 230–239.6 mbsf (Hole 1123C)
Age: late Miocene to Pliocene

Subunit IB encompasses a similar succession of alternating interglacial/glacial couplets as seen in Subunit IA. The sequence is of late Miocene age and extends from ~182 to 256 mbsf. It carries many of the lithologic features of Subunit IA except that IB is sufficiently indurated to be classified as chalk. The sequence, therefore, comprises mainly white (5Y 8/1) clayey nannofossil chalk interbedded with greenish gray (5GY 6/1) clayey nannofossil chalk.

As in Subunit IA, layers are typically between 1 and 1.5 m thick, and contacts between beds are bioturbated. Smear slides of samples from the white and greenish gray-colored chalk showed that both sediments have a similar composition compared to the oozes in Subunit IA. Bioturbation is again abundant, with an ichnofaunal assemblage (*Chondrites, Planolites, Thalassinoides, Zoophycus,* and *Terebellina*) similar to that in Subunit IA. The harder sediments of Subunit IB permit better

F7. A pyritized *Teichichnus* burrow, Unit I, **p. 61.**

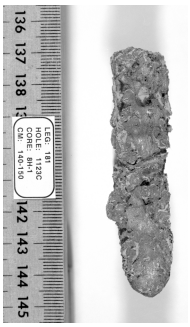

T3. Position and thickness of tephra layers, **p. 133.**

F8. Tephra layers vs. depth, **p. 62.**

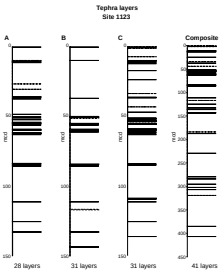

F9. A tephra layer from Unit I showing reworked tephra, **p. 63.**

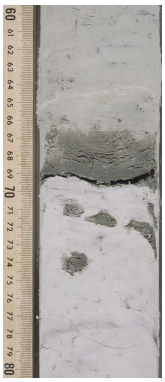

preservation of individual burrow structures than in Subunit 1A (e.g., Fig. F10), and, in some cases, these are highlighted by pyrite stains.

A noticeable difference between Subunits IA and IB is the infrequent occurrence of tephra layers in the latter. The chalk sequence of Subunit IB contains only two tephra layers, whereas at least 33 are present in the ooze of Subunit IA (Fig. F8). The younger late Miocene tephra have abundant pyrite toward their sharp bases, normal grading and bioturbated upper contacts with the overlying chalk. However, the firm sediment has been disrupted by pervasive drilling biscuits. Therefore, potential loss of the more poorly consolidated tephra layers (grain size of the tephra is in the silt to sand range) by washing out during drilling cannot be discounted.

F10. *Zoophycos* preserved in chalks, Subunit IIIA, p. 64.

Unit II

Interval: Sections 181-1123B-28X-5 through 48X-CC
Depth: 256.59–450.8 mbsf (Hole 1123B)
Age: middle to late Miocene

The sedimentary sequence exhibits a fairly uniform lithology between ~257 and ~451 mbsf. This uniformity is exemplified by the color recorded in hand specimen, which does not alter from light greenish gray (5BG 7/1). However, light reflectance data over this subunit show cyclicity too subtle to be recognized with the naked eye, and calibration of the spectrophotometer to proxy carbonate suggests that the percentage carbonate varies rhythmically between ~50% and 60% (Fig. F11). Nevertheless, moderate to abundant bioturbation has ensured extensive but subtle mottling of this subunit, associated with trace fossils such as *Chondrites, Planolites,* and *Skolithos,* together with abundant and conspicuous *Zoophycus* burrows. Beds have occasional very faint centimeter-scale color banding in pale green and pink. In smear-slide observations, these bands appear identical to the major lithology, except that they may contain slightly higher clay contents and possibly diatoms and silicoflagellates (concentrations in the "Present" category). Like the overlying unit, Unit II lithology is a clayey nannofossil chalk with a similar accessory assemblage. The noncarbonate mineralogy is dominated by clay and pyrite, with trace amounts of mica also present. The pyrite occurs as smears and occasionally within burrow fills.

F11. Proxy carbonate data for lithostratigraphic Unit II, p. 65.

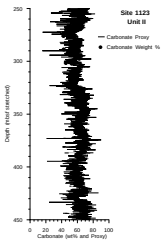

At least nine tephra beds occur in Unit II. The layers are typically 1–5 cm thick with a maximum of 7 cm, have sharp basal contacts, bioturbated tops, and exhibit pyritization toward their bases. One tephra layer (Section 181-1123B-29X-7) contains fine planar laminae toward its base. Some tephra beds are disrupted by the ubiquitous formation of drilling biscuits.

To fill the single coring break in the otherwise continuous record from Hole 1123B, Core 181-1123C-17X was recovered from 230–239.6 mbsf (within Subunit IB) during the wash-down phase of Hole 1123C. Rather than the containing the glacial/interglacial couplets of Subunit IB, as might be expected, the core contained a light greenish gray (5BG 7/1) clayey nannofossil chalk, with heavy bioturbation and common pyrite smears reminiscent of Unit II. The core was damaged during retrieval and required some reconstruction on the drill floor. Thus, the stratigraphy (particularly of Section 181-1123C-17X-4) is suspect. Nevertheless, with circumspection, we place Core 181-1123C-17X within Unit II.

Unit III

Unit III consists mainly of sediments reflecting a similar interglacial/glacial cyclic sedimentation pattern to that described for Subunit IB. The unit extends from 450.8 to 587.2 mbsf, where it is bounded below by the mid-Oligocene Marshall Paraconformity. A ~7-m-thick debris flow occurs within this sequence, allowing the division of the unit into three subunits (Fig. F5), with Subunit IIIB itself corresponding to the debris flow.

Subunit IIIA

Interval: Sections 181-1123B-48X-CC through 52X-CC; Sections 181-1123C-18X-1 through 24X-5
Depth: 450.8–489 mbsf (Hole 1123B); 484–542.9 mbsf (Hole 1123C)
Age: early to middle Miocene

Subunit IIIA, corresponding to the early to middle Miocene, extends from 450.8 to 542.9 mbsf. Its base corresponds to the upper contact of the deformed sediments of the underlying debris flow. Alternating light greenish gray (5BG 7/1) and greenish gray (5G 6/1) interbeds again dominate the sequence, with layers typically <1 m thick. Contacts are generally bioturbated, but the abundant biscuiting and brecciation makes the positions of many contacts subjective. Color differentiation is not as clear as in Unit I. The major difference in composition between this sequence and Unit I is the abundance of terrigenous clay present in the sediment. In addition to the light greenish gray clayey nannofossil chalk, clay concentrations are sufficient to classify the greenish gray layers as nannofossil mudstone, with a dominant nonbiogenic component of terrigenous clay, with nannofossils and micrite as a subordinate constituent, although not less than 40% of the total abundance.

Unlike the oozes and chalks of Unit I, the sediment appears comparatively barren of siliceous fauna, with only "Present" concentrations of sponge spicules in the smear slides. The noncarbonate mineralogy is dominated by clays with "Common" concentrations of diagenetic pyrite, and shows few compositional differences between layers. Only mica appears richer (concentrations from "Trace" to "Present") in the greenish gray layers. Pyrite occurs throughout the subunit as rare smears. Nannofossils are starting to recrystallize, and there is incipient micritization.

Most of Subunit IIIA is moderately bioturbated, with occasional intervals of more intense bioturbation. Mottling is therefore typically faint. Identified trace fossils include well-preserved examples of *Zoophycos, Planolites, Chondrites, Thalassinoides, Cylindrichnus, Terebellina, Teichichnus, Palaeophycos,* and *Skolithos*.

Subunit IIIB

Interval: Sections 181-1123C-24X-5 through 25X-3
Depth: 542.9–550.5 mbsf (Hole 1120C)
Age: early Miocene

A chaotic assemblage of plastically deformed clasts of clayey nannofossil chalk extends from 542.9 to 550.5 mbsf. The clasts are greenish gray (5GY 6/1) and light greenish gray (5BG 7/1) and of 0.5- to >7-cm diameter. The sediment matrix shows strongly contorted laminations, which are possibly flow lineations (e.g., Fig. F12). An intact block of

F12. Plastically deformed clayey nannofossil chalk, p. 66.

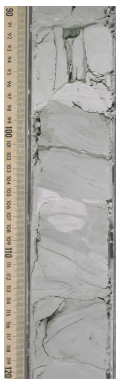

white (5Y 8/1) foraminifer-bearing micritic limestone fills the core between 547.8 and 548.6 mbsf. Although the upper contact of this subunit is conspicuous, the position of the basal contact is somewhat subjective, as the chaotic assemblage feathers out and grades to an intact sediment of a similar color but with disturbed bedding, probably caused by emplacement of the overlying bed. The sediment structure of Subunit IIIB is consistent with the instantaneous deposition of a debris flow originating from further upslope on Chatham Rise.

Subunit IIIC

Interval: Sections 181-1123C-25X-3 through 29X-2
Depth: 550.5–587.2 mbsf (Hole 1123C)
Age: early Miocene

Subunit IIIC extends from ~550 to 587 mbsf and is identical in lithology to Subunit IIIA. Of note is the paraconformity between early Miocene and early Oligocene ages (~12 m.y. gap; see **"Biostratigraphy,"** p. 13), which marks the base of Subunit IIIC (Fig. **F13**). This paraconformity, at 587.2 mbsf in Section 181-1123C-29X-2, manifests itself as a simple burrowed contact between greenish gray (5GY 6/1) nannofossil mudstone of Subunit IIIC and white (5Y 8/1) micritic limestone below (Unit IV). Beneath the contact (strictly Unit IV) are particularly well-preserved *Zoophycos* and *Chondrites,* containing fill from the overlying greenish gray mudstone. The contact closely resembles the shallow-water, onland occurrences of the Marshall Paraconformity (e.g., Concord Greensand on the Burnside Marl, at the abandoned Burnside cement quarry, Dunedin, New Zealand [R.M. Carter, pers. comm., 1998]).

F13. The Marshall Paraconformity, **p. 67.**

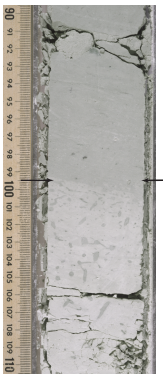

Unit IV

Interval: Sections 181-1123C-29X-2 through 33X-CC
Depth: 587.2–632.8 mbsf (Hole 1123C)
Age: late Eocene to early Oligocene

Below the paraconformity at 587.2 mbsf, the remainder of the cored section, to its base at 632.8 mbsf, is alternating white (5Y 8/1) and light gray (5Y 7/1) to light greenish gray (5BG 7/1) micritic limestone. Bioturbation is variable through Unit IV, ranging from rare to abundant. Observed ichnofauna include *Zoophycos, Skolithos, Chondrites, Teichichnus,* and *Planolites*. Core disturbance is variable, with moderate to extreme formation of drilling biscuits together with limited brecciation of some biscuits. Of special note is the presence of fine clay residues that mark out stylolitic surfaces through Core 181-1123C-30X (594.3–603.9 mbsf; Fig. **F14**). Such a feature indicates advanced diagenesis and pressure dissolution within the limestone.

F14. Stylolite contacts in Section IV, **p. 68.**

Discussion

Cyclicity

The alternations of light and dark colors in the sedimentary sequence of Site 1123 probably represent cool/warm climate cyclicity, as noted elsewhere off eastern New Zealand (e.g., Griggs et al., 1983; Nelson et al., 1986b; Weaver et al., 1998). The cyclicity is not always self-evident in hand specimen, as is the case for Unit II, but it is almost

invariably recorded by either or both the multisensor track and light reflectance measurements. Carbonate proxy values alternate between ~50% and 80% in the oozes of Unit I. These values are lower than those found at the isolated Campbell Plateau Site 1120 (see **"Carbonate and Organic Carbon,"** p. 20, in the "Site 1120" chapter), suggesting a greater terrigenous accumulation at Site 1123. The mica tracer work of Carter and Mitchell (1987) suggests that at least part of this terrigenous component was carried to Chatham Drift by the DWBC. This flow transported suspended load from the region of the Bounty Fan, which, in turn, derived sediment ultimately from the Southern Alps of the South Island.

A short kasten core from the vicinity of Site 1123 (Core CHAT 1K, from NIWA station S924), contains a succession of alternating light-colored, clayey nannofossil ooze and dark colored silty clay from the late Quaternary. On the basis of oxygen isotope curves for benthic foraminifers, foraminiferal assemblage data, and calcium carbonate profiles, Weaver et al. (1998) and Lean and McCave (1998) concluded that the light and dark layers represented interglacial and glacial phases of sedimentation, respectively. Interglacial sedimentation rates ranged over 1.8–2.3 cm/k.y., whereas glacial rates were 2.3–2.9 cm/k.y. Unpublished mass accumulation rates for Core CHAT 1K show that the slightly higher glacial sedimentation rates were largely caused by an increase in the noncarbonate flux of terrigenous and biogenic siliceous components. The nature of the elevated noncarbonate accumulation in glacial periods is not clear, but may result from an influx of waterborne and aeolian detritus together with increased biogenic silica production, supported by upwelling under increased glacial wind stress (R.M. Carter et al., unpubl. data). Organic carbon fluxes are distinctly higher during glacial Stages 2, 4, and 6, caused by higher productivity (Lean and McCave, 1998). Initial indications are that the recovered sediment from Site 1123 contains a record of Milankovitch-frequency colder/warmer cyclic sedimentation since at least the early Miocene.

The average late Quaternary sedimentation rate for Site 1123, estimated from the position of the Brunhes/Matuyama boundary (31.72 m; 0.78 Ma), is around 4 cm/k.y. The discrepancy between this rate and that reported above for Core CHAT 1K may reflect the different coring techniques; the kasten, being a gravity corer, probably compresses the section, whereas the piston of the APC may increase the natural thickness of the section by ~10% (see **"Composite Depths,"** p. 32).

Trace Fossils

Well-preserved trace fossils occur throughout this site. Their identification and assemblage provide some limited information on the paleoenvironment, which is summarized in Figure **F15.** The alternating sequences of clayey nannofossil ooze and clayey nannofossil chalk of Subunits IA and IB have similar ichnofauna, containing *Zoophycos, Chondrites, Planolites, Thalassinoides, Terebellina,* and *Teichichnus*. The ichnofauna assemblage alternates between *Cruziana* and *Zoophycos* ichnofacies in the upper ~80 mbsf of Subunit IA and throughout Subunit IB. Between these cyclic ichnofacies at ~80 and 180 mbsf, low diversity and a high abundance of dominant *Zoophycos* are consistent with a typical *Zoophycos* ichnofacies. Such an ichnofacies indicates a fairly quiescent deep-water environment with low mass accumulation rates, and moderate to low oxygen saturation of the overlying water (Pemberton and MacEachern, 1995). In contrast, the *Cruziana* ichnofacies is indica-

F15. Summary plot of major ichnofacies at Site 1123, **p. 69.**

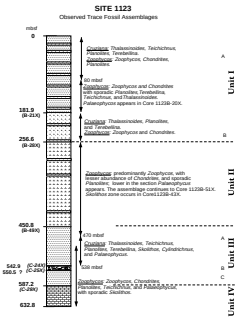

tive of a deep-water environment that is more energetic and better ventilated (for a detailed discussion of the recurring archetypal trace fossil associations [ichnofacies] and their common environmental implications, see Pemberton and MacEachern [1995]). The alternating ichnofacies in Units IA and IB are in a sequence consistent with the interglacial (*Zoophycus*)/glacial (*Cruziana*) cyclic sedimentation pattern of Unit I and may similarly reflect variability in the DWBC flow.

The monotonous clayey nannofossil chalk of Unit II, which has no visible color cyclicity, has an ichnofauna with abundant *Zoophycos* and lesser *Chondrites, Planolites,* and *Palaeophycos* continuing to ~470 mbsf. The resulting *Zoophycos* ichnofacies suggests that the middle to late Miocene was a period of relative quiescence, with slow DWBC flow and low oxygen concentrations. An isolated zone of *Skolithos* occurs in 181-1123B-43X and probably represents opportunistic colonization.

Subunit IIIA contains well-preserved *Zoophycos, Planolites, Chondrites, Skolithos, Thalassinoides, Terebellina, Palaeophycos, Teichichnus,* and *Cylindrichnus*. The presence of abundant *Skolithos, Cylindrichnus,* and *Thalassinoides* just below the Unit II/Unit III boundary at around 470 mbsf suggests an abrupt transition from the overlying *Zoophycos* to a robust *Cruziana* ichnofacies. The structure of the latter suggests a higher energy environment than is seen in the equivalent ichnofacies of Unit I. There is a gradual change through to Subunit IIIC with the *Cruziana* ichnofacies alternating with a lower energy *Zoophycos* ichnofacies and eventually becoming only a *Zoophycos* ichnofacies at 538 mbsf toward the Marshall Paraconformity.

These data suggest that DWBC activity was minimal in the early Miocene, but showed a gradual increase into the middle Miocene and then an abrupt decrease and relatively quiescent conditions through the late Miocene. It is tempting to suggest that this pattern may, to some extent, reflect a middle Miocene cooling event in Antarctica (e.g., Kennett, 1977).

In the upper Eocene and lower Oligocene micritic limestone of Unit IV, the trace-fossil assemblage is nearly identical to the *Zoophycos* ichnofacies in Subunit IIIC with *Zoophycos, Chondrites, Planolites,* and *Teichichnus*. Other observed trace fossils are generally robust burrows of opportunistic colonizers (e.g., *Teichichnus* and *Skolithos*).

Miocene Debris Flow

The zone of strongly deformed clayey nannofossil and nannofossil ooze with matrix-supported intraclasts (Subunit IIIB) is interpreted as part of a debris flow (e.g., Prior et al., 1984). The regional bathymetry suggests a flow source from the northern flank of Chatham Rise. The multichannel seismic line through Site 1123 sheds little light on the debris flow. It appears to coincide with a zone of short, discontinuous reflectors that are indistinguishable from the reflectors of in situ chalk higher up in the sequence. As the debris flow is only 7.2 m thick, it may simply be too small to detect on the large scale of the seismic line.

In contrast, the physical properties are a little more conclusive with respect to identifying the flow deposit. Magnetic susceptibility above and below the debris flow tends to decrease downcore, whereas susceptibility within the flow is fairly uniform. A prominent spike between 547.7 and 548.5 mbsf coincides with the block of white limestone incorporated within the debris flow. The light color of this block is also detected in the reflectance profile, although the remainder of the deposit did not produce a distinctive response. Similarly, the gamma-

ray attenuation porosity evaluator (GRAPE) density profile failed to define the deposit clearly. By comparison, paleomagnetic measurements detected a marked change in the debris flow. This change was a sharp departure from the normal polarity of sediments above (Chron C6n) and below (Chron C6n or C6 An) the flow. The change was a response to a fabric that was neither clearly normal or reversed. Changes were also revealed in the field in the underlying 4 m of sediment extending to 554 mbsf. Either the flow deposit is thicker than can be detected visually, or the magnetic fabric of the underlying beds has been disturbed slightly by the emplacement of the flow. The first option is less likely because the apparent bedding of the underlying layers is consistent with that of in situ clayey chalks. Furthermore, the paleomagnetic change in the underlying beds is less marked than that of the debris flow proper.

Plastic deformation affects the debris-flow matrix and some of the intraclasts. Deformed laminae are a feature of the matrix and probably reflect flow lines rather than original bedding, as the chalks above and below the debris flow are bioturbated and, therefore, poorly bedded. Intraclasts include soft clayey nannofossil chalk and an 80-cm-long cored section of a foraminifer-bearing micritic limestone. The microfauna within this block suggests an age that is contemporaneous with, or up to 1 m.y. older than, the flow. The lithified character of the block indicates it is older than the flow, which is tentatively assigned an age of 19.5 Ma on the basis of the magneto- and biostratigraphy.

We can only speculate upon the mechanism initiating the mass movement. The debris flow coincides with a period of active deformation that accompanied the onset of the present New Zealand collisional plate boundary (e.g., Rait et al., 1991). An increase in seismicity may have been sufficient to trigger the mass movement on what is normally a passive margin.

Volcanicity

A notable feature of Site 1123 is the presence of numerous macroscopic tephra layers from the middle Miocene to present (Fig. **F8**). Age estimates for individual tephra layers are given in **"Paleomagnetism,"** p. 26. Many of the tephra layers found at Site 1123 contain fresh glass and phenocrysts (plagioclase) suitable for radiometric dating (Pillans et al., 1996) and thus may become numerical stratigraphic calibration points (Shane et al., 1996). Since New Zealand is the only area in the Southwest Pacific with abundant rhyolitic volcanism during the late Cenozoic (Nelson et al., 1986a), it is the probable source for the tephra. For the late Quaternary, Carter et al. (1995) have shown that widespread downwind dispersal of tephra occurred from the Taupo Volcanic Zone (North Island, New Zealand). Voluminous eruptions have resulted in deposition of macroscopic tephra at least 1400 km from the source (e.g., the Kawakawa Tephra). For pre-Quaternary rhyolitic tephras, the probable eruptive source is the Coromandel region of northern North Island, which was active during the Neogene (Ballance, 1976; Suggate, 1978).

The frequency and level (in meters composite depth) of the recovered tephra layers show some differences between the three holes (Fig. **F8**). This includes a 22-cm-thick tephra layer recovered in Hole 1123C (Section 181-1123C-11H-6; 103.17–103.39 mbsf) of which no evidence is found in either Hole 1123A or Hole 1123B. This remains enigmatic.

Original spatial variability in burial (note the holes were each 30 m apart) or artifacts induced by the drilling are possible explanations.

The best-fit tephra stratigraphy is depicted against the composite section for Site 1123 in Figure F8. Forty-five tephra beds are recognized, the oldest of middle Miocene (~12 Ma) age. Naming individual tephra on the basis of stratigraphic position awaits onshore chemical analysis and dating. However, the two youngest tephra layers are almost certainly the well-documented Kawakawa Tephra (note this tephra is heavily bioturbated and its position is picked from magnetic susceptibility), which is dated at 22,590 radiocarbon years (Carter et. al., 1995), and the distinctive white-pink Omataroa Tephra (28,000 radiocarbon years; Froggatt and Lowe, 1990).

The composite tephra section suggests an event frequency of 1/27 k.y. for major eruptions. However, the tephra beds are not evenly distributed through time, and a major period of explosive activity occurred at ~1.60–1.35 Ma (~51–64 meters composite depth [mcd]). This could be related to the period of extensive volcanism inferred between 1.79–1.60 Ma from tephras of the southern North Island (Shane et al., 1996).

Additional lesser eruptions may be represented by the numerous green laminae in cores from Site 1123. These probably represent smectitic (i.e., bentonitic) alteration products of former tephra (Gardner et al., 1986). As Nelson et al. (1986a) suggest for Leg 90 sediments, the preservation potential for such inferred more basic material in highly calcareous sediment is lower than it is for the New Zealand-derived rhyolitic shards. Overall, however, the macroscopic tephra recorded at Site 1123, together with the continuous, astronomically tuned stratigraphy that may result for the site, will provide a unique record of Cenozoic volcanism in New Zealand and the Southwest Pacific region.

BIOSTRATIGRAPHY

Introduction and Summary

The micropaleontological biostratigraphy of Site 1123 is based mostly on the onboard study of core-catcher samples. Holes 1123A and 1123B samples were used for the uppermost part of the section, Hole 1123B samples for the middle part, and Hole 1123C samples for the lower part. Additional samples were taken from within selected cores to address specific age and paleoenvironmental questions. The absolute ages assigned to biostratigraphic datums follow the references listed in Tables T2, p. 59; T3, p. 60; T4, p. 63; T5, p. 64; all in the "Explanatory Notes" chapter; and Tables T5, T6, and T10 in this chapter.

Calcareous microfossils are diverse and abundant, but their preservation deteriorates gradually below 190 mbsf, especially in chalk. Strong differential dissolution in many samples has left only resistant species preferentially preserved. Radiolarians are generally abundant and well preserved throughout the sequence, except for three barren samples. Diatoms and silicoflagellates are present with good preservation in the upper 300 mbsf (uppermost Miocene to Pleistocene) and also in the upper Eocene/lower Oligocene interval recovered. Significant differential dissolution of planktonic foraminifers and calcareous nannofossils in Miocene and Pliocene sediments suggests that this site has frequently been bathed in corrosive bottom waters underneath the lysocline. In

contrast, the late Eocene–early Oligocene calcareous microplankton fossils are relatively better preserved, despite their deep burial.

As this site is north of the Subtropical Convergence, the presence of diverse temperate and subtropical assemblages in samples facilitates correlation with both the global standard zonations of low latitudes and with the New Zealand stages. The sequence is well dated by more than 100 datum levels from various fossil groups. Age assignments given by the five microfossil groups are in close agreement. A summary of zonation and major datum levels is presented in Figure **F16.** All the fossil groups suggest that Site 1123 recovered a continuous Neogene sequence of ~587 m back to ~20–21.5 Ma. This Neogene sequence terminates at a regional Oligocene unconformity (Marshall Paraconformity of Carter and Landis, 1972), which at this site separates lower Miocene (20–21.5 Ma) from lowest Oligocene–uppermost Eocene (~33 to 35 Ma) sediments.

Reworked Paleogene and early Miocene nannofossils and radiolarians are common in the upper part of the section. The presence of allochthonous subantarctic diatoms in the upper Neogene sediments at this site documents the influence of sediment input by contour currents flowing along the northern slope of Chatham Rise. The sharp contrast in preservation of calcareous microfossils between the Paleogene and Neogene, the presence of frequently reworked nannofossils, diatoms, and radiolarians in the upper sections, as well as the existence of a big hiatus (33 to ~21.5 Ma missing), suggests that the onset of the Deep Western Boundary Current took place after 33 Ma.

F16. Biostratigraphic summary chart, **p. 70.**

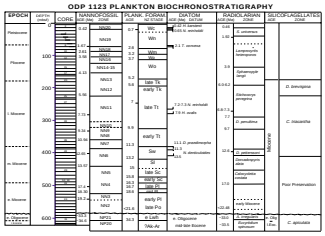

Age

Calcareous Nannofossils

Nannofossils in core catchers of Cores 181-1123A-1H to 17H, 181-1123B-18X to 52X, and 181-1123C-18X to 33X were examined. Additional samples were selected from within cores to increase the stratigraphic resolution. Nannofossils are abundant throughout the sequence, except for a few intervals where dissolution removed most of the species. Preservation of nannofossils is generally good in the top part of the sequence from Samples 181-1123A-1H-1, 40 cm, to 181-1123B-21X-CC (0–191.27 mbsf). Starting from 191 mbsf, the preservation deteriorates gradually. The identified species are tabulated in Table **T4.** Reworking is frequent throughout the sequence. The presence of many age-diagnostic species allows a detailed zonation of the sequence (Fig. **F16**). Twenty-two datum levels have been recognized. Their depths (mbsf) and age estimates are listed in Table **T5.** An age-depth relationship curve is shown in Figure **F17.** The upper 587.25 mbsf contains a continuous Neogene sequence (0 to ~21.6 Ma). A major disconformity is detected at ~587.2 mbsf between Samples 181-1123C-29X-2, 97 cm, and 29X-2, 114 cm. The sediments below this disconformity record a brief interval of the earliest Oligocene and latest Eocene (~33 to 35 Ma) (Figs. **F16, F17**). Compared to previous sites, the sedimentation rates of the Neogene sediments of this site are much lower (~33 m/m.y.).

T4. Identifications, range chart, and abundances of nannofossils, **p. 134.**

T5. Summary of nannofossil datum, age estimates, and references, **p. 138.**

F17. Age-depth relationship based upon calcareous nannofossil datums, **p. 71.**

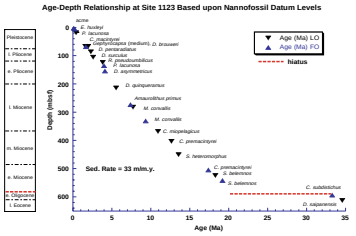

Pleistocene and Pliocene

The core catcher of the first core (Sample 181-1123A-1H-CC) indicates an age already older than the first age-diagnostic datum level, the first occurrence (FO) of *Emiliania huxleyi,* dated at 0.24 Ma (Naish et al., 1998). This datum was detected at Sample 181-1123A-1H-4, 75 cm,

which marks the base of Zone NN21. Within Zone NN21, a reversal of dominance from *Emiliania huxleyi* to *Gephyrocapsa oceanica* occurs between Samples 181-1123A-1H-2, 7 cm, and 1H-2, 145 cm, indicating an age of 0.085 Ma (Berggren et al., 1995a) at ~2.26 mbsf.

Although a few *Pseudoemiliania lacunosa* are present in samples above 15.61 mbsf, the genuine FO of this marker species at the base of Zone NN20 is its first abundant occurrence in Sample 181-1123A-3H-CC (23.21 mbsf). Because of the low sedimentation rates (~3–4 cm/k.y.) and coarse sampling, we were not able to detect all the bioevent datum levels of the Pleistocene as was possible at previous sites. Instead, two datum levels marking the beginning of the Pleistocene were detected: the FO of the medium-sized *Gephyrocapsa* and the last occurrence (LO) of *Calcidiscus macintyrei* at Sample 181-1123A-8H-CC (72.02 mbsf). These two events have been calibrated using paleomagnetic data slightly younger than the Olduvai Normal Event, at ~1.67 and 1.6 Ma, respectively (Raffi et al., 1993; Raffi and Flores, 1995).

The LO of *Discoaster brouweri* in Sample 181-1123A-8H-CC (72.02 mbsf) marks the top of Zone NN19 at 1.96 Ma (Raffia and Flores, 1995). Sample 181-1123A-10H-CC (91.88 mbsf) contains several *Discoaster* species, which represent the last stock of discoasterids before they became extinct at about the Pliocene/Pleistocene boundary. The common occurrence of *Discoaster pentaradiatus* indicates that the sediments were deposited before 2.2 to 2.4 Ma (Wei, 1993). The top of the Zone NN17 thus is defined in Core 181-1123A-10H. The last appearance of *D. surculus,* which defines the top of the Zone NN16 (2.55 Ma), occurs in Sample 181-1123A-12H-CC (110.76 mbsf). On the other hand, the LO of *Discoaster tamalis* (2.76 Ma; Raffi and Flores, 1995) in Sample 181-1123A-11H-CC (101.14 mbsf) appears to be conflicting. Considering the possibility that *D. tamalis* might be reworked, we chose the LO of *D. surculus* at 2.55 Ma as the age marker for this interval (Table **T5**).

The LO of *Reticulofenestra pseudoumbilicus* (the top of NN15 at 3.82 Ma) (Raffi and Flores, 1995) in Sample 181-1123A-14H-CC (129.66 mbsf) and the FO of *D. asymmetricus* (the bottom of NN14 at 4.13 Ma, Shackleton et al., 1995) in Sample 181-1123A-16H-CC (148.66 mbsf) allow a detailed zonation of the Pliocene. Furthermore, the FO of *Pseudoemiliania lacunosa* (4.0 Ma; Gartner, 1990) in Sample 181-1123A-14H-CC provides another good age marker. The absence of several important marker species for the early Pliocene, including *Ceratolithus rugosus* and *C. acutus,* makes it difficult to differentiate Zone NN12 from NN13. The appearance of *Discoaster quinqueramus* in Sample 181-1123B-24X-CC (220.5 mbsf) indicates that the Pliocene/Miocene boundary lies slightly above this level.

Late and Middle Miocene

Conventionally, the late Miocene in low-latitude regions can be subdivided into very fine zones based upon a series of fast-evolving *Discoaster, Amaurolithus,* and *Catinaster* species. However, the sporadic occurrence of *Amaurolithus* and *Discoaster* spp., aggravated by overgrowth, allows only partial recognition of the standard zones at this site. Nevertheless, several additional datum levels, which are not markers for the standard zonation, proved very useful for correlation in the mid-latitudes. For instance, the generally rare occurrence of *Amaurolithus primus* in this sequence casts doubt about the biochronologic value of its FO (7.39 Ma) in Sample 181-1123B-29X-CC (268.49 mbsf), but the LO (7.73 Ma) and FO (9.34 Ma) of a short-ranged species, *Minylitha convallis,* at 287.54 mbsf (Sample 181-1123B-31X-CC) and 326.02 mbsf

(Sample 181-1123B-35X-CC), respectively, helps to confirm the utility of *Amaurolithus primus* as a useful marker, despite its low abundance.

The middle/late Miocene boundary (~11.2 Ma) is approximated by the LO of *Coccolithus miopelagicus* (10.94 Ma) (Backman and Raffi, 1997) in Sample 181-1123B-40X-CC (374.06 mbsf). The LO of *Calcidiscus premacintyrei* (12.65 Ma) (Raffi and Flores, 1995) occurs in Sample 181-1123B-43X-CC (399.52 mbsf). This level has been reported to be slightly older than the top of Zone NN6 (Young et al., 1994). The zonal marker separating Zone NN5 from NN6, the LO of *Sphenolithus heteromorphus* (13.52 Ma) (Backman and Raffi, 1997), was found in Sample 181-1123B-49X-CC (457.06 mbsf).

Early Miocene

Most specimens of *Discoaster* spp. have been overgrown to the extent that species-level characters are unrecognizable. Not being able to differentiate to species, we only separated the *Discoaster variabilis* group from that of *D. deflandrei*. The transition from the *D. deflandrei* group to the *D. variabilis* group occurs at ~506 to 498 mbsf (Samples 181-1123C-20X-CC to 19X-CC), which marks generally the boundary between the early and middle Miocene. Although the early/middle Miocene boundary could be more precisely determined by the LO of *Helicosphaera ampliaperta,* which occurred slightly above the boundary, the virtual absence of this species in the sequence precludes its use as a marker at this site.

In the lower Miocene sequence, a few zonal markers were recognized. The LO of *Sphenolithus belemnos* in Sample 181-1123C-22X-6, 136 cm (526.26 mbsf), which defines the upper boundary of the Zone NN3, is a few meters lower than the FO of *Sphenolithus heteromorphus* in Sample 181-1123C-21X-CC (516.96 mbsf). Because neither *S. belemnos* nor *S. heteromorphus* were found in the particular sample (Sample 181-1123C-22X-5, 78 cm; 524.18 mbsf) that was taken between these two samples, we place the boundary between Zones NN3 and NN4 (18.3 Ma) right at this level (524.18 mbsf). Within Zone NN4, the FO of *Calcidiscus premacintyrei* in Sample 181-1123C-20X-3, 147 cm (504.48 mbsf), provides an additional age marker at 17.4 Ma.

The FO of *S. belemnos* was recorded in Sample 181-1123C-23X-CC (536.71 mbsf), indicating an age younger than 19.2 Ma (Berggren et al., 1995b). A major floral discontinuity was found between Samples 181-1123C-29X-2, 97 cm, and 29X-2, 114 cm. Early Oligocene assemblages occur below this floral break. Based upon the sedimentation rate of 20 m/m.y., calculated from the above three datum levels, the age of the oldest sediments immediately above the paraconformity is estimated to be 21.7 Ma.

Latest Eocene–Earliest Oligocene

Nannofossils from the chalky sediments below the paraconformity are generally abundant but have moderate to poor preservation. In the five samples below the paraconformity (Samples 181-1123C-29X-2, 114 cm, through 32X-2, 132 cm [587.39–616.42 mbsf]), the nannofossil assemblages are characterized by abundant *Chiasmolithus* spp. (difficult to be identified to the species level because of poor preservation), *Dictyococcites abisectus, Reticulofenestra umbilicus,* and *Zygrhablithus bijugatus*. The presence of *Isthmolithus recurvus,* a short-ranged species existing between 36 and ~32 Ma, constrains this interval to be in the early Oligocene to late Eocene. The occurrence of particularly abundant *Clausicoccus* spp. (listed as *C. subdistichus* in Table **T4**), centered around

Sample 181-1123C-29X-CC (593.31 mbsf), suggests that this interval is in the acme zone of *Clausicoccus,* which has been dated to be 33.3 Ma (Berggren et al., 1995b). *Discoaster saipanensis,* whose last occurrence defines the top of Zone NP20, occurs in Sample 181-1123C-32X-2, 132 cm (616.42 mbsf). Therefore, the sequence below this level down to the bottom of the Hole 1123C (625.76 mbsf) is assigned to Zone NP20 (34.2–35.4 Ma), slightly lower than the Eocene/Oligocene boundary (Berggren et al., 1995b).

Foraminifers

Throughout most of the Site 1123 section, the planktonic foraminiferal assemblages show evidence of variable, differential dissolution (Tables T6, T7). Benthic assemblages, which contain many relatively thick-walled taxa, appear more intact. However, this criterion may be misleading, since species content strongly varies between groups of samples, possibly the result of carbonate dissolution of benthic tests before their burial. Agglutinated benthic taxa are mostly rare to absent, except in Sample 181-1123C-22X-CC, where an acme of *Eggerella bradyi* occurs. Differential dissolution of planktonic foraminifer tests affected our ability to find all of the expected taxa of potential use in the biostratigraphy and led us to doubt the local stratigraphic distribution of some of the observed events. Also, the uncertainty attached to the age calibrations, coupled with the fact that the sampling depths of FO and LO events may be revised when samples in between core catchers are examined, demands caution in drawing detailed biochronological conclusions.

T6. Significant foraminifer and bolboformid datum levels, p. 139.

T7. Identifications, range chart, and abundances of planktonic foraminifers, p. 140.

We are most confident in the correlation potential of those bioevents that occur within evolutionary lineages (especially the *Globorotalia* lineages), where both ancestor and descendant forms are present in assemblages, below and above the datum. First and last appearance datum with no clear ancestral or descendant forms present may be less reliable for correlation (e.g., FO *G. praescitula,* FO *Zeaglobigerina nepenthes,* FO *Orbulina universa,* FO *O. suturalis,* FO *Globorotalia crassula,* and FO *G. truncatulinoides).* Members of the *G. fohsi* and *N. acostaensis* lineages are essentially absent.

Quaternary

The younger part of the Quaternary interval is not easily recognized biostratigraphically by using foraminifers. The uppermost sediment (Samples 181-1123B-1H-1, 0–2 cm; and 1H-1, 18–20 cm) is younger than 0.45 Ma, based on the presence of *Globorotalia hirsuta.* Despite intensive searching, this species was not found in any lower samples. The planktonic foraminiferal assemblage in Sample 181-1123A-1H-CC (6 mbsf) is dominated by *Globorotalia inflata* (first common occurrence [FCO] in subantarctic ~0.7 Ma) and also has common *Globorotalia truncatulinoides* (FO in subantarctic ~0.8 Ma). This indicates a late Pleistocene age (younger than 0.7 Ma, New Zealand Castlecliffian Stage).

Globorotalia inflata is still dominant in Sample 181-1123A-2H-CC (16 mbsf), but here the first *Globorotalia puncticuloides* (LO ~0.6 Ma) occurs downhole. The dominant globorotaliid from Sample 181-1123A-3H-CC to 11H-CC is *G. puncticuloides* (last common occurrence [LCO] ~0.7 Ma, FO ~3.6 Ma). It co-occurs with *Globorotalia inflata* (FO 3.7 Ma). Samples 181-1123A-3H-CC to 5H-CC (23–44 mbsf) also contain *Globorotalia truncatulinoides* (FO ~0.8 Ma in the subantarctic, but earlier in the subtropics) suggesting an age of ~0.7–0.8 Ma for this interval, although it

could be older, as this site is north of the STC. In Samples 181-1123A-2H-CC and 3H-CC, rare *G. crassaformis hessi* occurs. The latter is typical for the middle Pleistocene, the chronostratigraphic assignment is thus accepted for this interval. Samples down to 181-1123A-8H-CC (72 mbsf) are younger than 2.6 Ma because they also contain sporadic *Globorotalia crassula* (FO 2.6 Ma).

Pliocene

Samples 181-1123A-9H-CC and 10H-CC (82–92 mbsf) are late Pliocene (Mangapanian to early Nukumaruan Stages), because they contain a tightly constrained zone of dextral, unkeeled *Globorotalia crassaformis* (3.0–2.1 Ma).

Sample 181-1123A-11H-CC (101 mbsf) is mid-Pliocene (3.6–3.4 Ma, Waipipian Stage), based on the occurrence of *Globorotalia puncticuloides* (FO 3.6 Ma), *G. crassaconica* (LO 3.0 Ma), rare *G. pliozea* (LO ~3.4 Ma), and *G. inflata* (FO 3.7 Ma).

Sample 181-1123A-12H-CC (111 mbsf) is mid-Pliocene (~3.6–3.7 Ma, late Opoitian Stage), based on the occurrence of *Globorotalia inflata triangula* (FO 3.6 Ma), common *G. pliozea* (LCO 3.6 Ma), and *G. puncticulata* (LO 3.7 Ma).

Samples from 181-1123A-13H-CC to 181-1123B-19X-CC (120–172 mbsf) are of early Pliocene age (3.7–5.2 Ma, Opoitian Stage), based on the occurrence of common *Globorotalia puncticulata* (FO 5.2 Ma, LO 3.7 Ma), and supported by the presence of *G. pliozea* (3.4–5.4 Ma). The lower part of this interval can be further subdivided, as Sample 181-1123A-18X-CC (164 mbsf) is of earliest Pliocene age (~4.7–4.8 Ma, early Opoitian Stage), based on the occurrence of *Globorotalia crassaconica* (FO 4.7 Ma), *Globorotalia mons* (LO 4.8 Ma), and *Sphaeroidinella dehiscens* (FO 4.8 Ma).

Miocene

Sample 181-1123B-20X-4, 83–87 cm (177.65 mbsf), is latest Miocene (5.2–5.4 Ma, late Kapitean Stage), based on the occurrence of *Globorotalia sphericomiozea* (LO 5.2 Ma), *G. juanai* (LO 5.2 Ma in 181-1123B-20X-CC), and *G. pliozea* (FO 5.4 Ma). Sample 181-1123B-21X-CC (191 mbsf) is latest Miocene (5.5–5.6 Ma, middle Kapitean Stage), based on the presence of *Globorotalia sphericomiozea* (FO 5.6 Ma), *G. mons* (FO 5.5 Ma), and *G. miotumida* (LO 5.6 Ma). Also, no *G. crassaformis* was observed below this level.

Samples 181-1123B-22X-CC to 35X-CC (200–326 mbsf) are of undifferentiated late Miocene age (5.6–9.9 Ma), based on the dominance of sinistral *Globorotalia miotumida* (LO 5.6 Ma) and the occurrence of the distinctive *Globoquadrina dehiscens* (LO 9.9 Ma) in Sample 181-1123B-36X-CC (335 mbsf). *G. conoidea* Walters, the thick-walled form of *G. miotumida* Jenkins, is well represented. Within this long interval, the rare presence of *Bolboforma pentaspinosa* (LO 7 Ma) in Samples 181-1123B-27X-CC, 30-CC, and 32-CC assists to divide the upper Miocene interval into upper and lower parts. This is confirmed by the presence of *Sphaeroidinellopsis paenedehiscens* (FO ~8 Ma) in Sample 181-1123B-27X-CC (249 mbsf).

Samples 181-1123B-36X-CC to 40X-CC (336–374 mbsf) are earliest late Miocene (9.9–11.3 Ma, early Tongaporutuan Stage), based on the presence of *Globoquadrina dehiscens* (LO 9.9 Ma) and sporadic *Neogloboquadrina pachyderma* (FO 11.3 Ma; lowest occurrence in Sample 181-1123B-40X-CC). This agrees with the presence of *Zeaglobigerina druryi* (LO 11.3 Ma) in Samples 181-1123B-39X-CC and below. Sample 181-

1123B-40X-CC contains the highest stratigraphic level of *Catapsydrax parvulus,* longer ranging in Miocene strata.

The assemblage in Sample 181-1123B-41X-CC is sparse and contains no species that are diagnostic of differentiating the middle from late Miocene. The presence of *Neogloboquadrina nympha* and *Globorotalia miotumida* suggests these samples are younger than 13.2 Ma.

Samples 181-1123B-42X-CC to 46X-CC (388–428 mbsf) are late middle Miocene (11.3–13.2 Ma, Waiauan Stage), based on the presence of *Paragloborotalia mayeri* (LO 10.8 Ma; highest occurrence in Sample 181-1123B-42X-CC) and *Globorotalia miotumida* (LO 13.2 Ma; lowest occurrence in Sample 181-1123B-46X-CC), together with *Zeaglobigerina druryi* (LO 11.3 Ma), *Neogloboquadrina continuosa* (LO ~11 Ma), *Zeaglobigerina nepenthes* (FO 11.8 Ma; lowest occurrence in Sample 181-1123B-42X-CC), and *Globorotalia conica* (LO ~13 Ma; highest occurrence in Sample 181-1123B-45X-CC). Sample 181-1123B-46X-CC is latest Lillburnian Stage (13–13.2 Ma) based on the presence of *Globorotalia miotumida* (FO 13.2 Ma) and *Paragloborotalia partimlabiata* (LO 13 Ma).

Samples 181-1123B-47X-CC to 50X-CC (437–469 mbsf) are early middle Miocene (15.8–13.2 Ma, Clifdenian and Lillburnian Stages) based on the presence of *Globorotalia praemenardii* (LO 13.2 Ma, FO 15.8 Ma), supported by the presence of *Cibicidoides wuellerstorfi* (FO 16.4 Ma; lowest occurrence in Sample 181-1123B-49X-CC) and more sporadic occurrence of *Globorotalia amuria* (FO 16 Ma; lowest occurrence in Sample 181-1123B-48X-CC). The single occurrence of one specimen of *Globorotalia panda* (FO 15 Ma) in Sample 181-1123B-48X-CC tentatively assists with subdivision within this interval. From Sample 181-1123B-47X-CC downhole, *Globoquadrina praedehiscens* is common, whereas *Globorotalia mayeri* is absent.

Samples 181-1123B-51X-CC to 181-1123C-20X-CC (480–506 mbsf) span the early to middle Miocene boundary (16.7–15.8 Ma, late Altonian and early Clifdenian Stages) based on the presence throughout of *Globorotalia miozea* (FO 16.7 Ma, LO 15.8 Ma) supported by the presence of *Zeaglobigerina druryi* (FO 17.4 Ma) and common *Globoquadrina dehiscens* (local absence zone 18.6–17 Ma). It is possible that this core-catcher sampling interval spans a slightly wider age interval, using the common presence of *Catapsydrax stainforthi* and the LO of *Catapsydrax dissimilis* in Sample 181-1123-20X-CC. The latter two events have LOs of ~16.4 and 17.3 Ma, respectively, in temperate-subtropical realms. On the other hand, it is possible that the datum of one or several of the taxa involved may have to be revised, once more precise ranges are known, using samples selected from between core-catchers. This interval can be subdivided by the presence of *Paragloborotalia bella* (LO 16.3 Ma) in Sample 181-1123C-19X-CC. Above is early Clifdenian Stage and below is late Altonian Stage.

Sample 181-1123C-21X-CC (517 mbsf) is early Miocene (18.6–16.7 Ma, middle Altonian Stage) based on the occurrence of common *Globorotalia zealandica* (acme zone 18.6–16.7 Ma), *Sphaeroidinellopsis disjuncta* (FO 18.5 Ma), and absence of *Globoquadrina dehiscens* (local absence zone 18.6–17 Ma). Several *Bolboforma* taxa are present in this sample.

Sample 181-1123C-22X-CC has a sparse, partly dissolved planktonic assemblage, largely composed of *Catapsydrax dissimilis* and abundant benthic foraminifers.

Samples 181-1123C-23X-CC, 25X-2, 32–34 cm (limestone boulder in debris flow), 27X-CC, and 28X-CC (537–584 mbsf) contain *Globorotalia incognita* (FO 21.6, LO 18.5 Ma), indicative of an early Miocene age

(21.6–18.5 Ma, late Otaian and early Altonian Stages), supported by the presence of *Zeaglobigerina connecta* (FO ~22.2 Ma). Other samples within this interval have sparse assemblages of nonspecific probable early Miocene taxa, containing mostly *Catapsydrax dissimilis*.

Paleogene

Samples 181-1123C-29X-CC and 30X-CC (593–600 mbsf) are latest Eocene to early Oligocene (32–34.3 Ma; early Whaingaroan Stage) based on the occurrence of abundant *Subbotina angiporoides* (LO 30 Ma) and *Paragloborotalia gemma* (LO 32 Ma, FO 35 Ma), and absence of *Globigerinatheka index* (LO 34.3 Ma). Sample 181-1123C-30X-CC contains rare *Reticulophragmium* aff. *amplectens,* known to extend into the Oligocene of the Norwegian Sea.

Samples 181-1123C-31X-CC to 33X-CC (611–626 mbsf) are late Eocene in age (Runangan to Bortonian Stages), based on the occurrence of abundant *Globigerinatheka index* (LO 34.3 Ma), *Subbotina linaperta,* and *Porticulosphaera semiinvoluta* (LO 35.3 Ma, FO 38.4 Ma). In New Zealand, the latter species' recorded range is restricted to the Runangan Stage (dated ~35.5–34.3 Ma); hence, Hole 1123C probably bottomed in limestones of 35.3–35.5 Ma.

Sample 181-1123C-31X-CC also contains *Paragloborotalia gemma* (FO 35 Ma), indicating that the top of this interval is 34.3–35 Ma (late Runangan Stage). Present in Sample 181-1123C-33X-CC is the distinctive, cosmopolitan, deep-water benthic *Nuttallides truempyi,* which has a New Zealand LO of 37 Ma (Bortonian Stage), but extends to the top of the Eocene elsewhere. At DSDP Site 277, *Nuttallides truempyi's* youngest occurrence is in the early Kaiatan Stage (near the base of NP19, ~36 Ma, Hollis et al., 1997). The basal Sample 181-1123C-32C-XX also contains incomplete specimens of *Spiroplectammina* indistinguishable from *S. spectabilis*. This taxon is widely recorded in Eocene strata in the circum-North Atlantic and becomes extinct at the top of the Eocene (Kaminski et al., 1989).

Age Summary

The following is a summary of foraminiferal ages in terms of the New Zealand stage classification, and of local chronological calibration of these stages, according to Table **T2,** p. 59, in the "Explanatory Notes" chapter (see also Fig. **F16** in this chapter):

1. Nukumaruan (Wn), Castlecliffian (Wc), and Haweran (Wq), late Pliocene to Holocene (0–2.6 Ma): down to Sample 181-1123A-8H-CC (0–72 mbsf);
2. Mangapanian (Wm), late Pliocene (2.6–3.2 Ma): Sample 181-1123A-10H-CC (92 mbsf);
3. Waipipian (Wp), mid-Pliocene (3.2–3.7 Ma): Sample 181-1123A-11H-CC (101 mbsf);
4. Opoitian (Wo), early Pliocene (3.7–5.2 Ma): Samples 181-1123A-12H-CC to 181-1123B-19X-CC (111–172 mbsf);
5. Late Kapitean (late Tk), latest Miocene (5.2–5.5 Ma): Samples 181-1123B-20X-4, 83–87, to 21X-CC (178–191 mbsf);
6. Late Tongaporutuan and early Kapitean (late Tt-early Tk), late Miocene (9.9–5.5 Ma): Samples 181-1123B-22X-CC to 35X-CC (200–326 mbsf);
7. Early Tongaporutuan (early Tt), late Miocene (11.3–9.9 Ma): Samples 181-1123B-36X-CC to 40X-CC (336–374 mbsf);

8. Waiauan (Sw), middle Miocene (13.2–11.3 Ma): Samples 181-1123B-42X-CC to 47X-CC (388–437 mbsf);
9. Late Clifdenian (late Sc) and Lillburnian (Sl), middle Miocene (15.8–13.2 Ma): Samples 181-1123B-47X-CC to 50X-CC (437–469 mbsf);
10. Early Clifdenian (early Sc), middle Miocene (16.3–15.8 Ma): Sample 181-1123B-51X-CC (480 mbsf);
11. Late Altonian (late Pl), early Miocene (16.7–16.3 Ma): Samples 181-1123B-52X-CC, 181-1123C-18X-CC to 20X-CC (489–506 mbsf);
12. Middle Altonian (middle Pl), early Miocene (18.6–16.7 Ma): Sample 181-1123C-21X-CC (517 mbsf);
13. Late Otaian and early Altonian (late Po-early Pl), early Miocene (21.6–18.5 Ma): Samples 181-1123C-23X-CC to 27X-CC (537–575 mbsf);
14. Early Whaingaroan (early Lwh), latest Eocene and early Oligocene (32–34.3 Ma): Samples 181-1123C-29X-CC and 30X-CC (593–600 mbsf); and
15. Kaiatan (Ak) and Runangan (Ar), late Eocene (older than 34.3 Ma): Samples 181-1123C-31X-CC to 33X-CC (611–626 mbsf).

Diatoms and Silicoflagellates

Diatoms (Table T8) are present in varying abundance in the Pleistocene and are common in the Pliocene to uppermost Miocene sediments. In the upper to lower Miocene, diatoms are absent or so poorly preserved and rare that they are not useful for biostratigraphic dating. Only in the lower Oligocene to upper Eocene sediments below the unconformity recovered within Core 181-1123C-29X (587.3 mbsf) are diatoms again common.

T8. Species occurrences and relative abundance of diatoms and silicoflagellates, p. 142.

In spite of the common abundance of diatoms in upper Neogene sediments, stratigraphic marker species of the middle to low latitudes are rare and occur inconsistently. Reworking of older diatoms is also found in practically all samples, making biostratigraphic evaluation difficult. The few species that could be used for biostratigraphic assignment were *Nitzschia denticuloides, Denticulopsis praedimorpha, Hemidiscus ovalis, Nitzschia reinholdii,* and *Thalassiosira convexa* (Fig. F16). In addition, the *Hemidiscus karstenii* acme, which is found in the Antarctic and subantarctic regions in the Pleistocene, seems to be present in this area as well. Whether the presence of *H. karstenii* occurs at the same time in both hemispheres, and whether it results from the northward displacement of subantarctic diatoms has to be tested with more detailed studies later and by correlation of its abundance fluctuations against the oxygen isotope record at this site.

The relatively large and dissolution-resistant marker species *Cestodiscus reticulatus* was not found in the lower Oligocene sediments. Fragments of a large *Coscinodiscus* species, which may belong to *Coscinodiscus excavatus,* were encountered in Samples 181-1123-29X-CC and 30X-CC. This, together with the occurrence of species of the genus *Rocella* belonging to the complex of *R. vigilans,* place these cores into the early Oligocene. Samples 181-1123-31X-CC to 33X-CC are characterized by the presence of *Hemiaulus polycystinorum* var. *mesolepta, Hemiaulus caracteristicus, Riedelia lyriformi,* and *Riedelia claviger,* which place these cores into the middle to late Eocene.

Reworking of Eocene and Oligocene diatom valves (e.g., of the species *Paralia architecturalis, Pyxilla reticulata, Triceratium barbadense, T.*

kanayae, and *T. inconspicuum* var. *trilobata*) is observed throughout the Neogene, especially in the more clay-rich, green-gray sediment intervals. Occasionally, however, Miocene and Pliocene diatoms also are reworked into younger sediments.

Silicoflagellates are not common, but nevertheless provide age-diagnostic markers such as *Mesocena quadrangula* in the Pleistocene, *Dictyocha neonautica,* the characteristic species for the *D. fibula* Zone, which straddles the Miocene/Pliocene boundary, *Mesocena diodon borderlandensis,* which is characteristic of the late Miocene *D. brevispina* Zone, and *Mesocena diodon diodon* and *Paradictyocha apiculata,* which are characteristic of the Miocene *C. triacantha* Zone. Reworked species among the silicoflagellates include *Corbisema inermis minor, Dictyocha spinosa, Mesocena oamaruensis, M. occidentalis, Naviculopsis foliacea foliacea,* and *Valacerta tumidula.*

Radiolarians

Radiolarian biostratigraphy at Site 1123 is based on the examination of 70 core-catcher samples and two core samples (Table **T9**). Radiolarian faunas are generally abundant and well preserved throughout the section (Samples 181-1123A-1H-CC to 181-1123C-33X-CC, 0–625.76 mbsf). Extensive reworking of Paleocene and Eocene radiolarians is common throughout the section, and middle Miocene radiolarians occur frequently in the upper part of the section. Only three out of the processed samples proved to be barren (Samples 181-1123B-38X-CC, 50X-CC, and 181-1123C-23X-CC). Radiolarian datum levels applied at Site 1123 are shown in Table **T10,** and an age-depth plot using these radiolarian datum levels is shown in Figure **F18.** The radiolarian zones used at this site are of the low-latitude zonation of Sanfilippo and Nigrini (1998) and partly of the middle-latitude zonation of Foreman (1975) and Morley (1985).

T9. Identification and abundance of radiolarians, **p. 150.**

T10. Significant radiolarian datum levels, **p. 158.**

F18. Age-depth relationship based upon radiolarian datum, **p. 72.**

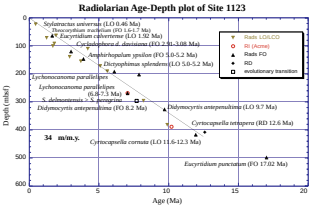

Pliocene–Pleistocene

The last occurrence of *Stylatractus universus* (LO 0.46 Ma) occurs in Sample 181-1123A-3H-CC, and this species was not found in the upper two samples (181-1123A-1H-CC and 2H-CC). The uppermost interval (0–23 mbsf), therefore, is younger than 0.46 Ma. In Sample 181-1123A-4H-CC (34.7 mbsf), the last occurrence of *Axoprunum angelinum* was also recognized. *Stylatractus universus* has been considered as a junior synonym of *Axoprunum angelinum* by some authors, or vice versa. The former taxon has been frequently recorded in the Southern Hemisphere, whereas the latter tends to occur in the Northern Hemisphere. However, examination of samples at this site reveals that both forms coexist in the same samples at the upper part of the section. They are morphotypically different and *A. angelinum* has a much longer stratigraphic range. For this reason, both species are listed as legitimate taxa and used for correlation at this site. The samples between 181-1123A-3H-CC and 5H-CC (23–44 mbsf) are assigned to the *Stylatractus universus* Zone, based on the occurrence of a single specimen of *Eucyrtidium matuyamai* in Sample 181-1123A-6H-CC.

Sample 181-1123A-7H-CC (63 mbsf) contains the FO datum of *Theocorythium trachelium* (FO 1.6–1.7 Ma in the equatorial Pacific) and the LO of *Eucyrtidium calvertense* (LO 1.92 Ma in the subantarctic). A middle to early Pleistocene age (0.46–1.8 Ma) is indicated for the interval between Samples 181-1123A-3H-CC and 7H-CC (23–63 mbsf).

Sample 181-1123B-16H-CC indicates an age of 3.9 Ma, based on the FO of *Amphirhopalum ypsilon,* which is consistently present in the upper section. Sample 181-1123B-17H-CC (158.57 mbsf) also indicates an age of 3.7 Ma, based on the LO of *Lychnodictyum audax*.

The interval between Samples 181-1123A-15H-CC and 181-1123B-21X-CC (140–191 mbsf) is assigned to the *Sphaeropyle langii* Zone of Foreman (1975), based on the last occurrence of *Stichocorys peregrina* (LO ~2.9 Ma) in Sample 181-1123A-15H-CC and the FO of *Sphaeropyle langii* (6.0–6.2 Ma) in Sample 181-1123B-21X-CC. A Pliocene and latest Miocene age is indicated for this interval.

Miocene

Sample 181-1123B-19X-CC (172 mbsf) is of latest Miocene age (5.0–5.2 Ma) based on the *Dictyophimus splendens* (LO 5.0–5.2 Ma in the North Pacific). It first occurs in Sample 181-1123B-27X-CC and last occurs in Sample 181-1123B-19X-CC, and is, therefore, a good short-range marker species (172–250 mbsf) in this section. In addition, *Lychnocanoma parallelipes* (LO 5.6 Ma; FO 6.8–7.3 Ma in the Northwest Pacific) also shows a short range from Samples 181-1123B-21X-CC to 29X-CC (191–268 mbsf), which reinforces the age assignment of latest Miocene (5.2–7.3 Ma) for this interval.

Samples between 181-1123B-21X-CC and 32X-CC (191–296 mbsf) are assigned to the *Stichocorys peregrina* Zone of Foreman (1975), the base of which is defined by the evolutionary transition (7.7 Ma in the northwest Pacific) from *Stichocorys delmontensis* to *Stichocorys peregrina* in Sample 181-1123B-32X-CC. This zone spans the time interval from 5.0–6.2 to 7.7 Ma, and its base is diachronous between low and middle latitudes (e.g., 6.71 Ma; base of the *Stichocorys peregrina* (RN9) Zone of Sanfilippo and Nigrini, 1998).

Within the RN9 Zone, *Stylacontarium aquilonium* first occurs in Sample 181-1123B-22X-CC (201 mbsf), and the datum of rapid increase in abundance of *Stichocorys peregrina* (RI event at 6.8–7.3 Ma) is recognized in Sample 181-1123B-29X-CC (268.5 mbsf). The interval between 296 and 326 mbsf is of middle late Miocene (8.2–9.7 Ma) age, based on the presence of *Didymocyrtis antepenultima* (LO 8.2 Ma, FO 9.7 Ma) in Samples 181-1123B-32X-CC and 35X-CC.

Cyrtocapsella japonica is sporadically present in varying abundances in the lower part of the section (181-1123B-41X-CC to 181-1123C-28X-CC). Its LO (9.9 Ma) and acme (10.2 Ma) horizons are recorded in Samples 181-1123B-41X-CC and 42X-CC, respectively. However, these horizons may occur higher than this apparent position, because the paucity of these forms or barren radiolarian occurrence in the higher Samples from 181-1123B-37X-CC to 39X-CC (345–364 mbsf).

The interval between Samples 181-1123B-42X-CC and 45X-CC (388–415.6 mbsf) contains abundant *Stichocorys delmontensis, Cyrtocapsella tetrapera, Cyrtocapsella japonica, Lithopera neotera,* and *Didymocyrtis laticonus,* which is assigned to the *Diartus petterssoni* (RN6) Zone of Sanfilippo and Nigrini (1998). The LO of *Cyrtocapsella cornuta* occurs in Sample 181-1123B-45X-CC (417 mbsf), which indicates an age of 11.6–12.3 Ma.

Common *Cyrtocapsella tetrapera* occurs consistently throughout the lower part of the section from Samples 181-1123B-44X-CC to 181-1123C-27X-CC (408.3–574.96 mbsf) and decreases rapidly between 408.3–399.52 mbsf, which suggests that Sample 181-1123B-44X-CC is of late middle Miocene age, based upon the dated age of 12.6 Ma for this rapid decrease event of this species.

Samples 181-1123B-46X-CC and 49X-CC (428–457 mbsf) are middle Miocene in age, based on faunas characterized by *Botrystrobus miralestensis, Eucyrtidium punctatum, Cyrtocapsella tetrapera, Theocorys redondoensis, Lithopera renzae,* and *Theocorys spongoconum*. The interval is assigned to the *Dorcadospyris alata* (RN5) Zone of Sanfilippo and Nigrini (1998).

In Sample 181-1123C-19X-CC (498 mbsf), the radiolarian fauna is characterized by the presence of common *Cyrtocapsella tetrapera,* common *Cyrtocapsella cornuta,* rare *Cyrtocapsella japonica,* and few *Eucyrtidium punctatum* (FO 17.02 Ma), together with rare *Carpocanopsis bramlettei, Dorcadospyris alata,* rare *Stichocorys wolfii, Theocorys spongoconum,* and few *Phormocyrtis alexandrae*. In addition, the LO of *Phormocyrtis alexandrae* (= *Eucyrtidium* sp. B of Sakai) is placed in the same sample, whereas this species is known to occur in the lower half of the *Dorcadospyris alata* Zone (Sakai, 1980). Furthermore, *Phormocyrtis alexandrae* and *Theocorys spongoconum* co-occur in the basal part of the *Dorcadospyris alata* Zone (Sakai, 1980). This suggests that the sample is early to middle Miocene (15–17 Ma) in age, and it correlates with the basal part of the *Dorcadospyris alata* (RN5) Zone and the *Calocycletta costata* (RN4) Zone of Sanfilippo and Nigrini (1998).

The interval between Samples 181-1123C-20X-CC and 23X-CC (506–536.7 mbsf) yields few radiolarians, including *Cyrtocapsella tetrapera* and *Cyrtocapsella japonica,* which suggests an age of middle to lower Miocene.

The interval between Samples 181-1123C-24X-CC and 27X-CC (546–575 mbsf) contains rare, but some age-diagnostic species including *Stichocorys delmontensis* (FO 20.53 Ma), *Cyrtocapsella tetrapera* (FO 23.62 Ma), *Dorcadospyris alata, Lychonocanoma elongata* (FO 24.6 Ma), *Dorcadospyris mahulangi, Anthocyrtidium marieae,* and *Phormocyrtis alexandrae.* This interval indicates an early Miocene age (17.5–20 Ma), because the last three species are known to occur from the lower Miocene Puriri Formation, Kaipara Harbour, New Zealand (O'Connor, 1994, 1997a, 1997b) and are correlated to the upper *Stichocorys delmontensis* Zone or lower *Stichocorys wolffii* Zone.

An age-depth plot for Site 1123 was constructed as shown in Figure **F18**, by using radiolarian datum levels including the FO, LO, RD (rapid decrease horizon), RI (rapid increase horizon), and an evolutionary transition. Accordingly, the sedimentation rate for the section (0–417 mbsf) is ~34 m/m.y., which is concordant with the rates calculated based upon other microfossil biochronologies and magnetostratigraphy.

Paleogene

Samples 181-1123C-29X-CC and 30X-CC, from a white to light gray limestone, contain well-preserved radiolarian assemblages dominated by *Stylacontarium bispiculum, Lophocyrtis longiventer, Lophocyrtis dumitricai,* and *Aphetocyrtis gnomabox*. This fauna is assigned to the *Axoprunum*(?) *irregularis* Zone of Takemura and Ling (1997), based on the rare occurrence of *Eucyrtidium antiquum* (FO 32.8–33.1 Ma), which indicates an early Oligocene age (~33 Ma).

Samples 181-1123C-31X-CC and 32X-CC (611–617 mbsf) contain common *Eucyrtidium spinosum* (LO 31.7–31.9 Ma) and rare *Eucyrtidium antiquum* (FO 32.8–33.1 Ma) together with abundant *Lophocyrtis longiventer* and few *Lophocyrtis aspera*. The two samples are assigned to the lower *Axoprunum* (?) *irregularis* Zone and upper *Eucyrtidium spinosum* Zone of Takemura and Ling (1997) because *Eucyrtidium spinosum* co-

occurs with *Eucyrtidium antiquum* in Sample 181-1123C-31X-CC but not in Sample 181-1123C-32X-CC. The estimated age for these samples is placed at about the Oligocene/Eocene boundary (31.7–33.5 Ma).

Sample 181-1123C-33X-CC (625.76 mbsf) yields a radiolarian fauna containing abundant *Lychnocanoma amphitrite, Calocyslas* (?) *nakasekoi, Lophocyrtis dumitricai,* and *Dicolocapsa microcephala,* indicative of a late Eocene age.

Paleoenvironment

Foraminifers

Only in the uppermost part (upper Pleistocene) of the hole are the foraminiferal assemblages well preserved and lacking indications of selective dissolution to varying degrees. It is clear that the site was below the lysocline for much of the Miocene and Pliocene. In many instances, the remaining foraminiferal assemblages are particularly sparse and required washing large core-catcher samples to obtain ~100 planktonic specimens. A preliminary study of pairs of dark-colored (cool hemipelagic) and light-colored (warm pelagic) lithologies within the lower Miocene and Pliocene indicates that planktonic foraminiferal percentages and abundances are lower in the darker lithologies than in the lighter ones. This suggests that dissolution was stronger during the cooler periods than during the warmer ones and, possibly, that planktonic productivity was higher during the warmer intervals. Dissolution is prevalent, however, throughout both cool and warm intervals.

Many of the planktonic assemblages lack or have very few representatives of dissolution-susceptible species (not always thin-walled). For example, particularly severe corrosion by dissolution removed or broke most specimens of *Globigerina, Globigerinoides, Praeorbulina, Orbulina,* and *Globorotalia panda* in the middle Miocene, and *Globorotalia praescitula* in the early Miocene.

Many of the early Miocene assemblages are dominated by thick-walled *Catapsydrax,* a taxon that in adjacent New Zealand rarely composes more than 10% of even a deep-water planktonic assemblage of the same age. Typically, the Neogene planktonic assemblages contain thick-walled, less porous, larger planktonics (e.g., the genera *Globorotalia, Sphaeroidinellopsis, Neogloboquadrina,* and *Catapsydrax*) that appear to have survived dissolution on the seafloor and become preferentially concentrated in the assemblage. These large forms are accompanied by an apparently random sprinkling of often thinner walled, smaller planktonic species that have perhaps survived by being moved down into the sediment by bioturbation soon after their arrival on the seafloor. Fragmented, partially dissolved, planktonic tests and chambers are common in most samples. Many of the surviving larger specimens have the last, less calcified chamber dissolved (e.g., *Globorotalia miozea* lineage forms).

The evidence suggests that, throughout most of the Neogene, the site was swept by corrosive bottom waters. This is most marked in the Miocene, where many assemblages have fewer than 10% planktonic foraminifers, compared with a normal oceanic assemblage above the lysocline, which would have >99% planktonic forms.

Site 1123 planktonic assemblages exhibit considerable evidence of their location north of the Subtropical Convergence. Numerous subtropical and temperate taxa not found in previous sites to the south (Sites 1119–1122), occur here: *Catapsydrax parvulus, C. stainforthi, Globi-*

gerinoides bolli, G. conglobatus, G. ruber, Globorotalia juanai, G. tumida, G. tosaensis, Neogloboquadrina acostaensis, Sphaeroidinella dehiscens, Sphaeroidinellopsis paenedehiscens, Zeaglobigerina druryi, and *Z. nepenthes*.

The early Oligocene and late Eocene foraminiferal assemblages have more normal planktonic foraminiferal compositions in both abundance (~99% of foraminifers) and diversity, reflecting oceanic conditions at lower bathyal depths.

The middle Miocene to Holocene benthic foraminiferal assemblages are relatively constant and typical of mid-bathyal to upper abyssal depths. Common taxa include *Chilostomella, Cibicidoides pachyderma, C. wuellerstorfi, Eggerella bradyi, Epistominella exigua, Globocassidulina, Gyroidina, Laticarinina pauperata, Martinotiella communis, Melonis barleeanum, M. pompilioides, Nodosaria longiscata, Oridorsalis umbonatus, Pyrgo murrhina, Pullenia bulloides, P. quinqueloba, Quinqueloculina venusta, Sigmoilopsis schlumbergeri, Sphaeroidina bulloides,* and *Uvigerina dirupta.* It is difficult to determine to what degree dissolution has modified the benthic assemblages, but undoubtedly selective dissolution has removed many thin-walled or more porous taxa and concentrated the more solution-resistant taxa (e.g., *Oridorsalis*). Much detailed quantitative study will be required to determine significant benthic assemblage changes through the section that may have been influenced by oceanographic changes.

Significant changes in the benthic foraminiferal assemblages are apparent in the upper Eocene, such as the loss of common *Nuttallides truempyi,* and in the upper lower Miocene, such as the loss of *Planulina renzi* and the appearance of *Cibicidoides wuellerstorfi*.

The clasts within the debris flow in Cores 181-1123C-24 and 25 contain foraminiferal assemblages of early Miocene age and of bathyal to abyssal depth, similar characteristics to the fauna of the section into which they were emplaced.

Diatoms

The diatom assemblages are temperate to subtropical and show two special characteristics: (1) dominance by high-productivity species belonging to *Thalassionema* and *Thalassiothrix,* along with resting spores of *Chaetoceros;* (2) displaced subantarctic diatoms, which are inferred to have been entrained into the sediments by the contour current formed by the upper Lower Circumpolar Deep Water throughout the latest Miocene to Pleistocene. In the Paleogene sediments, no such influence is recognizable.

PALEOMAGNETISM

Core archive halves from Holes 1123A, 1123B, and 1123C were measured on the shipboard pass-through cryogenic magnetometer. Declination, inclination, intensity of natural remanent magnetization (NRM), and a 20-mT alternating field (AF) demagnetization step were measured at 5-cm intervals. The first few cores of each hole were also measured after a 10-mT demagnetization step; this step added little extra information and, because of time constraints, only the 20-mT step was continued. In situ tensor tool data were collected for all APC cores, but a problem with the shipboard pass-through cryogenic magnetometer prevented the use of declination for polarity determination in the APC cores. Therefore, only inclination could be used to determine magnetic

polarity in Holes 1123A, 1123B, and 1123C. At least two discrete oriented samples were collected from the working half of each core interval for progressive AF and thermal demagnetization and for rock magnetic studies. Whole-core magnetic susceptibility was measured on all cores using a Bartington susceptibility loop on the automated multisensor track (MST).

A composite paleomagnetic record was constructed for Site 1123 using data from Hole 1123C (0–140 mcd and 500–635 mcd) and Hole 1123B (140–500 mcd). Hole 1123A was not used in constructing a composite record, as paleomagnetic results for the uppermost 90 mcd were not easy to interpret and not reproduced in Holes 1123B and 1123C. Discussion with the drilling team suggested that possible early failure of the shear pin may have contributed to this difference in paleomagnetic signal. A slower rate of penetration of the piston core and, hence, more disturbance of the core occurred during piston firing. Intensity of magnetic remanence varied markedly with depth in the composite record (Fig. F19). The upper 280 mcd has average NRM intensities of 4×10^{-4} A/m and these intensities increase steadily downcore to 1×10^{-3} A/m at 550 mcd. The lowermost 38 m (597–635 mcd) has average NRM intensities on the order of 10^{-5} A/m.

F19. Composite magnetostratigraphic record from Site 1123, p. 73.

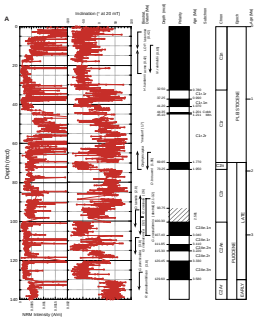

Paleomagnetic Behavior and Rock Magnetism

NRM measurements displayed consistent, steeply positive (downcore) inclinations ranging between +70° and +80°, consistent with a drill-string overprint induced during coring. The single 20-mT AF demagnetization step proved very effective in removing the overprint and elucidating a polarity reversal stratigraphy (Fig. F19). Figure F20 shows representative acquired isothermal remanence magnetizations (IRM) to saturation (SIRM) and backfield SIRM.

All samples above 597 mcd exhibited very uniform behavior, were saturated by 500 mT, and had backfield coercivities of remanence (B_{cr}) values of 40–80 mT (Fig. F20A). Alternating field and thermal demagnetization of the SIRM of these samples demonstrated moderate to soft magnetization with 60%–90% of intensity of remanence lost by the 60-mT AF demagnetization step (Fig. F21). Samples from the Eocene/Oligocene limestones beneath the hiatus at 597 mcd (see "Lithostratigraphy," p. 4) all had much harder magnetizations that did not saturate until IRM fields of 1 T (Fig. F20B). AF demagnetization was less effective in removing saturation magnetizations from discrete samples. Thermal demagnetization to zero intensity was not possible in samples above 597 mcd, as alteration of clay components of the sediment from stepwise heating caused new mineral growth above 500°C. This was detected by an increase in magnetic susceptibility, and further heating was discontinued. The general trend in each case was to zero remanence around 580°C (Fig. F21A, F21B). This, along with low coercivity and low B_{cr} values, suggests that the main remanence carrier is magnetite of distributed grain size. Below the hiatus at 597 mcd, however, intensity of remanence persisted above 600°C in all cases (Fig. F21C). The high unblocking temperature spectra, the high saturation IRM fields, and higher B_{cr} values (up to 100 mT) suggest hematite may contribute to the magnetic remanence of lithostratigraphic Unit IV.

F20. Isothermal remanent magnetization, p. 79.

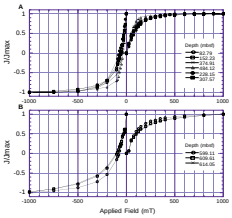

F21. Plots of normalized intensity of magnetization, p. 80.

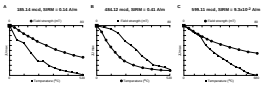

Magnetostratigraphy

Interpretation of magnetic polarity from the composite inclination record for Site 1123 (Fig. F19) is well constrained by key foraminiferal, nannofossil, and diatom datums from each of the core-catcher samples (see "Biostratigraphy," p. 13; also see "Biostratigraphy," p. 10, in the "Explanatory Notes" chapter). The inclination record for the upper 130 mcd of the composite record is taken from Hole 1123C and, when compared with the Geomagnetic Polarity Time Scale (Cande and Kent, 1995; Berggren et al., 1995), it provides a near-complete record of the Brunhes (C1n), Matuyama (C1r-C2r), and Gauss (C2An) magnetochrons (Fig. F19A). The uppermost 32.5 mcd of the polarity record is entirely normal, contains the last occurrences of the diatom *Nitzschia reinholdii* (0.65 Ma), nannofossil *Pseudoemiliania lacunosa* (0.42 Ma), and acme first occurrence (FO) of *Hemidiscus karstenii* (diatom, 0.42 Ma) and is assigned to the Brunhes (C1n) Chron. The characteristic normal-reversed-normal-reversed-normal pattern of the Gauss Chron occurs between 100 and 130 mcd, constrained by the LO of nannofossils *Reticulofenestra pseudoumbilicus* (3.8 Ma) and *Discoaster tamalis* (2.8 Ma), and foraminiferal datums *Globorotalia puncticulata* (LO, 3.8 Ma), *G. crassaconica* (LO, 3.2 Ma), *G. crassula* (FO, 2.6 Ma), and the range of the dextral form of *G. crassaformis* (2.1–3.2, Fig. F19A). Between 32.5 and 130 mcd, the polarity is mostly reversed with three short normal events. Two of these short normal polarity events immediately underlie the Brunhes Chron and are assigned to the Jaramillo (C1r.1n) and Cobb Mountain Subchrons, respectively. The other short normal polarity event occurs between 70 and 73 mcd and, constrained by nannofossils *Gephyrocapsa* (medium) (FO, 1.7 Ma) and *D. brouweri* (LO, 1.96 Ma), is assigned to Chron C2n (Olduvai). The inclination record between 94 and 100 mcd is ambiguous and not able to be designated as normal or reversed polarity. It is labeled "unknown" in Figure F19A, though it most likely lies within the upper part of Subchron C2An.1n (upper Gauss).

The inclination record between 130 and 260 mcd (Fig. F19B) is taken from Hole 1123B. It is more noisy than that for the upper 130 mcd but still allows interpretation of polarity zones. Between 130 and 213 mcd, polarity is mostly reversed with five short normal polarity events. Several foraminiferal events (short range of *G. sphericomiozea,* ~5.6 Ma, FO *G. puncticulata,* 5.2 Ma, FO *G. crassaconica,* 4.7 Ma, and LO *G. mons,* 4.8 Ma) and the FO of *D. asymmetricus* (nannofossil, 4.1 Ma) constrain this interval to the Gilbert Reversed Chron (C2Ar-C3n-C3r). The four short normal polarity subchrons between 150 and 185 mcd are characteristic of Chron C3n and are correlated with the Cochiti (C3n.1n), Nunivak (C3n.2n), Sidufjall (C3n.3n), and Thvera (C3n.4n) Subchrons, respectively. The lowermost of these (Thvera, C3n.4n, 177–185 mcd) is not well defined because most of the record at that depth was disturbed during the drilling process. The characteristic R-N-R-N polarity record of the latest Miocene (Chrons C3Ar and C3An) is observed between 213 and 265 mcd, and marks the base of the Gilbert Chron (Fig. F19B). It is constrained by the LO of the nannofossil *D. quinqueramus* (5.5 Ma) and by *Bolivinita pentaspinosa* (~7 Ma). The short interval of normal polarity between 200 and 201.5 mcd has no equivalent in the polarity time scale of Cande and Kent (1995).

The remaining polarity record of the late Miocene is very complex with many short reversals that make correlation with the GPTS difficult. However, the long normal polarity chron, C5n (9.74–10.95 m.y.),

is quite characteristic and marks the early part of the late Miocene record. A thick interval of normal polarity is observed between 350 and 380 mcd in the composite magnetic polarity record of Site 1123 (Fig. F19B). Constrained by the nannofossil datums LO *Minylitha convallis* (9.34 Ma) and FO *Coccolithus miopelagicus* (10.9 Ma) and foraminiferal datums LO *G. druryi* (11.2 Ma) and LO *Globoquadrina dehiscens* (10.1 Ma), this interval of normal polarity is correlated with Chron C5n.2n of the GPTS. Between 260 and 350 mcd, nine normal polarity intervals of the GPTS are recognized, and, like the GPTS, they are grouped into two distinct intervals: the upper five mark an interval that is of dominantly normal polarity between 265 and 300 mcd. These events are correlated with the subchrons of Chrons C3Bn–C4n. The remaining four normal polarity intervals lie directly above C5n and are separated from the upper five normal polarity intervals by a moderately thick interval of reversed polarity (300–319 mcd) that contains the FO of the nannofossil *D. quinqueramus* (8.3 Ma) and the diatom *Hemidiscus ovalis* (7.9 Ma) and is correlated with Chron C4r of the GPTS. The lower four normal polarity intervals are correlated with Chron C4An and Subchrons C4Ar.1n, C4Ar.2n, and C5n.1n, respectively (Fig. F19C). The very short normal event, C4r.1n, is not observed in the record from Site 1123. These correlations show that the late Miocene record at Site 1123 is remarkably complete and possesses strikingly uniform sedimentation rates.

The middle Miocene polarity record is equally complex and comprises 12 normal and 12 reversed chrons and subchrons. Again, the earliest part of the epoch is marked by a long chron, this time of reversed polarity (Chron C5Br). The correlative polarity record from Site 1123 (380–505 mcd, Fig. F19C, F19D) is complicated by poor recovery in the lowermost interval of Hole 1123B (see summary log in "Lithostratigraphy," p. 4). However, a thick interval of reversed polarity between 482 and 499 mcd contains the foraminiferal evolutionary transition of *G. miozea* to *G. praemenardii* dated in New Zealand at ~15.8 Ma (Scott, 1979; Morgans et al., 1996; see "Biostratigraphy," p. 13) and is correlated with C5Br. Between 380 and 482 mcd of Hole 1123B, no less than 13 individual normal polarity events were recognized in initial observations of the polarity record. This suggests that the polarity record is complete, despite the poor recovery. It is surmised that the loss of recovery (between 40% and 60%) must be distributed throughout each individual coring interval, most likely by abrasive loss of material at drilling-induced breaks in the core from the XCB drilling process. The retained core thus represents a compression of the 9.5-m-long cored interval into the reduced record actually recovered. In order to test this hypothesis, the whole-core magnetic susceptibility and inclination records from each core interval (see "Composite Depths," p. 32) were stretched linearly from their recorded length to fill each 9.5-m coring interval (Fig. F22), and the stretched records compared with the downhole logging record of magnetic susceptibility. The stretched whole-core magnetic susceptibility is very comparable to the downhole log susceptibility record and was, therefore, used to characterize the magnetic polarity stratigraphy for Cores 181-1123B-41X through 50X (Fig. F19D). The resulting stretched polarity record is, on average, of reversed polarity and more detailed correlation with the GPTS is afforded by several foraminiferal and nannofossil events. Between 380 and 404 mcd polarity is mostly reversed and correlated with C5r of the GPTS. At ~405 mcd, the LO of the nannofossil *Calcidiscus premacintyrei* and the diatom *N. denticuloides* (12.2–12.6 Ma and 11.3–13.5 Ma, respectively)

F22. Comparison of whole-core susceptibility and inclination, p. 81.

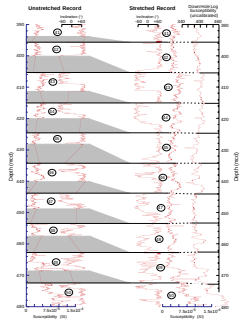

suggests that the N-R-N polarity pattern between 404 and 421 mcd (Fig. F19D) correlates with Chron C5A of the GPTS. The foraminiferal evolutionary transition of *G. praemenardii* to *G. miotumida* (~13 Ma) between ~435 and 455 mcd suggests that the normal polarity events in this interval correlate with Subchrons C5Ar.1n, C5Ar.2n, and Chron C5AAn, respectively. The LO of the nannofossil *Sphenolithus heteromorphus* (13.5–13.6 Ma) at ~463 mcd suggests that the normal polarity events between 457 and 482 mcd correlate with Chrons C5Abn, C5Acn, C5ADn and Subchrons C5Bn.1n and C5Bn.2n. Within the upper Miocene, two short reversals are recognized in the polarity record from Site 1123 that do not have equivalents in the GPTS (Fig. F19D). A short reversed polarity interval separates Subchron C5Ar.1n (432.6–435.3 mcd) into two normal polarity events, and another short reversed polarity interval separates Chron C5ADn (471.6–474.45 mcd) into two normal polarity events.

Foraminifer and nannofossil events (see "Biostratigraphy," p. 13) define a long hiatus in the record from Site 1123 where lowermost Oligocene strata are separated from middle to lower Miocene strata by a distinct *Cruziana* ichnofacies horizon at 596.7 mcd (see "Lithostratigraphy," p. 4). The early Miocene polarity record in Hole 1123C is complete down to and including Chron C6n and the upper part of Chron C6r (Fig. F19D, F19E). The acme of the foraminifer *G. zealandica* (16.7–18.6 Ma), the FO of *G. miozea* (16.7 Ma), the FO of the nannofossil *C. premacintyrei* (17.4 Ma), and the LO of the foraminifer *G. bella* (16.3 Ma) constrain the four normal polarity events between 499 and 522 mcd to the three subchrons of Chron C5Cn and Chron C5Dn, respectively, and the reversed polarity interval between 522 and 534 mcd to Chron C5Dr (Fig. F19E). Continuing down, still constrained by the acme of the foraminifer *G. zealandica* (16.7–18.6 Ma) and also by the FO of the nannofossil *S. heteromorphus,* the R-N-R pattern between 522 and 546 mcd correlates with Chrons C5Dr, C5En, and C5Er (Fig. F19E). A debris flow between 552 and 562 mcd (see "Lithostratigraphy," p. 4) complicates interpretation of the remaining early Miocene polarity record, but the complication is not severe as we consider it a single instantaneous event. Two biostratigraphic datum events occur within the material of the debris flow: the LO of the foraminifer *G. incognita* (18.5–19.4 Ma) and the FO of the nannofossil *S. belemnas* (19.2 Ma). Although the ~10-m sampling interval of core catchers prevents precise location of datums, and the fossils have been reworked from older strata, they still afford age constraints on the debris flow, as it must be younger than the fauna that it contains. By inference, the strata immediately overlying the debris flow must also be younger than the fauna contained within the debris flow; hence, the interval of normal polarity between 546 and 552 mcd must correlate with the upper part of Chron C6n of the GPTS. The inclination pattern between 552 and 562 mcd provides additional constraint on the thickness of strata affected by the debris flow. The signal is both noisy and of intermediate direction, rather than of truly normal or reversed polarity, and probably represents a fabric direction imparted by the debris-flow regime. It is assumed that the deposition of the debris flow was essentially instantaneous and also that because it was in a depositing phase it did not cause much erosion at its base. Using these constraints and assuming similar sedimentation rates beneath the debris flow as those above, and also constrained by the FO of *G. incognita* (21.6 Ma) within the hiatus at 597 mcd, the normal polarity between 562 and 579 mcd is correlated with the remainder of Chron C6n

and the underlying reversed polarity interval (579–697 mcd) with Chron C6r (Fig. F19E).

The hiatus at 597 mcd is not constrained by magnetic polarity as it occurs within an interval of continuously reversed polarity. Beneath the hiatus, however, the nannofossil *C. subdistichus* acme (33.3 Ma) suggests an earliest Oligocene age for the strata immediately underlying the hiatus and that the normal-reversed polarity events represent C13n and the lowermost part of C12r, respectively. Three more datums confirm that the record beneath the hiatus extends into latest Eocene time; the FO of the foraminifer *Paragloborotalia gemma* (~35 Ma), the LO of *G. index* (34.3 Ma), and the LO of the nannofossil *D. saipanensis* (34.2–35.4 Ma). The nannofossil *Isthmolithus recurvus* occurs to the base of Hole 1123C and its first occurrence must be lower than the base of Hole 1123C. Its FO is ~36 Ma (Wei, 1992; Wilson et al., 1998) and the base of Hole 1123C must therefore be younger than 36 Ma. Despite poor recovery and a weak and noisy paleomagnetic signal, a normal polarity event is identified between 625 and 627 mcd and is correlated with C15n, and reversed polarity is identified between 609 and 625 mcd and is correlated with Chron C13r. It is possible that, with further work, the interval between 616 and 619 mcd may prove to be normal and thus correlate with C15n and move the polarity interpretation to be slightly older, but present analysis of the polarity of this interval is still ambiguous.

In the 597-m Neogene composite record of Site 1123, all but two polarity subchrons of the GPTS are present. Absent are the Reunion normal polarity subchron (C2r.1n) and Subchron C5r.2n. However, three new polarity events are recognized: one is a normal polarity event within Chron C3r (Fig. F19B), the other two are reversed polarity events within Subchrons C5Ar.1n and C5An, respectively. A paleomagnetic age model for Site 1123, listing depths and ages of magnetic polarity reversal events, is given in Table T11.

T11. Compilation of age data, p. 159.

An age-depth summary for Site 1123, using the GPTS reversal polarity ages given in Berggren et al. (1995b), is given in Figure F23. The average sedimentation rate for lithostratigraphic Units I and II (alternating drift and pelagic sediments, see "Lithostratigraphy," p. 4) is 35 m/m.y. and remarkably uniform. Small variations in average sedimentation rate are separated by well-defined inflection points. Between three inflection points at ~170, 265, and 400 mcd, respectively, slightly faster and slower average sedimentation rates are recorded (47 m/m.y., between 170 and 265 mcd, and 28 m/m.y., between 260 and 400 mcd). Possible small hiatuses or condensed intervals of less than 100 k.y. are noted at 270 and 340 mcd. A major inflection point at 465 mcd (~13.5 Ma) denotes a major change in sedimentation at Site 1123 and separates the relatively fast sedimentation of lithostratigraphic Units I and II from the much slower sedimentation of Unit III, which is a solely pelagic nannofossil mudstone and chalk. Average sedimentation rates are ~15 m/m.y between this inflection point and the hiatus at 597 mcd and also in the Eocene/Oligocene micritic limestone of Unit IV beneath the hiatus. The debris flow between 552 and 652 mcd is clearly a single depositional event that does not represent much time. It is denoted on Figure F23 as a vertical line. The hiatus between Units III and IV represents almost exactly 12 m.y. of missing time (21–33 m.y.) and is presumably correlative, in part, with the Marshall Paraconformity (Carter, 1985; Fulthorpe et al., 1996). In most onshore localities in New Zealand, the paraconformity separates lower Oligocene and upper Oligocene sediments, and the hiatus at the type locality is 3–4 m.y. (32.4–

F23. Age model and correlation of the composite magnetic polarity record, p. 82.

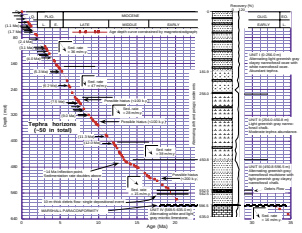

29.0 Ma) (Fulthorpe et al., 1996). In cases where the paraconformity spans longer intervals, it is generally inferred to be a result of erosion of older strata beneath, which extends the base of the unconformity in places to 36 Ma (Carter, 1985). Here, however, as for other offshore localities (Fulthorpe et al., 1996), the hiatus extends to younger strata, suggesting a prolonged phase of erosion/nondeposition.

Units I and II at Site 1123 contain more than 50 tephra horizons (see "Lithostratigraphy," p. 4). The age model presented in Figure F23 affords good constraints on the ages of these horizons.

COMPOSITE DEPTHS

Composite Section and Splice

A composite section for Site 1123 yielded overlapping records for the upper ~167 mcd. Data overlaps from Holes 1123A, 1123B, and 1123C document complete recovery of the sedimentary sequence to this depth. Two high-resolution data sets proved most useful for correlations at this site: magnetic susceptibility (MS), measured on whole cores on the MST, and spectral reflectance at 550 nm (the center wavelength of the range measured), measured on split cores. Reflectance records provided unambiguous ties for matching nearly all APC cores for the composite section, whereas MS provided reliable ancillary support for the majority of these ties. These two parameters are inversely correlated over the depth range of the splice, where the lithology alternates between white and green nannofossil ooze. The final composite section is illustrated in Figure F24.

Above ~40 mbsf, offsets between mbsf and mcd do not follow a clear trend (Fig. F25). We suggest these offsets are influenced by coring disturbance, including flow-in at the ends and in the middle sections of cores. Flow-in occurred in several APC cores from Holes 1123A and 1123B. The flow-in most likely resulted from slower-than-average APC strokes, which, when combined with ship heave, can introduce spurious material at any interval in a core. For example, in Core 181-1123A-4H, flow-in recovered in Section 4H-5 caused distortion of color reflectance and MS records of >2 m relative to the same stratigraphic intervals in Holes 1123B and 1123C (Fig. F24). Matches between different holes with and without flow-in can result in both negative and positive offsets relative to the mbsf scale. Data were edited to remove disturbed intervals before composite section development, and edited data are shown in Figure F24. Below ~40 mbsf, downhole core offsets in the composite section parallel a model of 10% stretch between the mbsf and mcd depth scales (Fig. F25). Table T12 (also in ASCII format) contains the offsets between the mbsf and mcd scales that result from composite section construction.

The continuous spliced record, based on MS and reflectance data (Fig. F26), extends to 167 mcd. The splice is composed entirely of records from Holes 1123B and 1123C. Coring difficulties, including several intervals of flow-in, complicated the upper section of Hole 1123A, making portions of the hole unsuitable for inclusion in the splice. Additionally, shipboard sampling was concentrated in Hole 1123A; therefore, post-cruise high-resolution sampling following the splice will benefit from splice concentration in Holes 1123B and 1123C. Wherever possible, splice tie points (Table T13, also in ASCII format) were picked at well-defined maxima or minima where the overlaps in data from

F24. Composite sections for magnetic susceptibility and color reflectance, p. 83.

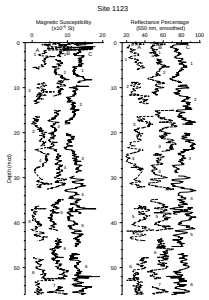

F25. Downhole depth offsets, p. 86.

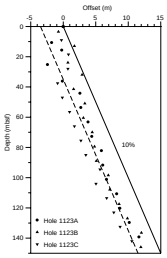

T12. Composite depth section, Site 1123, p. 160.

F26. Spliced record for Site 1123, p. 87.

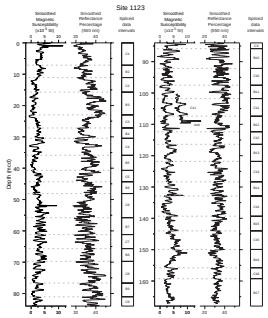

T13. Splice tie points, p. 171.

Holes 1123B and 1123C are correlated. Typically, parameter values differed by less than 10% at tie levels. In all cases, ties were selected so that the spliced record was as free from noise (high-frequency variability) as possible. (Note: Because of a proof-stage correction to the splice, Tables T12 and T13 are correct, but Figures F25–F29 have not been altered.)

Several tephras were recovered in only one of three holes, even in intervals where the major shapes of sedimentary cycles correlate between holes. Core 181-1123C-11H contains a particularly prominent example, where a 20-cm-thick tephra layer occurred near the base of the core (Fig. **F26**). Core 181-1123B-12H clearly spans other features recovered in Cores 181-1123C-11H and 181-1123C-12H (Fig. **F24**), though this thick tephra is missing. We did not include this tephra in the splice because (1) it was recovered in only one hole, and (2) it represents an "instantaneous" event that does not reflect the dominant pattern of sedimentation through this interval. If desired, one may add this (and other) features into the splice using the information in Tables **T12** and **T13.**

Overlap between Holes 1123B and 1123C was deliberately attempted deeper in the section. Hole 1123C was APC cored to refusal, washed down to approximately the base of Hole 1123B (~484 mbsf), then XCB cored to a depth of ~625 mbsf. The purpose of this drilling plan was to continue drilling deeper than the base of Hole 1123B, while recovering an overlapping section between the two holes. Magnetic susceptibility data document ~6 m of overlap between Cores 181-1123B-51X and 52X and Cores 181-1123C-18X and 19X (Fig. **F27**). The overlap illustrated here agrees with independent paleomagnetic results, which show a matching reversal at the boundary between paleomagnetic Chrons C5Br and C5Cn.1n in both holes (Fig. **F27**).

F27. Composite section overlap, **p. 88.**

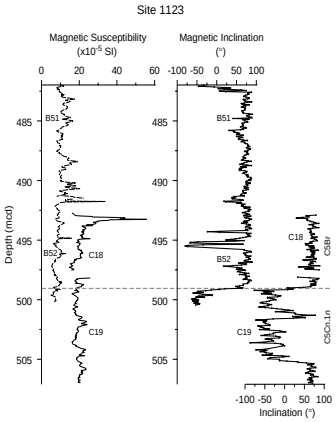

Stretching

Recovery (meters of core relative to meters advanced by the drill string) in XCB Cores 181-1123B-23X, 26X, 41X through 50X, and Core 181-1123C-20X was typically poor. However, through this interval, a complete sequence of paleomagnetic reversals was documented, a surprising result for poorly recovered intervals (see **"Paleomagnetism,"** p. 26). A comparison between core and log data supports the view that a more complete section is recovered than indicated by "core recovery" percentages. Rather than losing material at either end of an XCB core or from a continuous interval in the middle, shipboard data are consistent with the hypothesis that loss of material between XCB "biscuits" is distributed throughout the core, resulting in a compressed recovered section. To test whether recovery of the sedimentary signal at decimeter-meter scale is higher than indicated by meters of core retrieved, we "stretched" the core data for several XCB cores by linearly interpolating between fixed end-points for each core. The end-points in this scheme are (1) the top of the core fixed at its assigned mbsf depth, and (2) the bottom of the core fixed at 9.5 m below the top. The resulting "stretched" section compares well to downhole log magnetic susceptibility records from Hole 1123B (a continuous record of MS), with few cycles missing from the stretched core data (see Fig. **F22** for a core-log MS comparison including stretched paleomagnetic records). Based on this comparison, we suggest that the stretched core data represent a reasonable approximation of the real compositional variations (via MS and reflectance) through these intervals. To translate between mbsf and stretched mbsf, or mbsf and stretched mcd depths, refer to Table **T14.**

T14. Translation to stretched mbsf and mcd scales, **p. 172.**

Correlation and Time Scale Tuning

The continuity of the splice, plus good recovery in single-cored XCB sections, provides an excellent opportunity for development of a high-resolution, orbitally tuned time scale at this site. Figure **F28** illustrates a preliminary "map" between reflectance percentage (550 nm) and the benthic oxygen isotope record from eastern equatorial Pacific Site 846 for 0–3 Ma (Mix et al., 1995b). In many intervals, the shape and duration of features in the reflectance percentage curve mirror the oxygen isotope curve. Isotope stages are reflected in Site 1123 core data back to the end of the spliced record at ~4.6 Ma. This age model will be refined postcruise, incorporating revised biostratigraphic and paleomagnetic datums, and oxygen isotope stratigraphy.

F28. Color reflectance from Site 1123, **p. 89.**

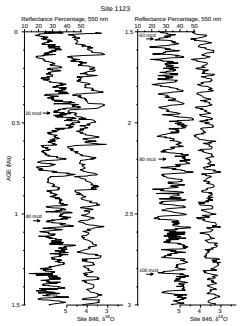

AGE MODELS AND SEDIMENTATION RATES

One of the discoveries of DSDP Leg 94, which explored the Feni and Gardar sediment drifts in the North Atlantic Ocean, was the presence of remarkable continuous stratigraphic sections, with few, if any, discernible hiatuses through the Pliocene–Pleistocene (Kidd and Hill, 1986). With the drilling of Site 1123, in hemipelagic drift sediments on north Chatham Rise, scientists on Leg 181 have now recovered similar continuous sections, not only for the Pliocene–Pleistocene, but also for most of the Miocene, starting near 20 Ma. Thus, Site 1123 offers the potential to improve the early and middle Miocene time scale (Hilgen et al., 1995), particularly if the carbonate/clastic cycle succession can be reconstructed for that stratigraphic interval. The quality of this carbonate record will particularly depend on continuous detail in the GRAPE density data, the downhole logging, and the hole splices. If it is possible to establish the ~20-m.y. Neogene cycle record by several parameters (reflectance, magnetic susceptibility, and others) it may be possible to correlate this to a calculated insolation tuning target (Laskar et al., 1993) to establish an astronomical time scale back into the late early and middle Miocene. The first order ties of the magnetostratigraphic and biostratigraphic datums to the cycle chronology can then be compared with those established for pieces of its record from other sites around the world (Hilgen et al., 1991a, 1991b, 1995; Shackleton et al., 1995; Shackleton and Crowhurst, 1997; Naish et al., 1997), and used for a Neogene time scale standard for southern Pacific stratigraphies. A remarkable set of data already exists, using information available from onboard studies, yielding a robust age-depth model based on magnetostratigraphic and biostratigraphic datums.

The combined nannofossil, foraminifer, diatom, and radiolarian biostratigraphy at Site 1123 yielded 112 event levels with a preliminary age assignment, using the shipboard stratigraphic framework (see **"Biostratigraphy,"** p. 10, in the "Explanatory Notes" chapter). The 112 levels are shown in Table **T15,** and consist of 51 FO events, 11 acme, FCO, or LCO events, and 50 LO events. Note that a tentative age of the FO of *Globoquadrina dehiscens* in Sample 181-1123C-28X-CC of 25 Ma cannot be verified without a continuous stratigraphic section across this interval. Hence, this level was not taken into account in the calculation of average sedimentation rates (see below). In Figure **F29,** all levels are plotted according to their observed depths at Site 1123 and ages defined in **"Biostratigraphy,"** p. 10, in the "Explanatory Notes" chapter. The position of the arrows in Figure **F29** may be extended uphole (down-

T15. Biostratigraphic events identified at Site 1123, **p. 173.**

F29. Age-depth plot, **p. 90.**

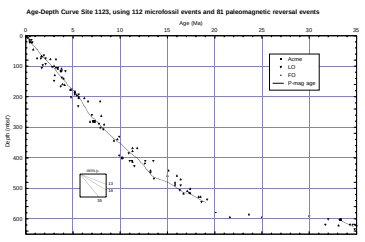

hole) for last occurrences (first occurrences) because of the limited sampling density for shipboard analysis. For comparative purposes, the magnetostratigraphic age model (see "Paleomagnetism," p. 26) is shown as a line in Figure F29. Because of the size of the plot, strongly or fully overlapping event positions may be obscured in the graphs. All depths are reported in meters composite depth (mcd; not mbsf) values.

Scrutiny of Figure F29 allows the following preliminary observations to be made. The event distributions in time show no obvious outliers, except for several first occurrences of taxa near 80, 205, and 450–460 mcd. A principal break in sedimentation exists near 560 mbsf. This level also marks a change from a low to a much higher rate, above which level the average rate is fairly steady, without any long-term trend. The plot of fossil events vs. sampling depth in the Miocene shows gaps between 14 and 15 Ma, 8.5 and 9.5 Ma, and 6 and 7 Ma. The gaps may change somewhat from changes in event age calibration, but also may have an underlying paleoceanographic meaning. Colder water-mass incursions might have limited immigration of taxa during these relatively short periods.

In the mid-Pliocene interval, between 80 and 120 mcd, LO events seem to "bunch up," as if terminated suddenly. A possible reason is the onset of severe paleoclimatic change, that is, drastic water-mass cooling and severe changes in surface circulation patterns, which affected evolutionary change. An increase in sampling resolution would not change the above observations, but changes in age calibration would do so.

Scatter of the event distribution in the vertical sampling depth scale will diminish with higher resolution sampling. FO events reported in the core catchers may have been estimated to be too shallow by several meters, which may pertain to the FOs of *Globorotalia amuria* (~16 Ma) at 457.69 mcd, of *Cibicidoides wuellerstorfii* (16.4 Ma) at 469.15 mcd, of *Orbulina suturalis* (15.1 Ma) at 440.35 mcd, of *Zeaglobоquadrina nepenthes* (11.8 Ma) at 366.83 mcd, of *Sphaeroidinellopsis paenedehiscens* (~8 Ma) at 261.36 mcd, of *Sphaeropyle langii* (6.0–6.2 Ma) at 203.31 mbsf, and of *Globorotalia tosaensis* (3.2 Ma) at 75.87 mcd (Fig. F29). In particular, the obvious and relatively large offset between the polarity chron trend and the six foraminifer FO events between 15 and 17 Ma may require adjustment, once more samples between the core catchers are studied. On the other hand, the *G. amuria* and *O. suturalis* events, among these six, plus the *G. tosaensis* LO event, are relatively rare, defined by few specimens per sample, which hampers a search for the "top." Thus, no correction may be forthcoming for these event positions.

LO events reported in the core catchers may have been estimated to be too deep by at least several meters and include the last appearance of *Sphenolithus heteromorphus* (13.57 Ma) at 469.15 mcd, of *Globorotalia conica* (~11.5 Ma) at 428.6 mcd, the acme (10.2 Ma) and the last occurrence (9.9 Ma) of *Cyrtocapsella japonica* at 400.34 and 394.14 mcd, respectively, the last occurrence of *Discoaster quinqueramus* (5.56 Ma) at 232.49 mcd, of *Lychnodictium audax* (3.7 Ma) at 167.57 mcd, and of *Stichocorys peregrina* (<3Ma) at 149.38 mcd. Berggren et al. (1995b) discuss at length problems around the diverging age assignments for the last occurrence of the nannofossil *S. heteromorphus*. If there is no change in sampling depth of the event, the Site 1123 evidence suggests the event was estimated to be too young by 0.5 Ma.

Forty-six calcareous microfossil events that were considered to be relatively reliable, at least for local age calibration, were combined with the magnetostratigraphy. The paleomagnetic age model at Site 1123 is

shown by a solid line in Figure **F29.** No polarity chrons appear to be missing (see **"Paleomagnetism,"** p. 26), and the record tracks the central tendency of the "events channel" remarkably well. The already rather tight fit of the age assignments for the microfossil events and the polarity chrons provides an excellent opportunity to use the record in Figure **F29** for future biochronologic calibration in the southwestern Pacific realm and possibly beyond. For example, the LOs of *Globorotalia puncticulata* and of *Zeaglobigerina druryi* appear too old by 0.6 Ma or more, whereas the FO of *Sphaeroidinellopsis paenedehiscens* at ~8 Ma might shift to 7 Ma. More detailed studies are needed to resolve these differences. Ultimately, a table may be drawn up of recalibrated event ages in the temperate to subtropical Southwest Pacific, as compared also to the North Atlantic realm, involving all microfossil groups studied onboard ship.

Sedimentation rates through time at Site 1123, using a slightly smoothed data set of polarity chron ages vs. depth for the Neogene and biostratigraphic age interpretation for older strata, are shown in Figure **F30.** The rates are corrected for compaction in the following manner. First, over 200 porosity measurements from Site 1123 (see **"Physical Properties,"** p. 41) were analyzed for trends, using the programs DEPOR and BURSUB (Stam et al., 1987; Gradstein et al., 1989). Grain density was averaged at 2700 kg/m^3. A clear trend in porosity with depth exists, with porosity exceeding 71% at the top, and decreasing more or less linearly to almost 30% at the bottom of the Hole 1123C. Program runs were executed for the fine-grained lithologies at the site. Next, compacted and restored rates of sedimentation were derived, with the age intervals slightly smoothed, as shown in Table **T16.** Thickness restoration resulted in a near-doubling of the older Neogene and Paleogene rates, from 5–25 m/m.y. to 15–35 m/m.y., with negligible effects on younger rates; this is in accord with the measured porosity-depth trend. In general, higher sedimentation rates, up to 45 m/m.y. on average in the late Neogene, were preceded by average rates of 35 m/m.y. in the early Neogene, and ~15 m/m.y. in the late Eocene and early Oligocene.

F30. Restored sedimentation rate, **p. 91.**

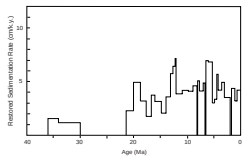

T16. Age-depth data, **p. 175.**

A simple burial diagram, without paleo–water depth but corrected for compaction, is shown in Figure **F31.** Age levels used are five or more meters apart. Burial was remarkably steady and constant for this drift.

F31. Burial curve for late Eocene through Neogene, **p. 92.**

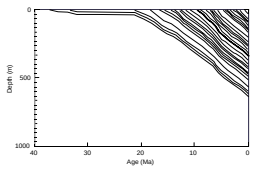

The principal feature of the sedimentation rate and age-depth curves (Figs. **F23, F29**) is remarkable uniformity over the past 20 Ma. The evidence suggests that the mixture of biopelagic skeletal remains and hemipelagic terrigenous sediment has remained rather constant over this period, testifying to long-term stability in both the productivity regime and the sediment delivery system. The early Miocene rate of ~15 m/m.y. ends at a marked slow-down in sedimentation at 15–13.5 Ma corresponding to the middle Miocene shift in $\delta^{18}O$ and growth in the Antarctic Ice Sheet. It remains to be determined whether the effect was to increase the flow speed and reduce sedimentation rate through winnowing or to decrease flow rate and, consequently, sediment delivery. Following this near-hiatus, sedimentation rate increases sharply to 38 m/m.y. and from 12 Ma steadies at 28 m/m.y. until 7 Ma, when there is a further sharp increase to ~47 m/m.y. This probably corresponds to increased delivery of sediment to Bounty Trough caused by sharp uplift of the Southern Alps in response to a pronounced phase of compression deformation along the plate boundary (Walcott, 1998). From 5 Ma to the present a constant sedimentation rate of 36 m/m.y. has prevailed with no apparent interference from climatic or tectonic changes. This

probably reflects the constancy of the sediment delivery system dominated by the DWBC. Three phases or pulses of volcanism are recognized: a late Miocene phase (7.5–9.0 Ma; 280-320 mcd) probably coincident with early compression at the New Zealand plate boundary (Walcott, 1998), a phase in the mid-Pliocene (3.1–4.0 Ma; 110–145 mcd), and a recent phase in the Quaternary (<1.7 Ma; <75 mcd) coincident with the opening of the Taupo Volcanic Zone (Shane et al., 1996). Earlier volcanism is marked by tephras at 385 and 485 mcd (~11.3 and 12.0 Ma, respectively).

INORGANIC GEOCHEMISTRY

Interstitial Waters

Forty-seven interstitial-water samples were collected at this site: 28 from Hole 1123A at depths ranging from 1.40 to 154.50 mbsf, 13 from Hole 1123B between 151.80 and 483.65 mbsf, and 6 from Hole 1123C between 494.35 and 609.75 mbsf. Insufficient sample volume was obtained for measurements from the two lowermost intervals of Hole 1123C, which are micritic limestones of lithostratigraphic Unit IV (see "Lithostratigraphy," p. 4). Therefore, only chloride, sulfate, magnesium, and calcium concentrations were measured from Sample 181-1123C-31X-4, 135–150 cm, and no measurements were made on the lowermost Sample 181-1123C-33X-1, 123–135 cm. Sampling frequency is one sample per 3 m for the upper 50 mbsf and one sample per 10 m thereafter to 100 mbsf. Below 100 mbsf one sample per 30 m was taken downhole to the total depth. Results from these three holes are considered to constitute a single depth profile and the data are plotted together in Figure F32. The upper part of the profiles (<200 mbsf) are shown separately in Figure F33. Analytical results are summarized in Table T17 (also in ASCII format).

Salinity, Chloride, and pH

The salinity profile shows a stepwise decrease from the subsurface value of 34.5 to 33.5 at 151.80 mbsf. Taking the relatively low precision of salinity measurements (0.5) into account, this stepwise decrease with depth may be interpreted as a gradual decrease in salinity with depth. On the other hand, chloride (Cl^-) concentrations increase from 555 mM at 1.40 mbsf to 562 mM at 26.50 mbsf. Below 26.50 mbsf, chloride increases slightly downhole, but also shows some fluctuations.

Interstitial water pH values increase from 7.45 at 1.40 mbsf to 7.66 at 22.80 mbsf. From 22.80 to 97.50 mbsf, pH values remain in a narrow range between 7.56 and 7.66, showing some erroneous values probably caused by instrument error (7.92 at 42.00 mbsf and 7.75 at 59.50 mbsf). The pH decreases rapidly below 97.50 mbsf to a minimum value of 7.19 at 135.50 mbsf. Below 135.50 mbsf, pH values again remain close to 7.2, although erroneous data occur at 293.60, 466.25, 483.65, and 532.85 mbsf.

Sulfate, Alkalinity, Phosphate, and Ammonium

Sulfate, alkalinity, phosphate, and ammonium concentrations are controlled by sulfate reduction, which occurs in the upper part of the hole. The sulfate (SO_4^{2-}) concentration decreases gradually from 27.9

F32. Depth profiles of interstitial-water constituents at Site 1123, p. 93.

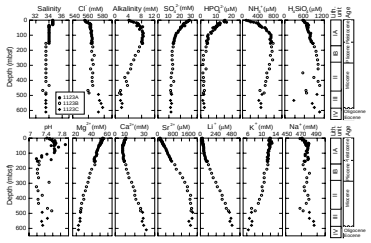

F33. Upper depth profiles of interstitial-water constituents, p. 94.

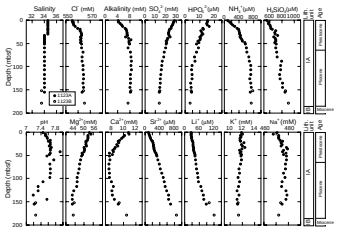

T17. Composition of interstitial waters, p. 176.

mM at 1.40 mbsf to 13 mM at ~200 mbsf (Fig. F33); below this depth sulfate values remain almost constant (Fig. F32).

The alkalinity of interstitial water increases with depth to 8.1 mM at 69.00 mbsf; below this depth, alkalinity remains almost constant to ~120 mbsf. Alkalinity shows a relatively small maximum value of 8.5 mM at 107.00 mbsf, compared to maxima observed at Sites 1119 (26.7 mM) and 1122 (40.5 mM), but it is about three times higher than the maximum value that occurred at Site 1121 (3.2 mM). The increase in alkalinity results from the production of bicarbonate ions during bacterial degradation of organic matter by sulfate reduction. A rather steep alkalinity decrease in the topmost part of the hole (<20.00 mbsf) presumably represents an interval of relatively intensive sulfate reduction (Fig. F33). Below 120 mbsf, alkalinity decreases downhole to 1.7 mM at 466.25 mbsf, probably caused by carbonate recrystallization, which depletes the bicarbonate ion in the interstitial water. Small fluctuations of alkalinity in the bottom part of the hole may be attributed to contamination resulting from drilling disturbance.

The intensity of sulfate reduction is governed by several factors, most importantly the abundance of organic matter and the sedimentation rates. The sedimentation rate of the upper part of the hole is not high compared to Sites 1119 and 1122 which show intensive sulfate reduction. However, a relatively high organic carbon content compared to normal deep-sea carbonate sediments may have caused moderate sulfate reduction at this site (see "Organic Geochemistry," p. 40).

Ammonium (NH_4^+) concentrations increase with depth to a maximum of 779 µM at 151.80 mbsf, which is located ~50 m below the alkalinity maximum. Below this interval, ammonium values decrease gradually downhole to the bottom. An increase in the ammonium concentration reflects the intensive bacterial degradation of organic matter, whereas a decrease indicates the results of ion exchange reactions with clay minerals and/or the subsequent incorporation into diagenetically formed clay minerals.

The phosphate (HPO_4^{2-}) concentrations decrease from a subseafloor value of 15.2 µM at 1.5 mbsf to ~4 µM at 151.80 mbsf, at which depth the ammonium maximum occurs. Below this depth, phosphate concentrations generally remain smaller than 3 µM. A rapid decreasing trend in the upper part of the hole suggests a diagenetic uptake of dissolved phosphate into sedimentary mineral phases.

Dissolved Silica

Dissolved silica (H_4SiO_4) concentrations increase gradually from a value of 546 µM at 1.50 mbsf to a local maximum value of 1014 µM at 293.60 mbsf. This is a result of diffusion driven by the concentration difference between seawater and the sediments and/or upward porefluid migration resulting from burial compaction of sediments. The values of samples below 351.00 mbsf are more variable, ranging from 274 to 1062 µM. This interval corresponds to lithostratigraphic Units II and III, which consist of nannofossil chalk overlain by an unconformity located at 587 mbsf (Fig. F34; see "Lithostratigraphy," p. 4). Dissolved silica concentrations show three pronounced minima at 351.00, 466.25, and 532.85 mbsf. A local decrease of dissolved silica in the deeper part of the hole is usually attributed to chert formation (DSDP Site 315, Gieskes and Lawrence, 1981; and Site 1121, see "Inorganic Geochemistry," p. 19, in the "Site 1121" chapter). However, no chert layers are found at this site (see "Lithostratigraphy," p. 4). Therefore,

F34. Depth profiles of dissolved silica in interstitial water, p. 95.

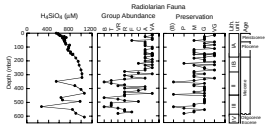

these local decreases of dissolved silica are not likely to be caused by silica diagenesis. The preservation of radiolarian fauna is generally good at this site (see "Biostratigraphy," p. 13); only three core-catcher samples are barren of radiolarians (Sample 181-1123B-38X-CC, 354.79 mbsf; 181-1123B-50X-CC, 468.6 mbsf; and 181-1123C-23X-CC, 536.71 mbsf). Each of these three samples corresponds to a sharp decrease in the dissolved silica concentration, suggesting possible changes in paleoproductivity of siliceous planktonic organisms including radiolarians and diatoms. Partly consolidated chalk layers of low permeability might contribute to the preservation of low dissolved silica concentrations, even accounting for the smoothing effect caused by fluid migration and diffusion. Low abundance of diatoms mirrored by low silica concentrations in interstitial waters has been reported from Paleogene sediments of the Ceara Rise in the Atlantic (Mikkelsen and Barron, 1997).

Calcium, Magnesium, and Strontium

The calcium (Ca^{2+}) concentration shows a near-seawater value in the shallowest sample (10.8 mM at 1.40 mbsf) and decreases with depth to a minimum of 7.55 mM at 78.50 mbsf, followed by a steady increase downhole to a maximum value of 31.6 mM at 609.75 mbsf. Magnesium (Mg^{2+}) also has a near-seawater value in the shallowest sample (53.29 mM at 1.40 mbsf). There is a steadily decreasing trend in the magnesium concentration throughout the hole, to a minimum value of 22.5 mM at 580.95 mbsf. At most DSDP and Ocean Drilling Program (ODP) sites, decreases of magnesium concentrations with depth have been reported, and magnesium transport from the surface downhole is interpreted to be controlled primarily by alteration reactions involving volcanic or igneous minerals (Gieskes, 1981).

The strontium (Sr^{2+}) concentration shows a steadily increasing trend with depth to ~400 mbsf. The content of strontium in inorganically precipitated calcite is about a factor of three lower than in biogenic calcite (Baker et al., 1982). Therefore, calcite diagenesis increases the strontium in the surrounding interstitial waters (calcite purification). The steady decrease in strontium concentration may be caused by carbonate recrystallization. Below 400 mbsf depth, strontium concentration remains in the relatively narrow range between 1481 and 1702 mM, suggesting the termination of active carbonate recrystallization. Another possible explanation for the constant dissolved strontium concentration in the interval is that celestite ($SrSO_4$) formation masks the increase of dissolved strontium concentration. Concentrations of strontium and sulfate in the lower part of this site (>400 mbsf) are ~1600 µM and 10 mM, respectively, and these values are close to those at DSDP Leg 90 sites on the Lord Howe Rise in the Tasman Sea where celestite nodules were recovered (Baker and Bloomer, 1988).

Potassium, Lithium, and Sodium

The potassium (K^+) concentration steadily decreases downhole to a minimum of 6.3 mM at 609.75 mbsf. Potassium normally decreases with increasing burial depth at deep-sea sites.

Up to ~150 mbsf, concentrations of lithium (Li^+) increase slowly with depth. Below 150 mbsf, the slope of the depth-concentration profile becomes slightly steeper. The lithium concentration generally tracks the profile of the calcium concentration. Although lithium concentrations are related to the opal transformation process, including biogenic

silica dissolution as described at some DSDP sites (Gieskes, 1981), the lithium profile of this site is apparently not influenced by the silica concentration.

Sodium (Na^+) concentrations are related to chloride concentrations, showing a local maximum of 479 mM at 51.50 mbsf and a minimum of 468 mM at 466.25 mbsf.

Summary of Interstitial Water Results

Interstitial water compositions are dominantly controlled by the high carbonate content of the sediments. Sulfate reduction is moderate in the upper part of the hole, probably related to relatively high organic carbon content compared to normal deep-sea carbonate sediments. Sulfate decreases gradually with depth to 13 mM at ~200 mbsf and remains almost constant below this depth. Alkalinity shows a maximum value of 8.5 mM at 107 mbsf. Carbonate diagenetic reactions are inferred from the profiles of dissolved calcium, magnesium, and strontium. The variation of dissolved silica in the lower part of the hole may imply a possible paleoproductivity change.

ORGANIC GEOCHEMISTRY

Volatile Hydrocarbons

As part of the shipboard safety and pollution-prevention monitoring program, hydrocarbon gases were analyzed in each core of Hole 1123A, in each core below 150 mbsf of Hole 1123B, and in each core below 490 mbsf of Hole 1123C by the headspace technique. Gas pockets were not encountered. The headspace methane concentrations are very low (<10 ppm). Despite the relatively high organic-carbon concentrations (see **"Carbonate and Organic Carbon,"** p. 40), this finding indicates low amounts of metabolizable organic matter and is corroborated by interstitial sulfate concentrations above 10 mM (see **"Inorganic Geochemistry,"** p. 37).

Carbonate and Organic Carbon

The abundance of total, inorganic, and organic carbon and of calcium carbonate in sediments from Holes 1123A, 1123B, and 1123C is summarized in Table **T18** (also in **ASCII format**). Random sampling of all lithologies was performed for carbonate analysis, and one sample per core was analyzed for organic carbon.

Carbonate contents vary between 10.3 and 84.3 wt% with an average of 57.5 wt% (Fig. **F35**). Variations are higher in the upper 180 mbsf (lithostratigraphic Subunit IA; see **"Lithostratigraphy,"** p. 4) and below 470 mbsf (Units III and IV) than in the section in between (Units IB and II). The upper boundary may reflect the Miocene/Pliocene boundary, whereas the lower one does not correspond to a chronostratigraphic transition. The sample with the value of 84.3 wt% (Sample 181-1123C-25X-2, 38–39 cm; 548.08 mbsf) is from the debris flow within the sequence.

Sediments at Site 1123 average 0.59 wt% organic carbon (Fig. **F36**), which is twice the average for deep-sea sediments of 0.3% compiled by McIver (1975) for DSDP Legs 1 through 33. The highest values were found in the uppermost samples and concentrations decrease slightly

T18. Organic chemistry data for sediments from Holes 1123A, 1123B, and 1123C, **p. 177.**

F35. Carbonate contents in sediments from Holes 1123A, 1123B, and 1123C, **p. 96.**

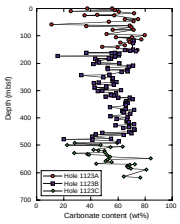

F36. Organic carbon contents in sediments from Holes 1123A, 1123B, and 1123C **p. 97.**

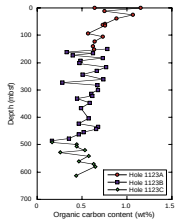

with increasing depth. The variations are high and without any apparent correlation with lithology. Despite the relatively high concentrations of organic carbon, there is no indication for present-day bacterial degradation of organic matter as indicated by low methane concentrations. Thus, the organic matter may be already reworked by bacteria, or large amounts are derived from terrigenous sources and are thus more refractory.

Organic Matter Source Characterization

The source of organic matter in Site 1123 samples was determined by either atomic organic carbon/nitrogen values or by Rock-Eval pyrolysis. Algal organic matter generally has C/N values of between 5 and 10, whereas organic matter derived from land plants has values of between 20 and 100 (e.g., Premuzic et al., 1982; Meyers, 1994).

Atomic organic carbon/nitrogen values were calculated for Site 1123 samples using total organic carbon and total nitrogen concentrations. The C/N ratios vary from 3.2 to 25.9 with an average of 10.9 (Table T18), without apparent correlation with depth, age, or lithology. These values suggest a predominantly marine source with varying amounts of terrestrial organic matter. Alternatively, the initial predominantly terrigenous organic material was affected by postdepositional diagenetic processes, and, thus, C/N values were altered. Degradation of organic matter in organic carbon–poor marine sediments tends to lower C/N values as nitrogenous compounds break down to produce ammonia, which is retained by clay minerals (Müller, 1977), and the produced CO_2 diffuses out of the sediment.

Rock-Eval analyses were conducted for 10 selected samples with organic carbon contents higher than 0.5% (Table T19). In general, volatile hydrocarbons (S_1), and hydrocarbons (S_2) generated by thermal cracking of kerogen can only be detected in very low concentrations, and, thus, the results must be interpreted carefully to eliminate a possible artifact caused by measurement error. Plotted in a van Krevelen–type diagram as hydrogen index (HI) vs. oxygen index (OI) values, the data suggest that the sediments contain Type III (terrigenous) organic matter (Fig. F37). This source assignment conflicts with the intermediate C/N values for these samples. The contradiction between the Rock-Eval source characterization and the elemental source characterization indicates that the organic matter has been heavily oxidized, probably by microbial reworking.

In summary, an unambiguous source assignment by determination of C/N values and Rock-Eval parameters is not possible because of strong organic matter degradation.

T19. Result of Rock-Eval pyrolysis of selected samples from Site 1123, p. 180.

F37. Rock-Eval van Krevelen–type diagram, p. 98.

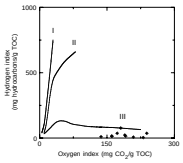

PHYSICAL PROPERTIES

Index Properties

Index properties measurements were made at a resolution of one sample for every two sections in the cores from all Site 1123 holes. Index properties were determined by a gravimetric method (see "Physical Properties," p. 24, in the "Explanatory Notes" chapter). Values of index properties (void ratio, porosity, water content, bulk density, and grain density) are presented in Table T20 (also in ASCII format). The properties measured from Holes 1123B and 1123C show gradual down-

T20. List of index properties measured from Holes 1123A, 1123B, and 1123C, p. 181.

hole changes to 540 mbsf (Fig. F38). Decreasing bulk density between 540 and 550 mbsf corresponds to a debris-flow deposit (see "Lithostratigraphy," p. 4). Over this same interval, the porosity increases from 40% to 60%. Below 550 mbsf, wet-bulk density increases from 1.4 to 2.2 g/cm³, and porosity decreases from 75% to 30% downhole. The index properties at Site 1123 reflect the effects of an increasing overburden.

Multisensor Track Measurements

The shipboard physical properties program at Site 1123 included nondestructive measurements of bulk density, magnetic susceptibility, and natural gamma-ray activity on whole sections of all cores using the MST (Figs. F39, F40). Magnetic susceptibility was measured at 4-cm intervals and at high sensitivity (4-s measurement time) in all Site 1123 holes. Low magnetic susceptibility values above 450 mbsf and below 590 mbsf in Hole 1123C are associated with a higher carbonate content (see "Organic Geochemistry," p. 40). Magnetic susceptibility increases below 451 mbsf, the boundary between lithostratigraphic Units II and III, and then decreases below the debris-flow deposits to the bottom of the hole. Natural gamma radiation was measured with a 15-s count every 14 cm in all Site 1123 holes. Natural gamma radiation values range from 0 to 30 counts/s. High values of natural gamma radiation indicate a relative high abundance of clay minerals. The low natural gamma radiation observed at Site 1123 indicates less clay-rich sediment than at previous Leg 181 sites. High natural gamma radiation values below 451 mbsf in Hole 1123C correlate with high magnetic susceptibility. Natural gamma radiation data from APC cores in Hole 1123A show cyclic variations above 70 mbsf, which reflect changes in mineral composition between carbonate-rich and clay-rich sediment layers. Below 70 mbsf, sediments are dominated by carbonate. The high natural gamma radiation peaks in the upper part of the section (<70 mbsf) are similar in value to those in lithostratigraphic Unit III. The high natural gamma radiation values in the upper part of the section may reflect the presence of tephra layers.

The GRAPE bulk density measurements were made at 4-cm intervals at all Site 1123 holes. A comparison of GRAPE density with the wet-bulk density determined from discrete samples shows general agreement, although GRAPE density values are generally higher than bulk density values obtained by index properties measurements in the upper portion of the cores (APC cores) (Fig. F41). The GRAPE density values increase generally with increasing burial depth. The decrease in GRAPE density at 160 mbsf coincides with the switch from APC to XCB coring. The XCB cores tend to be biscuit-like solid chunks of core material separated by layers of ground sediment. Voids between the biscuit-like core material and the core liner may cause the GRAPE density values to be lower than the actual values.

The *P*-wave velocity measurements (PWL) were made at 4-cm intervals at all Site 1123 holes. PWL measurements were only collected from APC cores. High values of *P*-wave velocity from Hole 1123A are associated with tephra layers. The highest *P*-wave velocity values are seen around 50 and 60 mbsf, where tephra layers are abundant. The peak around 50 mbsf probably occurs in carbonate-rich tephra-bearing sediments and is different from the peak around 60 mbsf, which occurs in clay-rich tephra-bearing sediments. Consistently high *P*-wave velocity values indicate sediment with high carbonate content and tephra lay-

F38. Index properties measurements from cores from Holes 1123B and 1123C, p. 99.

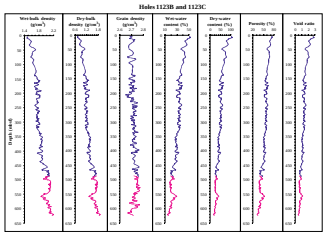

F39. MST measurements from Hole 1123A, p. 100.

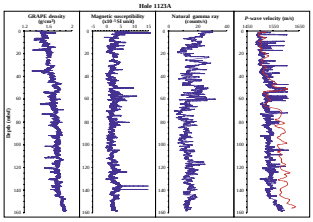

F40. MST measurements from Holes 1123B and 1123C, p. 101.

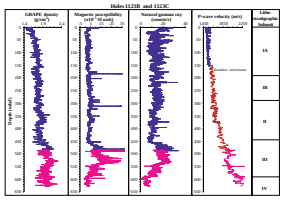

F41. Density measurements in Holes 1123B and 1123C, p. 102.

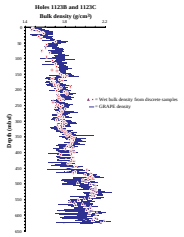

ers, while clay-rich tephra-bearing layers show scattered peaks of increased *P*-wave velocity. In general, calcareous sediments have higher *P*-wave velocities than clay-rich sediment.

Shear Strength

Measurements of shear strength, using a mechanical vane, were made on split cores from all Site 1123 holes (Fig. F42). Samples were generally taken in the fine-grained sediments at a resolution of one per section. No measurements were made on XCB cores. Shear strength values range from 5 to 130 kPa. There is a general increase in shear strength downhole. The highest shear strength values occurred above 130 mbsf in Hole 1123A and above 140 mbsf in Hole 1123B.

F42. Distribution of shear strength in cores from Holes 1123B and 1123C, p. 103.

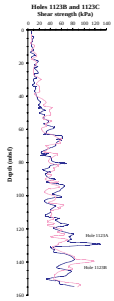

Compressional-Wave Velocity

Compressional-wave velocity (*P*-wave velocity) was measured parallel to the core axis on split cores from Hole 1123A using the DSV (Digital Sound Velocimeter). Sediments were more tightly compacted below 65 mbsf in Hole 1123A, and, therefore, the Hamilton frame velocimeter was used to measure sound propagation perpendicular to the long axis of the core below this depth. *P*-wave velocity measured from the DSV in Hole 1123A correlates well with the data from the *P*-wave logger on the MST. However, *P*-wave velocity values are higher from the Hamilton velocimeter measurement than from the DSV measurement. This may result from the fact that the pressure was applied to the discrete sample when lowering the transducers of the Hamilton Velocimeter onto the half core in the liner and may have caused the sediment samples to become more dense during the actual *P*-wave velocity measurement. The *P*-wave velocity was also taken by the Hamilton velocimeter from XCB cores recovered from Holes 1123B and 1123C. A sharp peak in *P*-wave velocity from 1800 to 2250 m/s occurring around 550 mbsf is associated with a lithified block of limestone contained in the debris-flow unit. The *P*-wave velocity values of this peak are similar to those measured from limestone in lithostratigraphic Unit IV. This limestone block also produces distinctive responses in the magnetic susceptibility and natural gamma radiation records.

DOWNHOLE MEASUREMENTS

Logging Operations

Downhole logging was performed in Hole 1123B. The drill string was placed at 100 mbsf as the logging tools were lowered to the bottom of the hole. Before logging, the drill string was raised to 86 mbsf. The drill string had to be maintained at 86 mbsf to keep the upper hole wall from collapsing.

Three tool string configurations were run in Hole 1123B, in the following order: the triple combination, the FMS-sonic, and the GHMT (see "Downhole Measurements," p. 29, in the "Explanatory Notes" chapter). A repeat interval was measured with the triple combination, and two full passes were made with the FMS-sonic. Logging operations are summarized in Figure F43. Logging operations began at 1100 hr on 18 September 1998 and finished at 0700 hr on 19 September 1998. There was between 3 and 4 m of heave, and the wireline heave compen-

F43. Logging operations in Hole 1123B, p. 104.

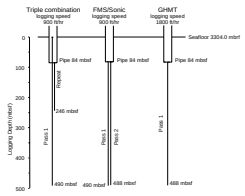

sator was used during all measurements. With the exception of the uppermost 65 m, the hole conditions were good, with a relatively uniform borehole diameter (~13.5 in) throughout (Fig. F44A). The NMRS sonde on the GHMT again failed to work.

Data Quality and Log/Core Correlation

The quality of the data is excellent, with very few erroneous readings caused by hole washouts. The only section of the hole to yield relatively poor-quality data was the uppermost 65 m (86–150 mbsf), where the borehole was regularly greater than 15 in and occasional more than 18 in diameter. Because the FMS pads only extend to 15 in, readings cannot be made where the borehole exceeds this value. Where the borehole is greater than 18 in, the data from the HLDS and the APS are unreliable. The upper section of the sonic log contained around 5 cycle skips, which have been edited out (Fig. F44B).

A comparison of log-based lithodensity with index bulk density determined from discrete samples shows general agreement, although log-based lithodensity values are higher below 150 mbsf (Fig. F45). At 150 mbsf, XCB coring began, indicating that the change in coring techniques could be partially responsible for the discrepancy between log and core-based results.

The downhole bulk density log was converted into a density-porosity log, using a matrix density of 2.71 g/cm^3 and a fluid density of 1.03 g/cm^3 for seawater (Fig. F46). In the above calculation, the matrix density value was determined by plotting a histogram of all the index-based matrix densities. This plot exhibited a single dominant peak at 2.71 g/cm^3.

Overall, neutron porosity correlates well with the other porosity proxies (density and sonic velocity) (Fig. F44A). There are, however, a few regions of disagreement (see "Preliminary Interpretation," p. 46). Most notably, between 245 and 267 mbsf, neutron porosity shows a dramatic increase, but bulk density only shows a narrow zone of decrease, and there is no appreciable change in sonic velocity (Figs. F46, F44B). The FMS shows this section of the hole to be a conductive region, but the FMS shows increased conduction starting at 233.5 mbsf. The caliper is steady throughout and the resistivity data fail to show any change in this region (Fig. F44A).

The top of the log also shows deviation between the neutron porosity log and the lithodensity/sonic logs (Fig. F44A, F44B). Some of the lack of agreement could be caused by fluctuating caliper values and, in some places, by a caliper too wide for the neutron porosity and lithodensity tools to record usable values, but much of the record appears to be reliable.

Between 150 and 460 mbsf, XCB coring produced ~50%–60% recovery in some cores, which were frequently "biscuity." Downhole magnetic susceptibility was correlated with core-based magnetic susceptibility in an effort to place the drilling biscuits at their proper depths within the cored interval. The results are consistent with the biscuits representing an even sampling of the entire 9.5-m cored interval, compressed into the lower part of the core liner (Fig. F47) (see also "Paleomagnetism," p. 26).

Sonic data show steadily increasing velocity downhole. Velocity at the top of the hole is 1.6 km/s and around 2.2 km/s in the lithified zone at the base of the hole (see "Lithostratigraphy," p. 4). The sonic velocity data were converted into a downhole integrated traveltime, for the

F44. Log data and logging units from Hole 1123B, p. 105.

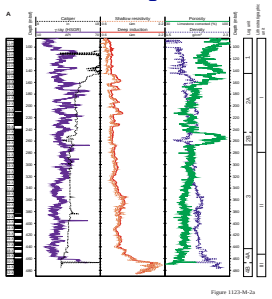

F45. Log bulk density and core-based index bulk density, p. 107.

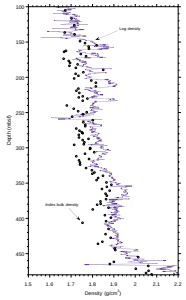

F46. Density and neutron porosities, p. 108.

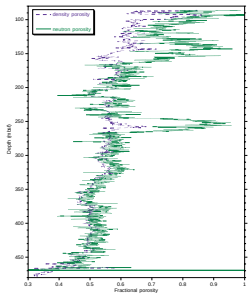

F47. Log and core magnetic susceptibility comparison, p. 109.

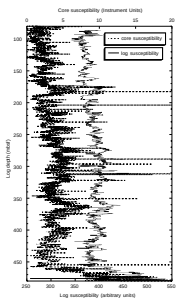

purpose of assessing the depth of reflectors evident on the site survey seismic profile.

The temperature tool was run at the base of the triple combination. Because of a failure of the MAXIS depth recording software, conversion of the data from temperature vs. time to temperature vs. depth could not be made.

Logging Units

Excellent data quality from Hole 1123B has enabled the results to be subdivided confidently into distinct logging units (Fig. **F44A, F44B**). The majority of data acquired have a rhythmically varying response to the sediments in the borehole wall, though the overall range of fluctuations in the data is slight. For example, resistivity values only vary between ~0.6 and 2.1 Ωm, and magnetic susceptibility shows less than a twofold increase downhole (Fig. **F44A, F44B**). Magnetic susceptibility values appear to show very little long-term variation, except for a sharp increase at the base of the log (Fig. **F44B**).

The base of log Subunit 2B correlates with the bottom of lithostratigraphic Unit I, and the base of log Unit 3 correlates with the bottom of lithostratigraphic Unit II (Fig. **F44A, F44B**). The log units identified in Hole 1123B are outlined below (Fig. **F44A, F44B**).

Log Unit 1: Base of Pipe to 145 mbsf

This unit is characterized by relatively constant, low resistivity values (mean = 0.757 ± 0.035 Ωm), high neutron porosities (0.79 ± 0.078), and slow sonic travel times (179.5 ± 8.75 µs/ft).

Log Subunit 2A: 145–245 mbsf

At 145 mbsf the logs show a distinct change in character: resistivity, density, and photoelectric effect all increase sharply at this point, and porosities and sonic traveltimes decrease. Throughout Subunit 2A, resistivity shows abrupt and periodic increases that can be correlated with increases in bulk density and photoelectric effect and with decreases in porosity.

Log Subunit 2B: 245–267 mbsf

In this subunit, the resistivity values remain at a relatively constant level, in line with the minimum values recorded in Subunit 2A. Sonic velocities fluctuate, and the photoelectric effect decreases toward the base of this subunit. Neutron porosity values show a sharp increase within this subunit, in conjunction with a slight decrease in density.

Log Unit 3: 267–443 mbsf

The top of Unit 3 is characterized by a slight rise in resistivities and photoelectric effect and a decrease in sonic traveltimes. With the exception of natural gamma and magnetic susceptibility, all of the log data within this unit show small-scale fluctuations. An overall compaction trend with depth is reflected in a gradual increase in density and a decrease in porosity and sonic velocity.

Log Subunit 4A: 443–466 mbsf

Resistivity values within this subunit increase steadily with depth. This trend is accompanied by a more acute increase in density and decrease in porosity. The top of this unit is also marked by a noticeable decrease in sonic traveltime.

Log Subunit 4B: 466–488 mbsf

Magnetic susceptibility and resistivities show a sharp rise and reach their maximum values at the top of this subunit. Toward the base of this subunit, the resistivity and magnetic susceptibility values begin to decrease.

Preliminary Interpretation

The spectral gamma-ray results show that downhole variations in thorium and potassium correlate (Fig. F48). Uranium values, however, appear to fluctuate independently of both thorium and potassium. Changes in the thorium and potassium values may be indicative of variations in the terrestrial clay content, whereas fluctuations in the uranium may be controlled by variations in organic material and/or redox potentials at the time of deposition.

The increase in neutron porosity vs. density porosity at 245–267 mbsf (Fig. F46) could be a result of bound water in clays or micas. The neutron porosity log is based on hydrogen in the formation. In clean formations, all the hydrogen is assumed to be in water and so the neutron log is a good indicator of porosity. Clays and micas, however, contain bound water in their molecular structure and the neutron log is unable to distinguish between different carriers of hydrogen. For this reason the discrepancies seen here could reflect an increase in clay or mica content. However, an increase in clay content would also be reflected in an increase in the natural gamma-ray; this is not observed at 245–267 mbsf (Fig. F44A). The reason for the sharp increase in neutron porosity within log Subunit 2B requires further postcruise investigation.

Particularly interesting results were obtained from Subunit 2A. Regular, correlative fluctuations in resistivity, density, and photoelectric effect can be seen throughout this unit (Fig. F44A, F44B). These responses in the log data, which are most clearly seen in the resistivity results, may reflect cycles of sedimentation. Looking upsection, resistivity values increase sharply, then gradually decrease back to their original value (Fig. F49).

F48. Potassium, thorium, and uranium results, p. 110.

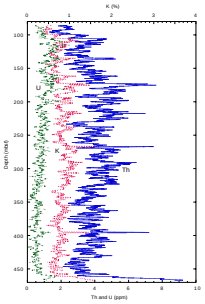

F49. Detailed view of logging subunit 2A, p. 111.

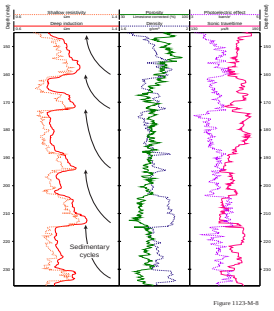

REFERENCES

Alexandrovich, J.M., 1989. Radiolarian biostratigraphy of ODP Leg 111, Site 677, eastern equatorial Pacific, late Miocene through Pleistocene. *In* Becker, K., Sakai, H., et al., *Proc. ODP, Sci. Results,* 111: College Station, TX (Ocean Drilling Program), 245–262.

Backman, J., and Raffi, I., 1997. Calibration of Miocene nannofossil events to orbitally tuned cyclostratigraphies from Ceara Rise. *In* Shackleton, N.J., Curry, W.B., Richter, C., and Bralower, T.J. (Eds.), *Proc. ODP, Sci. Results,* 154: College Station, TX (Ocean Drilling Program), 83–99.

Baker, P.A., and Bloomer, S.H., 1988. The origin of celestite in deep-sea carbonate sediments. *Geochim. Cosmochim. Acta,* 52:335–339.

Baker, P.A., Gieskes, J.M., and Elderfield, H., 1982. Diagenesis of carbonates in deep-sea sediments: evidence from Sr^{2+}/Ca^{2+} ratios and interstitial dissolved Sr^{2+} data. *J. Sediment. Petrol.,* 52:71–82.

Ballance, P.F., 1976. Evolution of the Upper Cenozoic magmatic arc and plate boundary in northern New Zealand. *Earth Planet. Sci. Lett.,* 28:356–370.

Berggren, W.A., Hilgen, F.J., Langereis, C.G., Kent, D.V., Obradovich, J.D., Raffi, I., Raymo, M.E., and Shackleton, N.J., 1995a. Late Neogene chronology: new perspectives in high-resolution stratigraphy. *Geol. Soc. Am. Bull.,* 107:1272–1287.

Berggren, W.A., Kent, D.V., Swisher, C.C., III, and Aubry, M.-P., 1995b. A revised Cenozoic geochronology and chronostratigraphy. *In* Berggren, W.A., Kent, D.V., Aubry, M.-P., and Hardenbol, J. (Eds.), *Geochronology, Time Scales and Global Stratigraphic Correlation*. Spec. Publ.—Soc. Econ. Paleontol. Mineral. (Soc. Sediment. Geol.), 54:129–212.

Campbell, H.J., Andrews, P.B., Beu, A.G., Maxwell, P.A., Edwards, R.A., Laird, M.G., Hornibrook, N. de B., Mildenhall, D.C., Watters, W.A., Buckeridge, J.S., Lee, D.E., Strong, C.P., Wilson, G.J., and Hayward, B.W., 1993. Cretaceous-Cenozoic geology and biostratigraphy of the Chatham Islands, New Zealand. *Inst. Geol. Nucl. Sci. Monogr.,* 2:269.

Cande, S.C., and Kent, D.V., 1995. Revised calibration of the geomagnetic polarity timescale for the Late Cretaceous and Cenozoic. *J. Geophys. Res.,* 100:6093–6095.

Carter, L., and McCave, I.N., 1994. Development of sediment drifts approaching an active plate margin under the SW Pacific deep western boundary current. *Paleoceanography,* 9:1061–1085.

Carter, L., and Mitchell, J.S., 1987. Late Quaternary sediment pathways through the deep ocean, east of New Zealand. *Paleoceanography,* 2:409–422.

Carter, L., Nelson, C.S., Neil, H.L., and Froggatt, P.C., 1995. Correlation, dispersal, and preservation of the Kawakawa Tephra and other late Quaternary tephra layers in the Southwest Pacific Ocean. *N. Z. J. Geol. Geophys.,* 38:29–46.

Carter, R.M., 1985. The mid-Oligocene Marshall Paraconformity, New Zealand: coincidence with global eustatic sea-level fall or rise? *J. Geol.,* 93:359–371.

Carter, R.M., Carter, L., and Davy, B., 1994. Seismic stratigraphy of the Bounty Trough, Southwest Pacific Ocean. *Mar. Pet. Geol.,* 11:79–93.

Carter, R.M., and Landis, C.A., 1972. Correlative Oligocene unconformities in southern Australasia. *Nature,* 237:12–13.

Caulet, J.-P., 1991. Radiolarians from the Kerguelen Plateau, Leg 119. *In* Barron, J., Larsen, B., et al., *Proc. ODP, Sci. Results,* 119: College Station, TX (Ocean Drilling Program), 513–546.

Fenner, J., Carter, L., and Stewart, R., 1992. Late Quaternary paleoclimatic and paleoceanographic change over northern Chatham Rise, New Zealand. *Mar. Geol.,* 108:383–404.

Foreman, H.P., 1975. Radiolaria from the North Pacific, Deep Sea Drilling Project, Leg 32. *In* Larson, R.L., Moberly, R., et al., *Init. Repts. DSDP,* 32: Washington (U.S. Govt. Printing Office), 579–676.

Froggatt, P.C., and Lowe, D.J., 1990. A review of late Quaternary silicic and some other tephra formations from New Zealand: their stratigraphy, nomenclature, distribution, volume and age *N.Z. J. Geol. Geophys.,* 33:89–109.

Fulthorpe, C.S., Carter, R.M., Miller, K.G., and Wilson, J., 1996. Marshall Paraconformity: a mid-Oligocene record of inception of the Antarctic Circumpolar Current and coeval glacio-eustatic lowstand? *Mar. Pet. Geol.,* 13:61–77.

Gardner, J.V., Nelson, C.S., and Baker, P.A., 1986. Distribution and character of pale green laminae in sediment from Lord Howe Rise: a probable late Neogene and Quaternary tephrostratigraphic record. *In* Kennett, J.P., von der Borch, C.C., et al., *Init. Repts. DSDP,* 90 (Pt. 2): Washington (U.S. Govt. Printing Office), 1145–1159.

Gartner, S., 1990. Neogene calcareous nannofossil biostratigraphy, Leg 116 (Central Indian Ocean). *In* Cochran, J.R., Stow, D.A.V., et al., *Proc. ODP, Sci. Results,* 116: College Station, TX (Ocean Drilling Program), 165–187.

Gieskes, J.M., 1981. Deep-sea drilling interstitial water studies: implications for chemical alteration of the oceanic crust, layers I and II. *In* Warme, J.E., Douglas, R.G., and Winterer, E.L. (Eds.), *The Deep Sea Drilling Project: A Decade of Progress.* Spec. Publ.—Soc. Econ. Paleontol. Mineral., 32:149–167.

Gieskes, J.M., and Lawrence, J.R., 1981. Alteration of volcanic matter in deep-sea sediments: evidence from the chemical composition of interstitial waters from deep sea drilling cores. *Geochim. Cosmochim. Acta,* 45:1687–1703.

Gradstein, F.M., Fearon, J.M., and Huang, Z., 1989. BURSUB and DEPOR version 3.50—two FORTRAN 77 programs for porosity and subsidence analysis. *Open-File Rep.—Geol. Surv. Can.,* 1283:1–10.

Griggs, G.B., Carter, L., and Kennett, J.P., and Carter, R.M., 1983. Late Quaternary marine stratigraphy southeast of New Zealand. *Bull. Geol. Soc. Am.,* 94:791–797.

Hilgen, F.J., 1991a. Astronomical calibration of Gauss to Matuyama sapropels in the Mediterranean and implication for the geomagnetic polarity time scale. *Earth Planet. Sci. Lett.,* 104:226–244.

————, 1991b. Extension of the astronomically calibrated (polarity) time scale to the Miocene/Pliocene boundary. *Earth Planet. Sci. Lett.,* 107:349–368.

Hilgen, F.J., Krijgsman, W., Langereis, C.G., Lourens, L.J., Santarelli, A., and Zachariasse, W.J., 1995. Extending the astronomical (polarity) time scale into the Miocene. *Earth Planet. Sci. Lett.,* 136:495–510.

Hollis, C.J., Waghorn, D.B., Strong, C.P., and Crouch, E.M., 1997. Integrated Paleogene biostratigraphy of DSDP Site 277 (Leg 29): foraminifera, calcareous nannofossils, radiolaria, and palynomorphs. *Inst. Geol. Nucl. Sci., Sci. Rep.,* 97/07.

Johnson, D.A., Schneider, D.A., Nigrini, C.A., Caulet, J.-P., and Kent, D.V., 1989. Pliocene-Pleistocene radiolarian events and magnetostratigraphic calibrations for the tropical Indian Ocean. *Mar. Micropaleontol.,* 14:33–66.

Kaminski, M.A., Gradstein, F.M., and Berggren, W.A., 1989. Paleogene benthic foraminifer biostratigraphy and paleoecology at Site 647, Southern Labrador Sea. *In* Srivastava, S.P., Arthur, M.A., Clement, B., et al., *Proc. ODP, Sci. Results,* 105: College Station, TX (Ocean Drilling Program), 705–730.

Kennett, J.P., 1977. Cenozoic evolution of Antarctic glaciation, the circum-Antarctic Ocean, and their impact on global paleoceanography. *J. Geophys. Res.,* 82:3843–3860.

Kidd, R.B., and Hill, P.R., 1986. Sedimentation on mid-ocean sediment drifts. *In* Summerhayes, C.P., and Shackleton, N.J. (Eds.), *North Atlantic Paleoceanography.* Geol. Soc. Spec. Publ., 21:87–102.

Laskar, J., Joutel, F., and Boudin, F., 1993. Orbital, precessional, and insolation quantities for the Earth from –20 Myr to +10 Myr. *Astron. Astrophys.,* 270:522–533.

Lazarus, D., 1992. Antarctic Neogene radiolarians from the Kerguelen Plateau, Legs 119 and 120. *In* Wise, S.W., Jr., Schlich, R., et al., *Proc. ODP, Sci. Results,* 120: College Station, TX (Ocean Drilling Program), 785–809.

Lean, C.M.B., and McCave, I.N., 1998. Glacial to interglacial mineral magnetic and palaeoceanographic changes at Chatham Rise, SW Pacific Ocean. *Earth Planet. Sci. Lett.,* 163:247–260.

McCave, I.N., and Carter, L., 1997. Recent sedimentation beneath the deep western boundary current off northern New Zealand. *Deep-Sea Res.,* 44:1203–1237.

McIver, R.D., 1975. Hydrocarbon occurrences from JOIDES Deep Sea Drilling Project. *Proc. Ninth Petrol. Congr.,* 269–280.

Meyers, P.A., 1994. Preservation of elemental and isotopic source identification of sedimentary organic matter. *Chem. Geol.,* 144:289–302.

Mikkelsen, N., and Barron, J.A., 1997. Early Oligocene diatoms on the Ceara Rise and the Cenozoic evolution of biogenic silica accumulation in the low-latitude Atlantic. *In* Shackleton, N.J., Curry, W.B., Richter, C., and Bralower, T.J. (Eds.), *Proc. ODP, Sci. Results,* 154: College Station, TX (Ocean Drilling Program), 483–490.

Mix, A.C., Harris, S.E., and Janecek, T.R., 1995a. Estimating lithology from nonintrusive reflectance spectra: Leg 138. *In* Pisias, N.G., Mayer, L.A., Janecek, T.R., Palmer-Julson, A., and van Andel, T.H. (Eds.), *Proc. ODP, Sci. Results,* 138: College Station, TX (Ocean Drilling Program), 413–427.

Mix, A.C., Pisias, N.G., Rugh, W., Wilson, J., Morey, A., and Hagelberg, T.K., 1995b. Benthic foraminifer stable isotope record from Site 849 (0–5 Ma): local and global climate changes. *In* Pisias, N.G., Mayer, L.A., Janecek, T.R., Palmer-Julson, A., and van Andel, T.H. (Eds.), *Proc. ODP, Sci. Results,* 138: College Station, TX (Ocean Drilling Program), 371–412.

Morgans, H.E.G., Scott, G.H., Beu, A.G., Graham, I.J., Mumme, T.C., George, W. St., and Strong, C.P., 1996. New Zealand Cenozoic Time Scale (version 11/96). *Rep.—Inst. Geol. Nucl. Sci.,* 96/38:1–12.

Morley, J.J., 1985. Radiolarians from the Northwest Pacific, Deep Sea Drilling Project Leg 86. *In* Heath, G.R., Burckle, L.H., et al., *Init. Repts. DSDP,* 86: Washington (U.S. Govt. Printing Office), 399–422.

Morley, J.J., and Nigrini, C., 1995. Miocene to Pleistocene radiolarian biostratigraphy of North Pacific Sites 881, 884, 885, 886, and 887. *In* Rea, D.K., Basov, I.A., Scholl, D.W., and Allan, J.F. (Eds.), *Proc. ODP, Sci. Results,* 145: College Station, TX (Ocean Drilling Program), 55–91.

Motoyama, I., and Maruyama, T., 1998. Neogene diatom and radiolarian biochronology for the middle-to-high latitudes of the Northwest Pacific region: calibration to the Kent's geomagnetic polarity time scales (CK 92 and CK 95). *J. Geol. Soc. Jpn.,* 104:171–183.

Müller, P.J., 1977. C/N ratios in Pacific deep sea sediments: effect of inorganic ammonium and organic nitrogen compounds sorbed by clays. *Geochim. Cosmochim. Acta,* 41:765–776.

Naish, T.R., Abott, S.T., Alloway, B.V., Beu, A.G., Carter, R.M., Edwards, A.R., Journeaux, T.D., Kamp, P.J.J., Pillans, B.J., Saul, G., and Woolfe, K.J., 1998. Astronomical calibration of a southern hemisphere Plio-Pleistocene reference section, Wanganui Basin, New Zealand. *Quat. Sci. Rev.,* 17:695–710.

Nelson, C.S., Cooke, P.J., Hendy, C.H., and Cuthbertson, A.M., 1993. Oceanographic and climatic changes over the past 160,000 years at Deep Sea Drilling Project Site 594 off southeastern New Zealand, Southwest Pacific Ocean. *Paleoceanography,* 8:435–458.

Nelson, C.S., Froggatt, P.C., and Gosson, G.J., 1986a. Nature, chemistry, and origin of late Cenozoic megascopic tephras in Leg 90 cores from the southwestern Pacific. *In* Kennett, J.P., von der Borch, C.C., et al., *Init. Repts. DSDP,* 90: Washington (U.S. Govt. Printing Office), 1161–1171.

Nelson, C.S., Hendy, C.H., Cuthbertson, A.M., and Jarrett, G.R., 1986b. Late Quaternary carbonate and isotope stratigraphy, subantarctic Site 594, Southwest Pacific. *In* Kennett, J.P., von der Borch, C.C., et al., *Init. Repts. DSDP,* 90: Washington (U.S.Govt. Printing Office), 1425–1436.

O'Connor, B., 1994. Seven new radiolarian species from the Oligocene of New Zealand. *Micropaleontology,* 40:337–350.

————, 1997a. Lower Miocene Radiolaria from Te Kopua Point, Kaipara Harbour, New Zealand. *Micropaleontology,* 43:101–128.

————, 1997b. New Radiolaria from the Oligocene and early Miocene of Northland, New Zealand. *Micropaleontology,* 43:63–100.

Pemberton, S.G., and MacEachern, J.A., 1995. The sequence stratigraphic significance of trace fossils: examples from the Cretaceous Foreland Basin of Alberta, Canada. *In* Van Wagoner, J.C., and Bertram, G.T. (Eds.), *Sequence Stratigraphy of Foreland Basin Deposits*. AAPG Mem., 64:429–475.

Pillans, B.J., Kohn, B.P., Berger, G., Froggatt, P., Duller, G., Alloway, B.V., and Hesse, P., 1996. Multi-method dating comparison for mid-Pleistocene Rangitawa Tephra, New Zealand. *Quat. Sci. Rev.,* 15:641–653.

Premuzic, E.T., Benkovitz, C.M., Gaffney, J.S., and Walsh, J.J., 1982. The nature and distribution of organic matter in the surface sediments of world oceans and seas. *Org. Geochem.,* 4:63–77.

Prior, D.B., Bornhold, B.D., and Johns, M.W., 1984. Depositional characteristics of a submarine debris flow. *J. Geol.,* 92:707–727.

Raffi, I., Backman, J., Rio, D., and Shackleton, N.J., 1993. Plio-Pleistocene nannofossil biostratigraphy and calibration to oxygen isotopes stratigraphies from Deep Sea Drilling Project Site 607 and Ocean Drilling Program Site 677. *Paleoceanography,* 8:387–408.

Raffi, I., and Flores, J.-A., 1995. Pleistocene through Miocene calcareous nannofossils from eastern equatorial Pacific Ocean. *In* Pisias, N.G., Mayer, L.A., Janecek, T.R., Palmer-Julson, A., and van Andel, T.H. (Eds.), *Proc. ODP, Sci. Results,* 138: College Station, TX (Ocean Drilling Program), 233–286.

Rait, G., Chanier, F., and Waters, D.W., 1991. Landward and seaward-directed thrusting accompanying the onset of subduction beneath New Zealand. *Geology,* 119:230–233.

Sakai, T., 1980. Radiolarians from Sites 434, 435, and 436, Northwest Pacific, Leg 56, Deep Sea Drilling Project. *In* von Huene, R., Nasu, N., et al., *Init. Repts. DSDP,* 56, 57 (Pt. 2): Washington (U.S. Govt. Printing Office), 695–733.

Sakai, T., and Aita, Y., 1994. Neogene siliceous microfossil-bearing sequences of the northern Kanto District. *Guide book for field trip for the post-conference excursion of INTERRAD VII, Osaka 1994. INTERRAD VII field excursion III (Cenozoic),* 63–88.

Sanfilippo, A., and Nigrini, C., 1998. Code numbers for Cenozoic low latitude radiolarian biostratigraphic zones and GPTS conversion tables. *Mar. Micropaleontol.,* 33:109–156.

Scott, G.H., 1979. The late Miocene to early Pliocene history of the *Globorotalia miozea* plexus from Blind River, New Zealand. *Mar. Micropaleontol.,* 4:341–361.

Shackleton, N.J., Baldauf, J.G., Flores, J.-A., Iwai, M., Moore, T.C., Jr., Raffi, I., and Vincent, E., 1995. Biostratigraphic summary for Leg 138. *In* Pisias, N.G., Mayer, L.A., Janecek, T.R., Palmer-Julson, A., and van Andel, T.H. (Eds.), *Proc. ODP, Sci. Results,* 138: College Station, TX (Ocean Drilling Program), 517–536.

Shackleton, N.J., and Crowhurst, S., 1997. Sediment fluxes based on an orbitally tuned time scale 5 Ma to 14 Ma, Site 926. *In* Shackleton, N.J., Curry, W.B., Richter, C., and Bralower, T.J. (Eds.), *Proc. ODP, Sci. Results,* 154: College Station, TX (Ocean Drilling Program), 69–82.

Shane, P.A.R., Black, T.M., Alloway, B.V., and Westgate, J.A., 1996. Early to middle Pleistocene tephrochronology of North Island, New Zealand: implications for volcanism, tectonism, and paleoenvironments. *Geol. Soc. Am. Bull.,* 108:915–925.

Stam, B., Gradstein, F.M., Lloyd, P., and Gillis, D., 1987. Algorithms for porosity and subsidence history. *Computers and Geosci.,* 13:317–349.

Suggate, R.P., 1978. *The Geology of New Zealand* (Vol. 1): Wellington (Govt. Printer).

Takemura, A., and Ling, H.Y., 1997. Eocene and Oligocene radiolarian biostratigraphy from the Southern Ocean: correlation of ODP Legs 114 (Atlantic Ocean) and 120 (Indian Ocean). *Mar. Micropaleontol.*, 30:97–116.

Walcott, R.I., 1998. Modes of oblique compression: late Cenozoic tectonics of the South Island of New Zealand. *Rev. Geophys.,* 36:1–26.

Warren, B.A., 1973. TransPacific hydrographic sections at latitudes 43S and 28S; the SCORPIO Expedition—deep water. *Deep-Sea Res.,* 20:9–38.

Weaver, P.P.E., Carter, L., and Neil, H., 1998. Response of surface watermasses and circulation to late Quaternary climate change, east of New Zealand. *Paleoceanography,* 13:70–83.

Weaver, P.P.E., Neil, H., and Carter, L., 1997. Sea surface temperature estimates from the Southwest Pacific based on planktonic foraminifera and oxygen isotopes. *Palaeogeogr., Palaeoclimatol., Palaeoecol.,* 131:241–256.

Wei, W., 1992. Updated nannofossil stratigraphy of the Ciros-1 core from McMurdo Sound (Ross Sea). *In* Wise, S.W., Jr., Schlich, R., et al., *Proc. ODP, Sci. Results,* 120: College Station, TX (Ocean Drilling Program), 1105–1117.

————, 1993. Calibration of Upper Pliocene-Lower Pleistocene nannofossil events with oxygen isotope stratigraphy. *Paleoceanography,* 8:85–99.

Wilson, G.S., Roberts, A.P., Verosub, K.L., Florindo, F., and Sagnotti, L., 1998. Magnetobiostratigraphic chronology of the Eocene-Oligocene transition in the CIROS-1 core, Victoria Land margin, Antarctica: implications for Antarctic glacial history. *Geol. Soc. Am. Bull.,* 110:35–47.

Wood, R.A., Andrews, P.B., Herzer, R.H., et al., 1989. Cretaceous and Cenozoic geology of the Chatham Rise region, South Island, New Zealand. *N. Z. Geol. Basin Stud.,* 3.

Wood, R.A., and Herzer, R.H., 1993. The Chatham Rise, New Zealand. *In* Ballance, P.F. (Ed.), *South Pacific Sedimentary Basins:* Amsterdam (Elsevier), Sedimentary Basins of the World Series, 2:329–349.

Young, J.R., Flores, J.A., Wei, W., 1994. A summary chart of Neogene nannofossil magnetostratigraphy. *J. Nannoplankton Res.,* 16:21–27.

Figure F1. Locality map of Site 1123, showing location of seismic line of Figure F2, p. 53.

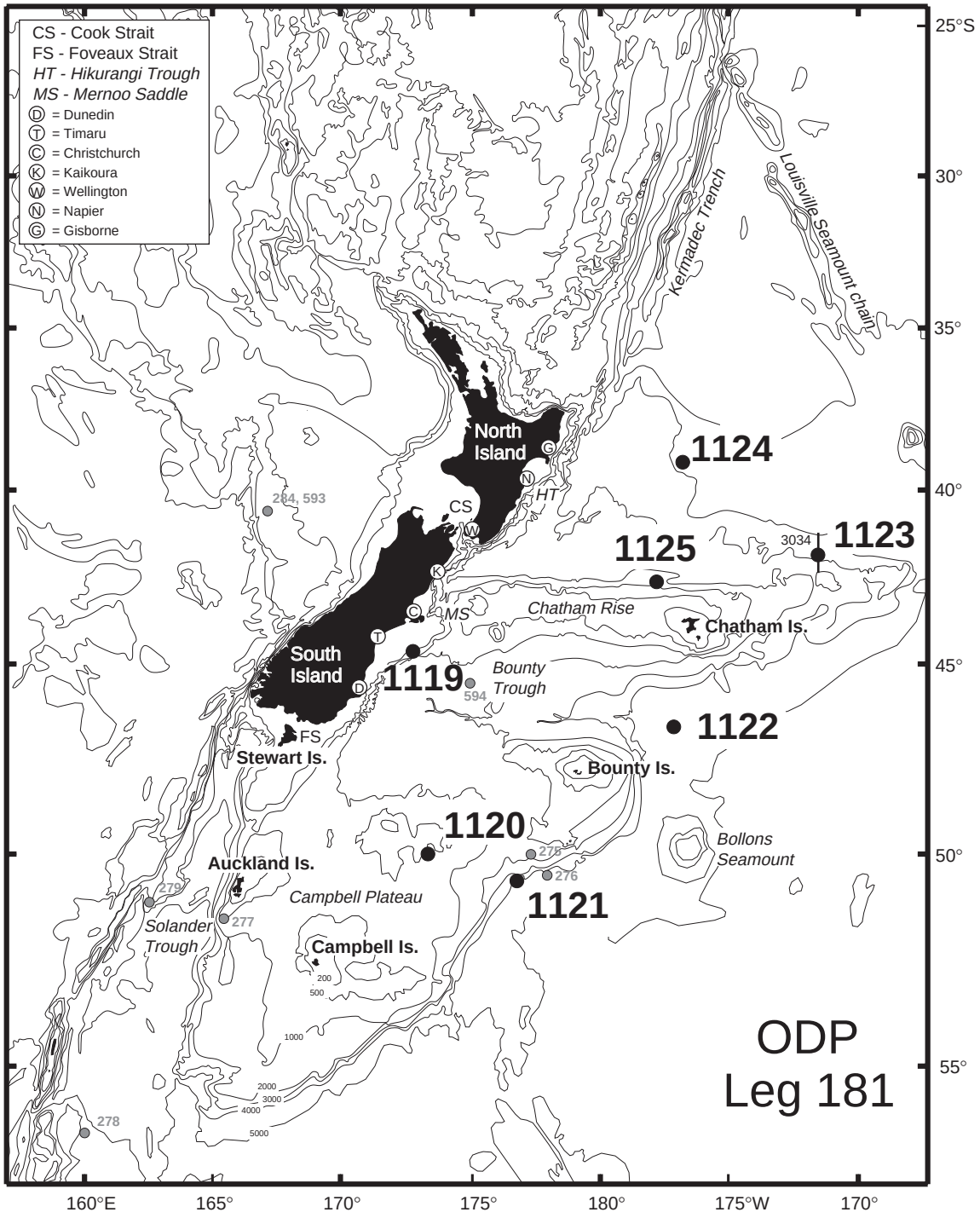

Figure F2. Portion of seismic line NIWA 3034 through Site 1123 (1930–2030 hr, 14 February 1997).

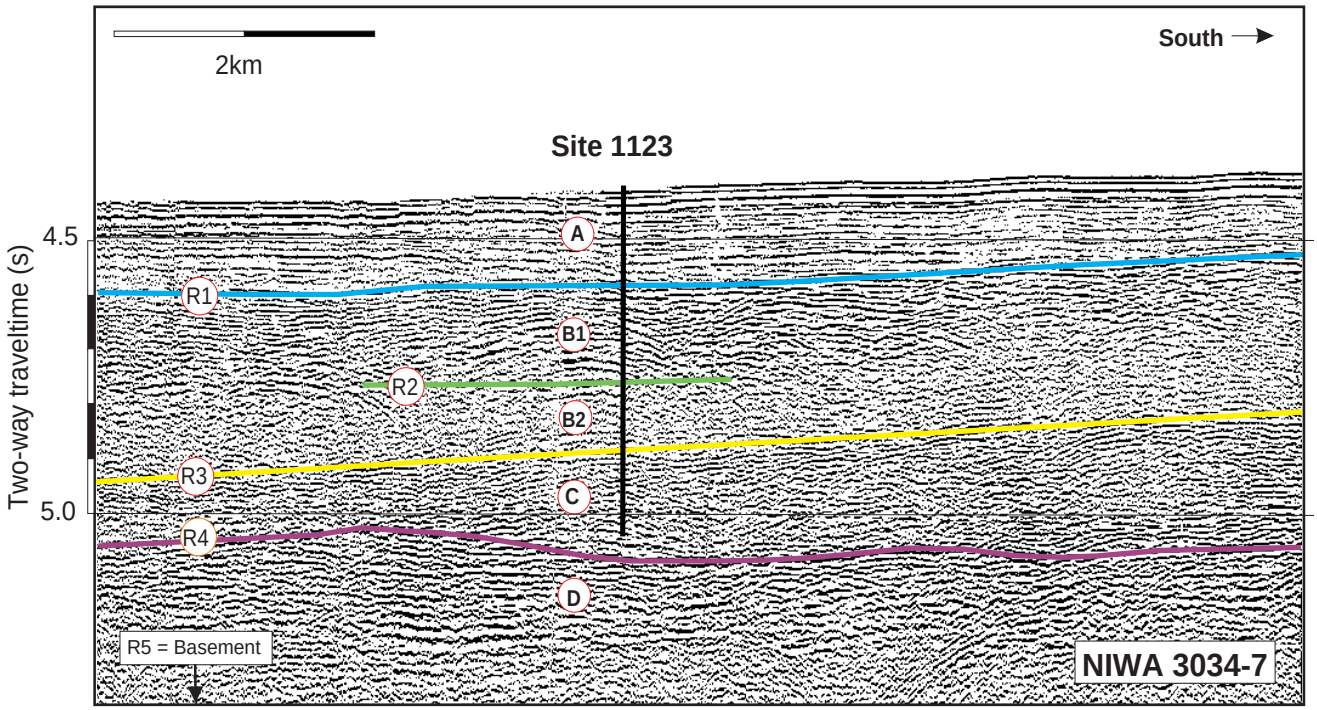

Figure F3. Portion of 3.5-kHz line NZOI 2050, lower slope of Chatham Rise near Site 1123.

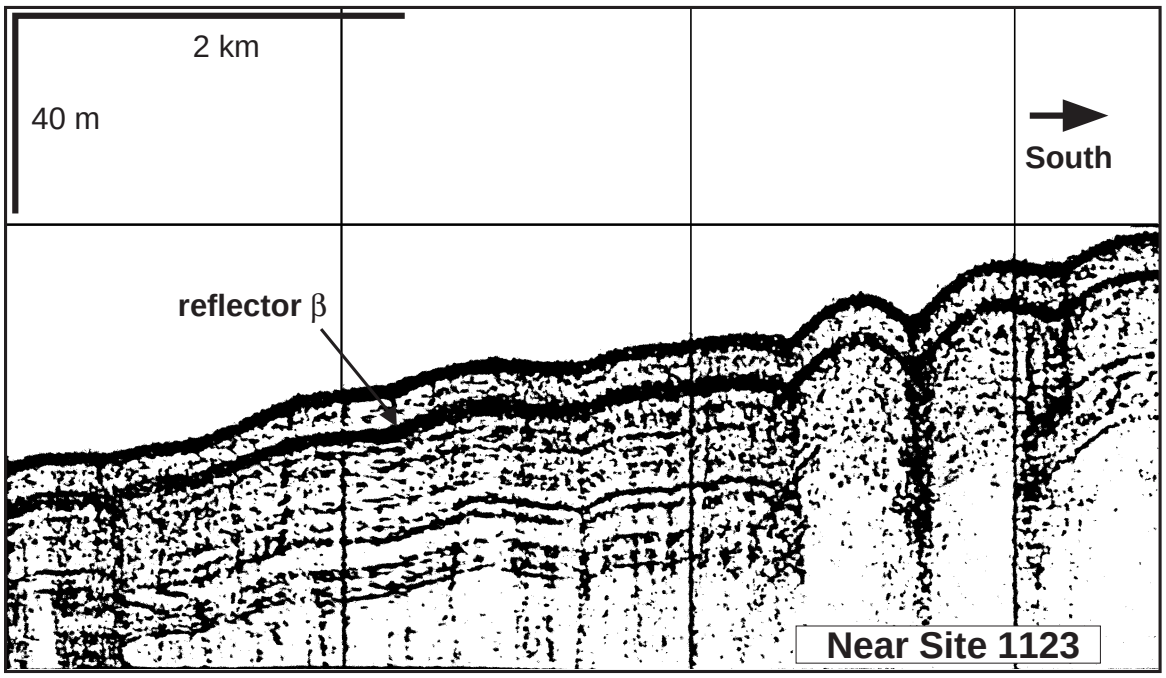

Figure F4. Synopsis of the summary log for Site 1123.

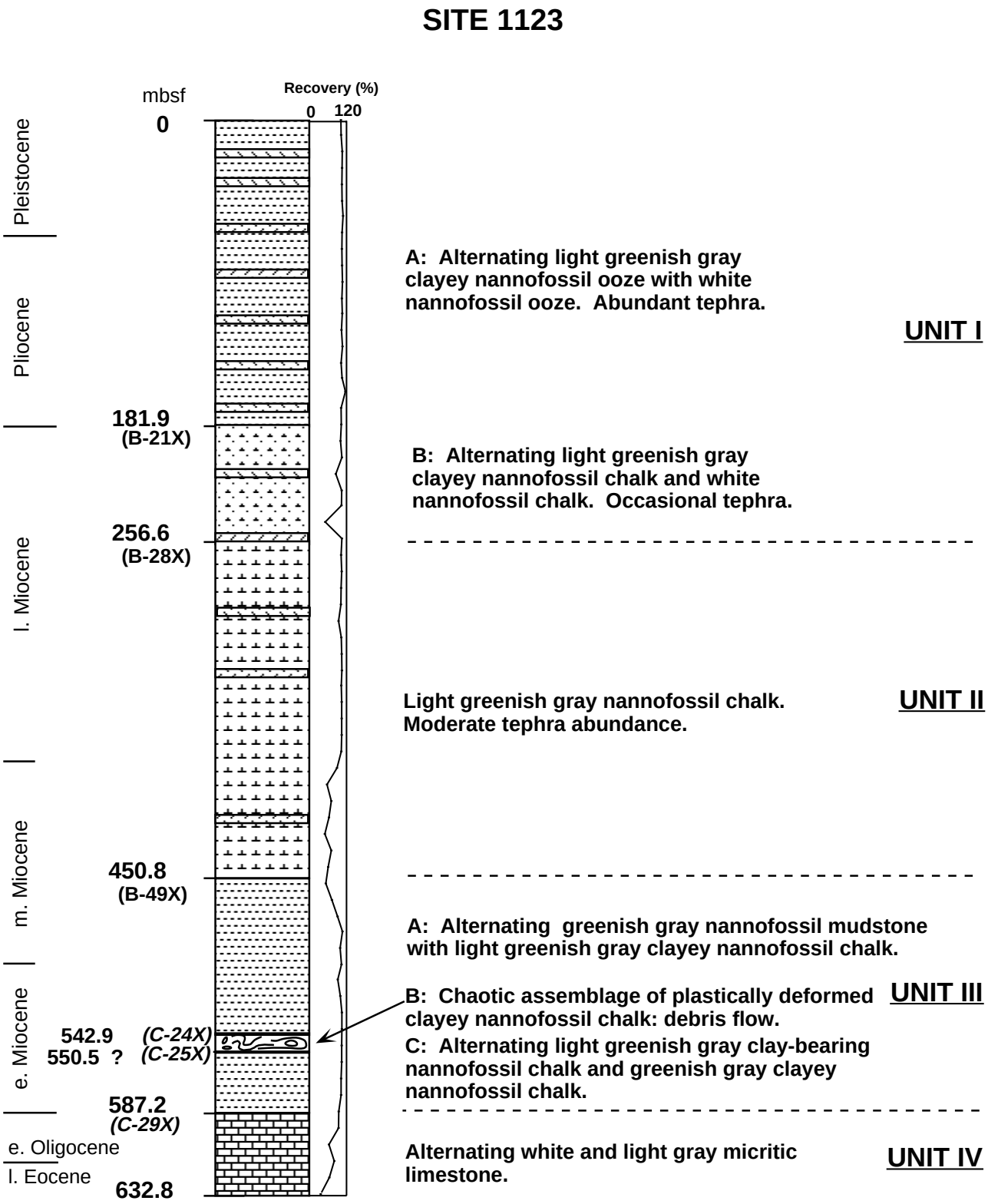

Figure F5. Summary log for Site 1123. (Continued on next three pages.)

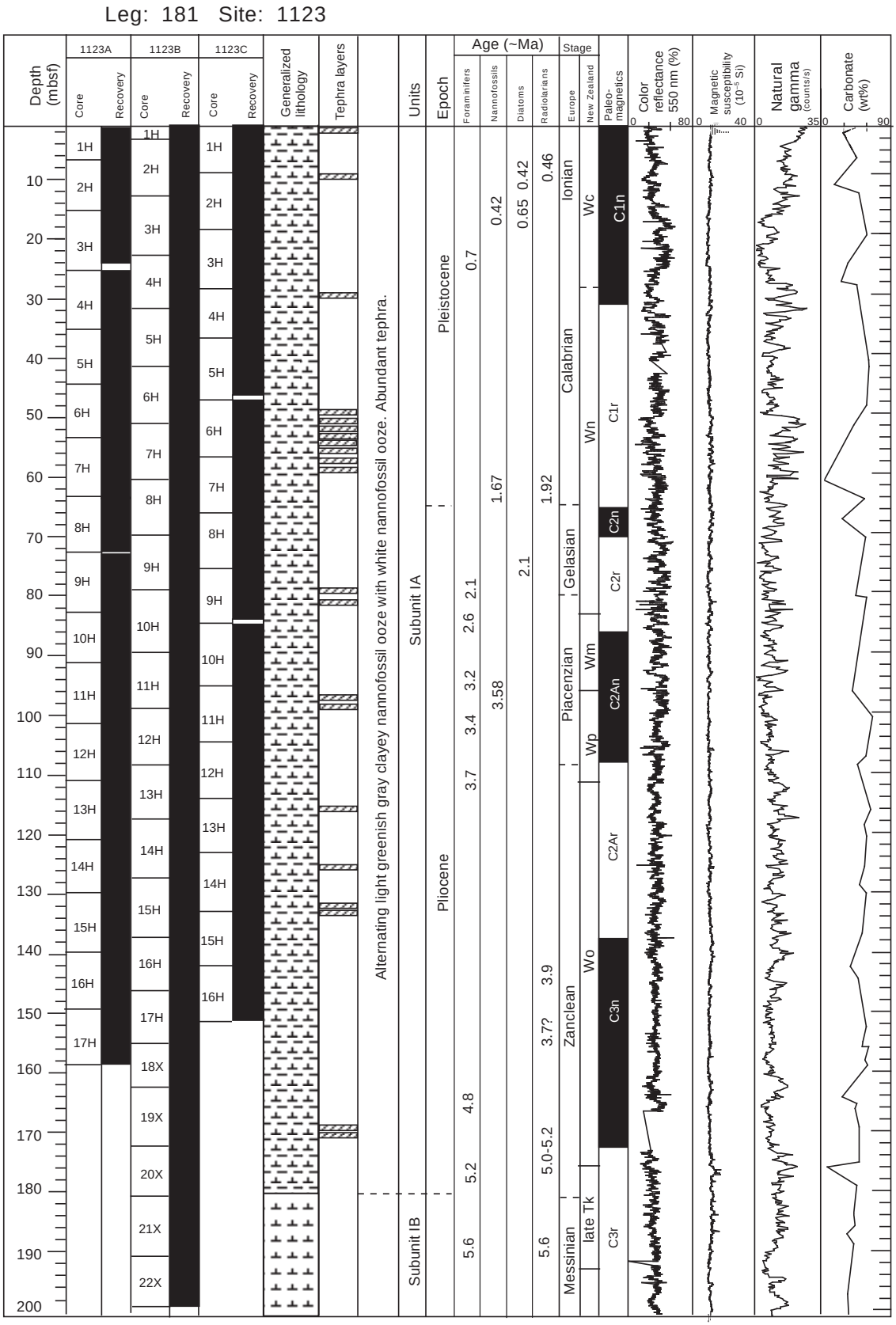

Figure F5 (continued).

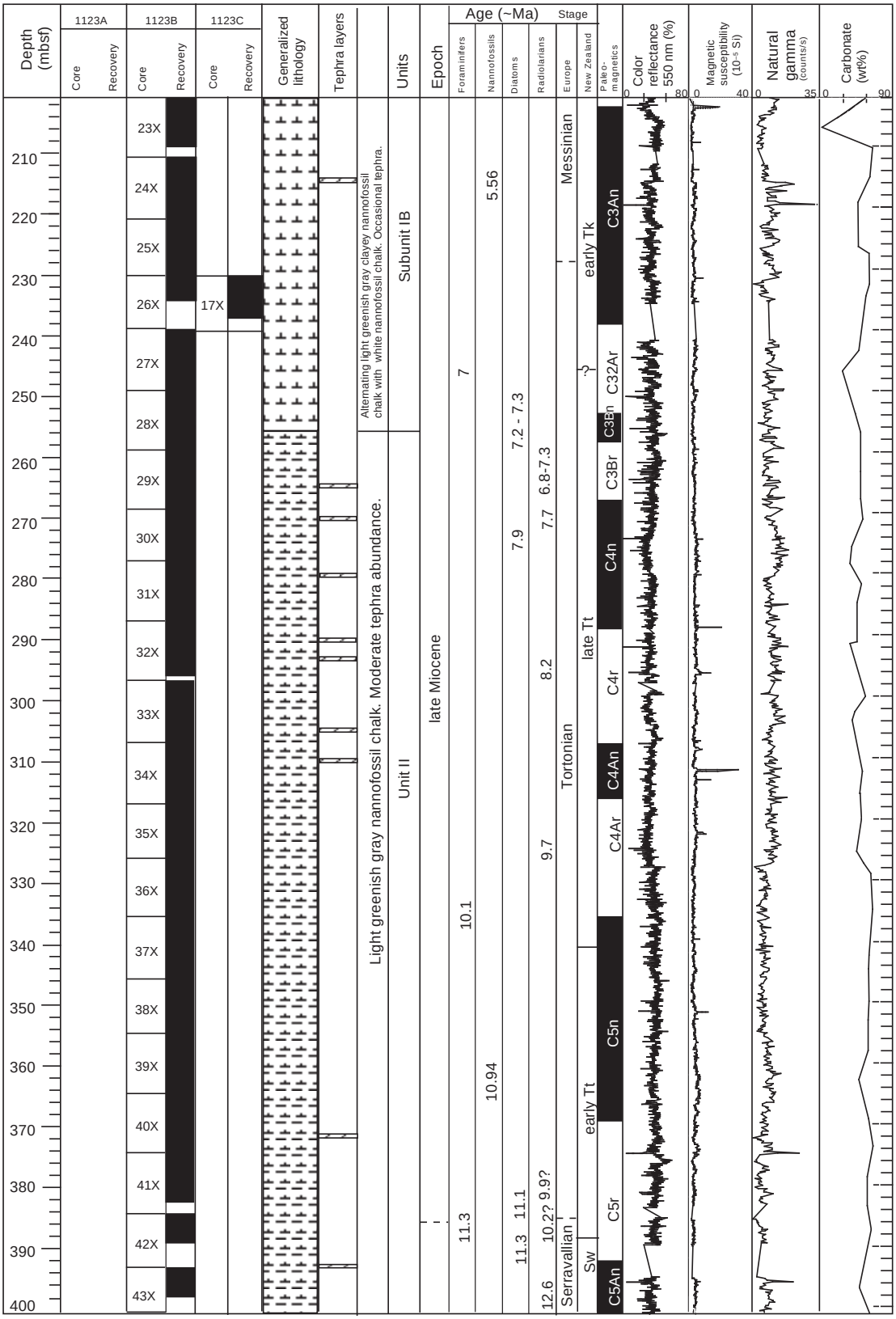

Figure F5 (continued).

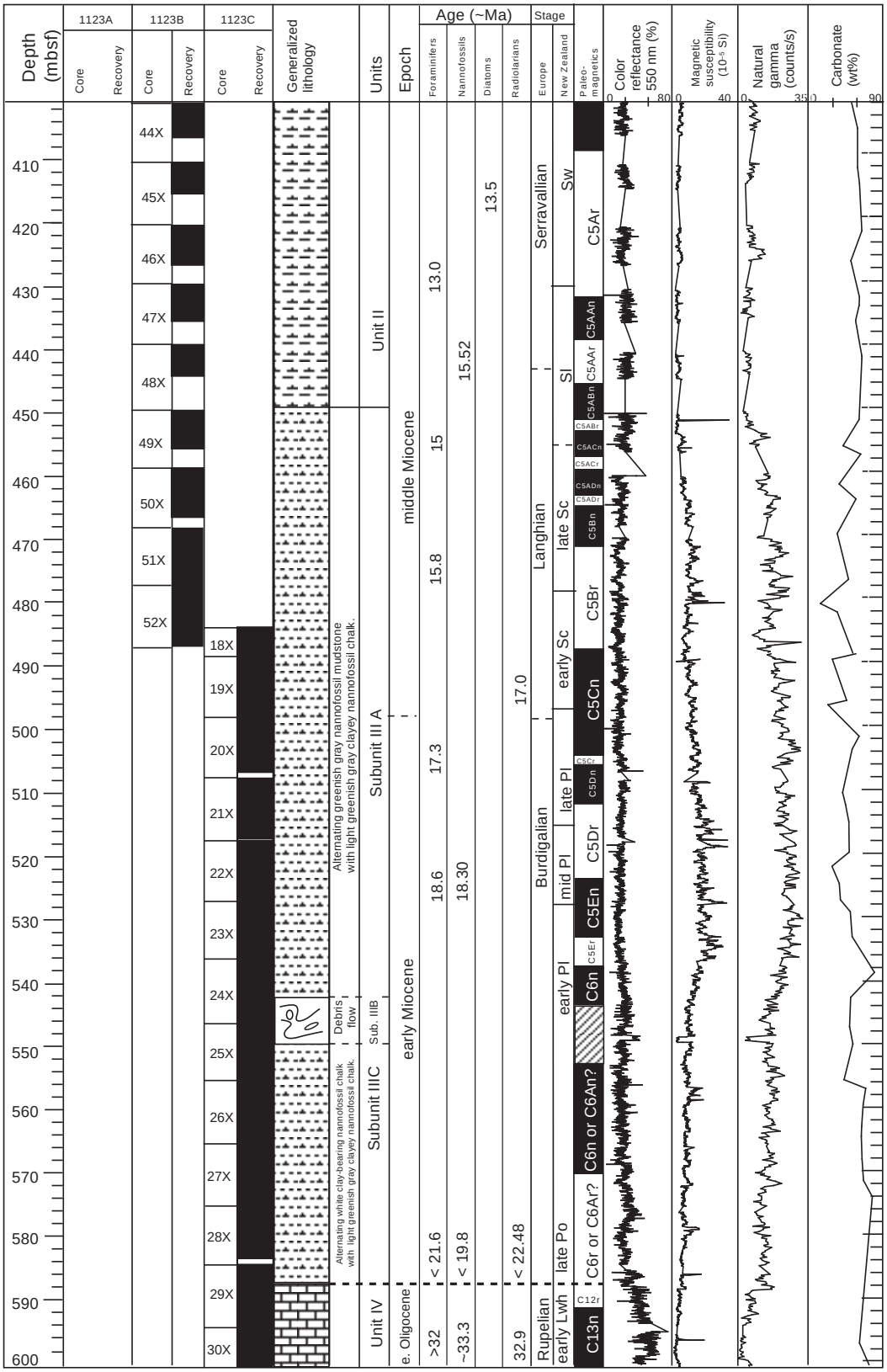

Figure F5 (continued).

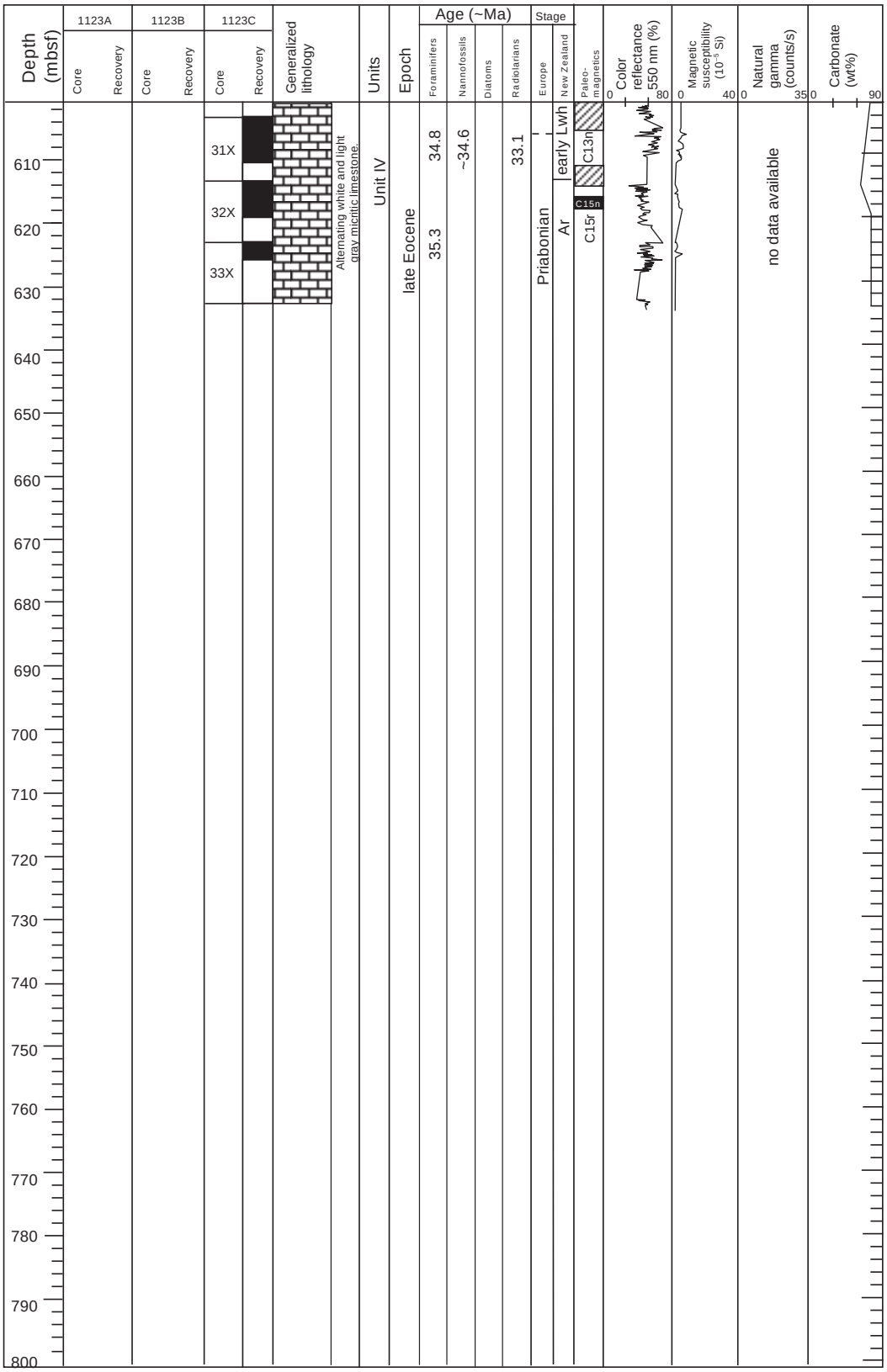

Figure F6. Light reflectance at 550 nm vs. carbonate percentage from Holes 1123A, 1123B, and 1123C.

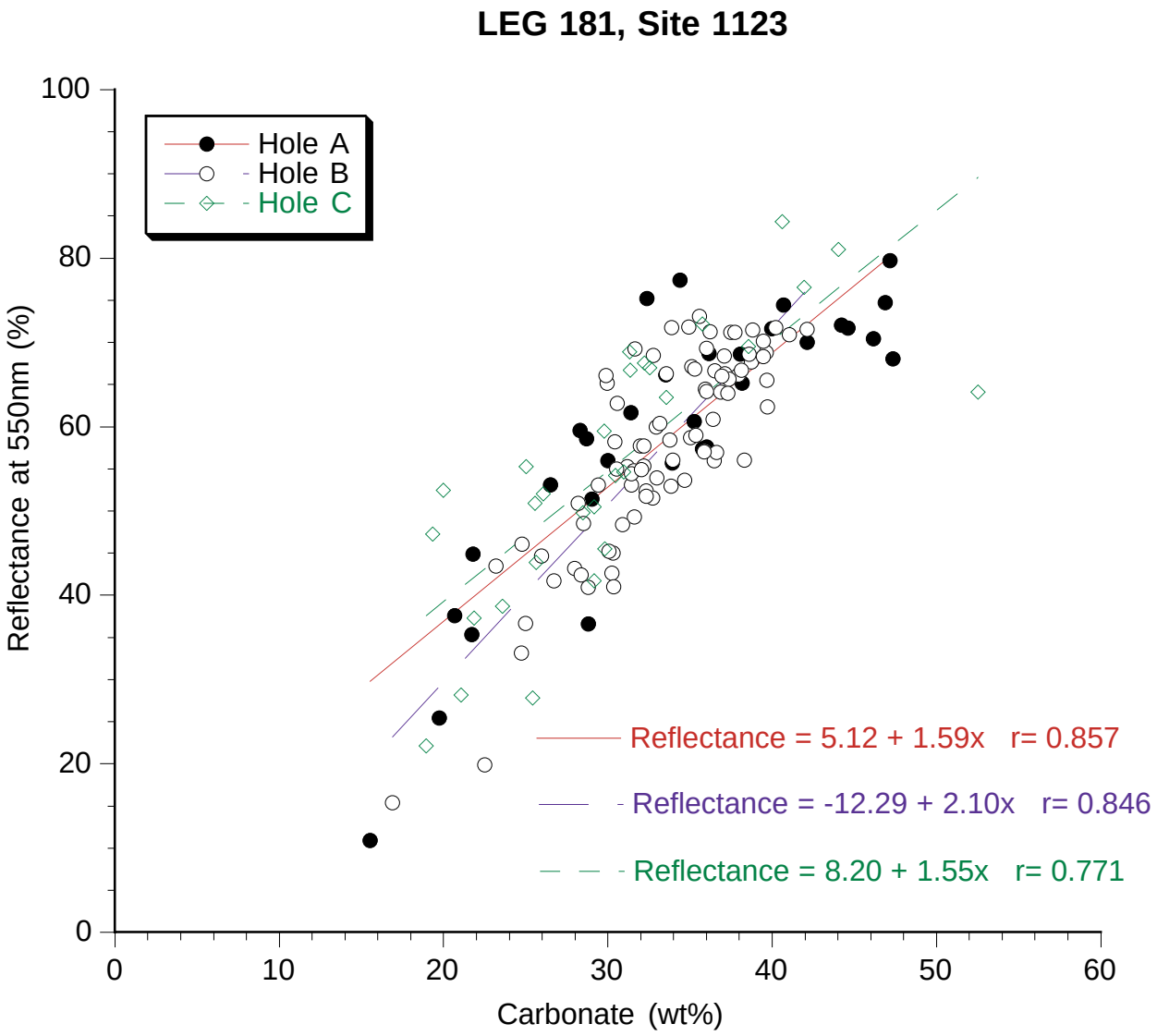

Figure F7. A pyritized *Teichichnus* burrow (top aspect) from Unit I (interval 181-1123C-8H-1, 136–145 cm; 67.36 mbsf).

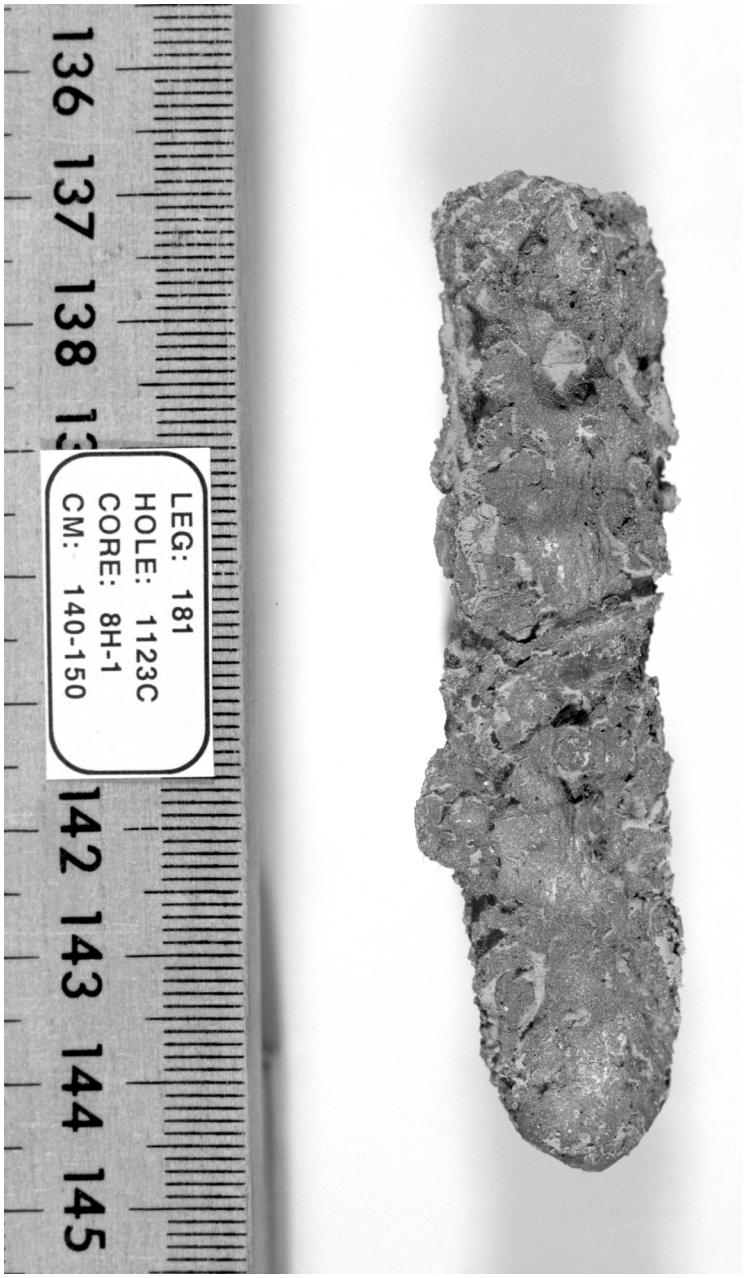

Figure F8. Tephra layers vs. depth (mcd) for Holes 1123A, 1123B, 1123C, together with the composite section showing tephra below 150 mcd. Thin solid lines represent tephra layers considered in situ; dashed lines indicate those considered to be disturbed or present as lenses. Thick lines are closely spaced, multiple tephra layers.

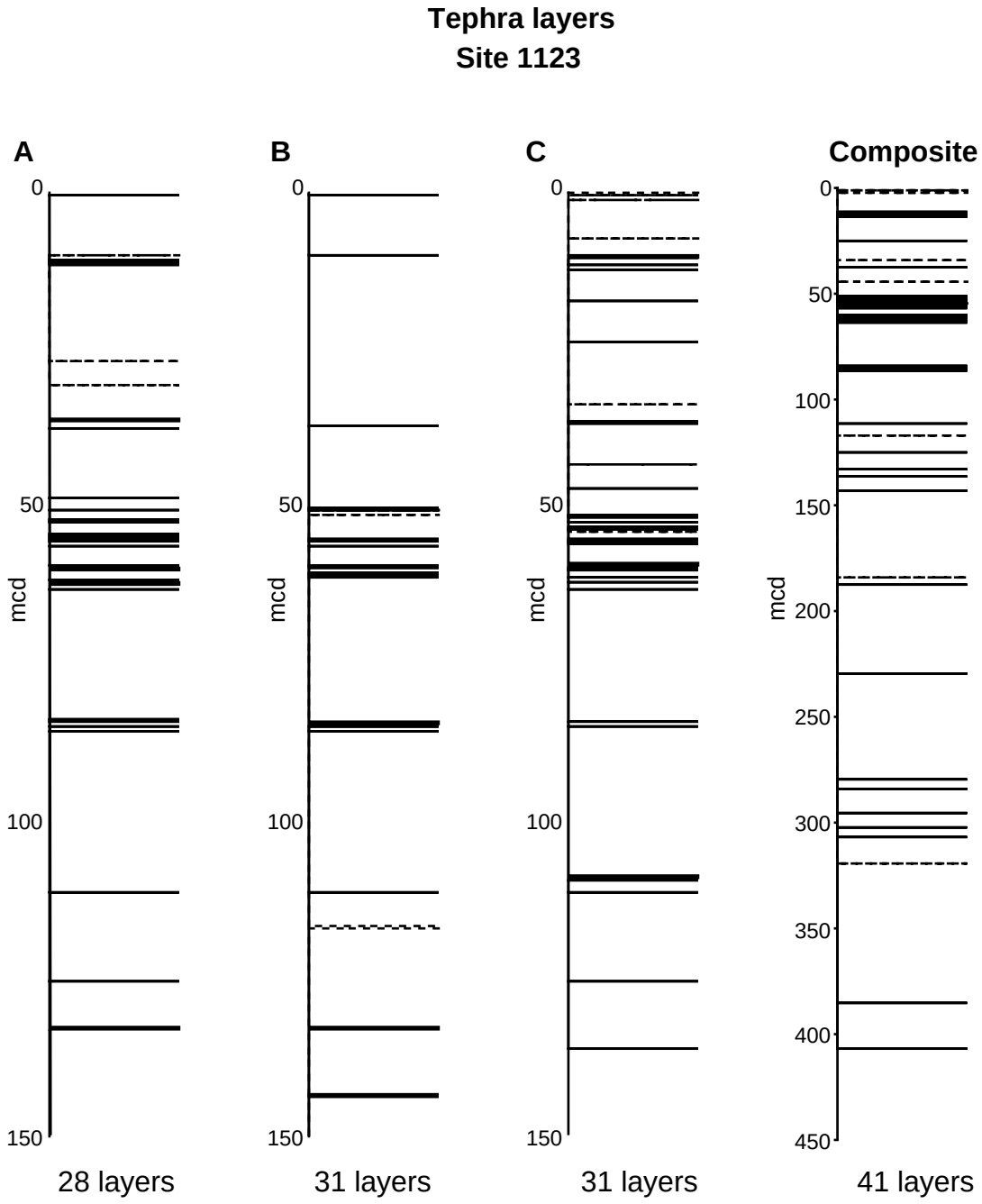

Figure F9. A tephra layer from Unit I showing reworked tephra contained within *Thalassinoides* burrows below the sharp basal contact (interval 181-1123C-13H-4, 60–80 cm; 118.60–118.80 mbsf).

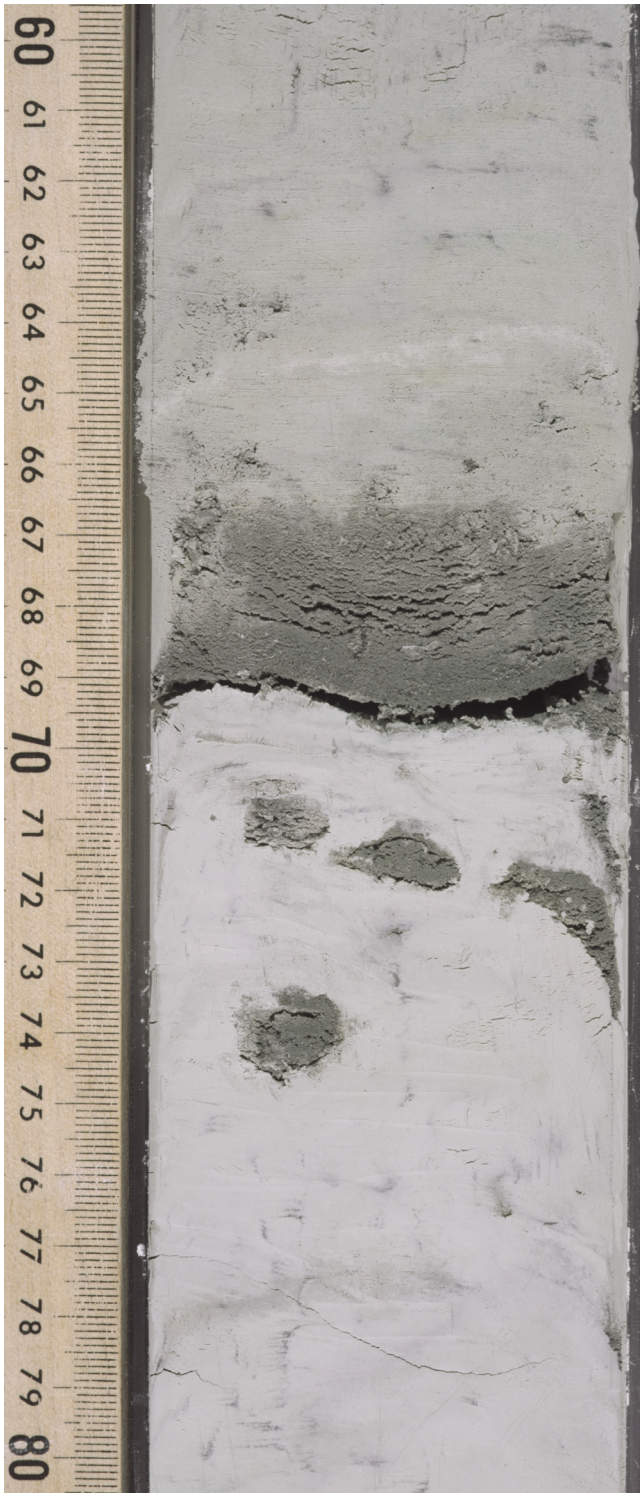

Figure F10. *Zoophycos* preserved in Subunit IIIA chalks (interval 181-1123C-22X-2, 10–30 cm; 519.00–519.20 mbsf).

Figure F11. Proxy and weight percentage carbonate data for lithostratigraphic Unit II, showing subtle cyclicity recorded by the spectrophotometer, although color changes are not evident to the naked eye. The proxy carbonate record has been stretched as outlined in "Composite Depths," p. 32.

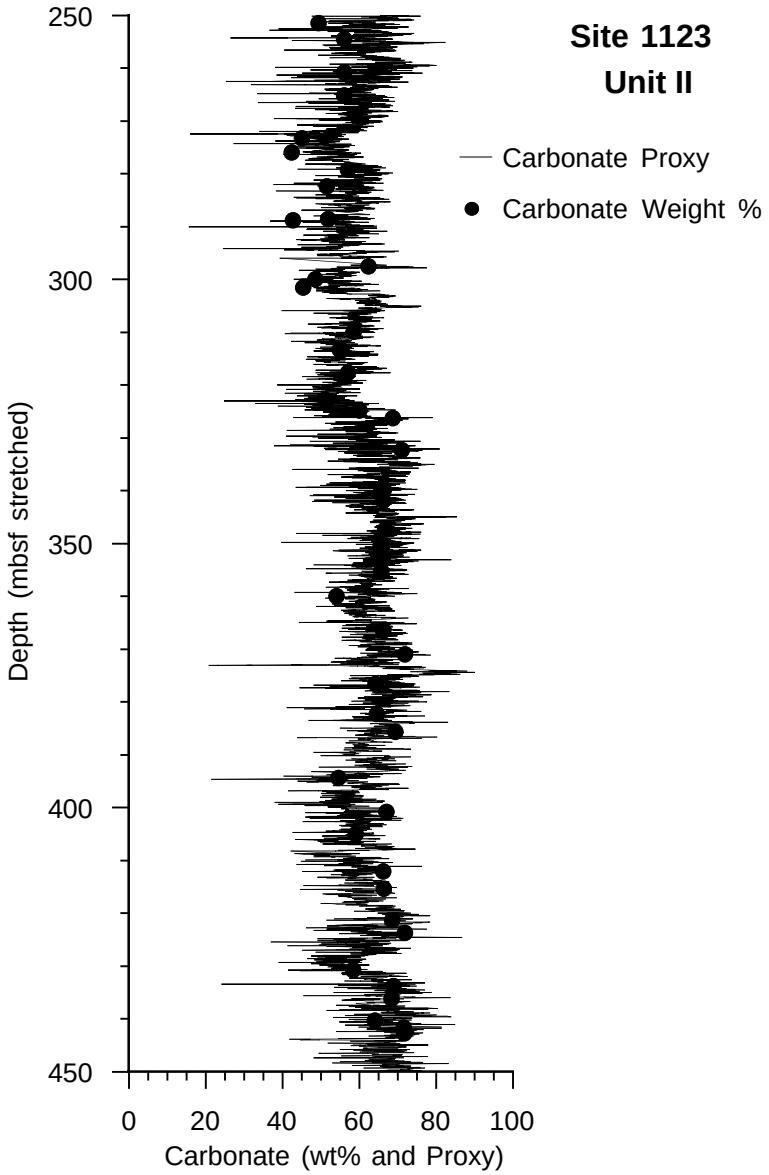

Figure F12. Plastically deformed clayey nannofossil chalk from the debris flow of Subunit IIIB (interval 181-1123C-24X-5, 90–120 cm; 543.50–543.80 mbsf).

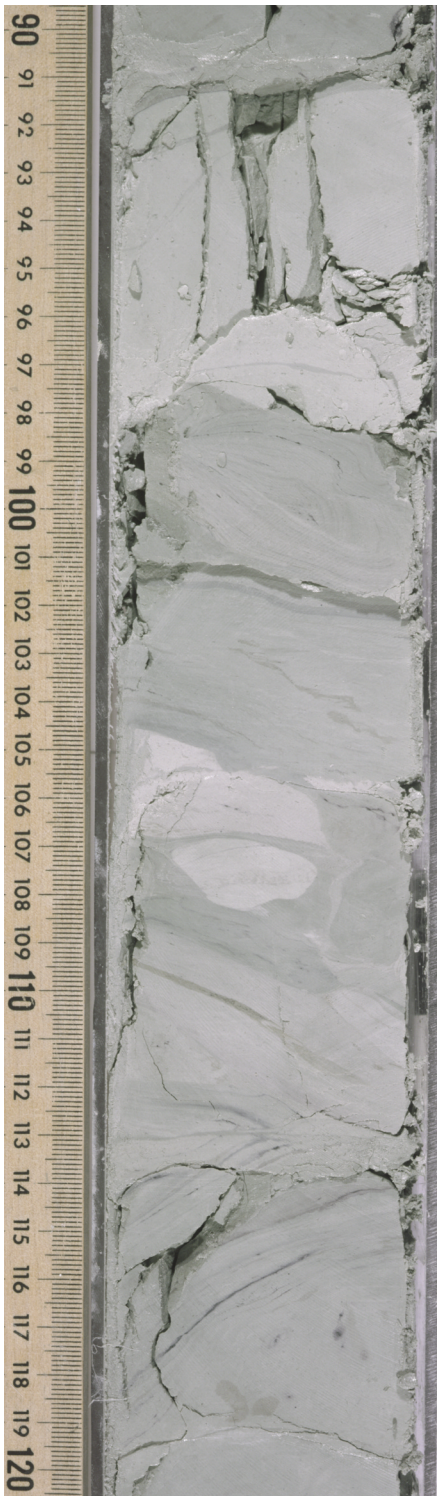

Figure F13. The Marshall Paraconformity (99.5 cm) at the contact between Subunit IIIC nannofossil-bearing mudstone and Subunit IV chalk (interval 181-1123C-29X-2, 90–110 cm; 587.10–587.30 mbsf).

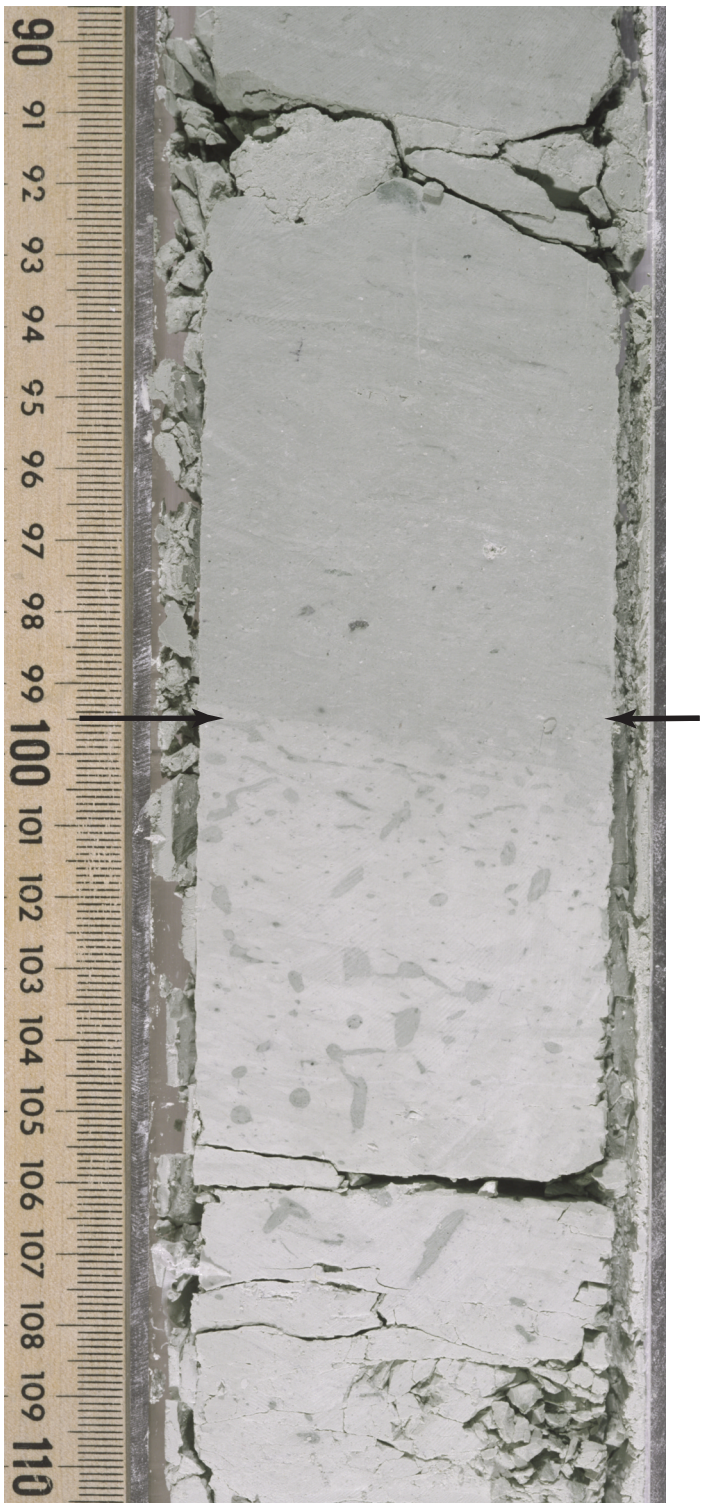

Figure F14. Stylolite contacts in Section IV (interval 181-1123C-30X-2, 0–15 cm; 595.80–595.95 mbsf).

Figure F15. Summary plot of major ichnofacies (underlined) at Site 1123.

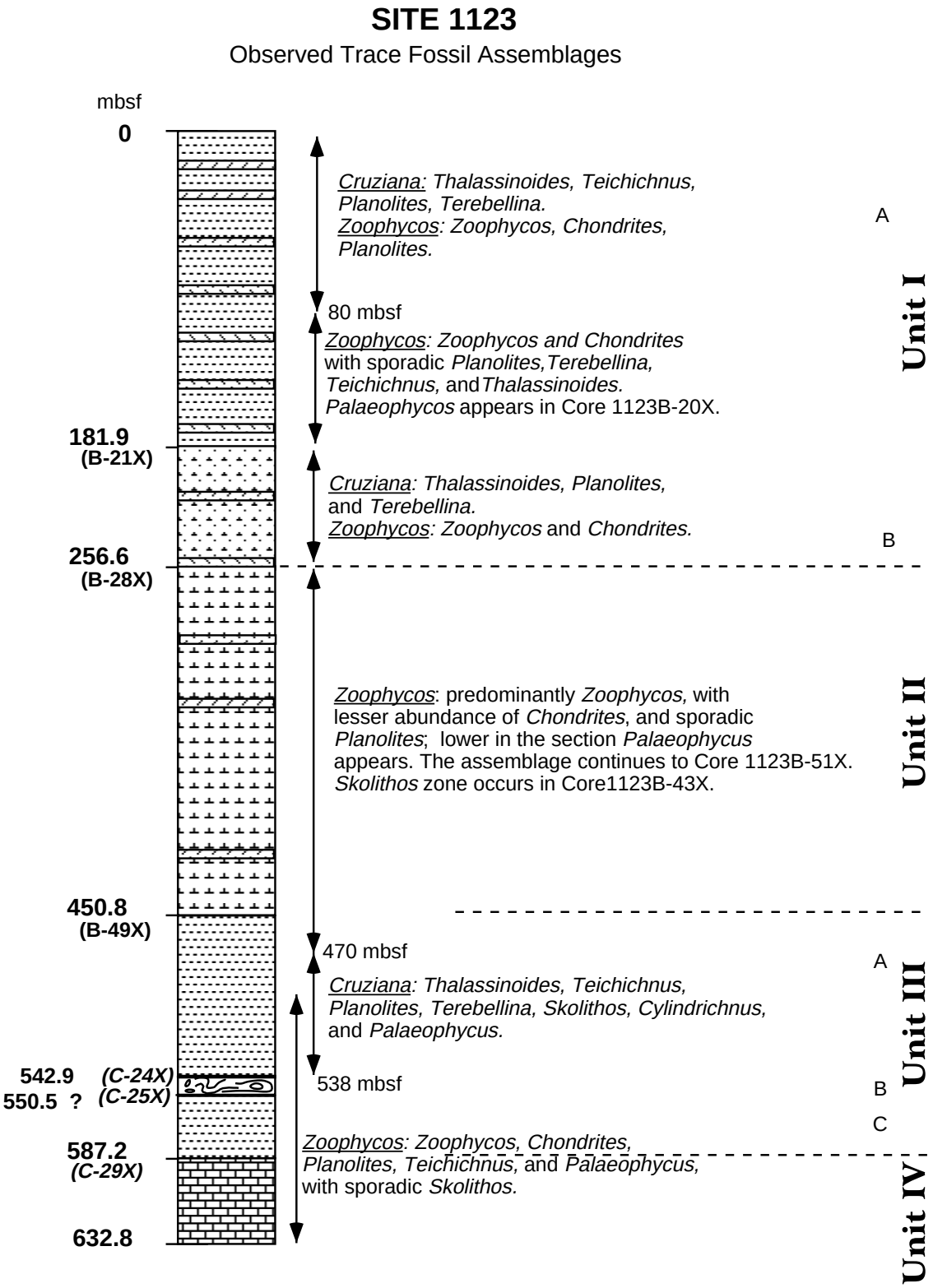

Figure F16. Biostratigraphic summary chart of Site 1123 showing correlation between the five planktonic microfossil biochronologies. See "Paleogene," p. 20, for New Zealand stage abbreviations.

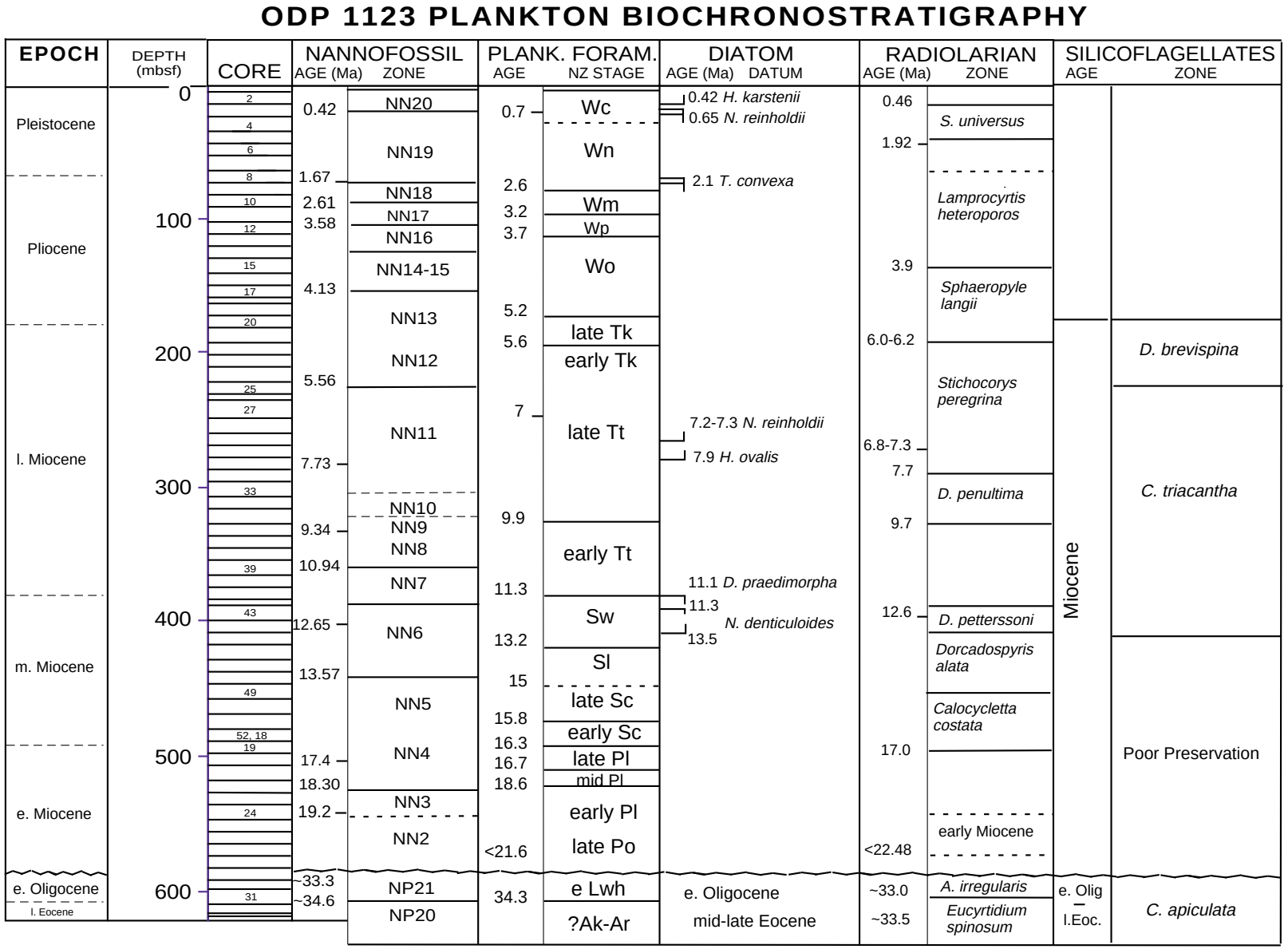

Figure F17. Age-depth relationship based upon calcareous nannofossil datums at Site 1123.

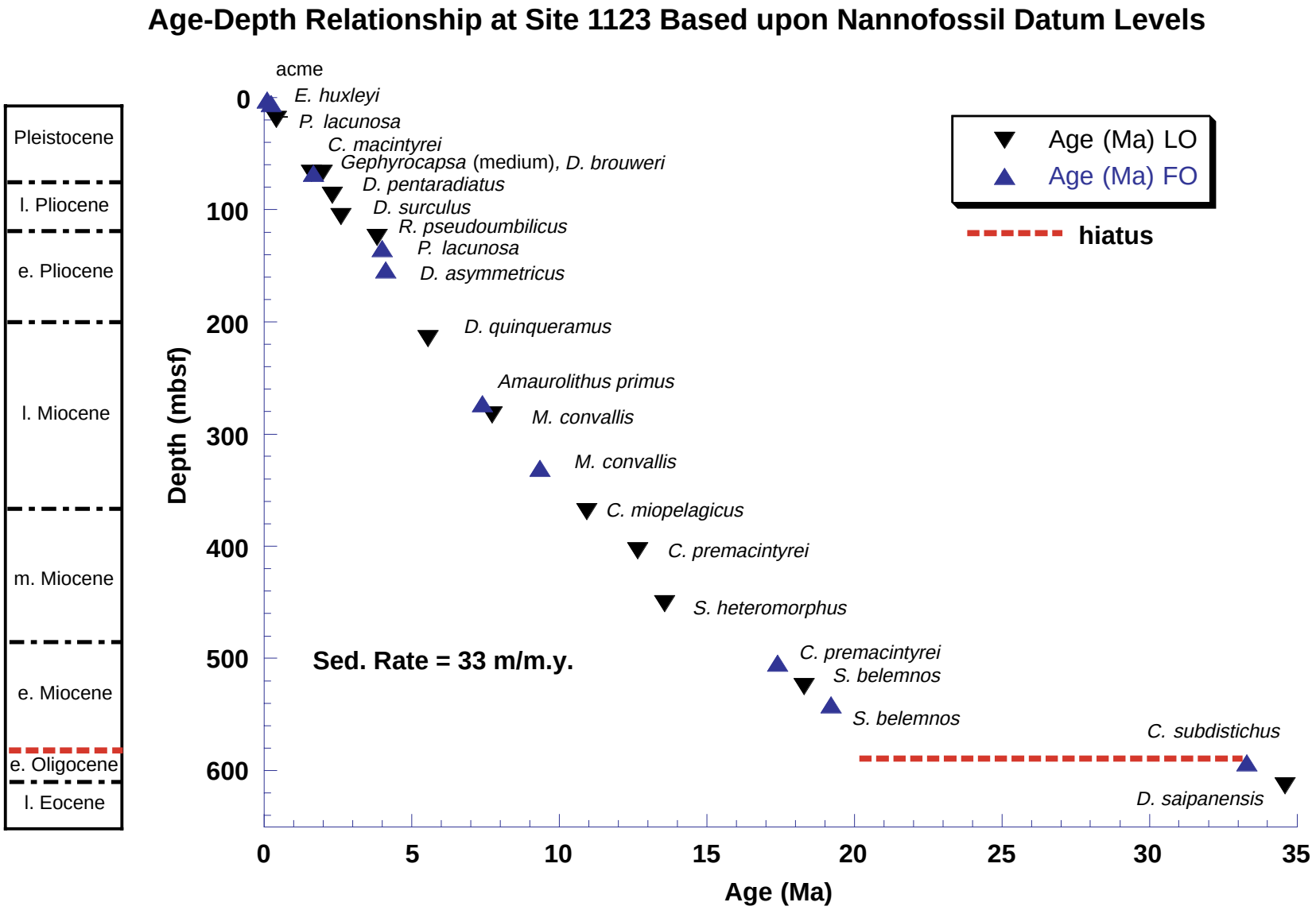

Figure F18. Age-depth relationship based upon radiolarian datums at Site 1123.

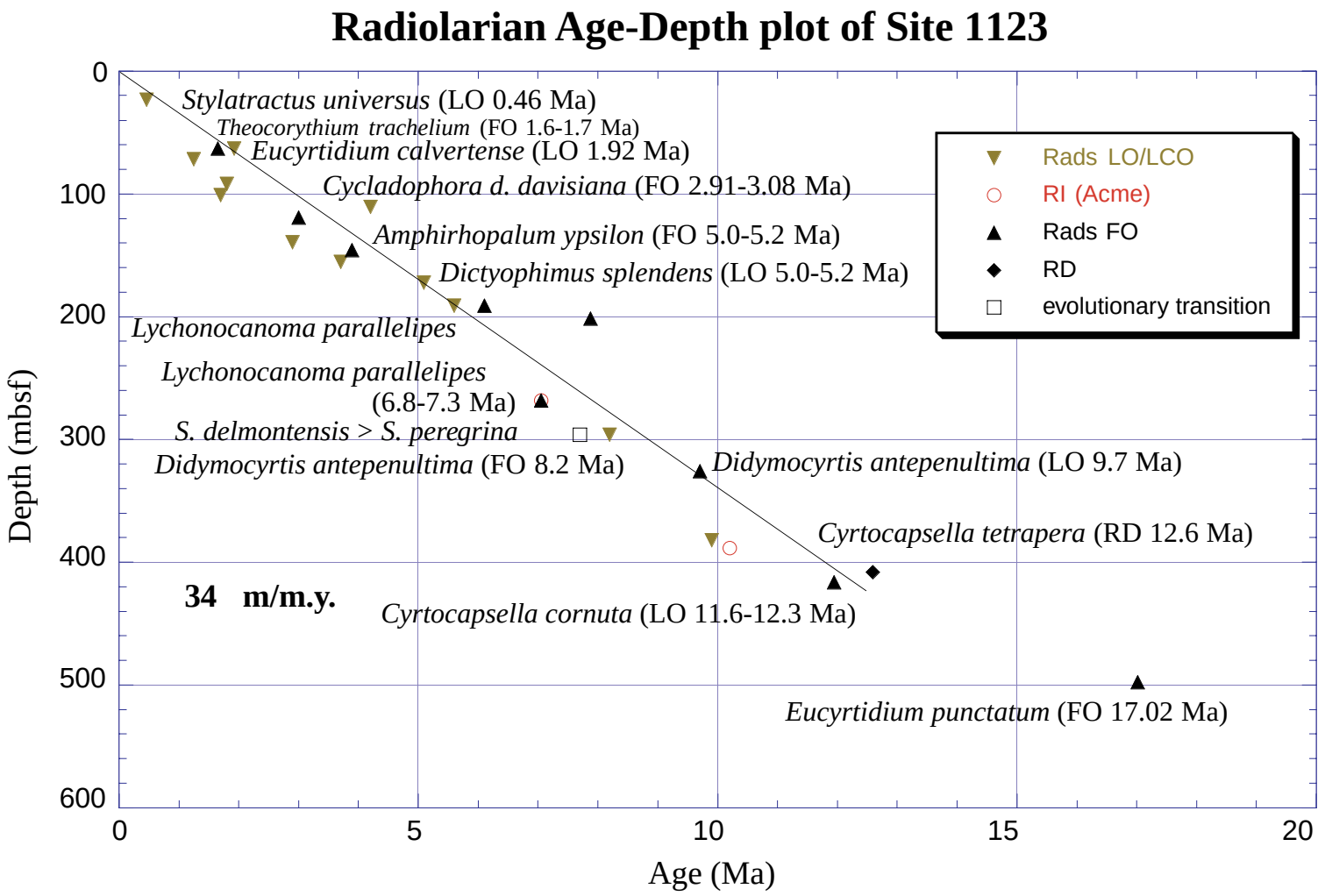

Figure F19. A–E. Composite magnetostratigraphic record from Site 1123. Depth scale is mcd from correlation between Holes 1123A, 1123B, and 1123C using whole-core magnetic susceptibility and reflectance data in combination with magnetic polarity datums (see **"Composite Depths,"** p. 32). Some intervals of the record use stretched mcd depths where low-recovery intervals are stretched linearly to cover the full 9.5-m cored interval (see Fig. **F22,** p. 81, and discussion in text). The inclination record is after a single demagnetization step of 20 mT. Black (white) represents normal (reversed) polarity and hatching defines intervals where polarity could not be determined because of drilling disturbances, flow-in, debris flow in core, or poor recovery intervals that were not able to be stretched. Ages for polarity reversal datums are from Berggren et al. (1995). Arrowheads represent core-catcher depths for fossil datums and arrow length represents possible error because of sampling intervals being confined to core-catcher samples (error bars extend up for last occurrences and down for first occurrences). Single occurrences and acme events have error bars extending to the core catcher sample above and below. (**Figure F19 shown on next five pages.**)

Figure F19 (Caption on previous page.)

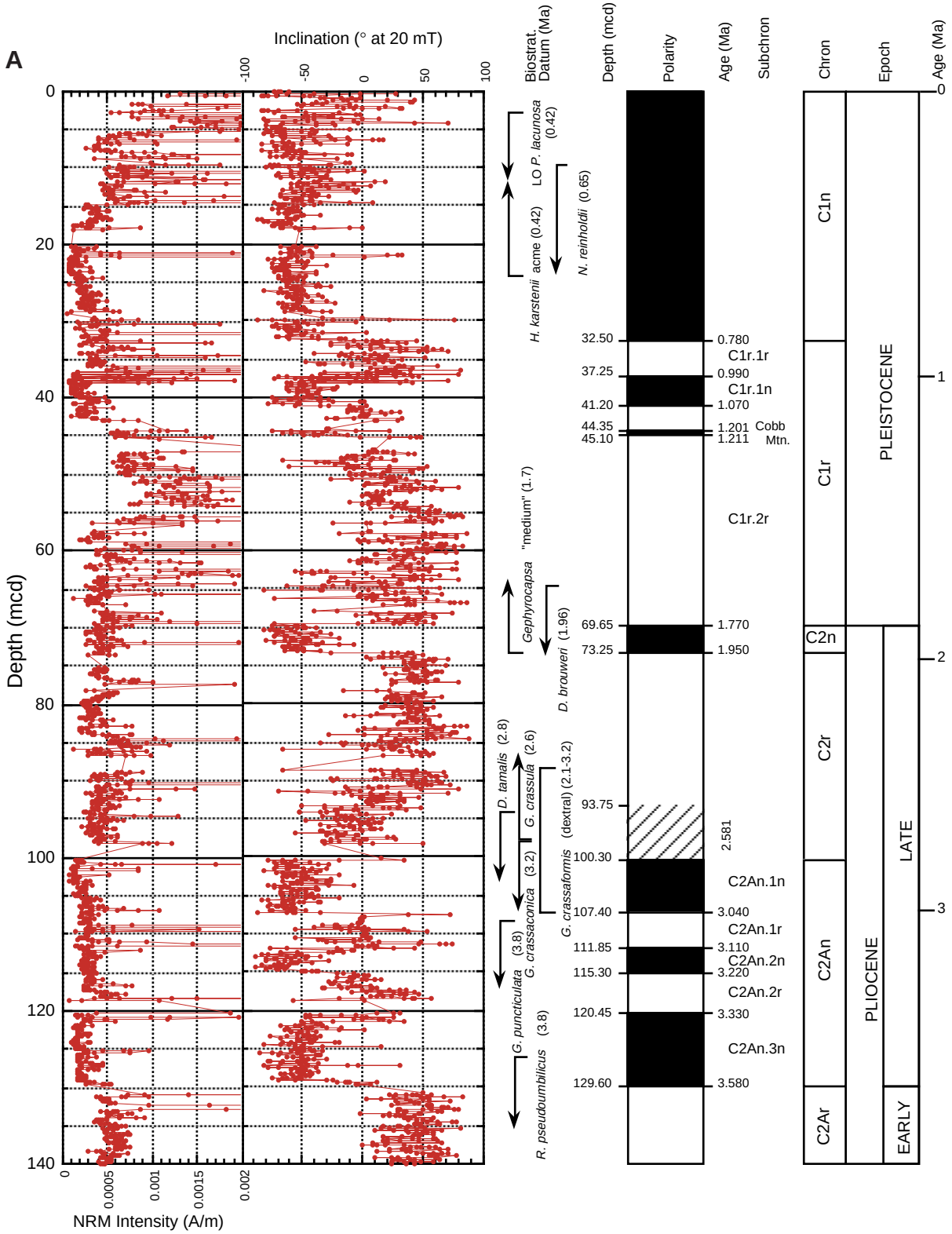

Figure F19 (continued).

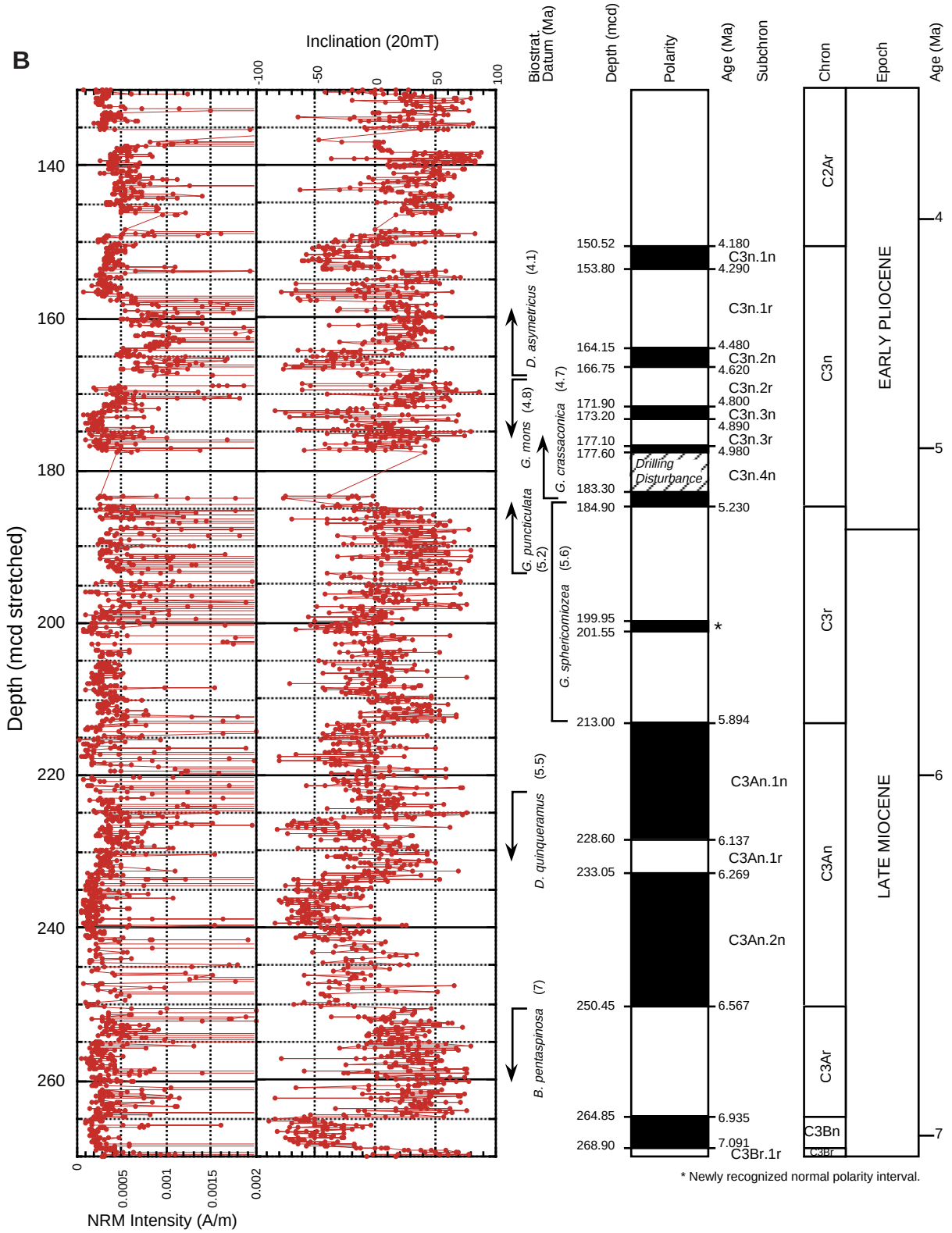

Figure F19 (continued).

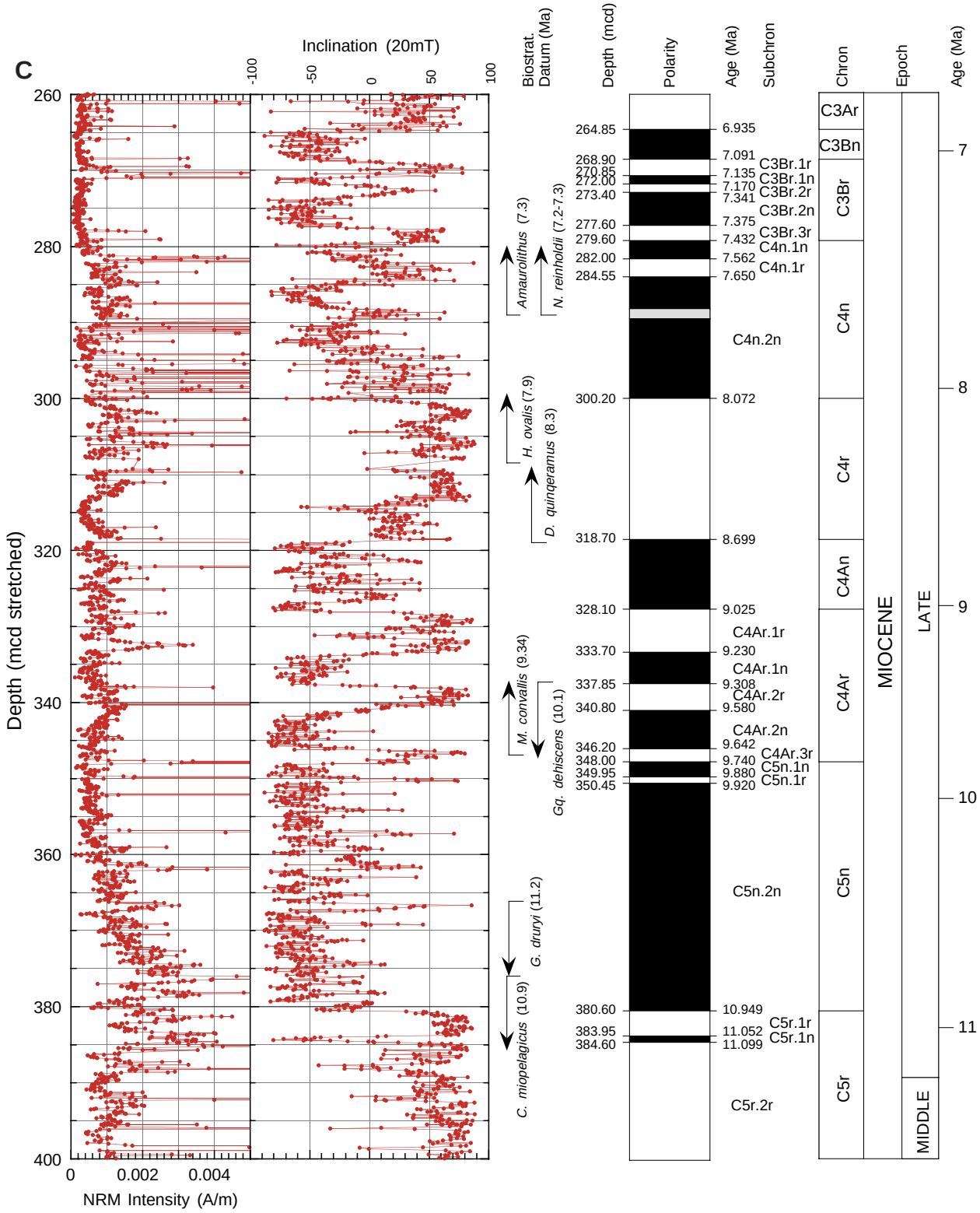

Figure F19 (continued).

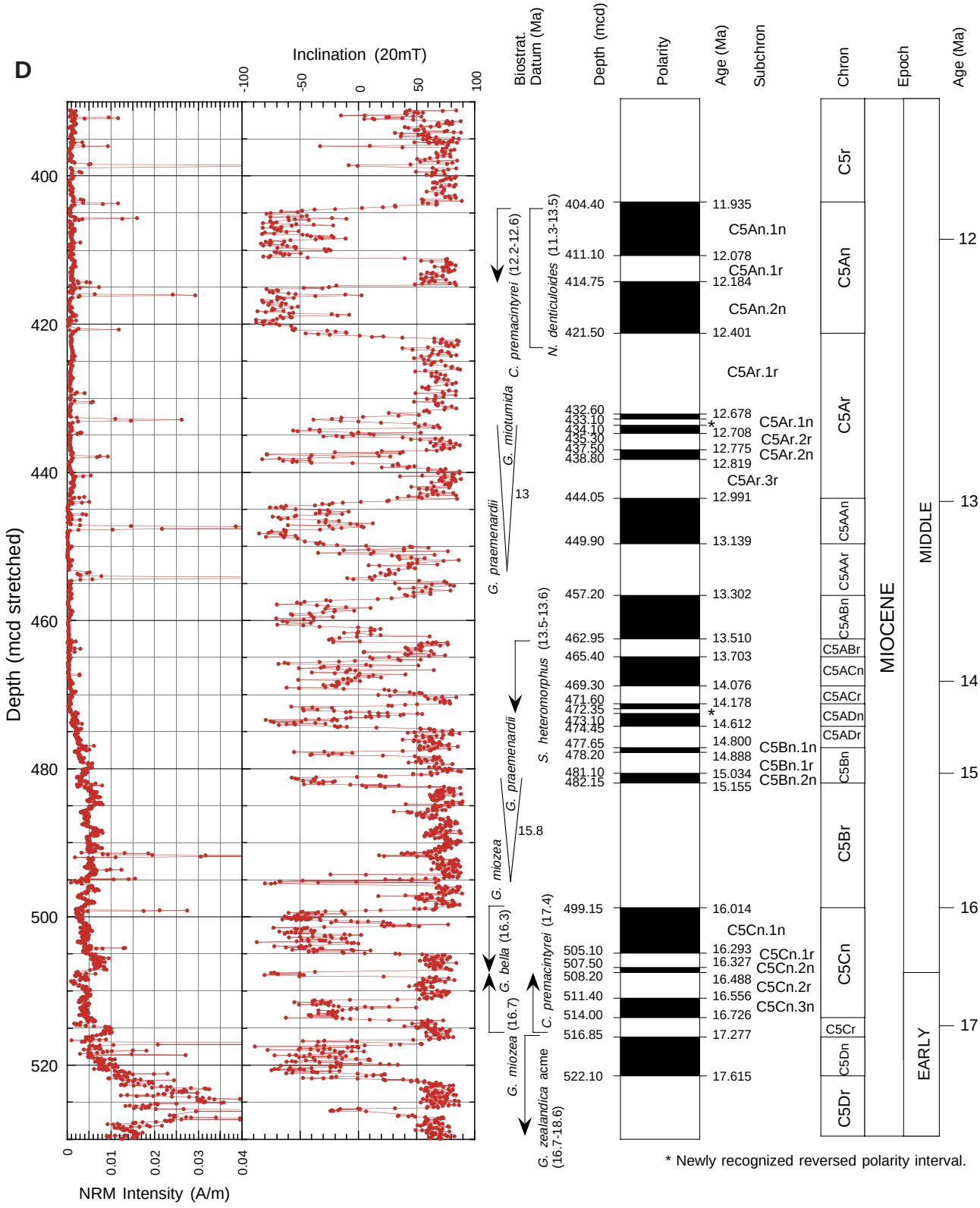

Figure F19 (continued).

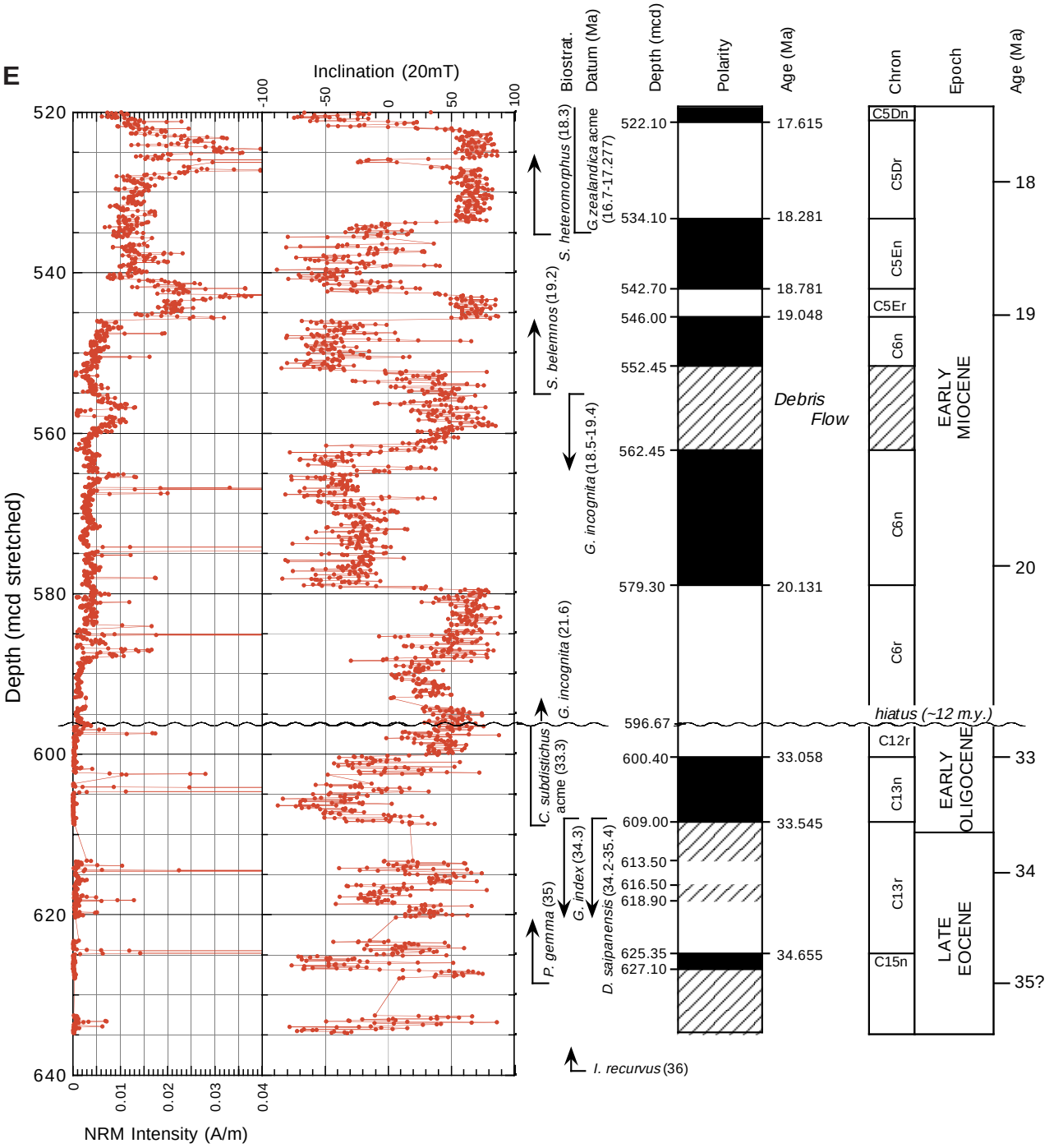

Figure F20. Isothermal remanent magnetization (IRM) and backfield acquisition curves for representative discrete samples from Site 1123. **A.** Samples from above 597 mcd (lithostratigraphic Units I–III), remanence saturates by 500 mT, and B_{cr} is between 25 and 75 mT. **B.** Samples from below 597 mcd (lithostratigraphic Unit IV), remanence saturates at ~1 T, and B_{cr} is between 75 and 100 mT.

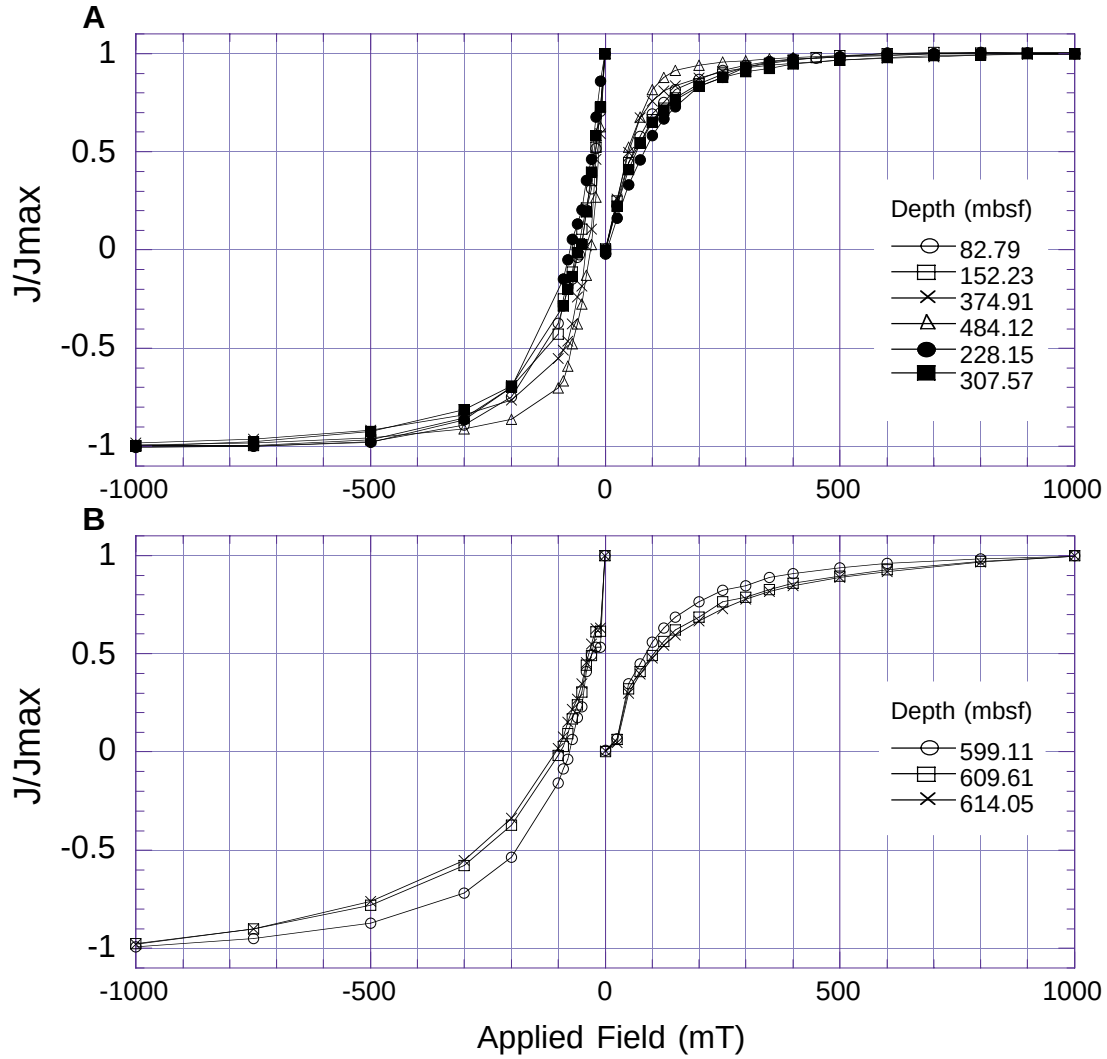

Figure F21. A–C. Plots of normalized intensity of magnetization with progressive AF and thermal demagnetization of saturation isothermal remanent magnetization (SIRM) for selected samples from Site 1123.

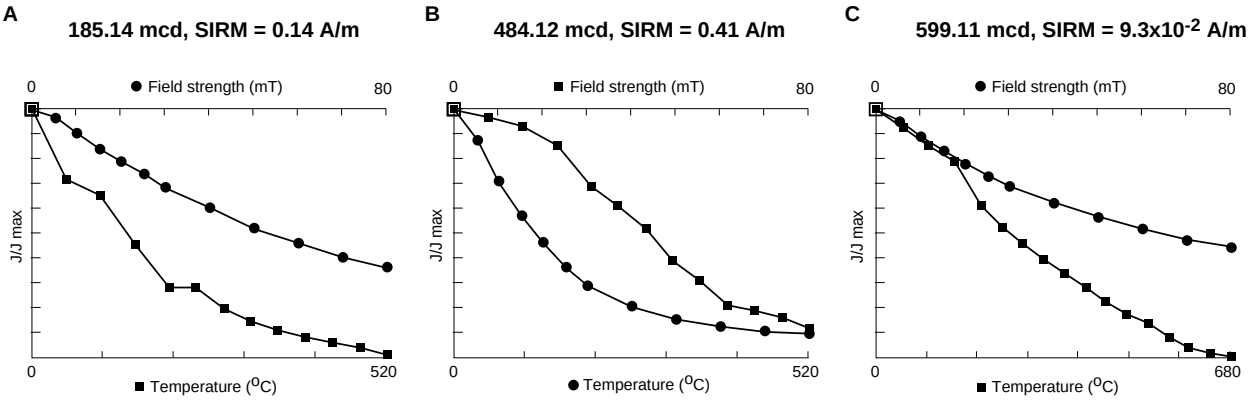

Figure F22. Comparison of whole-core susceptibility and inclination (after 20-mT demagnetization) for Cores 181-1123B-41X to 50X as recovered, with linearly stretched records of whole-core susceptibility and inclination and the downhole log susceptibility record. Stretching assumes distributed loss throughout each coring interval from coring-induced breakage. See **"Magnetostratigraphy,"** p. 28, for discussion.

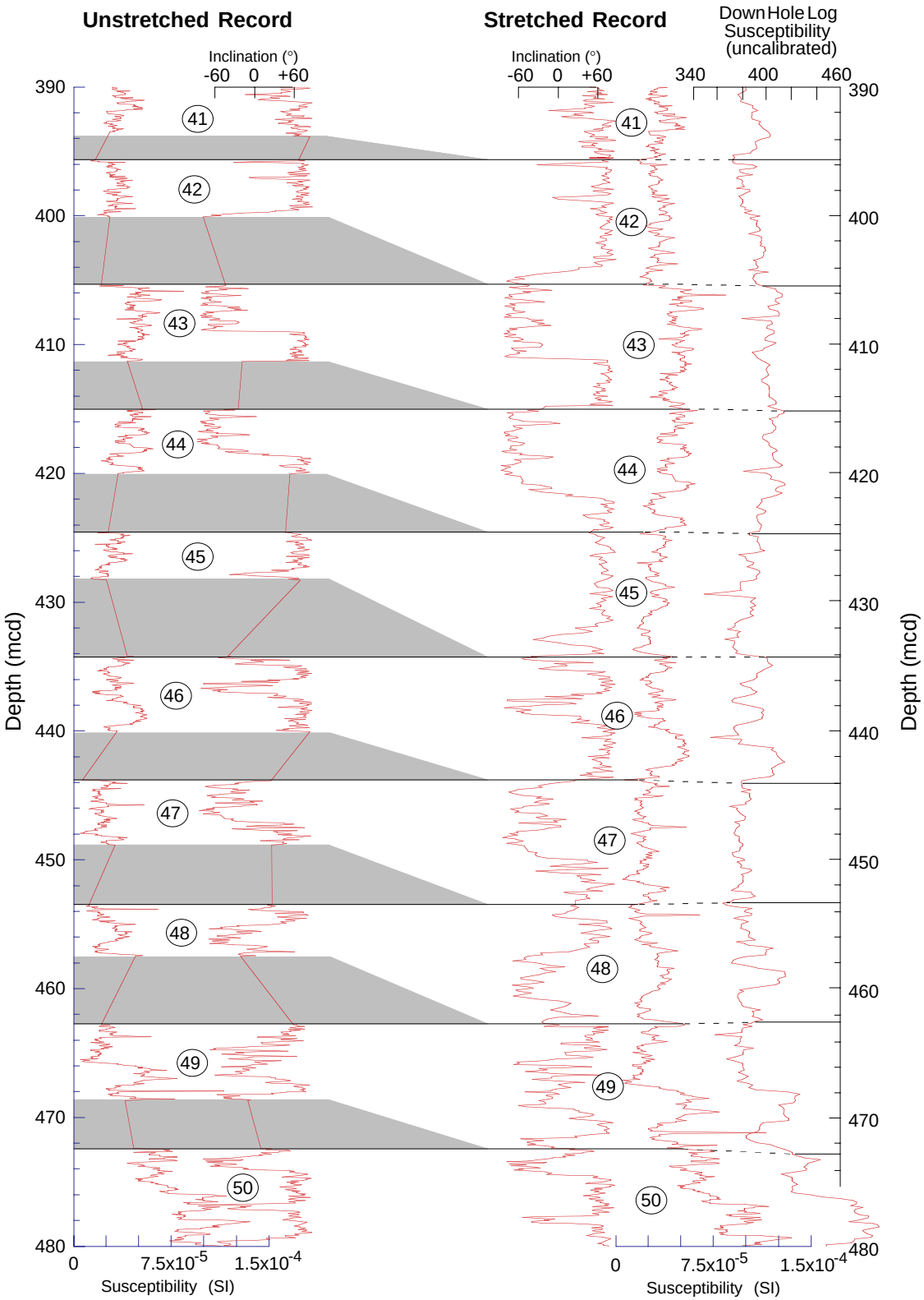

Figure F23. Age model and correlation of the composite magnetic polarity record for Site 1123. Magnetic polarity interpretations are given in Figure F19, p. 73, and individual reversal ages are from Berggren et al. (1985). Solid black line shows line of correlation. Undulating line indicates a hiatus. Lithostratigraphic summary is from "Lithostratigraphy," p. 4. Ages of tephra horizons are assigned from the age-depth model (Table T11, p. 159). The main features are discussed in "Age Models and Sedimentation Rates," p. 34.

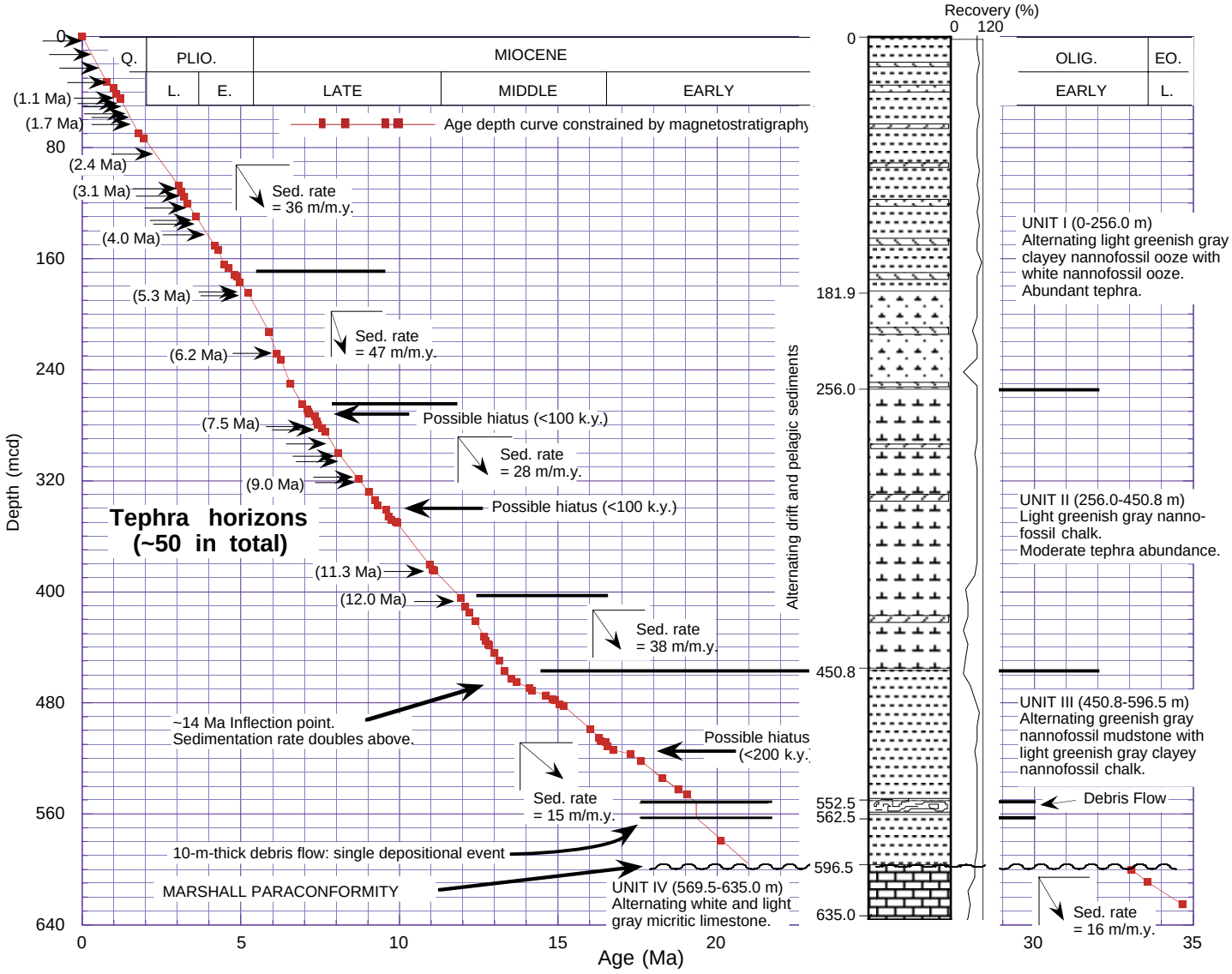

Figure F24. Composite sections for magnetic susceptibility and reflectance percentage at 550 nm. For convenience, MS values from Holes 1123B and 1123C are offset by 5 × 10^{-5} and 10 × 10^{-5}, respectively, and reflectance values are offset by 25% and 50%, respectively. Cores are indicated by small numbers. Data from disturbed intervals (typically "soupy" sediment at core tops and flow-in) have been removed. (Continued on next two pages).

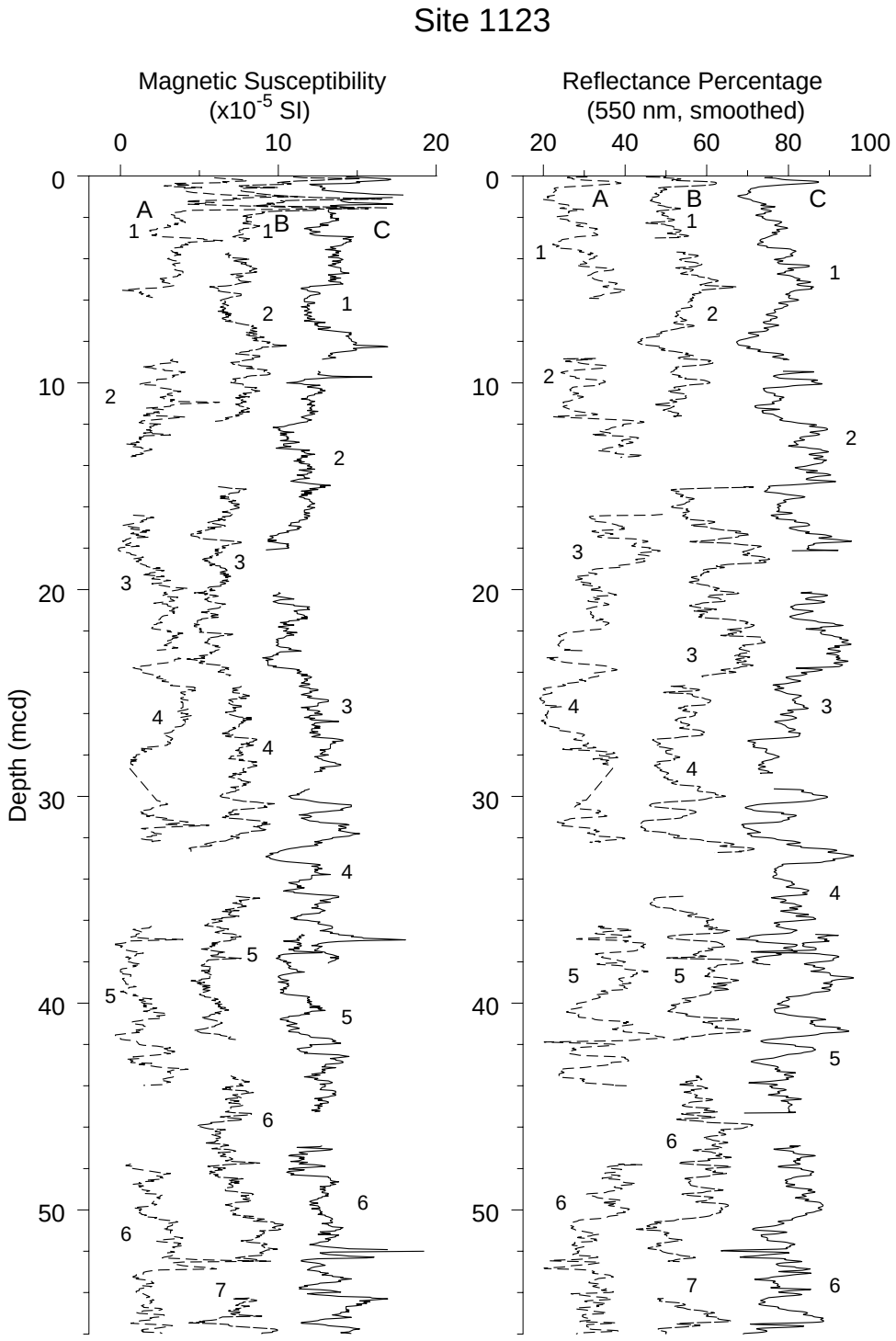

Figure F24 (continued).

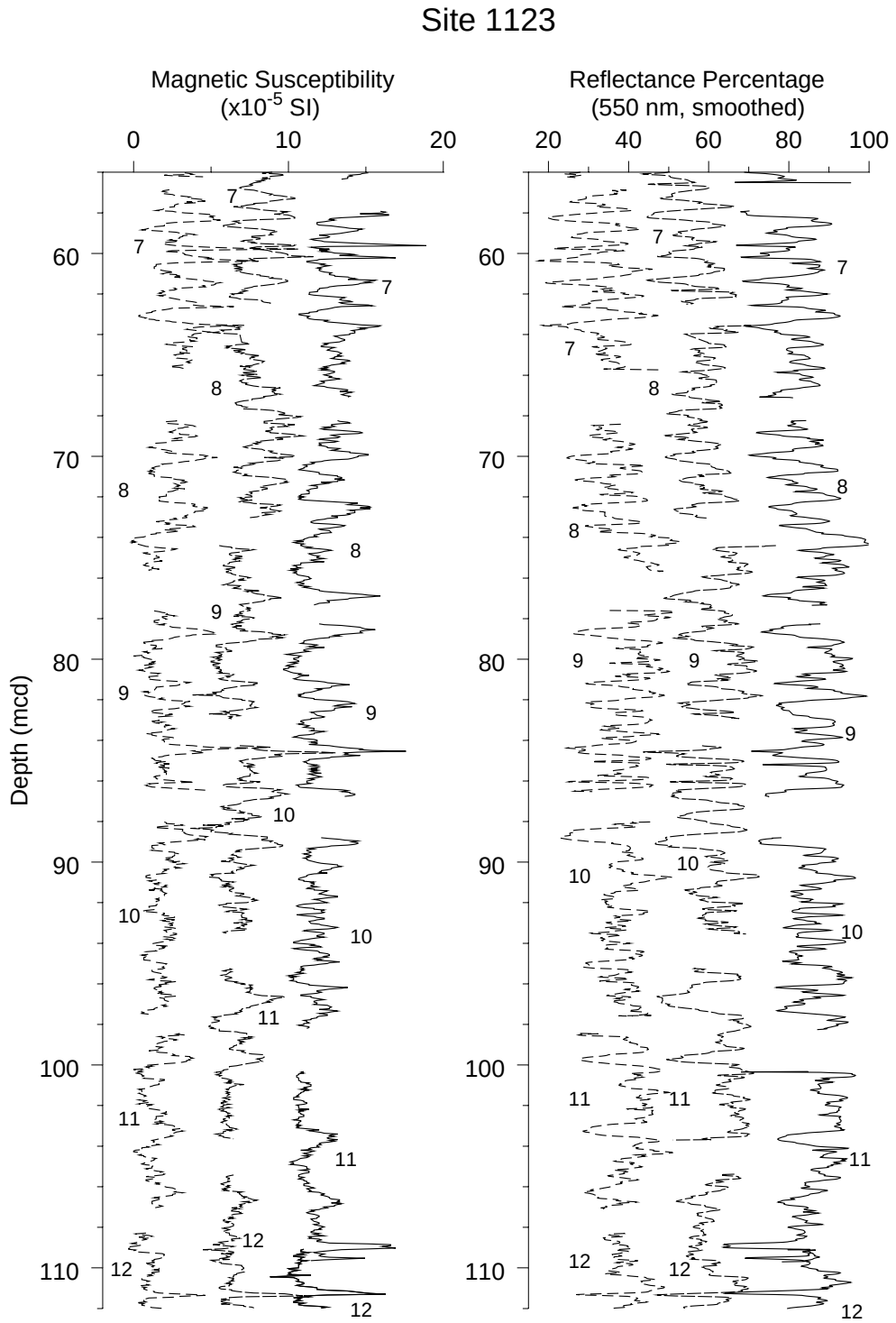

Figure F24 (continued).

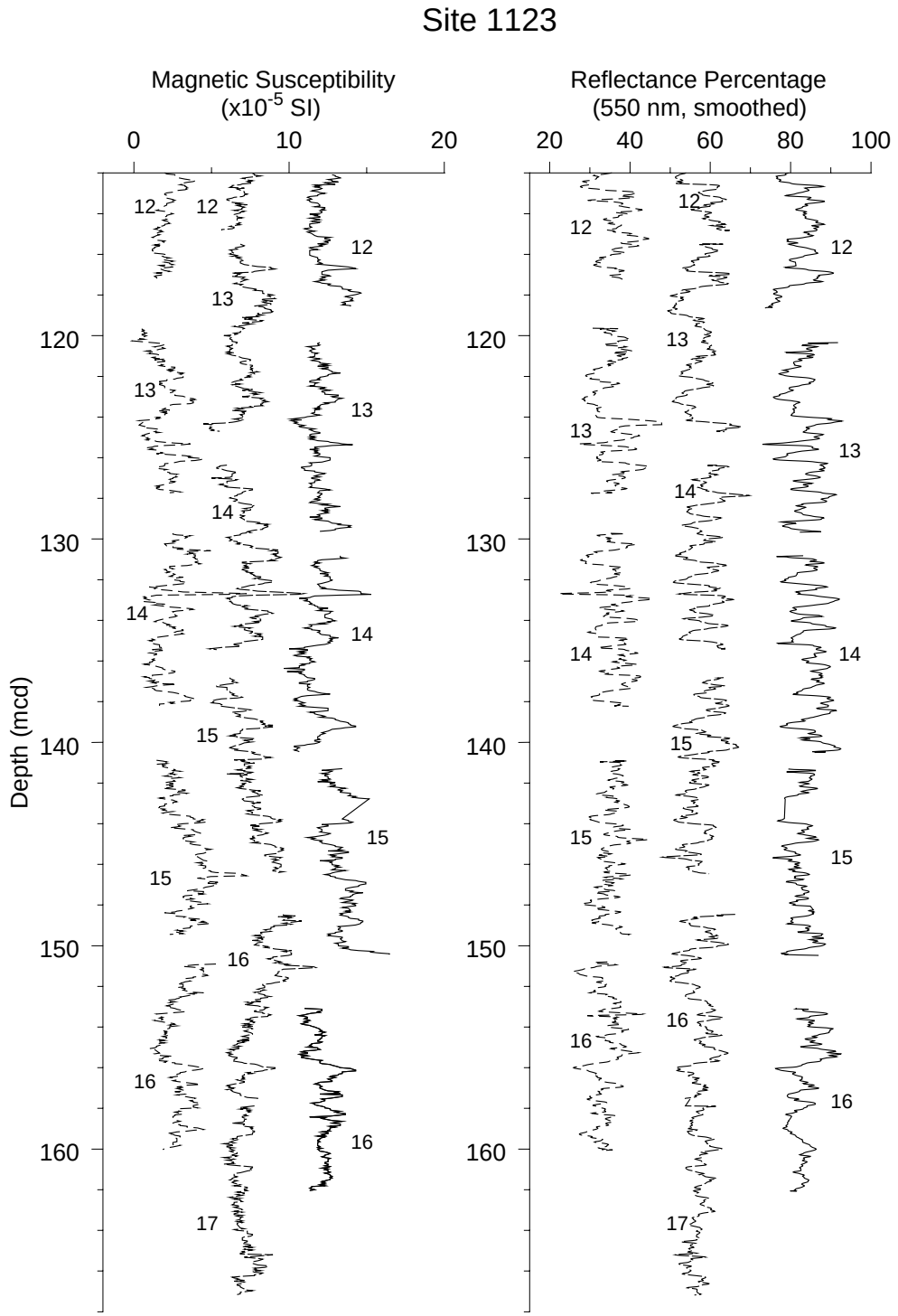

Figure F25. Downhole depth offsets between the mbsf and mcd scales for Site 1123. The solid line indicates the trend for a typical 10% stretch model between mbsf and mcd depths; the dashed line parallels this trend. Composite depth offsets below ~40 mbsf parallel the 10% stretch model.

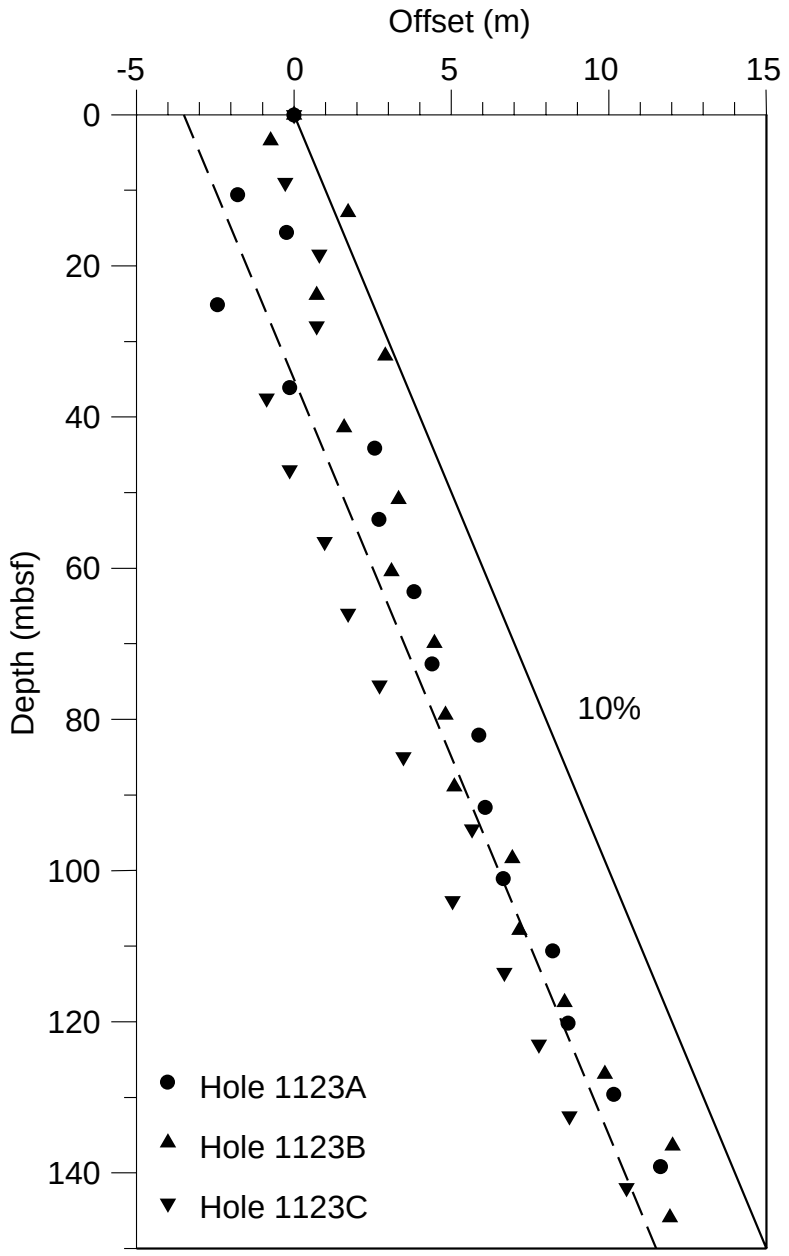

Figure F26. Spliced record for Site 1123. To reduce noise, MS and reflectance data illustrated were smoothed with a 13-cm Gaussian window. Core 181-1123C-11H is plotted in its entirety, offset from the splice, to illustrate the recovery of a 20-cm tephra in this core that was not recovered in Hole 1123A or 1123B (Fig. F24, p. 83). This tephra is excluded from the splice. C1 = Core 181-1123C-1H, B2 = Core 181-1123B-2H, and so on.

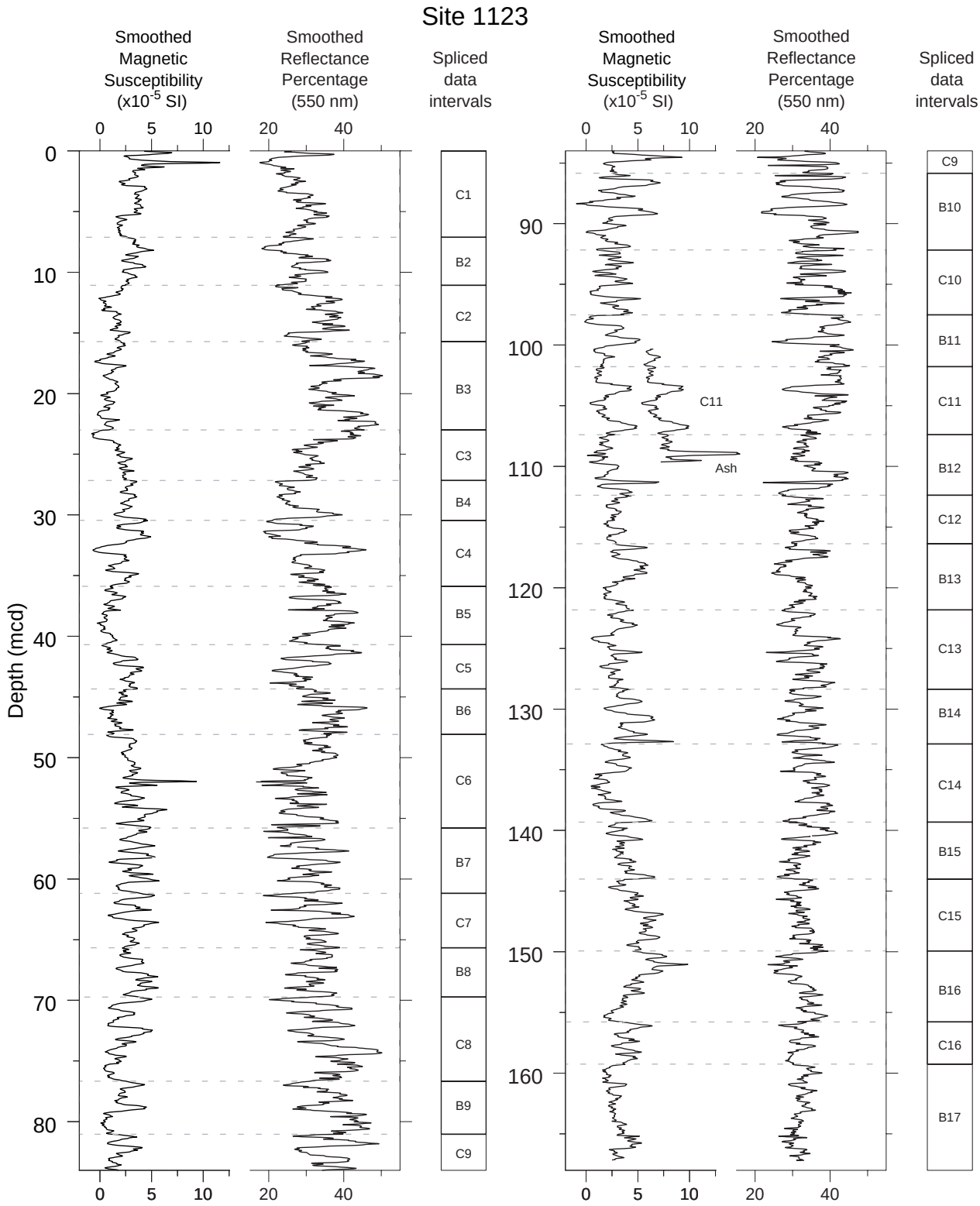

Figure F27. Overlap (composite section) for Cores 181-1123B-51X and 52X and Cores 181-1123C-18X and 19X illustrated with MS and paleomagnetic inclination data (after 20-mT alternating-field demagnetization). The paleomagnetic reversal between Chrons C5Br and C5Cn.1n is aligned between Holes 1123B and 1123C. The paleomagnetic excursion in Core 181-1123B-52X near 495.3 mcd does not appear in Core 181-1123C-18X, although the match between the two holes is unambiguous based on MS records. This excursion will be investigated postcruise.

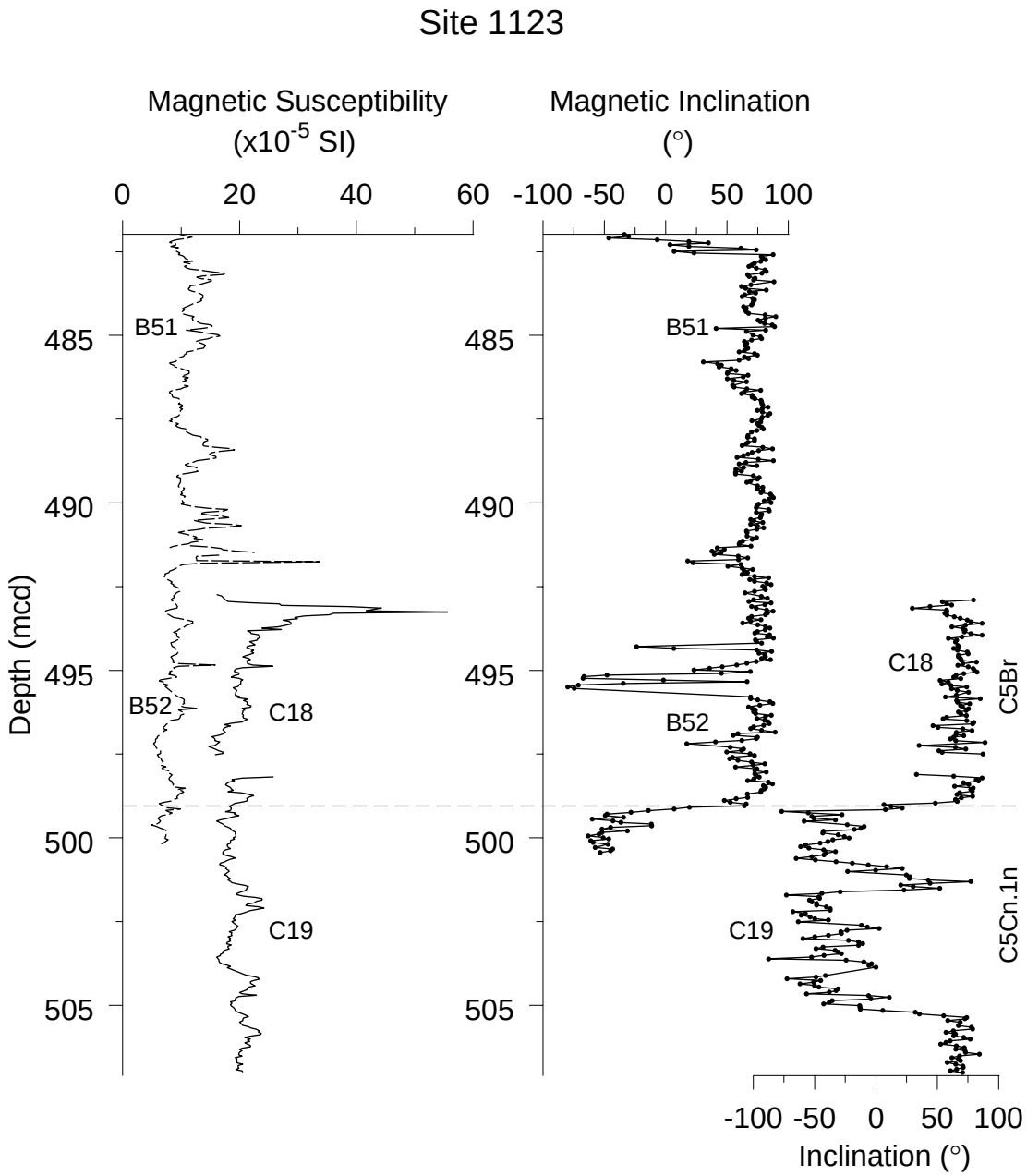

Figure F28. Reflectance percentage from Site 1123 with benthic oxygen isotope data from ODP Site 849 (Mix et al., 1995b) for 0–3 Ma. The shape of the reflectance data mirrors oxygen isotopes over much of the extent of the splice (to ~4.6 Ma) and will provide an excellent opportunity for development of an orbitally tuned age model at this site.

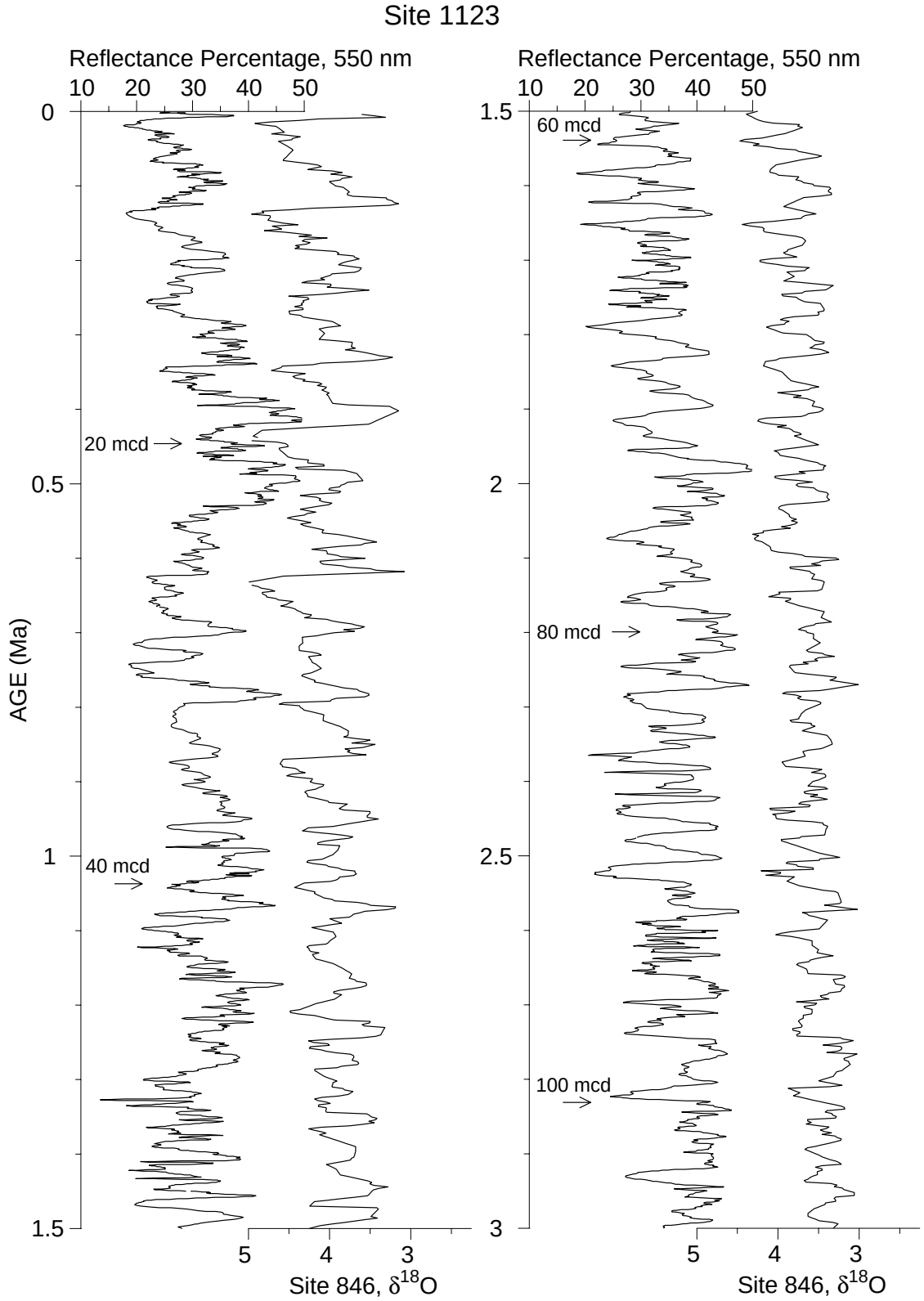

Figure F29. Age-depth plot using 112 foraminifer, nannofossil, diatom, and radiolarian age assignments for Site 1123. Because of the size of the plot, strongly or fully overlapping event positions may be obscured in the graph, seemingly accounting for fewer than 112 points. All depths are reported in mcd values. The plot of events is rather tightly clustered and shows fairly good coherence. The solid line indicates the paleomagnetic age model from **"Paleomagnetism,"** p. 26. It approximates a remarkably constant average rate of sedimentation through the last 20 Ma of ~3.5 cm/k.y. (35 m/m.y.). No estimates are available for the amount of sediment possibly eroded during middle to late Oligocene time, following late Eocene through early Oligocene sedimentation.

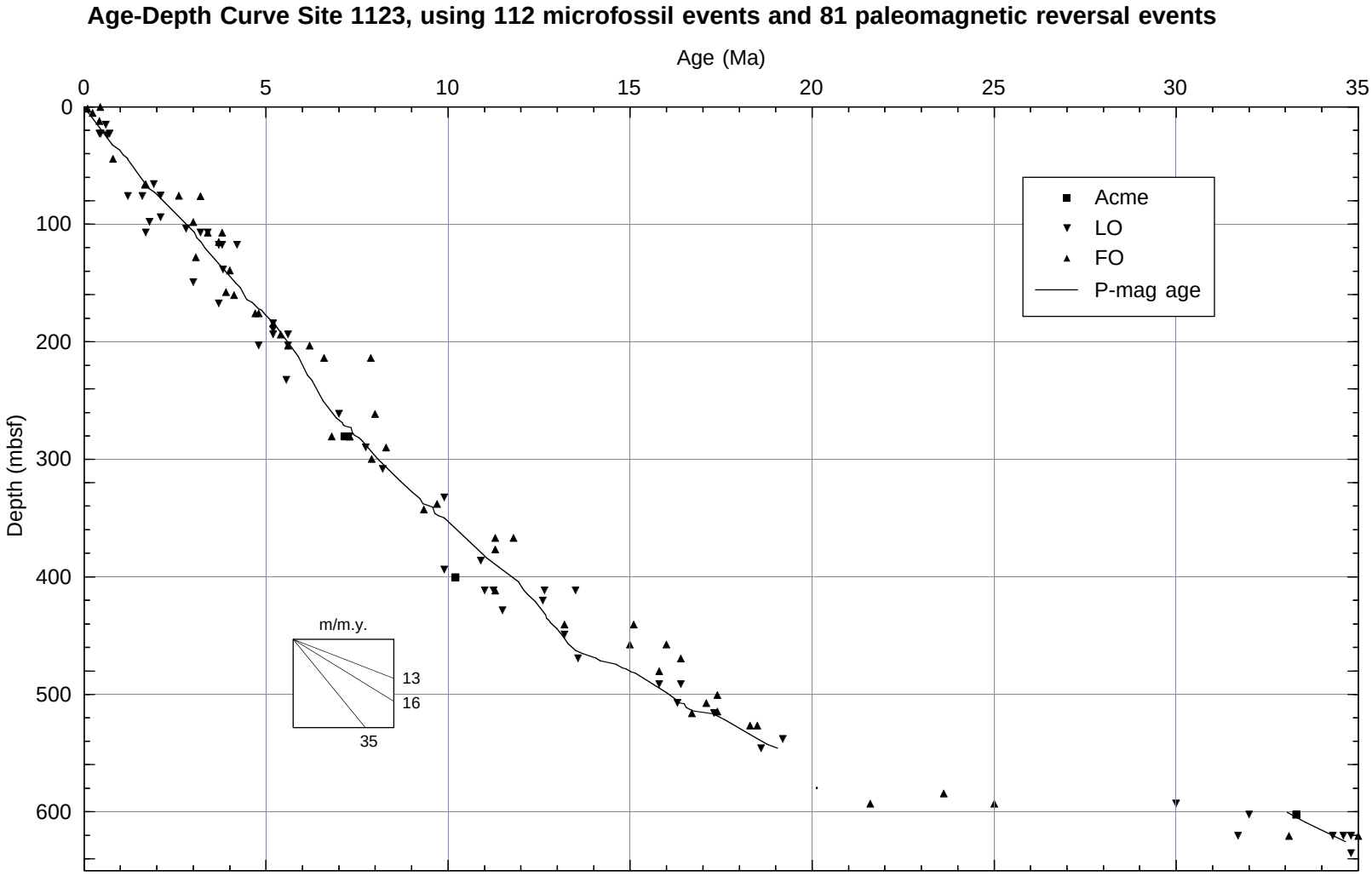

Figure F30. Site 1123 restored sedimentation rate for upper Eocene through Neogene strata.

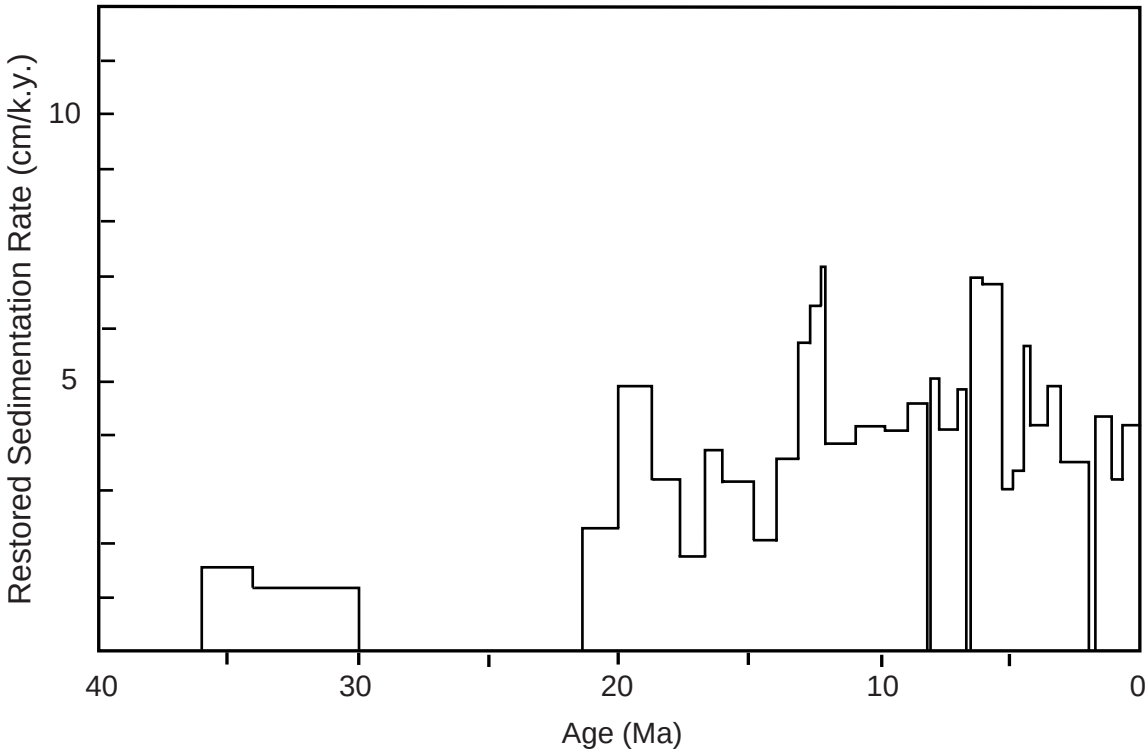

Figure F31. Burial curve for late Eocene through Neogene limestone, chalk, and ooze at Site 1123. Age levels have been smoothed to only encompass discrete levels of 5 m or more. No paleo–water depth has been taken into account.

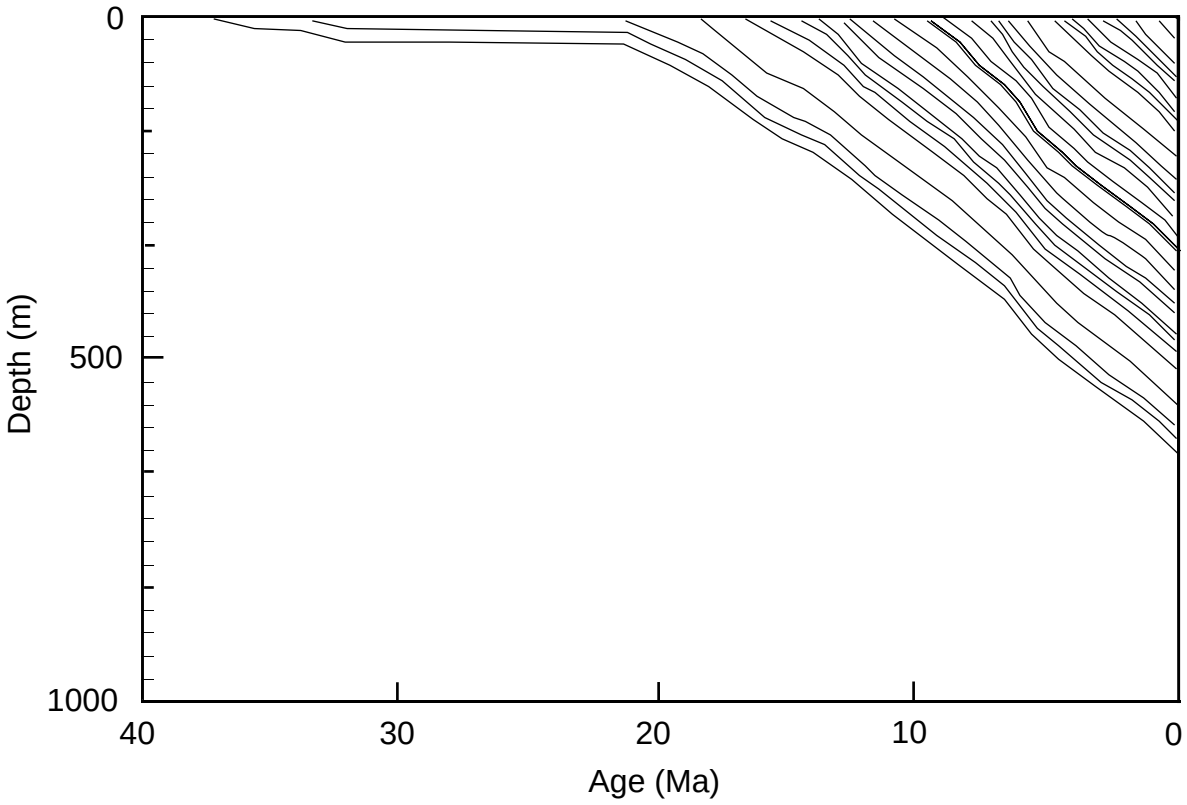

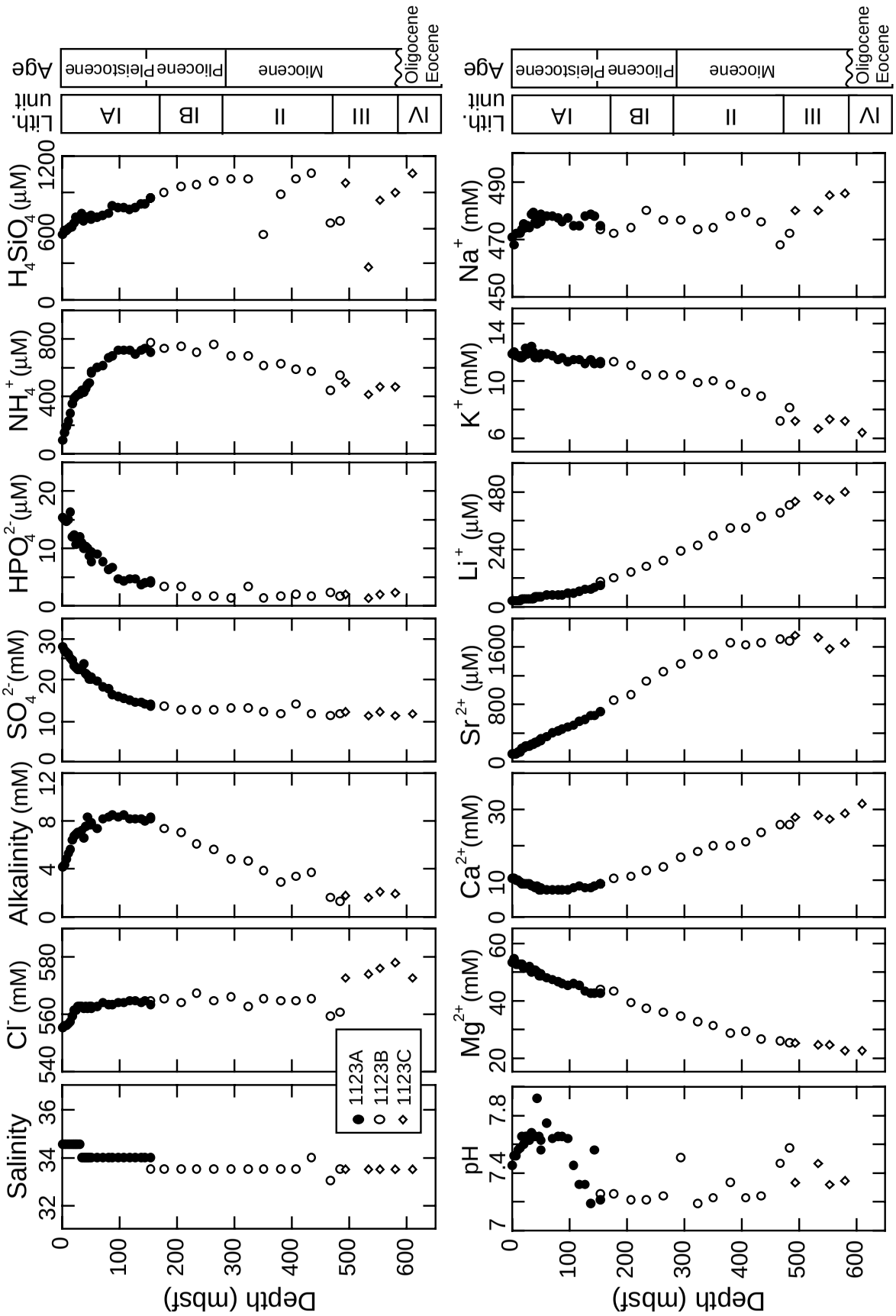

Figure F32. Depth profiles of interstitial-water constituents at Site 1123.

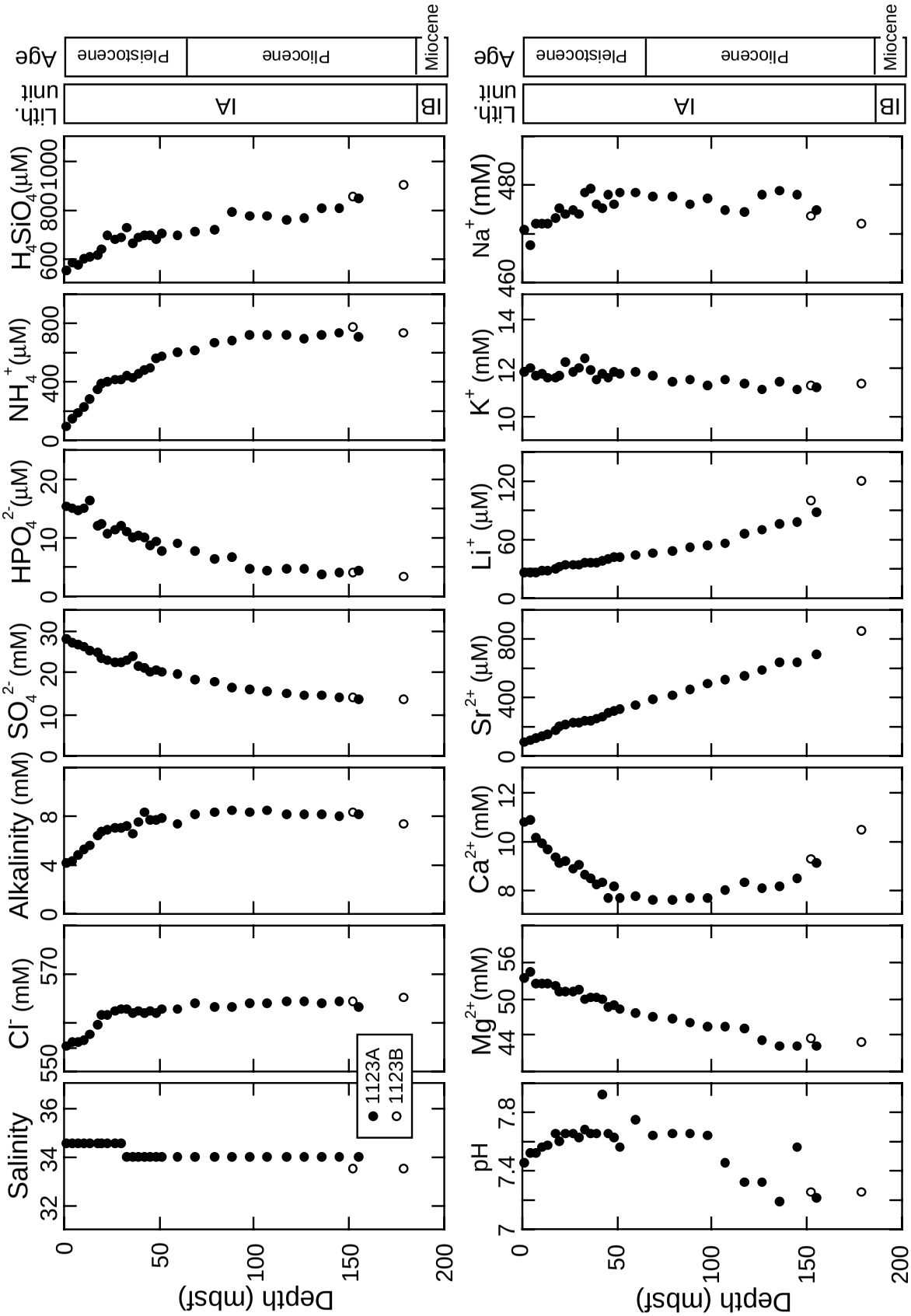

Figure F33. Depth profiles of interstitial-water constituents in the upper part of the section (<200 mbsf) at Site 1123.

Figure F34. Depth profiles of dissolved silica in interstitial water and group abundance and preservation of radiolarian fauna of core-catcher samples at Site 1121. Symbols of ranks based on microscopic observations are as follows: B = barren; T = trace; VR = very rare; R = rare; F = few; C = common; A = abundant; VA = very abundant, P = poor; M = moderate; G = good; VG = very good.

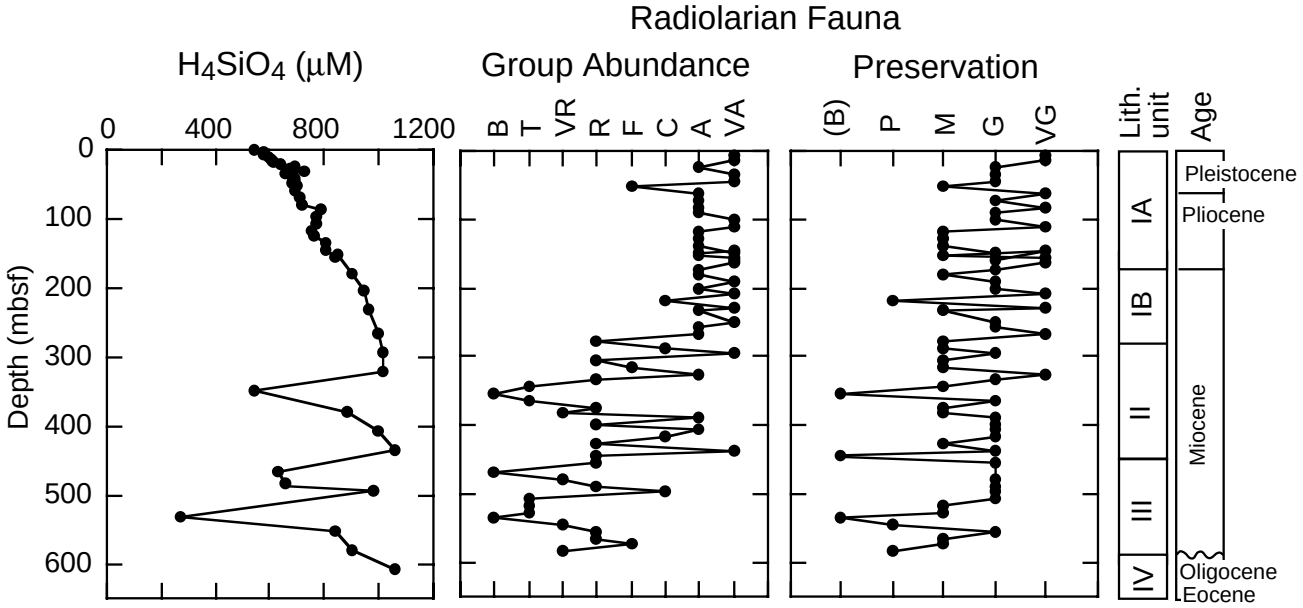

Figure F35. Carbonate contents in sediments from Holes 1123A, 1123B, and 1123C.

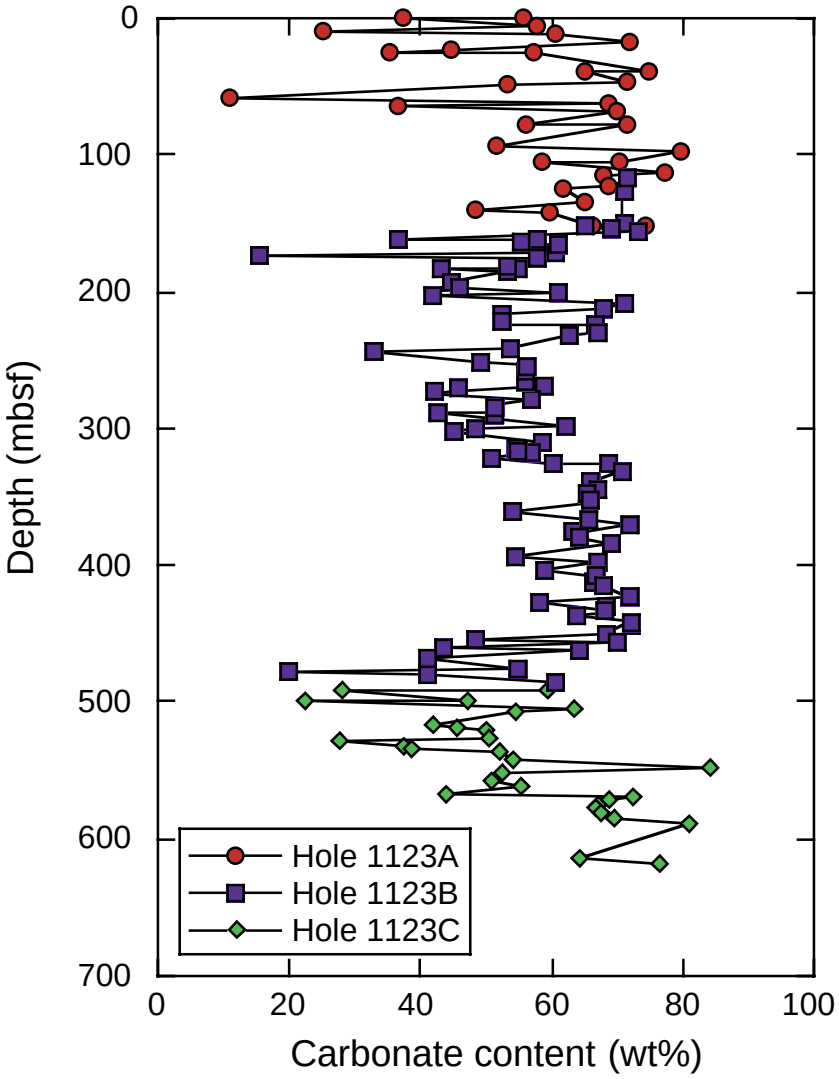

Figure F36. Organic carbon contents in sediments from Holes 1123A, 1123B, and 1123C.

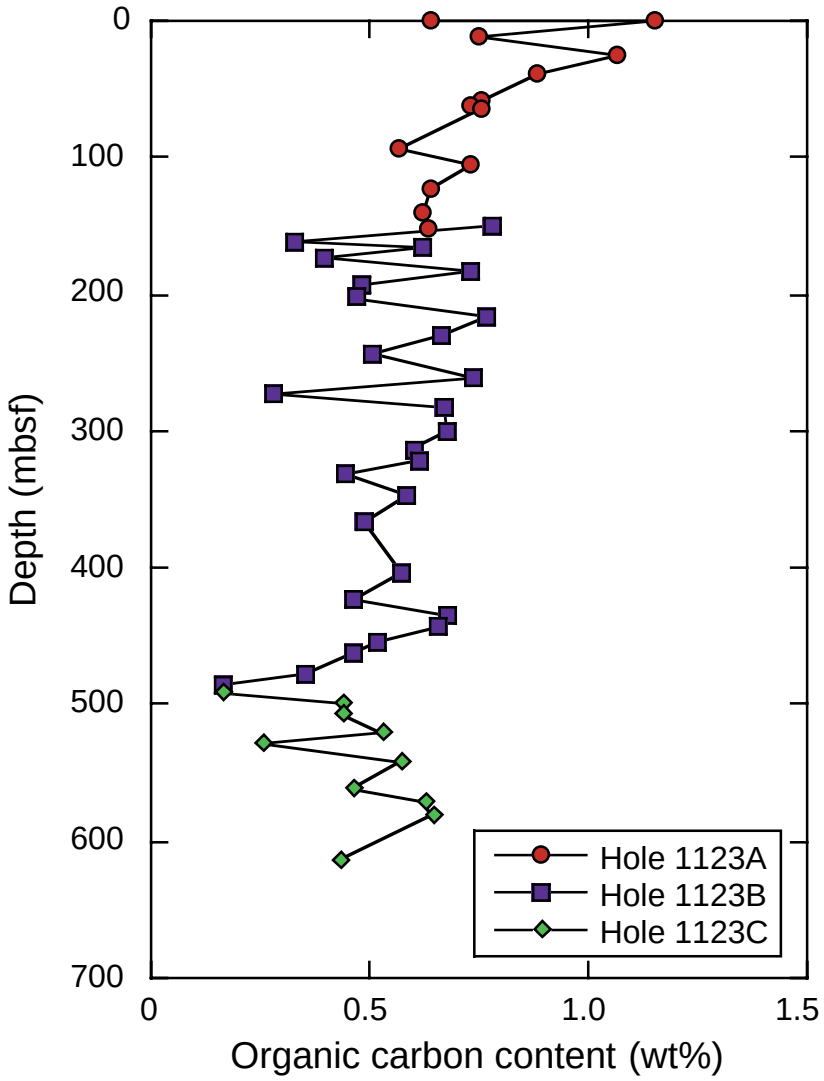

Figure F37. Rock-Eval van Krevelen–type diagram of samples from Site 1123 with kerogen-type lines (I–III).

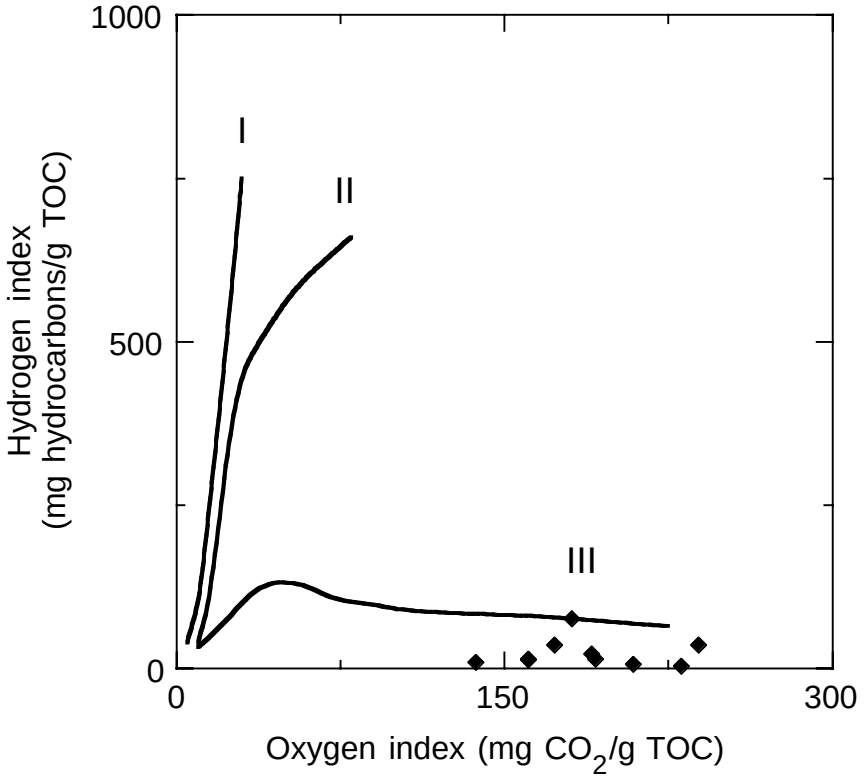

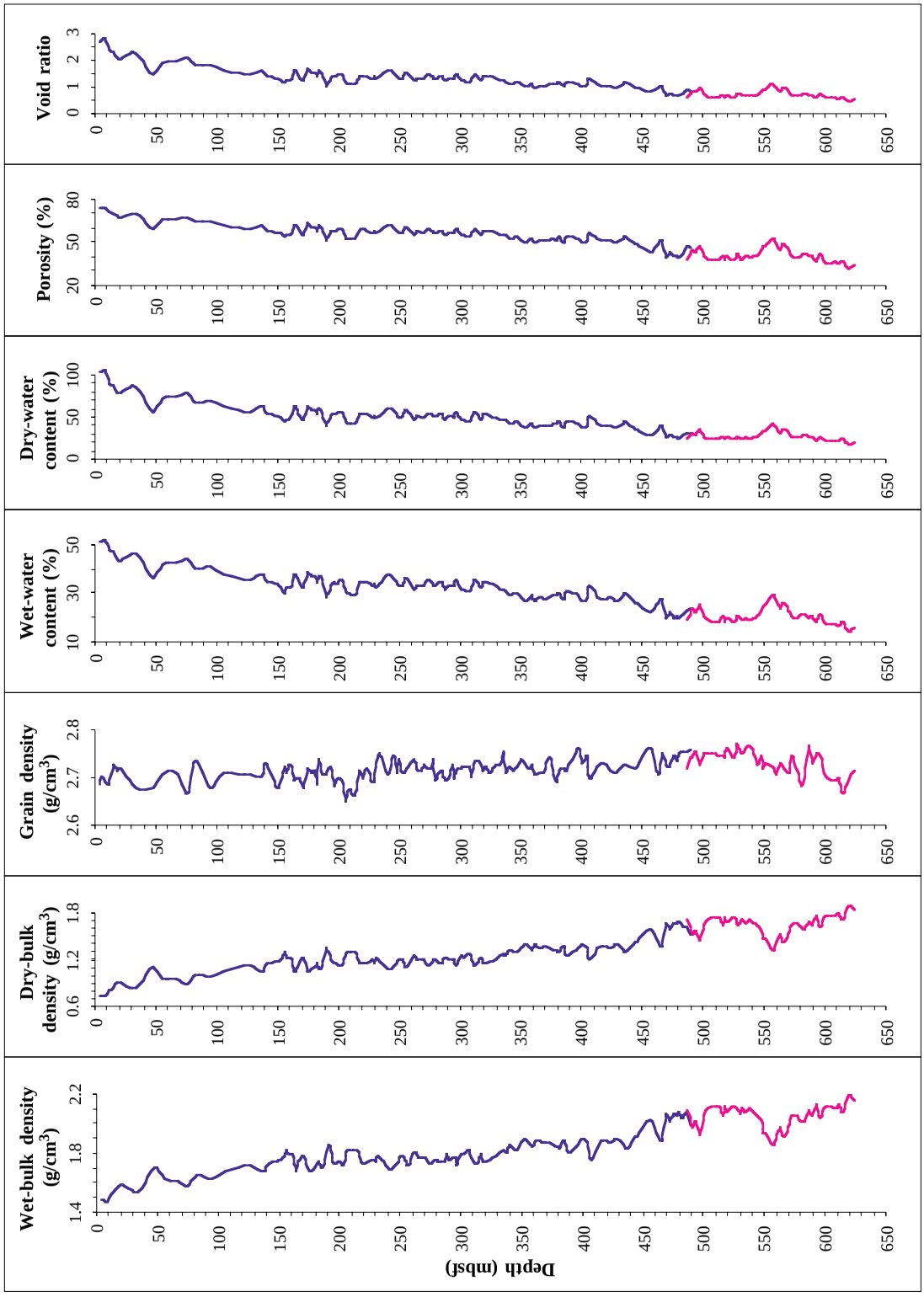

Figure F38. Index properties measurements from cores from Holes 1123B and 1123C.

Figure F39. MST measurements from Hole 1123A including GRAPE density magnetic susceptibility, natural gamma-ray intensity, and *P*-wave velocity. The smoothed *P*-wave velocity data were measured from split cores using the DSV and Hamilton frame velocimeter.

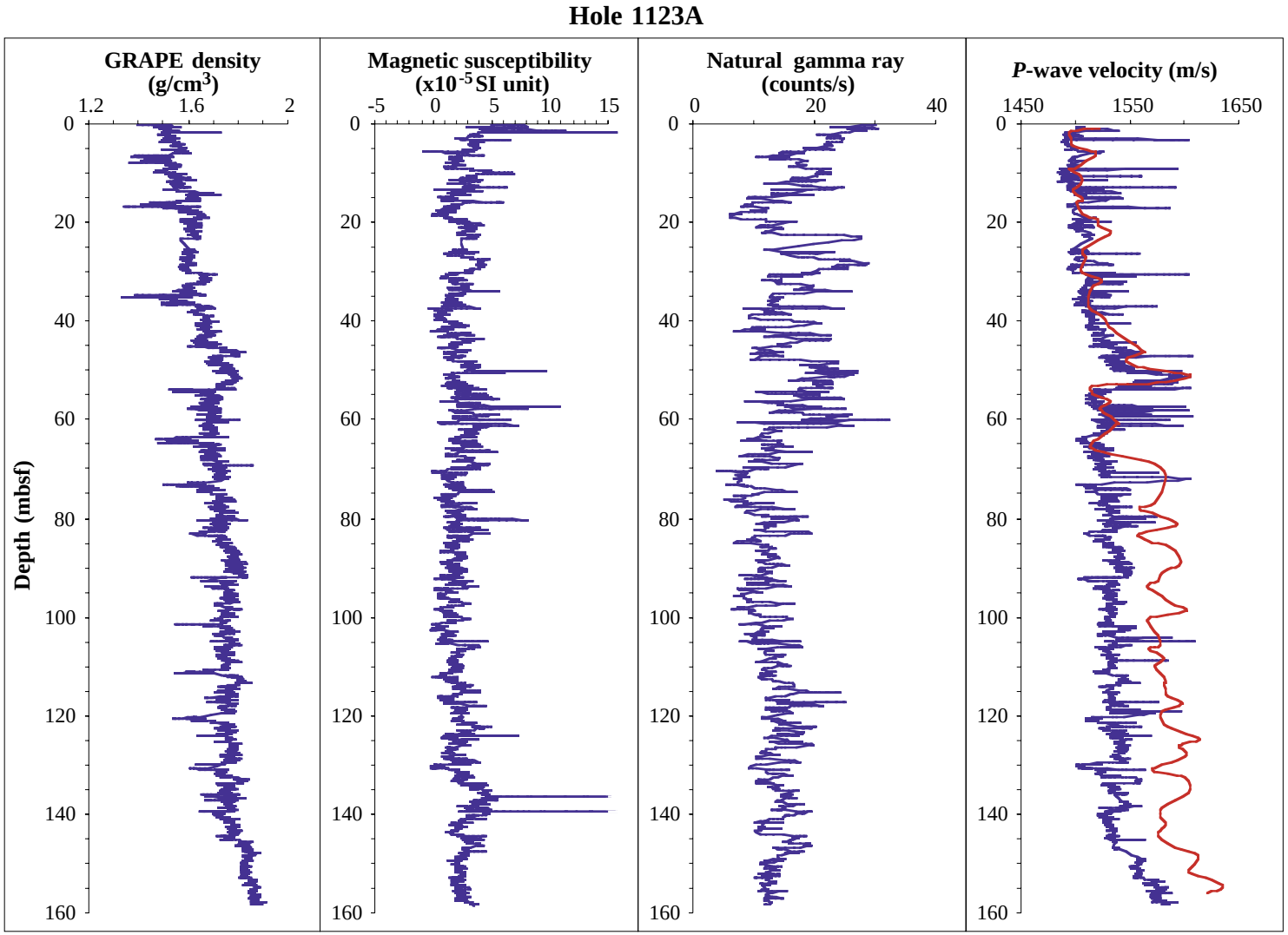

Figure F40. MST measurements from Holes 1123B and 1123C including GRAPE density magnetic susceptibility, natural gamma-ray intensity, and *P*-wave velocity. The Hamilton frame velocimeter was used to measure *P*-wave velocity on split XCB cores.

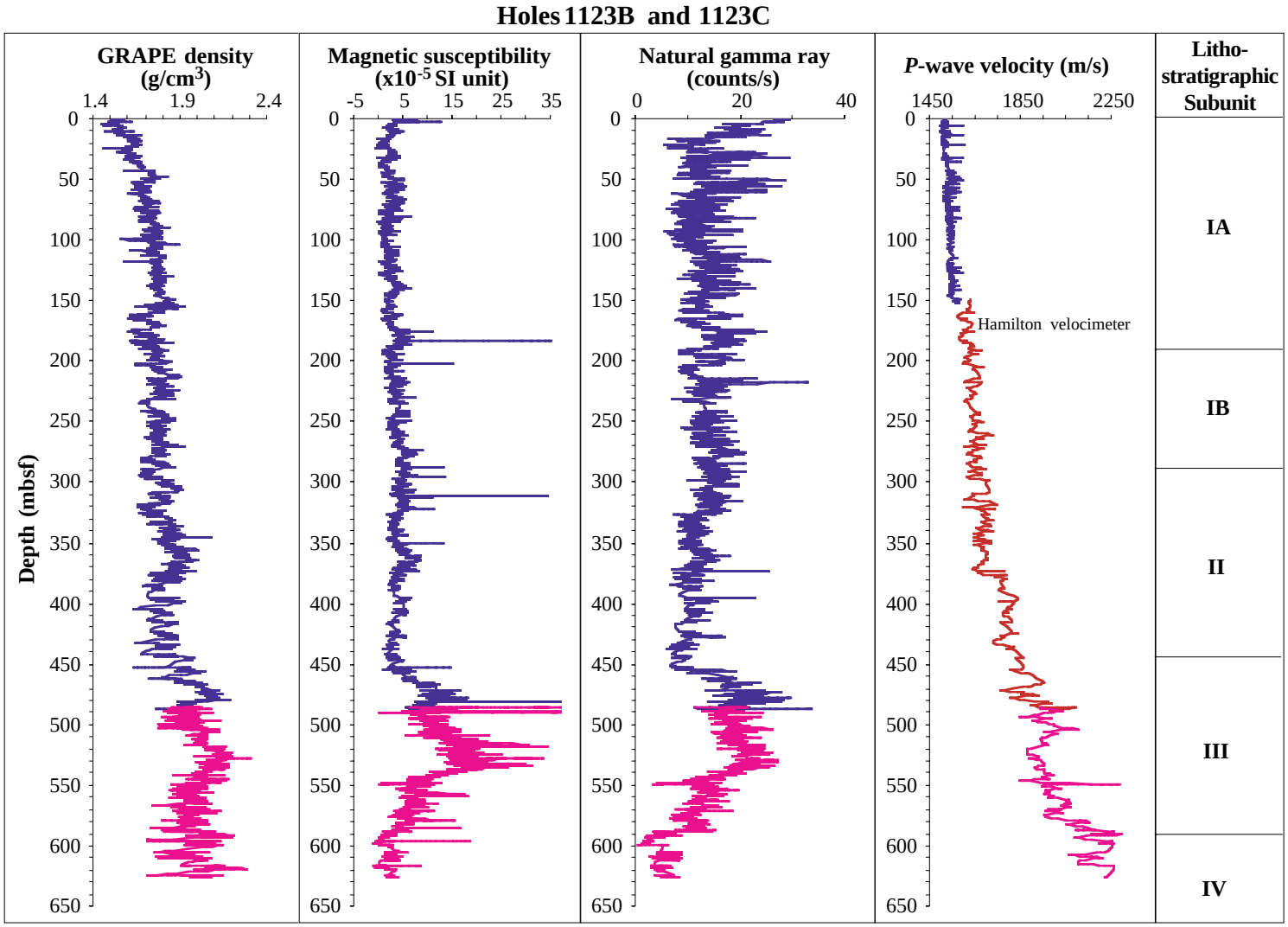

Figure F41. Density measurements in Holes 1123B and 1123C using the GRAPE instrument on the MST in comparison with index properties. The circle and triangle markers indicate the distribution of wet-bulk density based on index properties measurements in Holes 1123B and 1123C, respectively.

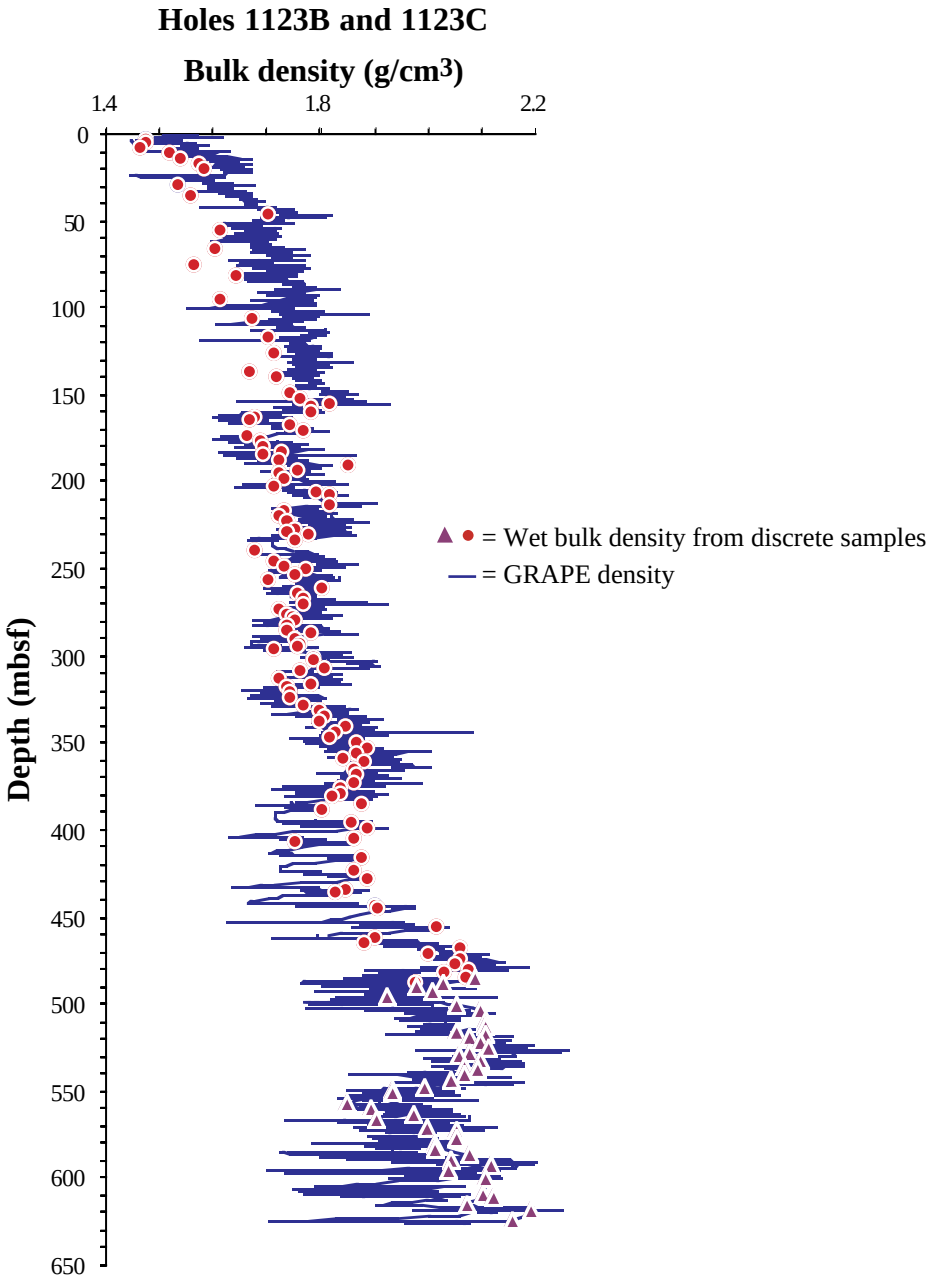

Figure F42. Distribution of shear strength in cores from Holes 1123B and 1123C.

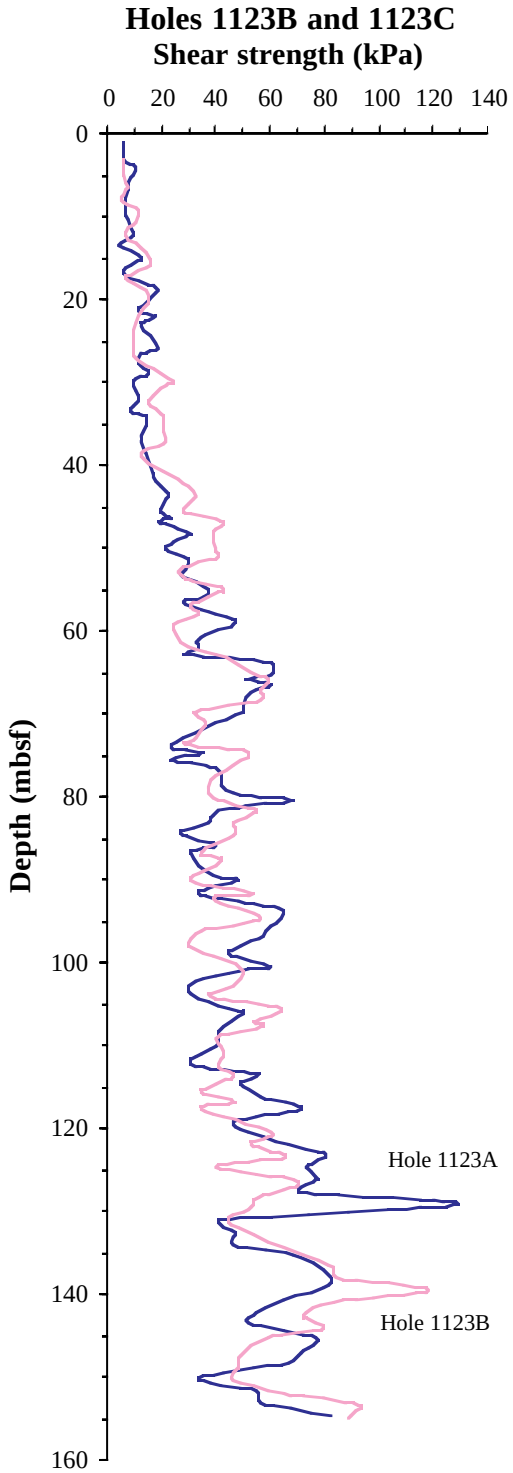

Figure F43. Logging operations in Hole 1123B. The solid lines extending vertically from the pipe show the intervals that were logged. The top of each line shows where logging stopped while the bottom shows where logging started.

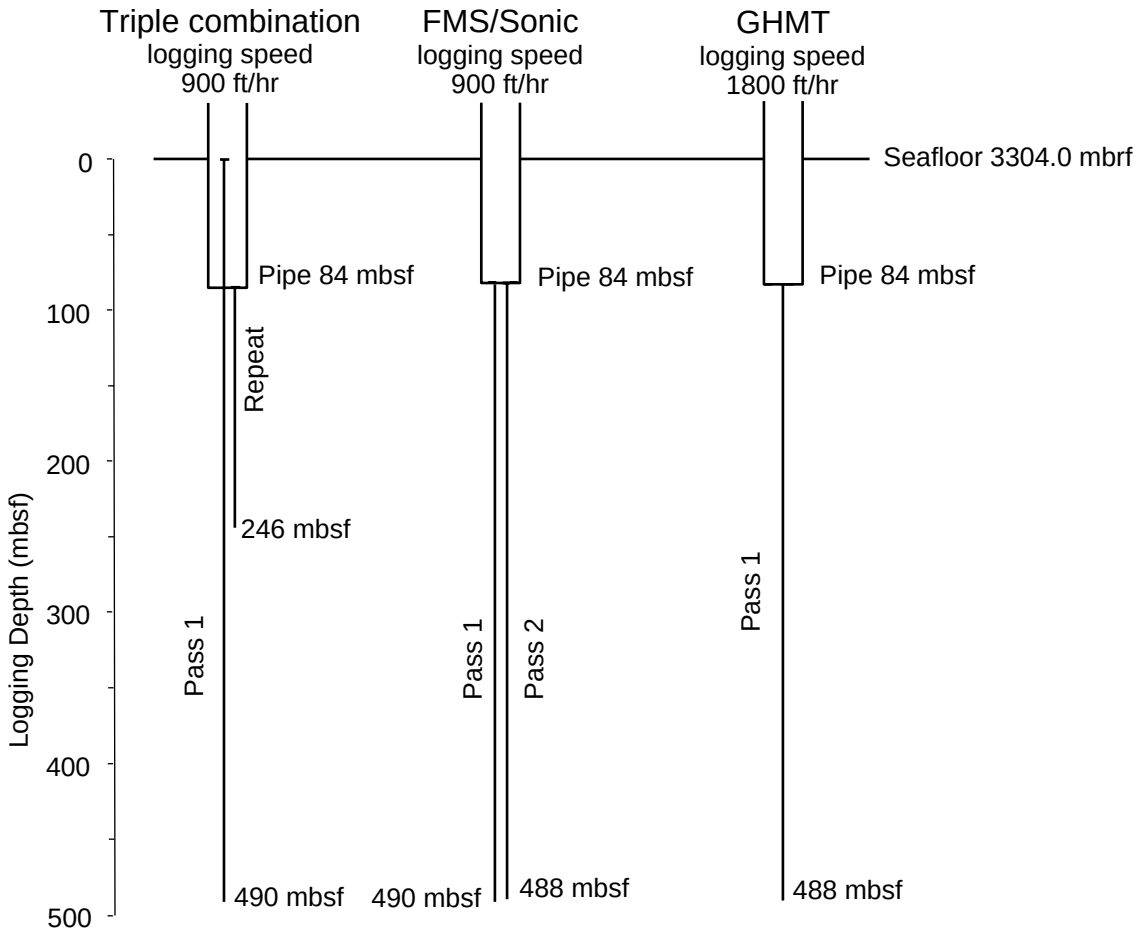

Figure F44. **A.** Caliper, gamma-ray, resistivity, density, and porosity data. (Continued on next page).

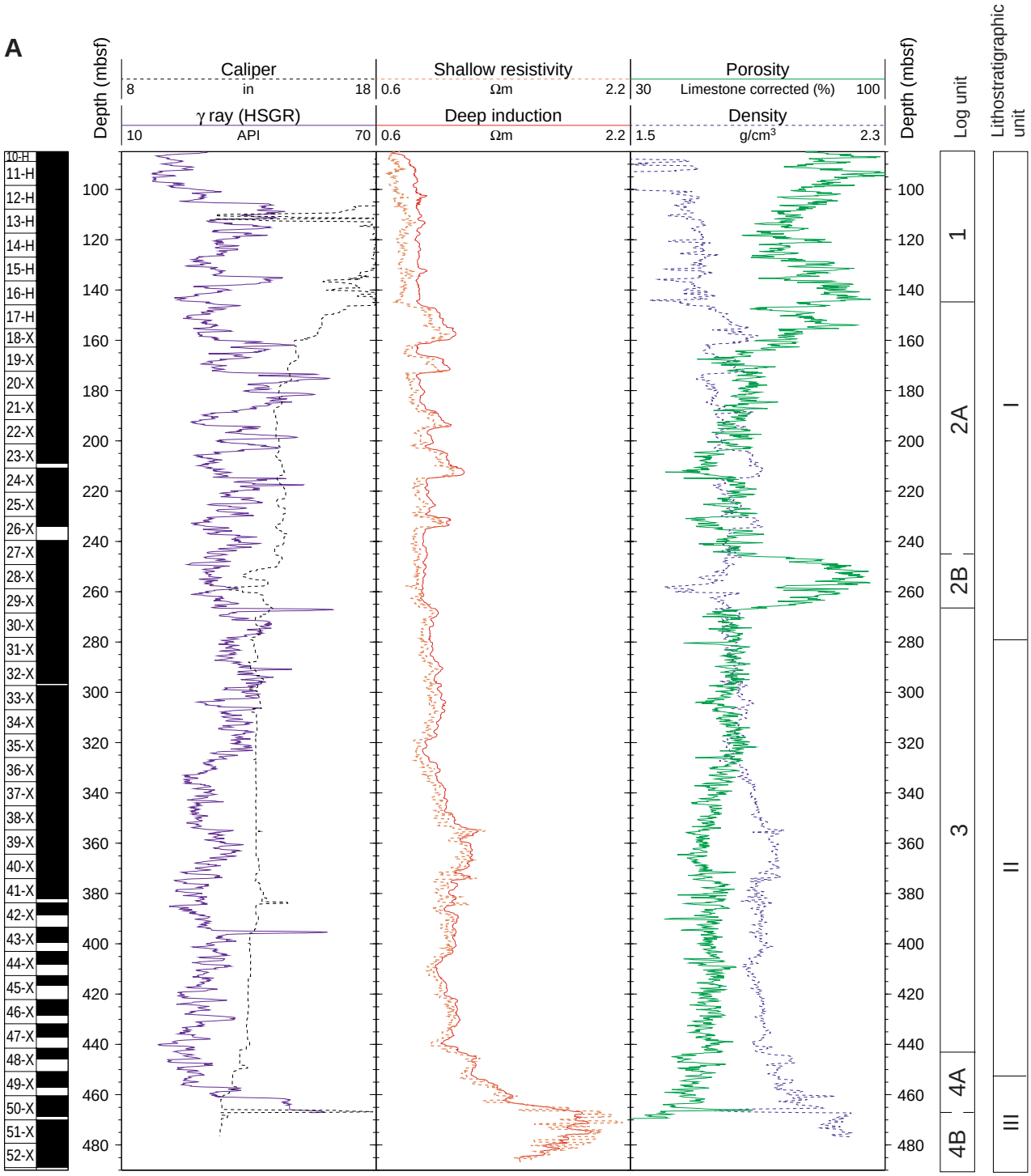

Figure F44 (continued). **B.** Sonic, photoelectric effect, and magnetic susceptibility data.

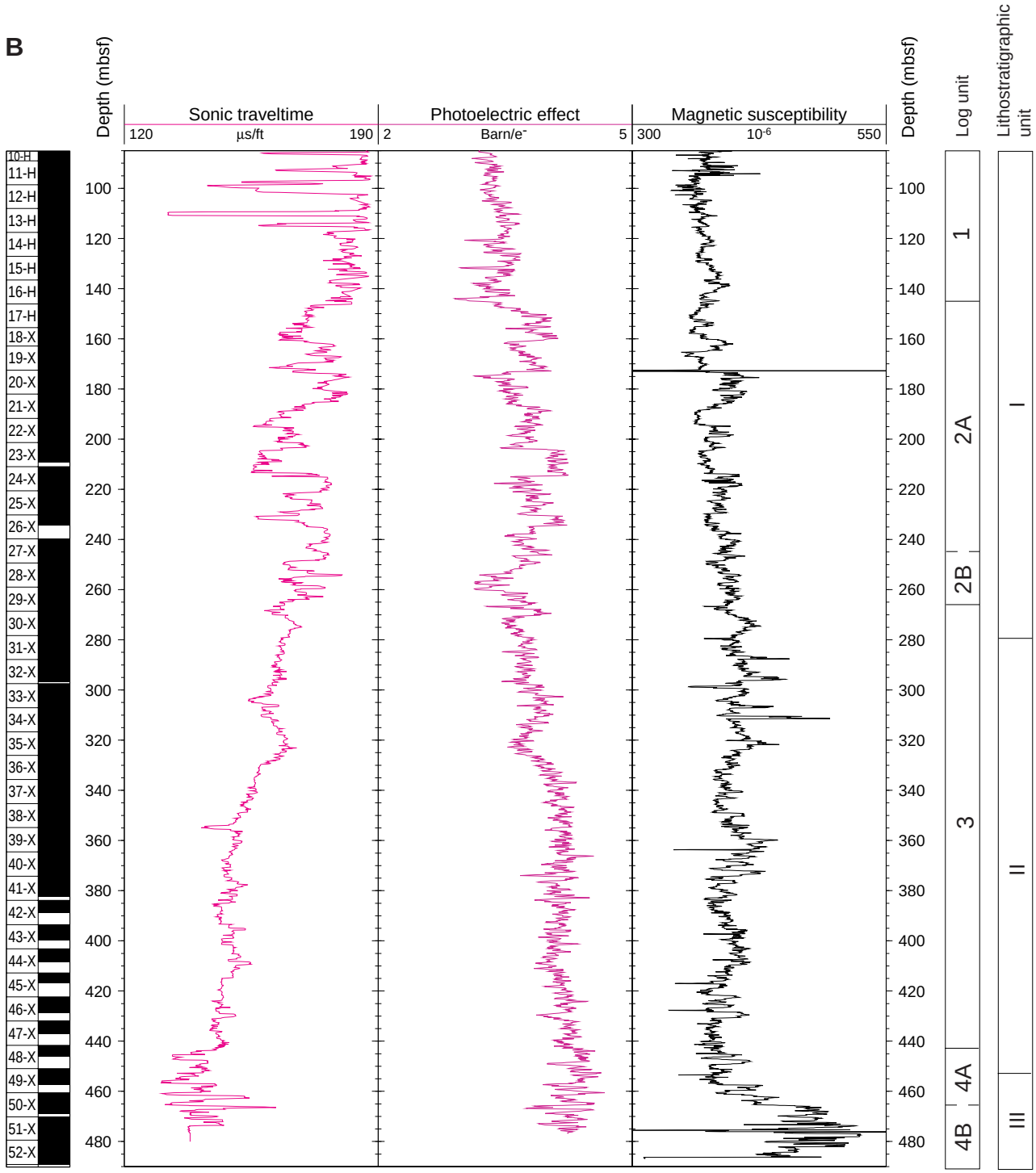

Figure F45. Log bulk density and core-based index bulk density.

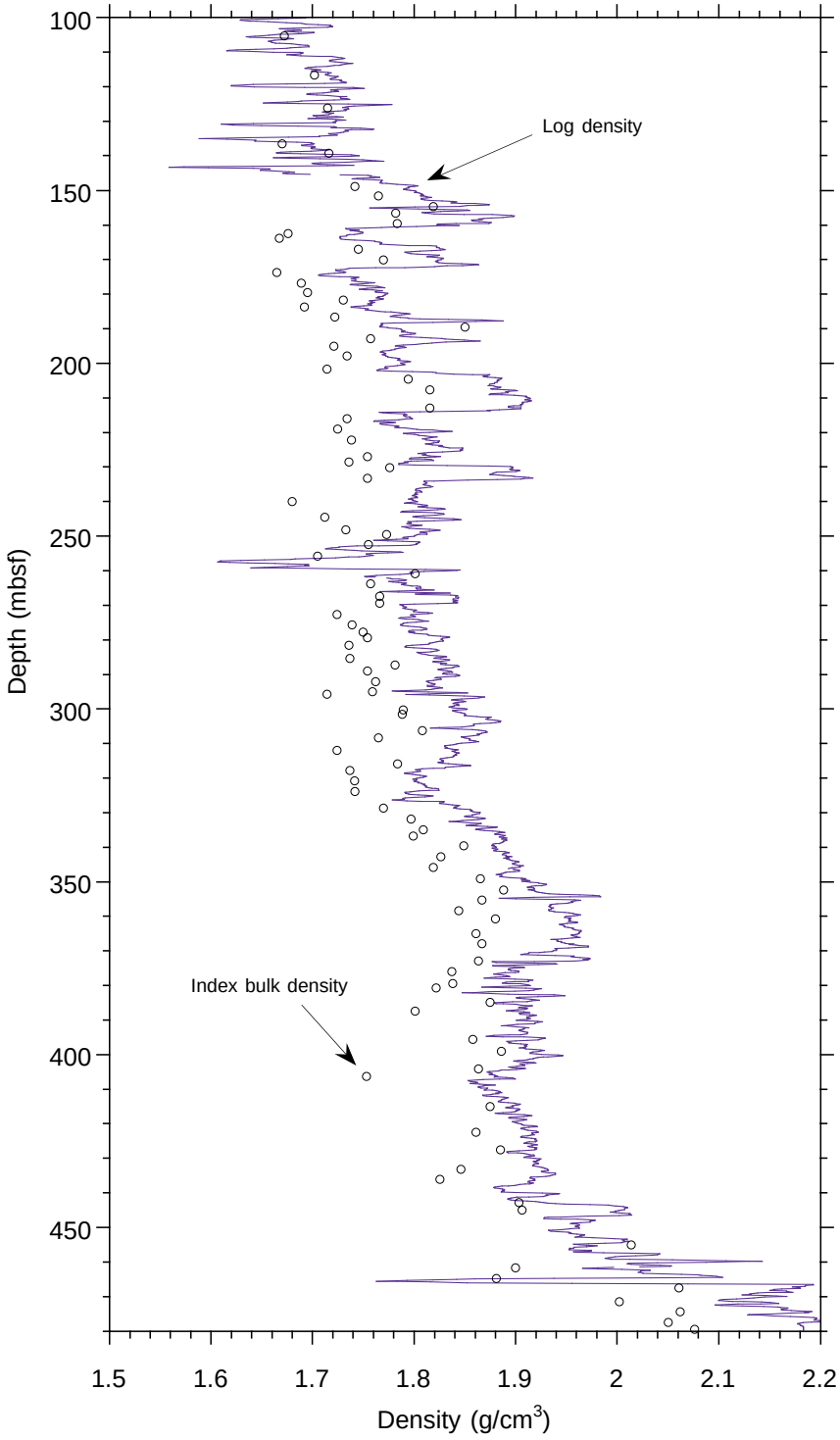

Figure F46. Density and neutron porosities. Density porosity was calculated using matrix density = 2.71 g/cm³ and fluid density = 1.03 g/cm³.

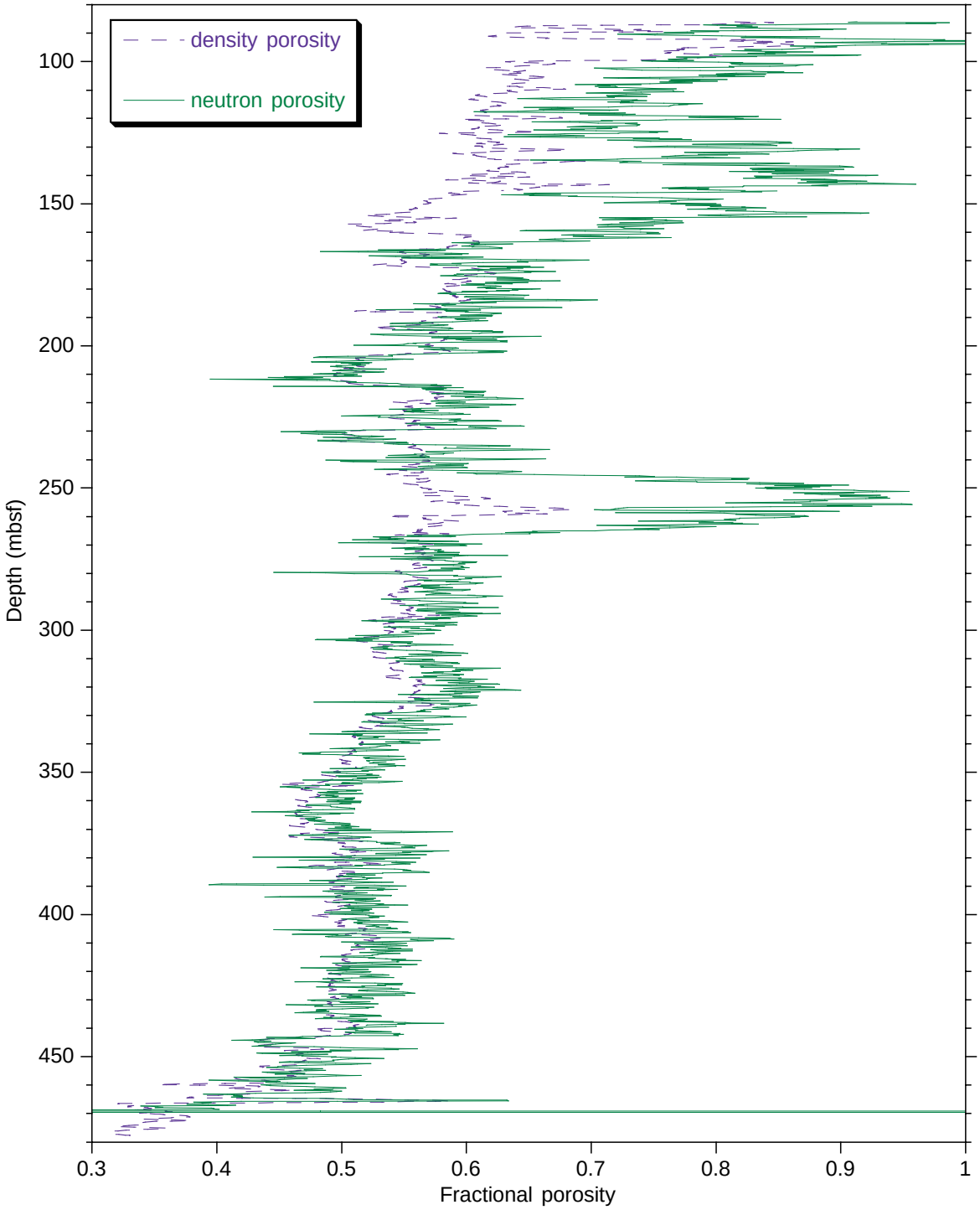

Figure F47. Log and core magnetic susceptibility comparison, after stretching the individual core results to equate with a full 9.5 m of recovery (see **"Paleomagnetism,"** p. 26).

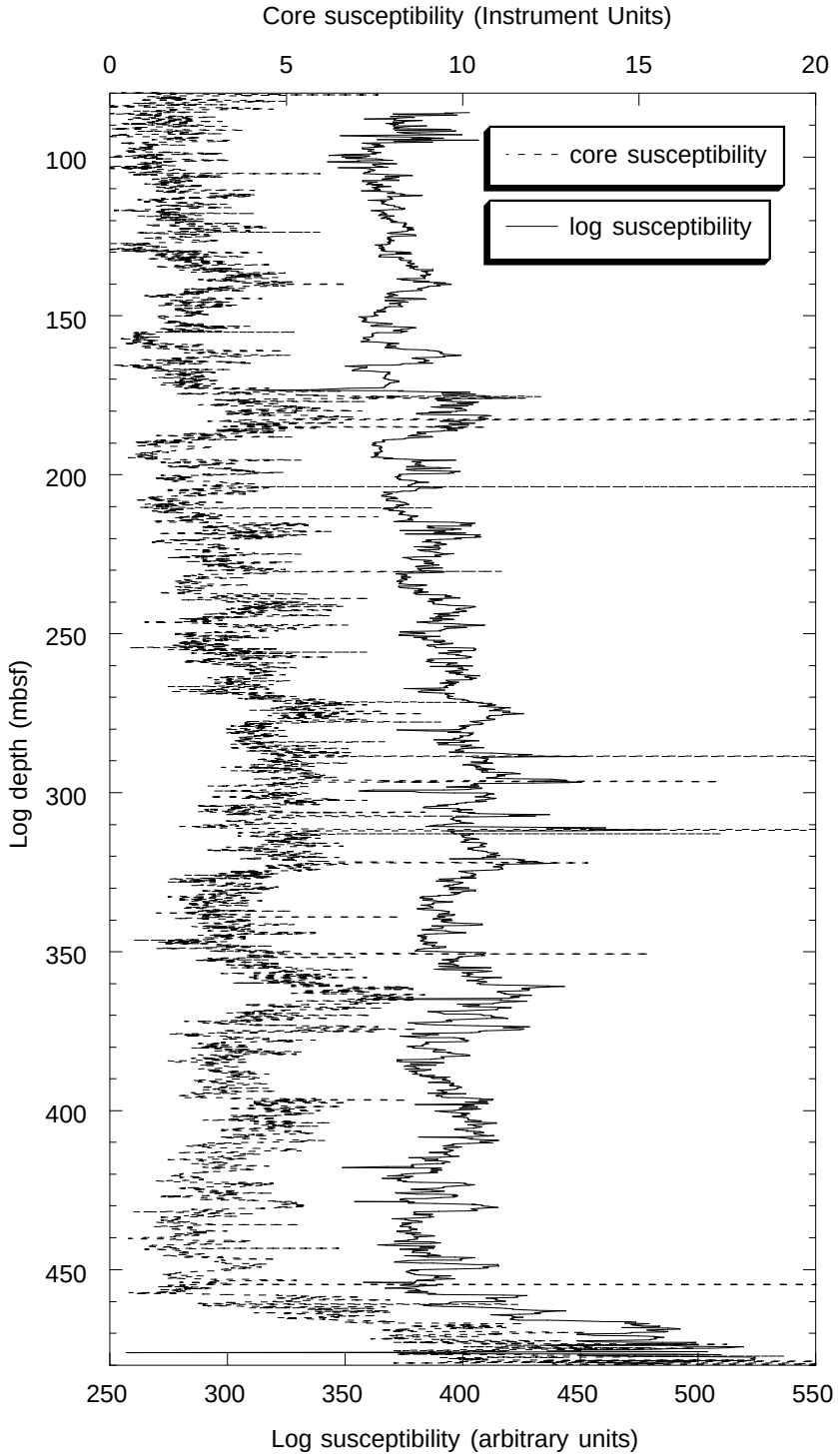

Figure F48. Potassium, thorium, and uranium results from the spectral gamma-ray log.

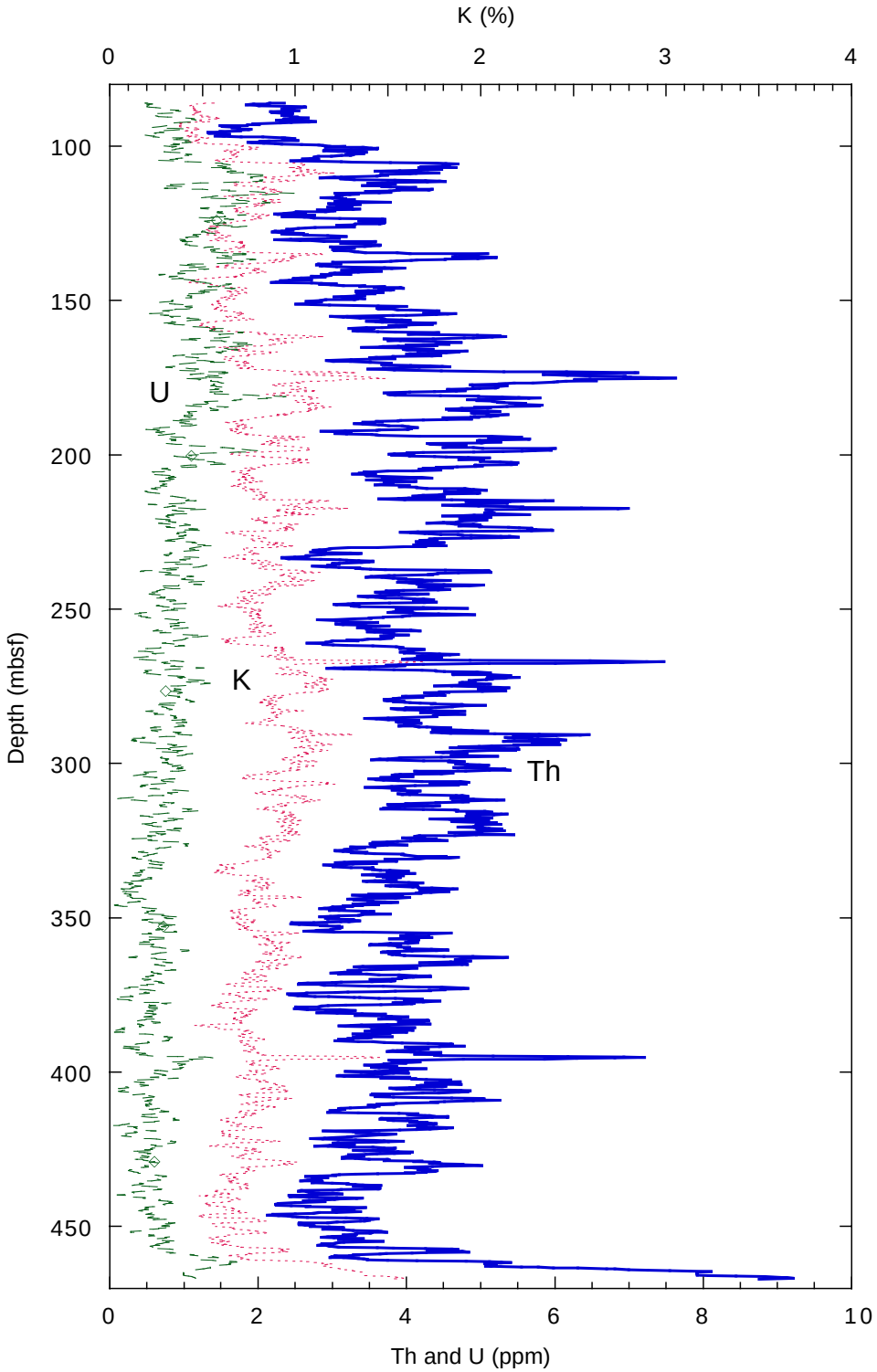

Figure F49. Detailed view of logging Subunit 2A, showing sedimentary cycles.

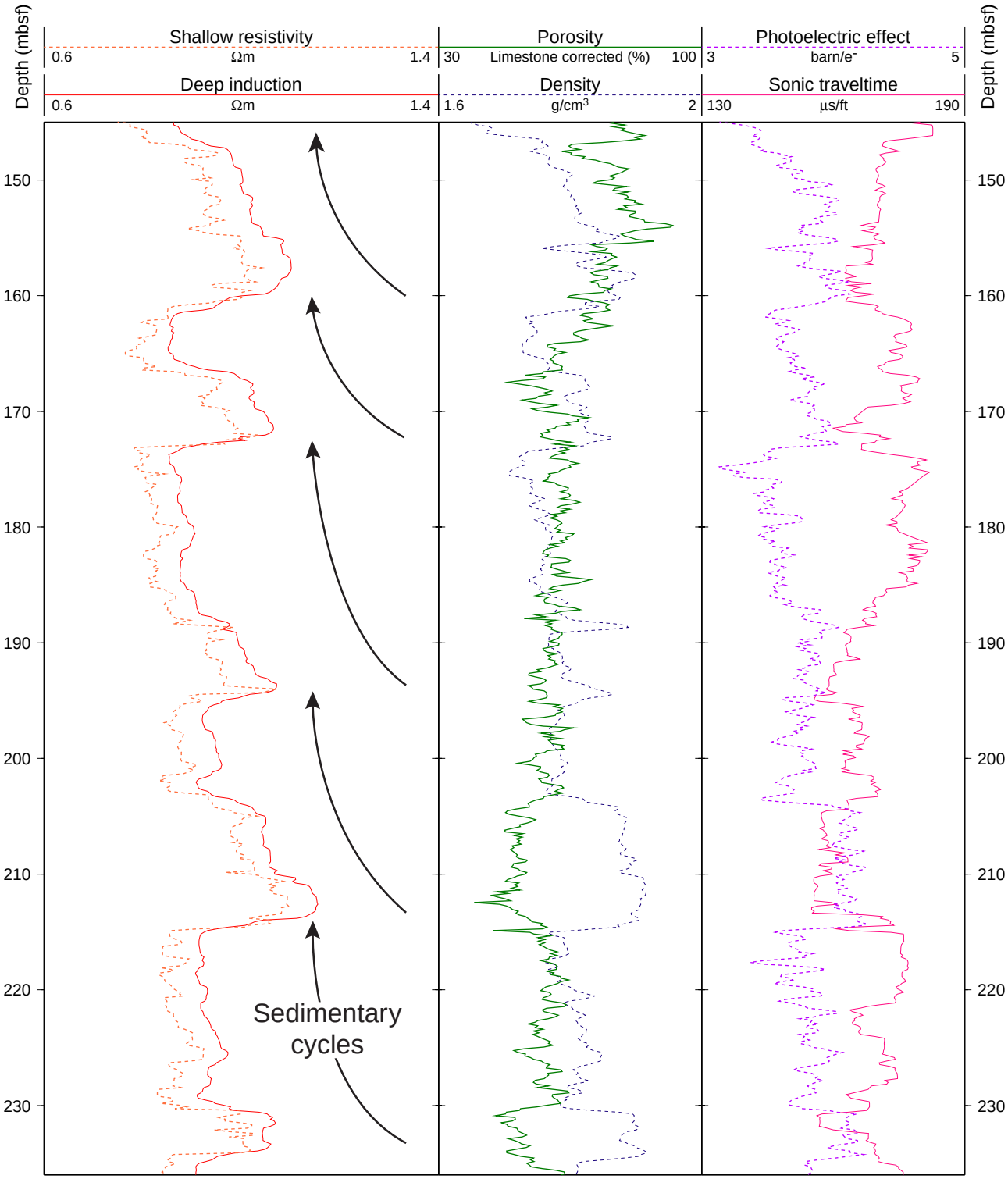

Table T1. Summary of main seismic units and reflectors for profile NIWA 3034-7 and Site 1123.

Reflectors	Unit	Time to base (ms)	Velocity (m/s)	Depth to reflector (m)	Thickness (m)	Cumulative thickness (m)	Character of reflectors within units
Seabed				0	0	0	
R-1	A	180	1656	149	149	149	Slightly discontinuous, but subparallel
R-2	B1	355	1740	309	160	309	Diffuse, with widespread diffractions
R-3	B2	475	1845	438	129	438	Semi-transparent, little continuity
						(626)	Drilled
R-4	C	680	2050	697	259	697	Diffuse, with widespread diffractions
R-5	D	1250	2200	1375	678	1375	Upper = strong diffractions; lower = transparent
Estimated seismic thickness to basement: 1375 m							

Table T2. Site 1123 expanded coring summary. (**See table note.** Continued on next 19 pages.)

Core	Date (September 1998)	Time (UTC)	Core depth (mbsf) Top	Core depth (mbsf) Bottom	Length (m) Cored	Length (m) Recovered	Recovery (%)	Section	Length (m) Liner	Length (m) Curated	Section depth (mbsf) Top	Section depth (mbsf) Bottom	Catwalk samples	Comment
181-1123A-														
1H	13	1645	0	6.1	6.1	6.1	100							
								1	1.5	1.5	0	1.5	IW	
								2	1.5	1.5	1.5	3		
								3	1.45	1.45	3	4.5	IW	
								4	1.5	1.5	4.45	5.95	HS	
								CC	0.15	0.15	5.95	6.1	PAL	All to PAL
									6.10	6.10				
2H	13	1745	6.1	15.6	9.5	9.61	101.2							
								1	1.5	1.5	6.1	7.6	IW	
								2	1.5	1.5	7.6	9.1		
								3	1.5	1.5	9.1	10.6	IW	
								4	1.5	1.5	10.6	12.1	HS	
								5	1.5	1.5	12.1	13.6	IW	
								6	1.5	1.5	13.6	15.1		
								7	0.35	0.35	15.1	15.45		
								CC	0.26	0.26	15.45	15.71	PAL	
									9.61	9.61				
3H	13	1840	15.6	25.1	9.5	7.71	81.2							
								1	1.5	1.5	15.6	17.1	IW	
								2	1.5	1.5	17.1	18.6		
								3	1.5	1.5	18.6	20.1	IW	
								4	1.5	1.5	20.1	21.6	HS	
								5	1.3	1.3	21.6	22.9	IW	
								6	0.31	0.31	22.9	23.21		
								CC	0.1	0.1	23.21	23.31	PAL	All to PAL
									7.71	7.71				
4H	13	2025	25.1	34.6	9.5	9.7	102.1							
								1	1.5	1.5	25.1	26.6	IW	
								2	1.5	1.5	26.6	28.1		
								3	1.5	1.5	28.1	29.6	IW	
								4	1.5	1.5	29.6	31.1		
								5	1.5	1.5	31.1	32.6	IW	
								6	1.5	1.5	32.6	34.1	HS	
								7	0.6	0.6	34.1	34.7		
								CC	0.1	0.1	34.7	34.8	PAL	All to PAL
									9.7	9.7				
5H	13	2130	34.6	44.1	9.5	9.69	102							
								1	1.5	1.5	34.6	36.1	IW	
								2	1.5	1.5	36.1	37.6		
								3	1.5	1.5	37.6	39.1	IW	
								4	1.5	1.5	39.1	40.6	HS	
								5	1.5	1.5	40.6	42.1	IW	
								6	1.5	1.5	42.1	43.6		
								7	0.59	0.59	43.6	44.19		
								CC	0.1	0.1	44.19	44.29	PAL	All to PAL
									9.69	9.69				
6H	13	2225	44.1	53.6	9.5	9.72	102.3							

Table T2 (continued).

Core	Date (September 1998)	Time (UTC)	Core depth (mbsf) Top	Core depth (mbsf) Bottom	Length (m) Cored	Length (m) Recovered	Recovery (%)	Section	Length (m) Liner	Length (m) Curated	Section depth (mbsf) Top	Section depth (mbsf) Bottom	Catwalk samples	Comment
								1	1.5	1.5	44.1	45.6	IW	
								2	1.5	1.5	45.6	47.1		
								3	1.5	1.5	47.1	48.6	IW	
								4	1.5	1.5	48.6	50.1	HS	
								5	1.5	1.5	50.1	51.6	IW	
								6	1.5	1.5	51.6	53.1		
								7	0.62	0.62	53.1	53.72		
								CC	0.1	0.1	53.72	53.82	PAL	All to PAL
									9.72	9.72				
7H	13	2325	53.6	63.1	9.5	9.65	101.6							
								1	1.5	1.5	53.6	55.1		
								2	1.5	1.5	55.1	56.6		
								3	1.5	1.5	56.6	58.1		
								4	1.5	1.5	58.1	59.6	IW	
								5	1.5	1.5	59.6	61.1	HS	
								6	1.5	1.5	61.1	62.6		
								7	0.44	0.44	62.6	63.04		
								CC	0.21	0.21	63.04	63.25	PAL	
									9.65	9.65				
8H	14	25	63.1	72.6	9.5	8.97	94.4							
								1	1.5	1.5	63.1	64.6		
								2	1.5	1.5	64.6	66.1		
								3	1.5	1.5	66.1	67.6		
								4	1.5	1.5	67.6	69.1	IW	
								5	1.5	1.5	69.1	70.6	HS	
								6	1.31	1.31	70.6	71.91		
								CC	0.16	0.16	71.91	72.07	PAL	
									8.97	8.97				
9H	14	125	72.6	82.1	9.5	9.83	103.5							
								1	1.5	1.5	72.6	74.1		
								2	1.5	1.5	74.1	75.6		
								3	1.5	1.5	75.6	77.1		
								4	1.5	1.5	77.1	78.6	IW	
								5	1.5	1.5	78.6	80.1	HS	
								6	1.5	1.5	80.1	81.6		
								7	0.56	0.56	81.6	82.16		
								CC	0.27	0.27	82.16	82.43	PAL	
									9.83	9.83				
10H	14	220	82.1	91.6	9.5	9.83	103.5							
								1	1.5	1.5	82.1	83.6		
								2	1.5	1.5	83.6	85.1		
								3	1.5	1.5	85.1	86.6		
								4	1.5	1.5	86.6	88.1	IW	
								5	1.5	1.5	88.1	89.6	HS	
								6	1.5	1.5	89.6	91.1		
								7	0.63	0.63	91.1	91.73		
								CC	0.2	0.2	91.73	91.93	PAL	
									9.83	9.83				
11H	14	315	91.6	101.1	9.5	9.64	101.5							
								1	1.5	1.5	91.6	93.1		

Table T2 (continued).

Core	Date (September 1998)	Time (UTC)	Core depth (mbsf) Top	Core depth (mbsf) Bottom	Length (m) Cored	Length (m) Recovered	Recovery (%)	Section	Length (m) Liner	Length (m) Curated	Section depth (mbsf) Top	Section depth (mbsf) Bottom	Catwalk samples	Comment
								2	1.5	1.5	93.1	94.6		
								3	1.5	1.5	94.6	96.1		
								4	1.5	1.5	96.1	97.6	IW	
								5	1.5	1.5	97.6	99.1	HS	
								6	1.5	1.5	99.1	100.6		
								7	0.43	0.43	100.6	101.03		
								CC	0.21	0.21	101.03	101.24	PAL	
									9.64	9.64				
12H	14	410	101.1	110.6	9.5	9.76	102.7							
								1	1.5	1.5	101.1	102.6		
								2	1.5	1.5	102.6	104.1		
								3	1.5	1.5	104.1	105.6		
								4	1.5	1.5	105.6	107.1	IW	
								5	1.5	1.5	107.1	108.6	HS	
								6	1.5	1.5	108.6	110.1		
								7	0.53	0.53	110.1	110.63		
								CC	0.23	0.23	110.63	110.86	PAL	
									9.76	9.76				
13H	14	500	110.6	120.1	9.5	9.14	96.2							
								1	1.5	1.5	110.6	112.1		
								2	1.5	1.5	112.1	113.6		
								3	1.05	1.05	113.6	114.65		
								4	1.5	1.5	114.65	116.15	IW	
								5	1.5	1.5	116.15	117.65	HS	
								6	1.5	1.5	117.65	119.15		
								7	0.4	0.4	119.15	119.55		
								CC	0.19	0.19	119.55	119.74	PAL	
									9.14	9.14				
14H	14	600	120.1	129.6	9.5	9.66	101.7							
								1	1.5	1.5	120.1	121.6		
								2	1.5	1.5	121.6	123.1		
								3	1.5	1.5	123.1	124.6		
								4	1.5	1.5	124.6	126.1	IW	
								5	1.5	1.5	126.1	127.6	HS	
								6	1.5	1.5	127.6	129.1		
								7	0.44	0.44	129.1	129.54		
								CC	0.22	0.22	129.54	129.76	PAL	
									9.66	9.66				
15H	14	655	129.6	139.1	9.5	9.99	105.2							
								1	1.5	1.5	129.6	131.1		
								2	1.5	1.5	131.1	132.6		
								3	1.5	1.5	132.6	134.1		
								4	1.5	1.5	134.1	135.6	IW	
								5	1.5	1.5	135.6	137.1	HS	Replaced liner
								6	1.5	1.5	137.1	138.6		
								7	0.73	0.73	138.6	139.33		
								CC	0.26	0.26	139.33	139.59	PAL	
									9.99	9.99				
16H	14	755	139.1	148.6	9.5	9.61	101.2							
								1	1.5	1.5	139.1	140.6		

Table T2 (continued).

Core	Date (September 1998)	Time (UTC)	Core depth (mbsf) Top	Core depth (mbsf) Bottom	Length (m) Cored	Length (m) Recovered	Recovery (%)	Section	Length (m) Liner	Length (m) Curated	Section depth (mbsf) Top	Section depth (mbsf) Bottom	Catwalk samples	Comment
								2	1.5	1.5	140.6	142.1		
								3	1.5	1.5	142.1	143.6	IW	
								4	1.5	1.5	143.6	145.1	HS	
								5	1.5	1.5	145.1	146.6		
								6	1.5	1.5	146.6	148.1		
								7	0.35	0.35	148.1	148.45		
								CC	0.26	0.26	148.45	148.71	PAL	
									9.61	9.61				
17H	14	1050	148.6	158.1	9.5	10.02	105.5							
								1	1.5	1.5	148.6	150.1		
								2	1.5	1.5	150.1	151.6		
								3	1.5	1.5	151.6	153.1		
								4	1.5	1.5	153.1	154.6	IW	
								5	1.5	1.5	154.6	156.1	HS	
								6	1.5	1.5	156.1	157.6		
								7	0.75	0.75	157.6	158.35		
								CC	0.27	0.27	158.35	158.62	PAL	
									10.02	10.02				
				Totals:	158.1	158.63	100.30							
181-1123B-														
1H	14	1330	0	3.4	3.4	3.36	98.8							
								1	1.5	1.5	0	1.5	PAL	
								2	1.5	1.5	1.5	3		
								3	0.21	0.21	3	3.2		
								CC	0.15	0.15	3.21	3.36	PAL	All to PAL
									3.36	3.36				
2H	14	1420	3.4	12.9	9.5	9.45	99.5							
								1	1.5	1.5	3.4	4.9		
								2	1.5	1.5	4.9	6.4		
								3	1.5	1.5	6.4	7.9		
								4	1.5	1.5	7.9	9.4		
								5	1.5	1.5	9.4	10.9		
								6	1.5	1.5	10.9	12.4		
								7	0.24	0.24	12.4	12.64		
								CC	0.21	0.21	12.64	12.85	PAL	
									9.45	9.45				
3H	14	1515	12.9	22.4	9.5	9.84	103.6							
								1	1.5	1.5	12.9	14.4		
								2	1.5	1.5	14.4	15.9		
								3	1.5	1.5	15.9	17.4		
								4	1.5	1.5	17.4	18.9		
								5	1.5	1.5	18.9	20.4		
								6	1.5	1.5	20.4	21.9		
								7	0.63	0.63	21.9	22.53		
								CC	0.21	0.21	22.53	22.74	PAL	
									9.84	9.84				
4H	14	1615	22.4	31.9	9.5	9.8	103.2							
								1	1.5	1.5	22.4	23.9		
								2	1.5	1.5	23.9	25.4		
								3	1.5	1.5	25.4	26.9		

Table T2 (continued).

Core	Date (September 1998)	Time (UTC)	Core depth (mbsf) Top	Core depth (mbsf) Bottom	Length (m) Cored	Length (m) Recovered	Recovery (%)	Section	Length (m) Liner	Length (m) Curated	Section depth (mbsf) Top	Section depth (mbsf) Bottom	Catwalk samples	Comment
								4	1.5	1.5	26.9	28.4		
								5	1.5	1.5	28.4	29.9		
								6	1.5	1.5	29.9	31.4		
								7	0.6	0.6	31.4	32		
								CC	0.2	0.2	32	32.2	PAL	
									9.80	9.80				
5H	14	1735	31.9	41.4	9.5	9.77	102.8							
								1	1.5	1.5	31.9	33.4		
								2	1.5	1.5	33.4	34.9		
								3	1.5	1.5	34.9	36.4		
								4	1.5	1.5	36.4	37.9		
								5	1.5	1.5	37.9	39.4		
								6	1.5	1.5	39.4	40.9		
								7	0.6	0.6	40.9	41.5		
								CC	0.17	0.17	41.5	41.67	PAL	
									9.77	9.77				
6H	14	1830	41.4	50.9	9.5	9.78	102.9							
								1	1.5	1.5	41.4	42.9		
								2	1.5	1.5	42.9	44.4		
								3	1.5	1.5	44.4	45.9		
								4	1.5	1.5	45.9	47.4		
								5	1.5	1.5	47.4	48.9		
								6	1.5	1.5	48.9	50.4		
								7	0.53	0.53	50.4	50.93		
								CC	0.25	0.25	50.93	51.18		
									9.78	9.78				
7H	14	1950	50.9	60.4	9.5	10.12	106.5							
								1	1.5	1.5	50.9	52.4		
								2	1.5	1.5	52.4	53.9		
								3	1.5	1.5	53.9	55.4		
								4	1.5	1.5	55.4	56.9		
								5	1.5	1.5	56.9	58.4		
								6	1.5	1.5	58.4	59.9		
								7	0.75	0.75	59.9	60.65		
								CC	0.37	0.37	60.65	61.02	PAL	
									10.12	10.12				
8H	14	2045	60.4	69.9	9.5	9.79	103.1							
								1	1.5	1.5	60.4	61.9		
								2	1.5	1.5	61.9	63.4		
								3	1.5	1.5	63.4	64.9		
								4	1.5	1.5	64.9	66.4		
								5	1.5	1.5	66.4	67.9		
								6	1.5	1.5	67.9	69.4		
								7	0.59	0.59	69.4	69.99		
								CC	0.2	0.2	69.99	70.19	PAL	
									9.79	9.79				
9H	14	2145	69.9	79.4	9.5	9.76	102.7							
								1	1.5	1.5	69.9	71.4		
								2	1.5	1.5	71.4	72.9		
								3	1.5	1.5	72.9	74.4		

Table T2 (continued).

Core	Date (September 1998)	Time (UTC)	Core depth (mbsf) Top	Core depth (mbsf) Bottom	Length (m) Cored	Length (m) Recovered	Recovery (%)	Section	Length (m) Liner	Length (m) Curated	Section depth (mbsf) Top	Section depth (mbsf) Bottom	Catwalk samples	Comment
								4	1.5	1.5	74.4	75.9		
								5	1.5	1.5	75.9	77.4		
								6	1.5	1.5	77.4	78.9		
								7	0.66	0.66	78.9	79.56		
								CC	0.1	0.1	79.56	79.66		
									9.76	9.76				
10H	14	2245	79.4	88.9	9.5	9.79	103.1							
								1	1.5	1.5	79.4	80.9		
								2	1.5	1.5	80.9	82.4		
								3	1.5	1.5	82.4	83.9		
								4	1.5	1.5	83.9	85.4		
								5	1.5	1.5	85.4	86.9		
								6	1.5	1.5	86.9	88.4		
								7	0.34	0.34	88.4	88.74		
								CC	0.45	0.45	88.74	89.19	PAL	
									9.79	9.79				
11H	14	2355	88.9	98.4	9.5	9.91	104.3							
								1	1.5	1.5	88.9	90.4		
								2	1.5	1.5	90.4	91.9		
								3	1.5	1.5	91.9	93.4		
								4	1.5	1.5	93.4	94.9		
								5	1.5	1.5	94.9	96.4		
								6	1.5	1.5	96.4	97.9		
								7	0.7	0.7	97.9	98.6		
								CC	0.21	0.21	98.6	98.81	PAL	
									9.91	9.91				
12H	15	55	98.4	107.9	9.5	9.76	102.7							
								1	1.5	1.5	98.4	99.9		
								2	1.5	1.5	99.9	101.4		
								3	1.5	1.5	101.4	102.9		
								4	1.5	1.5	102.9	104.4		
								5	1.5	1.5	104.4	105.9		
								6	1.5	1.5	105.9	107.4		
								7	0.55	0.55	107.4	107.95		
								CC	0.21	0.21	107.95	108.16	PAL	
									9.76	9.76				
13H	15	150	107.9	117.4	9.5	9.88	104							
								1	1.5	1.5	107.9	109.4		
								2	1.5	1.5	109.4	110.9		
								3	1.5	1.5	110.9	112.4		
								4	1.5	1.5	112.4	113.9		
								5	1.5	1.5	113.9	115.4		
								6	1.5	1.5	115.4	116.9		
								7	0.67	0.67	116.9	117.57		
								CC	0.21	0.21	117.57	117.78	PAL	
									9.88	9.88				
14H	15	245	117.4	126.9	9.5	9.58	100.8							
								1	1.5	1.5	117.4	118.9		
								2	1.5	1.5	118.9	120.4		
								3	1.5	1.5	120.4	121.9		

Table T2 (continued).

Core	Date (September 1998)	Time (UTC)	Core depth (mbsf) Top	Core depth (mbsf) Bottom	Length (m) Cored	Length (m) Recovered	Recovery (%)	Section	Length (m) Liner	Length (m) Curated	Section depth (mbsf) Top	Section depth (mbsf) Bottom	Catwalk samples	Comment
								4	1.5	1.5	121.9	123.4		
								5	1.5	1.5	123.4	124.9		
								6	1.5	1.5	124.9	126.4		
								7	0.48	0.48	126.4	126.88		
								CC	0.1	0.1	126.88	126.98	PAL	All to PAL
									9.58	9.58				
15H	15	340	126.9	136.4	9.5	9.91	104.3							
								1	1.5	1.5	126.9	128.4		
								2	1.5	1.5	128.4	129.9		
								3	1.53	1.53	129.9	131.43		
								4	1.53	1.53	131.43	132.96		
								5	1.5	1.5	132.96	134.46		
								6	1.5	1.5	134.46	135.96		
								7	0.62	0.62	135.96	136.58		
								CC	0.23	0.23	136.58	136.81	PAL	
									9.91	9.91				
16H	15	655	136.4	145.9	9.5	9.46	99.6							
								1	1.5	1.5	136.4	137.9		
								2	1.5	1.5	137.9	139.4		
								3	1.5	1.5	139.4	140.9		
								4	1.5	1.5	140.9	142.4		
								5	1.5	1.5	142.4	143.9		
								6	1.5	1.5	143.9	145.4	PAL	
								7	0.36	0.36	145.4	145.76		
								CC	0.1	0.1	145.76	145.86	PAL	All to PAL
									9.46	9.46				
17H	15	840	145.9	155.4	9.5	9.78	102.9							
								1	1.5	1.5	145.9	147.4		
								2	1.5	1.5	147.4	148.9	PAL	
								3	1.5	1.5	148.9	150.4		
								4	1.5	1.5	150.4	151.9	IW	
								5	1.5	1.5	151.9	153.4	HS	
								6	1.5	1.5	153.4	154.9	PAL	
								7	0.38	0.38	154.9	155.28		
								CC	0.4	0.4	155.28	155.68	PAL	
									9.78	9.78				
18X	15	945	155.4	162.7	7.3	8.39	114.9							
								1	1.5	1.5	155.4	156.9		
								2	1.5	1.5	156.9	158.4		
								3	1.5	1.5	158.4	159.9		
								4	1.5	1.5	159.9	161.4		
								5	1.5	1.5	161.4	162.9		
								6	0.61	0.61	162.9	163.51		
								CC	0.28	0.28	163.51	163.79	PAL	
									8.39	8.39				
19X	15	1025	162.7	172.3	9.6	9.59	99.9							
								1	1.5	1.52	162.7	164.22		
								2	1.5	1.52	164.22	165.74		
								3	1.5	1.52	165.74	167.26		
								4	1.5	1.52	167.26	168.78		

Table T2 (continued).

Core	Date (September 1998)	Time (UTC)	Core depth (mbsf) Top	Core depth (mbsf) Bottom	Length (m) Cored	Length (m) Recovered	Recovery (%)	Section	Length (m) Liner	Length (m) Curated	Section depth (mbsf) Top	Section depth (mbsf) Bottom	Catwalk samples	Comment
								5	1.5	1.52	168.78	170.3	HS	
								6	1.5	1.52	170.3	171.82		
								7	0.26	0.26	171.82	172.08		
								CC	0.33	0.33	172.08	172.41	PAL	
									9.59	9.71				
20X	15	1130	172.3	181.9	9.6	9.65	100.5							
								1	1.5	1.52	172.3	173.82		
								2	1.5	1.52	173.82	175.34		
								3	1.5	1.52	175.34	176.86		
								4	1.5	1.5	176.86	178.36	IW, HS	
								5	1.5	1.52	178.36	179.88		
								6	1.5	1.52	179.88	181.4		
								7	0.4	0.4	181.4	181.8		
								CC	0.25	0.25	181.8	182.05	PAL	
									9.65	9.75				
21X	15	1935	181.9	191.6	9.7	9.47	97.6							
								1	1.5	1.5	181.9	183.4		
								2	1.5	1.5	183.4	184.9		
								3	1.5	1.5	184.9	186.4		
								4	1.5	1.5	186.4	187.9		
								5	1.5	1.5	187.9	189.4	HS	
								6	1.5	1.5	189.4	190.9		
								7	0.24	0.24	190.9	191.14		
								CC	0.23	0.23	191.14	191.37	PAL, PAL	
									9.47	9.47				
22X	15	2040	191.6	201.2	9.6	9.87	102.8							
								1	1.57	1.57	191.6	193.17		Other
								2	1.5	1.5	193.17	194.67		
								3	1.5	1.5	194.67	196.17		
								4	1.5	1.5	196.17	197.67		
								5	1.5	1.5	197.67	199.17	HS	
								6	1.5	1.5	199.17	200.67		
								7	0.44	0.44	200.67	201.11		
								CC	0.36	0.36	201.11	201.47	PAL, PAL	
									9.87	9.87				
23X	15	2155	201.2	210.8	9.6	7.76	80.8							
								1	1.5	1.5	201.2	202.7		
								2	1.5	1.5	202.7	204.2		
								3	1.5	1.5	204.2	205.7	IW	
								4	1.5	1.5	205.7	207.2	HS	
								5	1.5	1.5	207.2	208.7		
								CC	0.26	0.26	208.7	208.96	PAL	
									7.76	7.76				
24X	15	2310	210.8	220.4	9.6	9.75	101.6							
								1	1.5	1.5	210.8	212.3		Other
								2	1.5	1.5	212.3	213.8		
								3	1.5	1.5	213.8	215.3		
								4	1.5	1.5	215.3	216.8		
								5	1.5	1.5	216.8	218.3	HS	
								6	1.5	1.5	218.3	219.8		

Table T2 (continued).

Core	Date (September 1998)	Time (UTC)	Core depth (mbsf) Top	Core depth (mbsf) Bottom	Length (m) Cored	Length (m) Recovered	Recovery (%)	Section	Length (m) Liner	Length (m) Curated	Section depth (mbsf) Top	Section depth (mbsf) Bottom	Catwalk samples	Comment
								7	0.44	0.44	219.8	220.24		
								CC	0.31	0.31	220.24	220.55	PAL, PAL	
									9.75	9.75				
25X	16	20	220.4	230	9.6	9.7	101							
								1	1.5	1.5	220.4	221.9		
								2	1.5	1.5	221.9	223.4		
								3	1.5	1.5	223.4	224.9		
								4	1.5	1.5	224.9	226.4		
								5	1.5	1.5	226.4	227.9	HS	
								6	1.5	1.5	227.9	229.4		
								7	0.38	0.38	229.4	229.78		
								CC	0.32	0.32	229.78	230.1	PAL	
									9.70	9.70				
26X	16	130	230	239.6	9.6	4.18	43.5							
								1	1.5	1.5	230	231.5		
								2	1.5	1.5	231.5	233	IW	
								3	0.86	0.86	233	233.9	HS	
								CC	0.32	0.32	233.86	234.18	PAL	
									4.18	4.18				
27X	16	240	239.6	249.2	9.6	9.82	102.3							
								1	1.5	1.5	239.6	241.1		
								2	1.5	1.5	241.1	242.6		
								3	1.5	1.5	242.6	244.1		
								4	1.5	1.5	244.1	245.6		
								5	1.5	1.5	245.6	247.1	HS	
								6	1.5	1.5	247.1	248.6		
								7	0.46	0.46	248.6	249.06		
								CC	0.36	0.36	249.06	249.42	PAL	
									9.82	9.82				
28X	16	345	249.2	258.8	9.6	9.59	99.9							
								1	1.5	1.5	249.2	250.7		
								2	1.5	1.5	250.7	252.2		
								3	1.5	1.5	252.2	253.7		
								4	1.5	1.5	253.7	255.2		
								5	1.5	1.5	255.2	256.7	HS	
								6	1.5	1.5	256.7	258.2		
								7	0.36	0.36	258.2	258.56		
								CC	0.23	0.23	258.56	258.79	PAL	
									9.59	9.59				
29X	16	620	258.8	268.4	9.6	9.79	102							
								1	1.5	1.5	258.8	260.3		
								2	1.5	1.5	260.3	261.8		
								3	1.5	1.5	261.8	263.3		
								4	1.5	1.5	263.3	264.8	IW	
								5	1.5	1.5	264.8	266.3	HS	
								6	1.5	1.5	266.3	267.8		
								7	0.42	0.42	267.8	268.22		
								CC	0.37	0.37	268.22	268.59	PAL	
									9.79	9.79				
30X	16	740	268.4	278.1	9.7	9.65	99.5							

Table T2 (continued).

Core	Date (September 1998)	Time (UTC)	Core depth (mbsf) Top	Core depth (mbsf) Bottom	Length (m) Cored	Length (m) Recovered	Recovery (%)	Section	Length (m) Liner	Length (m) Curated	Section depth (mbsf) Top	Section depth (mbsf) Bottom	Catwalk samples	Comment
								1	1.5	1.5	268.4	269.9		
								2	1.5	1.5	269.9	271.4		
								3	1.5	1.5	271.4	272.9		
								4	1.5	1.5	272.9	274.4		
								5	1.5	1.5	274.4	275.9	HS	
								6	1.5	1.5	275.9	277.4		
								7	0.35	0.35	277.4	277.75		
								CC	0.3	0.3	277.75	278.05	PAL	
									9.65	9.65				
31X	16	845	278.1	287.7	9.6	9.49	98.9							
								1	1.5	1.5	278.1	279.6		
								2	1.5	1.5	279.6	281.1		
								3	1.5	1.5	281.1	282.6		
								4	1.5	1.5	282.6	284.1		
								5	1.5	1.5	284.1	285.6		
								6	1.5	1.5	285.6	287.1		
								7	0.27	0.27	287.1	287.37		
								CC	0.22	0.22	287.37	287.59	PAL	
									9.49	9.49				
32X	16	945	287.7	297.3	9.6	8.71	90.7							
								1	1.5	1.5	287.7	289.2		
								2	1.5	1.5	289.2	290.7		
								3	1.5	1.5	290.7	292.2		
								4	1.5	1.5	292.2	293.7	IW	
								5	1.5	1.5	293.7	295.2	HS	
								6	0.88	0.88	295.2	296.08		
								CC	0.33	0.33	296.08	296.41	PAL	
									8.71	8.71				
33X	16	1105	297.3	306.9	9.6	9.65	100.5							
								1	1.5	1.5	297.3	298.8		
								2	1.5	1.5	298.8	300.3		
								3	1.5	1.5	300.3	301.8		
								4	1.5	1.5	301.8	303.3	HS	
								5	1.5	1.5	303.3	304.8		
								6	1.5	1.5	304.8	306.3		
								7	0.4	0.4	306.3	306.7		
								CC	0.25	0.25	306.7	306.95	PAL	
									9.65	9.65				
34X	16	1210	306.9	316.5	9.6	9.78	101.9							
								1	1.5	1.5	306.9	308.4		
								2	1.5	1.5	308.4	309.9		
								3	1.5	1.5	309.9	311.4		
								4	1.5	1.5	311.4	312.9		
								5	1.5	1.5	312.9	314.4	HS	
								6	1.5	1.5	314.4	315.9		
								7	0.44	0.44	315.9	316.34		
								CC	0.34	0.34	316.34	316.68	PAL	
									9.78	9.78				
35X	16	1320	316.5	325.9	9.4	9.62	102.3							
								1	1.5	1.5	316.5	318		

Table T2 (continued).

Core	Date (September 1998)	Time (UTC)	Core depth (mbsf) Top	Core depth (mbsf) Bottom	Length (m) Cored	Length (m) Recovered	Recovery (%)	Section	Length (m) Liner	Length (m) Curated	Section depth (mbsf) Top	Section depth (mbsf) Bottom	Catwalk samples	Comment
								2	1.5	1.5	318	319.5		
								3	1.5	1.5	319.5	321		
								4	1.5	1.5	321	322.5	IW	
								5	1.5	1.5	322.5	324	HS	
								6	1.5	1.5	324	325.5		
								7	0.43	0.43	325.5	325.93		
								CC	0.19	0.19	325.93	326.12	PAL	
									9.62	9.62				
36X	16	1430	325.9	335.5	9.6	9.67	100.7							
								1	1.5	1.5	325.9	327.4		
								2	1.5	1.5	327.4	328.9		
								3	1.5	1.5	328.9	330.4		
								4	1.5	1.5	330.4	331.9		
								5	1.5	1.5	331.9	333.4	HS	
								6	1.5	1.5	333.4	334.9		
								7	0.44	0.44	334.9	335.34		
								CC	0.23	0.23	335.34	335.57	PAL	
									9.67	9.67				
37X	16	1550	335.5	345.1	9.6	9.8	102.1							
								1	1.5	1.5	335.5	337		
								2	1.5	1.5	337	338.5		
								3	1.5	1.5	338.5	340		
								4	1.5	1.5	340	341.5		
								5	1.5	1.5	341.5	343	HS	
								6	1.5	1.5	343	344.5		
								7	0.48	0.48	344.5	344.98		
								CC	0.32	0.32	344.98	345.3	PAL	
									9.8	9.8				
38X	16	1710	345.1	354.7	9.6	9.79	102							
								1	1.5	1.5	345.1	346.6		
								2	1.5	1.5	346.6	348.1		
								3	1.5	1.5	348.1	349.6		
								4	1.5	1.5	349.6	351.1	IW	
								5	1.5	1.5	351.1	352.6	HS	
								6	1.5	1.5	352.6	354.1		
								7	0.38	0.38	354.1	354.48		
								CC	0.41	0.41	354.48	354.89	PAL	
									9.79	9.79				
39X	16	1825	354.7	364.4	9.7	9.88	101.9							
								1	1.5	1.5	354.7	356.2		
								2	1.5	1.5	356.2	357.7		
								3	1.5	1.5	357.7	359.2		
								4	1.5	1.5	359.2	360.7		
								5	1.5	1.5	360.7	362.2	HS	
								6	1.5	1.5	362.2	363.7		
								7	0.49	0.49	363.7	364.19		
								CC	0.39	0.39	364.19	364.58	PAL	
									9.88	9.88				
40X	16	1940	364.4	374.1	9.7	9.76	100.6							
								1	1.5	1.5	364.4	365.9		

Table T2 (continued).

Core	Date (September 1998)	Time (UTC)	Core depth (mbsf) Top	Core depth (mbsf) Bottom	Length (m) Cored	Length (m) Recovered	Recovery (%)	Section	Length (m) Liner	Length (m) Curated	Section depth (mbsf) Top	Section depth (mbsf) Bottom	Catwalk samples	Comment
								2	1.5	1.5	365.9	367.4		
								3	1.5	1.5	367.4	368.9		
								4	1.5	1.5	368.9	370.4		
								5	1.5	1.5	370.4	371.9	HS	
								6	1.5	1.5	371.9	373.4		
								7	0.44	0.44	373.4	373.84		
								CC	0.32	0.32	373.84	374.16	PAL	
									9.76	9.76				
41X	16	2220	374.1	383.7	9.6	8.2	85.4							
								1	1.5	1.5	374.1	375.6		
								2	1.5	1.5	375.6	377.1		
								3	1.5	1.5	377.1	378.6		
								4	1.5	1.5	378.6	380.1	IW	
								5	1.5	1.5	380.1	381.6	HS	
								6	0.32	0.32	381.6	381.92		
								CC	0.38	0.38	381.92	382.3	PAL	
									8.2	8.2				
42X	16	2345	383.7	393.4	9.7	4.84	49.9							
								1	1.5	1.5	383.7	385.2		
								2	1.5	1.5	385.2	386.7		
								3	1.5	1.5	386.7	388.2	HS	
								CC	0.34	0.34	388.2	388.54	PAL	
									4.84	4.84				
43X	17	135	393.4	403	9.6	6.22	64.8							
								1	1.5	1.5	393.4	394.9		
								2	1.5	1.5	394.9	396.4		
								3	1.5	1.5	396.4	397.9	HS	
								4	1.48	1.48	397.9	399.38		
								CC	0.24	0.24	399.38	399.62	PAL	
									6.22	6.22				
44X	17	325	403	412.6	9.6	5.42	56.5							
								1	1.5	1.5	403	404.5		
								2	1.5	1.5	404.5	406		
								3	1.5	1.5	406	407.5	IW	
								4	0.62	0.62	407.5	408.12	HS	
								CC	0.3	0.3	408.12	408.42	PAL	
									5.42	5.42				
45X	17	510	412.6	422.2	9.6	4.06	42.3							
								1	1.5	1.5	412.6	414.1		
								2	1.5	1.5	414.1	415.6	HS	
								3	0.78	0.78	415.6	416.38		
								CC	0.28	0.28	416.38	416.66	PAL	
									4.06	4.06				
46X	17	655	422.2	431.8	9.6	6.21	64.7							
								1	1.5	1.5	422.2	423.7		
								2	1.5	1.5	423.7	425.2		
								3	1.5	1.5	425.2	426.7	HS	
								4	1.46	1.46	426.7	428.16		
								CC	0.25	0.25	428.16	428.41	PAL	
									6.21	6.21				

Table T2 (continued).

Core	Date (September 1998)	Time (UTC)	Core depth (mbsf) Top	Core depth (mbsf) Bottom	Length (m) Cored	Length (m) Recovered	Recovery (%)	Section	Length (m) Liner	Length (m) Curated	Section depth (mbsf) Top	Section depth (mbsf) Bottom	Catwalk samples	Comment
47X	17	845	431.8	441.5	9.7	5.26	54.2							
								1	1.5	1.5	431.8	433.3		
								2	1.5	1.5	433.3	434.8		
								3	1.5	1.5	434.8	436.3	IW	
								4	0.66	0.66	436.3	436.96	HS	
								CC	0.1	0.1	436.96	437.06	PAL	All to PAL
									5.26	5.26				
48X	17	1055	441.5	450.8	9.3	4.25	45.7							
								1	1.5	1.5	441.5	443		
								2	1.5	1.5	443	444.5	HS	
								3	1.1	1.1	444.5	445.6		
								CC	0.15	0.15	445.6	445.75	PAL	All to PAL
									4.25	4.25				
49X	17	1420	450.8	460.4	9.6	6.41	66.8							
								1	1.5	1.5	450.8	452.3		
								2	1.5	1.5	452.3	453.8		
								3	1.5	1.5	453.8	455.3	HS	
								4	1.5	1.5	455.3	456.8		
								CC	0.41	0.41	456.8	457.21	PAL	
									6.41	6.41				
50X	17	1620	460.4	470	9.6	8.35	87							
								1	1.5	1.5	460.4	461.9		
								2	1.5	1.5	461.9	463.4		
								3	1.5	1.5	463.4	464.9		
								4	1.5	1.5	464.9	466.4	IW	
								5	1.5	1.5	466.4	467.9	HS	
								6	0.31	0.31	467.9	468.21		
								CC	0.54	0.54	468.21	468.75	PAL	
									8.35	8.35				
51X	17	1825	470	479.3	9.3	9.72	104.5							
								1	1.5	1.5	470	471.5		
								2	1.5	1.5	471.5	473		
								3	1.5	1.5	473	474.5		
								4	1.5	1.5	474.5	476		
								5	1.5	1.5	476	477.5	HS	
								6	1.5	1.5	477.5	479		
								7	0.45	0.45	479	479.5		
								CC	0.27	0.27	479.45	479.72	PAL	
									9.72	9.72				
52X	17	2035	479.3	489	9.7	9.36	96.5							
								1	1.5	1.5	479.3	480.8		
								2	1.5	1.5	480.8	482.3		
								3	1.5	1.5	482.3	483.8	IW	
								4	1.5	1.5	483.8	485.3	HS	
								5	1.5	1.5	485.3	486.8		
								6	1.5	1.5	486.8	488.3		
								CC	0.36	0.36	488.3	488.66	PAL	
									9.36	9.36				
				Totals:	489.00	451.40	92.30							

Table T2 (continued).

Core	Date (September 1998)	Time (UTC)	Core depth (mbsf) Top	Core depth (mbsf) Bottom	Length (m) Cored	Length (m) Recovered	Recovery (%)	Section	Length (m) Liner	Length (m) Curated	Section depth (mbsf) Top	Section depth (mbsf) Bottom	Catwalk samples	Comment
181-1123C-														
1H	18	2355	0	9	9	9.02	100.2							
								1	1.5	1.5	0	1.5		
								2	1.5	1.5	1.5	3	EDDY	
								3	1.5	1.5	3	4.5		
								4	1.5	1.5	4.5	6		
								5	1.5	1.5	6	7.5		
								6	1.42	1.42	7.5	8.92		
								CC	0.1	0.1	8.92	9.02	PAL	All to PAL
									9.02	9.02				
2H	19	0050	9	18.5	9.5	9.53	100.3							
								1	1.5	1.5	9	10.5		
								2	1.5	1.5	10.5	12	EDDY	
								3	1.5	1.5	12	13.5		
								4	1.5	1.5	13.5	15		
								5	1.5	1.5	15	16.5		
								6	1.5	1.5	16.5	18		
								7	0.43	0.43	18	18.4		
								CC	0.1	0.1	18.43	18.53	PAL	All to PAL
									9.53	9.53				
3H	19	0155	18.5	28	9.5	9.79	103.1							
								1	1.5	1.5	18.5	20		
								2	1.5	1.5	20	21.5		
								3	1.5	1.5	21.5	23		
								4	1.5	1.5	23	24.5	EDDY	
								5	1.5	1.5	24.5	26		
								6	1.5	1.5	26	27.5		
								7	0.61	0.61	27.5	28.1		
								CC	0.18	0.18	28.11	28.29	PAL	
									9.79	9.79				
4H	19	0250	28	37.5	9.5	9.59	100.9							
								1	1.5	1.5	28	29.5		
								2	1.5	1.5	29.5	31	EDDY	
								3	1.5	1.5	31	32.5		
								4	1.5	1.5	32.5	34		
								5	1.5	1.5	34	35.5		
								6	1.5	1.5	35.5	37		
								7	0.43	0.43	37	37.4		
								CC	0.16	0.16	37.43	37.59	PAL	
									9.59	9.59				
5H	19	0345	37.5	47	9.5	8.85	93.2							
								1	1.5	1.5	37.5	39		
								2	1.5	1.5	39	40.5		
								3	1.5	1.5	40.5	42		
								4	1.5	1.5	42	43.5	EDDY	
								5	1.5	1.5	43.5	45		
								6	1.2	1.2	45	46.2		
								CC	0.15	0.15	46.2	46.35	PAL	
									8.85	8.85				
6H	19	0445	47	56.5	9.5	9.91	104.3							

Table T2 (continued).

Core	Date (September 1998)	Time (UTC)	Core depth (mbsf) Top	Core depth (mbsf) Bottom	Length (m) Cored	Length (m) Recovered	Recovery (%)	Section	Length (m) Liner	Length (m) Curated	Section depth (mbsf) Top	Section depth (mbsf) Bottom	Catwalk samples	Comment
								1	1.5	1.5	47	48.5		
								2	1.5	1.5	48.5	50		
								3	1.5	1.5	50	51.5		
								4	1.5	1.5	51.5	53		
								5	1.5	1.5	53	54.5	EDDY	
								6	1.5	1.5	54.5	56		
								7	0.67	0.67	56	56.7		
								CC	0.24	0.24	56.67	56.91	PAL	
									9.91	9.91				
7H	19	0540	56.5	66	9.5	9.85	103.7							
								1	1.5	1.5	56.5	58		
								2	1.5	1.5	58	59.5		
								3	1.5	1.5	59.5	61	EDDY	
								4	1.5	1.5	61	62.5		
								5	1.5	1.5	62.5	64		
								6	1.5	1.5	64	65.5		
								7	0.65	0.65	65.5	66.15		
								CC	0.2	0.2	66.15	66.35	PAL	
									9.85	9.85				
8H	19	0645	66	75.5	9.5	9.82	103.4							
								1	1.5	1.5	66	67.5		
								2	1.5	1.5	67.5	69		
								3	1.5	1.5	69	70.5		
								4	1.5	1.5	70.5	72	EDDY	
								5	1.5	1.5	72	73.5		
								6	1.5	1.5	73.5	75		
								7	0.64	0.64	75	75.6		
								CC	0.18	0.18	75.64	75.82	PAL	
									9.82	9.82				
9H	19	0735	75.5	85	9.5	8.65	91.1							
								1	1.5	1.5	75.5	77		
								2	1.5	1.5	77	78.5		
								3	1.5	1.5	78.5	80	EDDY	
								4	1.5	1.5	80	81.5		Archive half sampled
								5	1.5	1.5	81.5	83		
								6	1.1	1.1	83	84.1		
								CC	0.05	0.05	84.1	84.15	PAL	All to PAL
									8.65	8.65				
10H	19	0835	85	94.5	9.5	9.94	104.6							
								1	1.5	1.5	85	86.5		
								2	1.5	1.5	86.5	88		
								3	1.5	1.5	88	89.5		
								4	1.5	1.5	89.5	91		
								5	1.5	1.5	91	92.5		
								6	1.5	1.5	92.5	94	EDDY	
								7	0.79	0.79	94	94.8		
								CC	0.15	0.15	94.79	94.94	PAL	
									9.94	9.94				
11H	19	0930	94.5	104	9.5	9.71	102.2							
								1	1.5	1.5	94.5	96		

Table T2 (continued).

Core	Date (September 1998)	Time (UTC)	Core depth (mbsf) Top	Core depth (mbsf) Bottom	Length (m) Cored	Length (m) Recovered	Recovery (%)	Section	Length (m) Liner	Length (m) Curated	Section depth (mbsf) Top	Section depth (mbsf) Bottom	Catwalk samples	Comment
								2	1.5	1.5	96	97.5		
								3	1.5	1.5	97.5	99		
								4	1.5	1.5	99	100.5		
								5	1.5	1.5	100.5	102	EDDY	
								6	1.5	1.5	102	103.5		
								7	0.55	0.55	103.5	104.05		
								CC	0.16	0.16	104.05	104.21	PAL	
									9.71	9.71				
12H	19	1025	104	113.5	9.5	9.87	103.9							
								1	1.5	1.5	104	105.5		
								2	1.5	1.5	105.5	107		
								3	1.5	1.5	107	108.5		
								4	1.5	1.5	108.5	110		
								5	1.5	1.5	110	111.5	EDDY	
								6	1.5	1.5	111.5	113		
								7	0.63	0.63	113	113.6		
								CC	0.24	0.24	113.63	113.87	PAL	
									9.87	9.87				
13H	19	1125	113.5	123	9.5	9.74	102.5							
								1	1.5	1.5	113.5	115	EDDY	
								2	1.5	1.5	115	116.5		
								3	1.5	1.5	116.5	118		
								4	1.5	1.5	118	119.5		
								5	1.5	1.5	119.5	121		
								6	1.5	1.5	121	122.5		
								7	0.5	0.5	122.5	123		
								CC	0.24	0.24	123	123.24	PAL	
									9.74	9.74				
14H	19	1225	123	132.5	9.5	10.05	105.8							
								1	1.5	1.5	123	124.5	EDDY	
								2	1.5	1.5	124.5	126		
								3	1.5	1.5	126	127.5		
								4	1.5	1.5	127.5	129		
								5	1.5	1.5	129	130.5		
								6	1.5	1.5	130.5	132		
								7	0.73	0.73	132	132.7		
								CC	0.32	0.32	132.73	133.05	PAL	
									10.05	10.05				
15H	19	1325	132.5	142	9.5	9.59	100.9							
								1	0.97	0.97	132.5	133.47		Crushed liner
								2	1.5	1.5	133.47	134.97		Crushed liner
								3	1.5	1.5	134.97	136.47		
								4	1.5	1.5	136.47	137.97		
								5	1.5	1.5	137.97	139.47	EDDY	
								6	1.5	1.5	139.47	140.97		
								7	0.78	0.78	140.97	141.75		
								CC	0.34	0.34	141.75	142.09	PAL	
									9.59	9.59				
16H	19	1440	142	151.5	9.5	9.79	103.1							
								1	1.5	1.5	142	143.5		

Table T2 (continued).

Core	Date (September 1998)	Time (UTC)	Core depth (mbsf) Top	Core depth (mbsf) Bottom	Length (m) Cored	Length (m) Recovered	Recovery (%)	Section	Length (m) Liner	Length (m) Curated	Section depth (mbsf) Top	Section depth (mbsf) Bottom	Catwalk samples	Comment
								2	1.5	1.5	143.5	145		
								3	1.5	1.5	145	146.5		
								4	1.5	1.5	146.5	148	EDDY	
								5	1.5	1.5	148	149.5		
								6	1.5	1.5	149.5	151		
								7	0.52	0.52	151	151.5		
								CC	0.27	0.27	151.52	151.79	PAL	
									9.79	9.79				
17O	19	1830	151.5	230	0	0	N/A							
17X	19	1940	230	239.6	9.6	6.39	66.6							
								1	1.5	1.5	230	231.5		
								2	1.5	1.5	231.5	233		
								3	1.5	1.5	233	234.5		
								4	1.5	1.5	234.5	236		
								CC	0.39	0.39	236	236.39	PAL	
									6.39	6.39				
18O	20	745	239.6	484	0	0	N/A							
18X	20	925	484	488.5	4.5	4.95	110							
								1	1.5	1.5	484	485.5		
								2	1.5	1.5	485.5	487		
								3	1.5	1.5	487	488.5		
								CC	0.45	0.45	488.5	488.95	PAL	
									4.95	4.95				
19X	20	1110	488.5	498.1	9.6	9.7	101							
								1	1.5	1.5	488.5	490		
								2	1.5	1.5	490	491.5		
								3	1.5	1.5	491.5	493		
								4	1.5	1.5	493	494.5	IW	
								5	1.5	1.5	494.5	496	HS	
								6	1.5	1.5	496	497.5		
								7	0.35	0.35	497.5	497.85		
								CC	0.35	0.35	497.85	498.2	PAL	
									9.7	9.7				
20X	20	1315	498.1	507.7	9.6	8.44	87.9							
								1	1.5	1.5	498.1	499.6		
								2	1.5	1.5	499.6	501.1		
								3	1.5	1.5	501.1	502.6	HS	
								4	1.5	1.5	502.6	504.1		
								5	1.5	1.5	504.1	505.6		
								6	0.79	0.79	505.6	506.39		
								CC	0.15	0.15	506.39	506.54	PAL	All to PAL
									8.44	8.44				
21X	20	1520	507.7	517.4	9.7	9.41	97							
								1	1.5	1.5	507.7	509.2		
								2	1.5	1.5	509.2	510.7		
								3	1.5	1.5	510.7	512.2		
								4	1.5	1.5	512.2	513.7	HS	
								5	1.5	1.5	513.7	515.2		

Table T2 (continued).

Core	Date (September 1998)	Time (UTC)	Core depth (mbsf) Top	Core depth (mbsf) Bottom	Length (m) Cored	Length (m) Recovered	Recovery (%)	Section	Length (m) Liner	Length (m) Curated	Section depth (mbsf) Top	Section depth (mbsf) Bottom	Catwalk samples	Comment
								6	1.5	1.5	515.2	516.7		
								7	0.26	0.26	516.7	516.96		
								CC	0.15	0.15	516.96	517.11	PAL	All to PAL
									9.41	9.41				
22X	20	1710	517.4	527	9.6	9.81	102.2							
								1	1.5	1.5	517.4	518.9		
								2	1.5	1.5	518.9	520.4		
								3	1.5	1.5	520.4	521.9		
								4	1.5	1.5	521.9	523.4	IW	
								5	1.5	1.5	523.4	524.9	HS	
								6	1.5	1.5	524.9	526.4		
								7	0.43	0.43	526.4	526.83		
								CC	0.38	0.38	526.83	527.21	PAL	
									9.81	9.81				
23X	20	1910	527	536.6	9.6	9.81	102.2							
								1	1.5	1.5	527	528.5		
								2	1.5	1.5	528.5	530		
								3	1.5	1.5	530	531.5		
								4	1.5	1.5	531.5	533		
								5	1.5	1.5	533	534.5	HS	
								6	1.5	1.5	534.5	536		
								7	0.43	0.43	536	536.4		
								CC	0.38	0.38	536.43	536.81	PAL	
									9.81	9.81				
24X	20	2105	536.6	546.2	9.6	9.76	101.7							
								1	1.5	1.5	536.6	538.1		
								2	1.5	1.5	538.1	539.6		
								3	1.5	1.5	539.6	541.1		
								4	1.5	1.5	541.1	542.6		
								5	1.5	1.5	542.6	544.1	HS	
								6	1.5	1.5	544.1	545.6		
								7	0.41	0.41	545.6	546.01		
								CC	0.35	0.35	546.01	546.36	PAL	
									9.76	9.76				
25X	20	2250	546.2	555.7	9.5	9.66	101.7							
								1	1.5	1.5	546.2	547.7		
								2	1.5	1.5	547.7	549.2	HS	
								3	1.5	1.5	549.2	550.7		
								4	1.5	1.5	550.7	552.2	IW	
								5	1.5	1.5	552.2	553.7		
								6	1.5	1.5	553.7	555.2		
								7	0.4	0.4	555.2	555.6		
								CC	0.26	0.26	555.6	555.86	PAL	
									9.66	9.66				
26X	21	30	555.7	565.4	9.7	9.67	99.7							
								1	1.5	1.5	555.7	557.2		
								2	1.5	1.5	557.2	558.7		
								3	1.5	1.5	558.7	560.2		

Table T2 (continued).

Core	Date (September 1998)	Time (UTC)	Core depth (mbsf) Top	Core depth (mbsf) Bottom	Length (m) Cored	Length (m) Recovered	Recovery (%)	Section	Length (m) Liner	Length (m) Curated	Section depth (mbsf) Top	Section depth (mbsf) Bottom	Catwalk samples	Comment
								4	1.5	1.5	560.2	561.7		
								5	1.5	1.5	561.7	563.2	HS	
								6	1.5	1.5	563.2	564.7		
								7	0.36	0.36	564.7	565.06		
								CC	0.31	0.31	565.06	565.37	PAL	
									9.67	9.67				
27X	21	210	565.4	575.1	9.7	9.66	99.6							
								1	1.5	1.5	565.4	566.9		
								2	1.5	1.5	566.9	568.4		
								3	1.5	1.5	568.4	569.9		
								4	1.5	1.5	569.9	571.4		
								5	1.5	1.5	571.4	572.9		
								6	1.5	1.5	572.9	574.4		
								7	0.32	0.32	574.4	574.72		
								CC	0.34	0.34	574.72	575.06	PAL	
									9.66	9.66				
28X	21	355	575.1	584.7	9.6	8.78	91.5							
								1	1.5	1.5	575.1	576.6		
								2	1.5	1.5	576.6	578.1		
								3	1.5	1.5	578.1	579.6		
								4	1.5	1.5	579.6	581.1	IW	
								5	1.5	1.5	581.1	582.6	HS	
								6	1.13	1.13	582.6	583.73		
								CC	0.15	0.15	583.73	583.88	PAL	
									8.78	8.78				
29X	21	615	584.7	594.3	9.6	8.71	90.7							
								1	1.5	1.5	584.7	586.2		
								2	1.5	1.5	586.2	587.7		
								3	1.5	1.5	587.7	589.2		
								4	1.5	1.5	589.2	590.7		
								5	1.5	1.5	590.7	592.2	HS	
								6	0.82	0.82	592.2	593.02		
								CC	0.39	0.39	593.02	593.41	PAL	
									8.71	8.71				
30X	21	835	594.3	603.9	9.6	5.44	56.7							
								1	1.5	1.5	594.3	595.8		
								2	1.5	1.5	595.8	597.3		
								3	1.5	1.5	597.3	598.8	HS	
								4	0.69	0.69	598.8	599.49		
								CC	0.25	0.25	599.49	599.74	PAL	
									5.44	5.44				
31X	21	1105	603.9	613.6	9.7	7.28	75.1							
								1	1.5	1.5	603.9	605.4		
								2	1.5	1.5	605.4	606.9		
								3	1.5	1.5	606.9	608.4		
								4	1.5	1.5	608.4	609.9	IW	
								5	1.18	1.18	609.9	611.08	HS	
								CC	0.1	0.1	611.08	611.18	PAL	All to PAL

Table T2 (continued).

Core	Date (September 1998)	Time (UTC)	Core depth (mbsf) Top	Core depth (mbsf) Bottom	Length (m) Cored	Length (m) Recovered	Recovery (%)	Section	Length (m) Liner	Length (m) Curated	Section depth (mbsf) Top	Section depth (mbsf) Bottom	Catwalk samples	Comment
									7.28	7.28				
32X	20	1540	613.6	623.2	9.6	5.61	58.4							
								1	1.5	1.5	613.6	615.1		
								2	1.5	1.5	615.1	616.6	HS	
								3	1.5	1.5	616.6	618.1		
								4	0.58	0.58	618.1	618.68		
								CC	0.53	0.53	618.68	619.21	PAL	
									5.61	5.61				
33X	21	1910	623.2	632.8	9.6	2.66	27.7							
								1	1.35	1.35	623.2	624.55	IW	
								2	0.96	0.96	624.55	625.51	HS	
								CC	0.35	0.35	625.51	625.86	PAL	
									2.66	2.66				
				Totals:	309.90	289.44	93.40							

Notes: IW = interstitial water, HS = head space, PAL = paleontology, EDDY = geotechnical samples, N/A = not available. This table is also available in **ASCII format.**

Table T3. Position and thickness of tephra layers.

Core, section	Depth at base of tephra (cm)	Depth at base of tephra (mbsf)	Thickness of tephra (cm)	Comments
181-1123A-				
1H-1	101	1.01		Dispersed
1H-2	10	1.6	5	
2H-5	65	12.75	5	Not in situ
2H-5	138	13.48	0.8	
2H-6	20	13.8	7.6	
2H-6	70	14.3	5.5	
4H-4	62	30.22	1.5	Disturbed
4H-6	130	33.9	2	Disturbed
5H-2	100	37.1	9	
5H-3	68	38.28	0.5	
6H-2	109	46.69	0.2	
6H-3	140	48.5	0.1	
6H-4	134	49.94	5	
6H-5	21	50.31	3	
6H-6	66	52.26	0.3	
6H-6	127	52.87	1	
6H-7	16	53.26	0.5	
6H-7	42	53.52	0.5	
7H-1	55	54.15	3	
7H-3	51.5	57.115	5	
7H-3	112	57.72	8.5	
7H-4	111.5	59.215	2.5	
7H-5	36	59.96	6	
7H-5	60	60.2	1	
7H-5	128	60.88	2.5	
9H-5	102	79.62	10	
9H-5	143	80.03	4	
9H-6	60	80.7	4	
9H-7	10	81.7	5	
12H-3	60	104.7	3	
13H-5	100	117.15	6	
14H-3	93	124.03	4	
181-1123B-				
1H-2	9	1.59	4	Rotated
2H-6	95	11.85	5.5	Rotated
5H-1	2	31.51		Not in situ
5H-3	6	34.96	5	
6H-6	11	49.01	1	
6H-6	24.5	49.145	2	
6H-6	32	49.22	0.3	
6H-6	47	49.37	1	
6H-6	50	49.4		Burrow
6H-6	59	49.49		Burrow
6H-6	143	50.33	10	Disturbed
7H-1	132.5	52.225	4	
7H-2	40	52.8	6	
7H-2	92	53.32	6	
7H-4	94	56.34	0.5	
7H-4	148	56.88	5	
7H-5	75.5	57.655	0.5	
7H-5	117	58.07	1.5	
7H-6	15.5	58.555	4	
7H-6	110	59.5	15	Not in situ
10H-1	40	79.8	7	
10H-1	99	80.39	5	
10H-2	36	81.26	4	
12H-5	7	104.47	10	
13H-2	24.5	109.645	1	Lens
14H-5	76	124.16	9	
15H-5	37	133.33	1	
15H-5	64	133.6	1	
15H-6	135	135.81	2	
19X-6	126	171.56	0.3	Disturbed?
20X-2	143	175.25	1.5	
24X-5	72.5	217.525	6	
29X-7	7	267.87	3	
30X-3	102	272.41	3	
31X-4	68	283.28	1	Disturbed
32X-2	90	290.1	3	
32X-5	50	294.2	3	
33X-CC	2	306.72	1	Disturbed
40X-6	121	373.11	7	
43X-1	79	394.19	2	
181-1123C-				
1H-1	135	1.35	10	Lens?
1H-2	3	1.53	3	Lens?
1H-2	70	2.2	5	Lens?
1H-6	80	8.3	3	Lens?
2H-2	94	11.44	6	
2H-2	109	11.59	5	
2H-3	70	12.7	1	
2H-3	139	13.39	7	
2H-7	35	18.35	4	Disturbed
3H-4	86	23.86	2	
4H-4	120	33.7	2	Lens
4H-6	73	36.23	5	
5H-1	93	38.43	8	
5H-5	123	44.73	3	Lens
6H-1	78	47.78	1	
6H-3	130	51.3	1	Lens
6H-4	65	52.15	9	
6H-4	97	52.47	7	
6H-5	11	53.11	1	
6H-5	92	53.92	2	
6H-5	113	54.13	3	
6H-5	124	54.24	1	
6H-6	10	54.6	3	Lens
6H-6	120	55.7	4	
6H-7	18	56.18	5	
6H-7	67	56.67	8	
7H-2	67	58.67	7	
7H-2	127	59.27	8	
7H-3	4	59.54	4	
7H-3	135	60.85	2	
7H-4	63	61.63	7	
7H-5	13	62.63	4	
9H-5	35	81.85	5	
9H-5	101	82.51	3	
11H-6	139	103.39	22	
12H-2	77.5	106.275	13	
13H-4	69.5	118.695	3	
14H-4	57	128.07	9	Burrow fill

Table T4. Identification and abundance of nannofossils observed at Site 1123. (See table note. Continued on next three pages.)

Core, section, interval (cm)	Depth (mbsf)	Preservation	Group abundance	*Amaurolithus amplificus*	*Amaurolithus delicatus*	*Amaurolithus primus*	*Amaurolithus tricorniculatus*	*Calcidiscus leptoporus*	*Calcidiscus macintyrei*	*Calcidiscus premacintyrei*	*Calcidiscus tropicus*	*Ceratolithus rugosus*	*Chiasmolithus* spp.	*Clausicoccus subdistichus*	*Coccolithus eopelagicus*	*Coccolithus miopelagicus*	*Coccolithus pelagicus*	*Coronocyclus nitescens*	*Cyclicargolithus abisectus*	*Cyclicargolithus floridanus*	*Dictyococcites antarcticus*	*Dictyococcites bisectus*	*Dictyococcites productus*	*Discoaster adamanteus*	*Discoaster asymmetricus*	*Discoaster bellus*	*Discoaster bollii*	*Discoaster brouweri*	*Discoaster calcaris*	*Discoaster challengeri*	*Discoaster decorus*	*Discoaster deflandrei*	*Discoaster dilatus*	*Discoaster exilis*	*Discoaster intercalaris*	*Discoaster lodoensis*	*Discoaster loeblichii*	*Discoaster moorei*	*Discoaster pentaradiatus*	*Discoaster pseudovariabilis*	*Discoaster quinqueramus*	*Discoaster saipanensis*	*Discoaster sanmiguelensis*	*Discoaster surculus*	Comments
181-1123A-																																												
1H-1, 40	0.40	G	VA					C									C					R																							Big *C. pelagicus*
1H-2, 7	1.57	G	A					C								R				R											R													Big *C. pelagicus*
1H-2, 145	2.95	G	VA					C									A																												
1H-3, 80	3.80	G	VA					C								R				R																									
1H-4, 75	5.25	G	VA					C									A																												
1H-CC, 0-15	5.95	G	VA					C								R	C					R																							Big *C. pelagicus*
2H-6, 139	14.99	G	VA					F									A						A																					Big *C. pelagicus*
2H-CC, 16-26	15.61	G	VA					C									C															R												
3H-CC, 0-10	23.21	G	VA					C									A																												
4H-CC, 0-10	34.70	G	VA					F								R	F											R				R												
5H-CC, 0-10	44.19	G	VA					C									C					F		F																					
6H-CC, 0-10	53.72	G	VA					A								R	C		R	R				A																					
7H-CC, 11-21	63.15	G	VA					C				R				R	C			R		R																								
8H-CC, 11-16	72.02	G	VA					C	A				R			R	C			R								R																	
9H-CC, 17-27	82.33	G	VA														C																												
10H-CC, 15-20	91.88	G	VA					C	C	F							C											R								R			C						
11H-CC, 11-21	101.14	G	VA					C	F								C						A	R	F			C											C					
12H-CC, 13-23	110.76	G	VA					C	F								C								C			C				R							C				C	
13H-CC, 14-19	119.69	G	VA					C	C			R	R				C		R	R			C		C			C											C				C	
14H-CC, 12-22	129.66	G	VA					F	C			F				R	C								F			C																F	
15H-CC, 21-26	139.54	G	VA		C				C												C				F			C							R				C	R			R	
16H-6, 126	147.86	G	VA		C			C	C				R				C				C				C			C															C	
16H-CC, 21-26	148.66	G	VA		C			C	C								A				R	C			C			C															C	
17H-CC, 22-27	158.57	G	VA		R				A				R				C					A	C					F											R				R	
181-1123B-																																													
18X-CC, 18-28	163.69	G	VA		C			C	C								C				R	C	R	C				C				R					C				C		
19X-CC, 23-33	172.31	G	VA		F			C	F								F	R					C					F											F				F	
20X-CC, 20-25	182.00	G	VA		F			F	F								C					C		R						R		R	R			R			F	R		R		Many reworked
21X-CC, 13-23	191.27	G	VA					F	F		R		F			F	C				F	C	F	R				R																Many reworked
22X-CC, 26-36	201.37	G	VA		F	R			A								C	C																			R	R					
23X-CC, 21-26	208.91	G	VA														C				R	C	R					F																
24X-CC, 26-31	220.50	G	A	?	F	C	R										C											C							R				R		R		R	
25X-CC, 22-32	230.00	G	VA			R	R						R			R	C	R			R	A	R	A				C		R						R			F		R		R	
26X-CC, 22-32	234.08	G	VA			R			F								C	R			R	A		A				F									R		F		R		F	
27X-CC, 26-36	249.32	G	VA	R	F	R											C											C									R							
28X-CC, 18-23	258.74	M	VA	R				C	F				R				C					C		C															R	R				
29X-CC, 27-37	268.49	G	VA			R							R			R	C				F	A	R					F												F	R		F	
30X-CC, 25-30	278.00	G	VA					F	F							R	C					C	R					F			R				R	F	F	R		R		R	
31X-CC, 17-22	287.54	G	VA					C	C								A	F			F	C						R															
32X-CC, 23-33	296.31	G	VA					F	F													C					R	F									F	F	R					
33X-CC, 15-25	306.85	G	VA					C	C		R						A		R	R	A			R	R			F											R					
34X-CC, 19-34	316.53	G	A					F	F				R				A				R	C	R		R			R				R												

Table T4 (continued).

Core, section, interval (cm)	Depth (mbsf)	Preservation	Group abundance	*Discoaster tamalis*	*Discoaster triradiatus*	*Discoaster variabilis*	*Emiliania huxleyi*	*Ericsonia formosa*	*Geminilithella rotula*	*Gephyrocapsa* (medium)	*Gephyrocapsa parallela*	*Gephyrocapsa* (small)	*Helicosphaera carteri*	*Helicosphaera euphratis*	*Helicosphaera mediterranea*	*Helicosphaera paleocarteri*	*Helicosphaera perch-nielseniae*	*Helicosphaera sellii*	*Isthmolithus recurvus*	*Markalius inversus*	*Minylitha convallis*	*Pontosphaera* spp.	*Pseudoemiliania lacunosa*	*Pyrocyclus* spp.	*Reticulofenestra asanoi*	*Reticulofenestra lockerii*	*Reticulofenestra* (medium)	*Reticulofenestra pseudoumbilicus*	*Reticulofenestra* (small)	*Reticulofenestra umbilicus*	*Reticulofenestra* sp. *Z*	*Rhabdosphaera clavigera*	*Sphenolithus abies*	*Sphenolithus belemnos*	*Sphenolithus conicus*	*Sphenolithus dissimilis*	*Sphenolithus heteromorphus*	*Sphenolithus moriformis*	*Sphenolithus neoabies*	*Syracosphaera* spp.	*Umbilicosphaera sibogae*	*Watznauenia barnesae*	*Zygrhablithus bijugatus*	Comments
181-1123A-																																										
1H-1, 40	0.40	G	VA				A			A		C	C									R	R	R				A			C						C	F				
1H-2, 7	1.57	G	A				A			C		C	F					R				R															R	R				
1H-2, 145	2.95	G	VA				C			D	R		C																		R						R	F				
1H-3, 80	3.80	G	VA				F			D		C	F																		R											
1H-4, 75	5.25	G	VA				C			C		C	R																				R					R	R				
1H-CC, 0-15	5.95	G	VA							A	R		R					R				R	R					A			F							R				Big *C. pelagicus*
2H-6, 139	14.99	G	VA							A		A	R									R									R											Big *C. pelagicus*
2H-CC, 16-26	15.61	G	VA							A	R		C		R								R		R		C	R			F							F				
3H-CC, 0-10	23.21	G	VA						R	F		C	C									R	A		F	F										R		F				
4H-CC, 0-10	34.70	G	VA			R				R	R	F	C										A				C	F			R	R										
5H-CC, 0-10	44.19	G	VA						R	R		F	C					R				R	C				A		A		R											
6H-CC, 0-10	53.72	G	VA							R		C	C									R	C				A	F	A	R		R										
7H-CC, 11-21	63.15	G	VA							C			C					C					C					R														
8H-CC, 11-16	72.02	G	VA										A					A					A	R					D													
9H-CC, 17-27	82.33	G	VA										C					C					C				A		A													
10H-CC, 15-20	91.88	G	VA		R								C					C					C						A													
11H-CC, 11-21	101.14	G	VA	F									C					C					C				C		A													
12H-CC, 13-23	110.76	G	VA	C	F	F							F					C					C				A	R	A							R						
13H-CC, 14-19	119.69	G	VA	C		F			F				C					C					F				C	R	A													
14H-CC, 12-22	129.66	G	VA	F					C				F					F					F					C	A										R				
15H-CC, 21-26	139.54	G	VA		F	F																					C											R				
16H-6, 126	147.86	G	VA			C			F																		C	A				F						C		R		
16H-CC, 21-26	148.66	G	VA			C			C				C					R									C					F						C				
17H-CC, 22-27	158.57	G	VA						R				F									R					C	C	R			F						F				
181-1123B-																																										
18X-CC, 18-28	163.69	G	VA		F	C			F				F									R					C	C										C			R	R	
19X-CC, 23-33	172.31	G	VA		C	A			F				F														A	C	A			F						F				
20X-CC, 20-25	182.00	G	VA			C			C				F															A		R		F						F				R	Many reworked
21X-CC, 13-23	191.27	G	VA			C			F				F									R		F				A		R			F					F					Many reworked
22X-CC, 26-36	201.37	G	VA			C			F																		A	A		R			F					F				
23X-CC, 21-26	208.91	G	VA			C			F															F			C	A										R				
24X-CC, 26-31	220.50	G	A		R	C																		F				C										F				
25X-CC, 22-32	230.00	G	VA			C							F											F				C										F				
26X-CC, 22-32	234.08	G	VA			C		R	F															F			C	C	C	R												
27X-CC, 26-36	249.32	G	VA			C																						C														
28X-CC, 18-23	258.74	M	VA			C							R														A	F				R						F				
29X-CC, 27-37	268.49	G	VA			F																		F			A	C												F		
30X-CC, 25-30	278.00	G	VA		R	C							R								R							A										F			R	
31X-CC, 17-22	287.54	G	VA			R			F							R					F						A	C										F			F	
32X-CC, 23-33	296.31	G	VA		R				F												R			F				A														
33X-CC, 15-25	306.85	G	VA		R	C			F				R								F						F	A	C	R			C				R	F			F	
34X-CC, 19-34	316.53	G	A		R	C			F				R								F			F			C	A		R			C									

Table T4 (continued).

Core, section, interval (cm)	Depth (mbsf)	Preservation	Group abundance	*Amaurolithus amplificus*	*Amaurolithus delicatus*	*Amaurolithus primus*	*Amaurolithus tricorniculatus*	*Calcidiscus leptoporus*	*Calcidiscus macintyrei*	*Calcidiscus premacintyrei*	*Calcidiscus tropicus*	*Ceratolithus rugosus*	*Chiasmolithus* spp.	*Clausicoccus subdistichus*	*Coccolithus eopelagicus*	*Coccolithus miopelagicus*	*Coccolithus pelagicus*	*Coronocyclus nitescens*	*Cyclicargolithus abisectus*	*Cyclicargolithus floridanus*	*Dictyococcites antarcticus*	*Dictyococcites bisectus*	*Dictyococcites productus*	*Discoaster adamanteus*	*Discoaster asymmetricus*	*Discoaster bellus*	*Discoaster bollii*	*Discoaster brouweri*	*Discoaster calcaris*	*Discoaster challengeri*	*Discoaster decorus*	*Discoaster deflandrei*	*Discoaster dilatus*	*Discoaster exilis*	*Discoaster intercalaris*	*Discoaster lodoensis*	*Discoaster loeblichii*	*Discoaster moorei*	*Discoaster pentaradiatus*	*Discoaster pseudovariabilis*	*Discoaster quinqueramus*	*Discoaster saipanensis*	*Discoaster sanmiguelensis*	*Discoaster surculus*	Comments
35X-CC, 9-19	326.02	G	VA					C	F								C				C	R				C		R		R												
36X-CC, 13-23	335.47	P	C					F	F								C				F																						Fragmentation
37X-CC, 22-32	345.20	M	VA					F	F								F			R	C	R				F							R		R			R				Cold
38X-CC, 31-41	354.79	M	C														F						F					R														Fragmentation
39X-CC, 29-39	364.48	P	VA					C	C								F						C				R	C									R					Fragmentation
40X-CC, 22-32	374.06	M	A					F	F				R			F	F			R	F						R	R					F									Fragmentation
41X-CC, 28-38	382.20	P	C													F					C	R																				
42X-CC, 24-34	388.44	M	VA						C							C	C			F	C		C			F		F	R			F	F	F	R					R			
43X-CC, 14-24	399.52	G	A					F	F	R	R					C	C			C	C						R	F	R					F								
44X-CC, 20-30	408.32	M	VA					F	R	C			R			C	C			A	C	R									R										R	
45X-CC, 18-28	416.56	G	VA					R		C			R			C	C		R	C	A	R		F				F				F		F						R			
46X-CC, 20-25	428.36	M	VA					F		F						F	C			C	C							R			R	F									R	
47X-CC, 0-10	436.96	M	A					C		F						F	C			C	C																						Fragmentation
48X-CC, 0-15	445.60	M	A					R		F			R			F	A			A				F									F									Fragmentation
49X-CC, 26-41	457.06	M	C					F		F						F	A			A				R																		Fragmentation
50X-CC, 39-54	468.60	M	A							F						F	C			A	C											C										Fragmentation
51X-1, 117	471.17	G	VA							F			R			C	A			A	A	R	C									F										
51X-CC, 17-27	479.62	M	C					R		F						F	F			D	C											C										Fragmentation
52X-CC, 26-36	488.56	P	A					F		C						R	F			D	C																					Fragmentation
181-1123C-																																											
18X-CC, 35-45	488.85	M	A							F						F	C			D												C										
19X-CC, 25-35	498.10	M	C							F						F	C			A	F											C	C									
20X-3, 147	502.57	G	A					R		F						F	C			A												C	C									
20X-CC, 0-15	506.39	M	A													R	C			C	C											C	C									
21X-4, 138-138	513.58	G	A					R								F	F			C													C									
21X-CC, 0-15	516.96	M	A													F	C		R	A												C										
22X-5, 78-78	524.18	G	A					R			R						A			C	C											C										
22X-6, 136	526.26	G	A													F	A			C	C											C	C									
22X-CC, 23-38	527.06	M	A													F	A			D		R										A										
23X-CC, 28-38	536.71	P	A													F	F			A												A										
24X-CC, 25-35	546.26	M	VA													C	A			C		R										C	C									
25X-CC, 16-26	555.76	G	A					R									C			C												C										
26X-CC, 21-31	565.27	G	A										R			C	A			C	C	R										A										
27X-CC, 24-34	574.96	M	A													C	A			C												A										
28X-CC, 5-15	583.78	M	C										R			C	A			A	C	R	C	C								C										
29X-2, 97	587.17	M	A										R			F	A			C				C								C										Above the hiatus
29X-2, 119	587.39	M	A										F	C	C					F		A										F										Below the hiatus
29X-CC, 29-39	593.31	M	A										C	A	C		C					A																				
30X-CC, 15-25	599.64	M	A										F	C	C		A			F		C										R										
31X-CC, 0-10	611.08	M	A										C		C		C					C																			R		
32X-2, 132	616.42	M	A																	F		C										R								R		
32X-CC, 43-53	619.11	P	A																			D																				
33X-CC, 25-35	625.76	P	A																			D																				Bad preservation

Note: Preservation: G = good, M = moderate, and P = poor; total abundance of calcareous nannofossils: VA = very abundant, A = abundant, and C = common; relative abundance of species: D = dominant, A = abundant, C = common, F = few, and R = rare.

Table T4 (continued).

Core, section, interval (cm)	Depth (mbsf)	Preservation	Group abundance	*Discoaster tamalis*	*Discoaster triradiatus*	*Discoaster variabilis*	*Emiliania huxleyi*	*Ericsonia formosa*	*Geminilithella rotula*	*Gephyrocapsa* (medium)	*Gephyrocapsa parallela*	*Gephyrocapsa* (small)	*Helicosphaera carteri*	*Helicosphaera euphratis*	*Helicosphaera mediterranea*	*Helicosphaera paleocarteri*	*Helicosphaera perch-nielseniae*	*Helicosphaera sellii*	*Isthmolithus recurvus*	*Markalius inversus*	*Minylitha convallis*	*Pontosphaera* spp.	*Pseudoemiliania lacunosa*	*Pyrocyclus* spp.	*Reticulofenestra asanoi*	*Reticulofenestra lockerii*	*Reticulofenestra* (medium)	*Reticulofenestra pseudoumbilicus*	*Reticulofenestra* (small)	*Reticulofenestra umbilicus*	*Reticulofenestra* sp. *Z*	*Rhabdosphaera clavigera*	*Sphenolithus abies*	*Sphenolithus belemnos*	*Sphenolithus conicus*	*Sphenolithus dissimilis*	*Sphenolithus heteromorphus*	*Sphenolithus moriformis*	*Sphenolithus neoabies*	*Syracosphaera* spp.	*Umbilicosphaera sibogae*	*Watznaueria barnesae*	*Zygrhablithus bijugatus*	Comments
35X-CC, 9-19	326.02	G	VA			F			F												R			F			A	A													
36X-CC, 13-23	335.47	P	C			R																					C	A														Fragmentation
37X-CC, 22-32	345.20	M	VA			F																		R			A	A		R								R			R	Cold
38X-CC, 31-41	354.79	M	C			R																					C	A										R				Fragmentation
39X-CC, 29-39	364.48	P	VA			C			F															F			A	A									F	F				Fragmentation
40X-CC, 22-32	374.06	M	A			R																		F			A	A		R							F					Fragmentation
41X-CC, 28-38	382.20	P	C																																							
42X-CC, 24-34	388.44	M	VA			R			F															F			A	A									F	F				
43X-CC, 14-24	399.52	G	A			C			F				R														C	A									F	R				
44X-CC, 20-30	408.32	M	VA			F																						A		R							F		R		R	
45X-CC, 18-28	416.56	G	VA			C			R															F			A	C									C	F			F	
46X-CC, 20-25	428.36	M	VA			F			F															F			C	A									F	F				
47X-CC, 0-10	436.96	M	A			F			F				F			F										C	A	C								F	F				Fragmentation
48X-CC, 0-15	445.60	M	A			C			F				F														C	F									F				F	Fragmentation
49X-CC, 26-41	457.06	M	C			R			R				F											R			C								F	F				F	Fragmentation
50X-CC, 39-54	468.60	M	A			C			R															R										R		F	F				Fragmentation
51X-1, 117	471.17	G	VA						R				R			R													C	R				R		F	C				
51X-CC, 17-27	479.62	M	C			C			F																			F									R					Fragmentation
52X-CC, 26-36	488.56	P	A			C							F	R		R												R				F			F	C	C				Fragmentation
181-1123C-																																										
18X-CC, 35-45	488.85	M	A						F				F	R		R											C							R		C		C				
19X-CC, 25-35	498.10	M	C			A																					C								F	C	C			F	
20X-3, 147	502.57	G	A																								A	F							F	C	C			F	
20X-CC, 0-15	506.39	M	A			C																		R			A								F	C	C				
21X-4, 138-138	513.58	G	A						R															F		F				C				F	C	C				
21X-CC, 0-15	516.96	M	A						R																		C			C				F	C	C				
22X-5, 78-78	524.18	G	A						R																		C			C						C					
22X-6, 136	526.26	G	A													R											C			C			C			C					
22X-CC, 23-38	527.06	M	A																					R			A			C			F			C				R	
23X-CC, 28-38	536.71	P	A																								A			R	C		R		R					
24X-CC, 25-35	546.26	M	VA																								C			R				R	C	C				
25X-CC, 16-26	555.76	G	A						R															R		F								R	F					
26X-CC, 21-31	565.27	G	A														R					R					C			R	F			F	F	C			R	
27X-CC, 24-34	574.96	M	A																								F			R					R					
28X-CC, 5-15	583.78	M	C																							F					F				F	A				
29X-2, 97	587.17	M	A						R																					R	F				C				R	Above the hiatus
29X-2, 119	587.39	M	A																C											C					C				C	Below the hiatus
29X-CC, 29-39	593.31	M	A																C											A					C				C	
30X-CC, 15-25	599.64	M	A																F								C			A					C				F	
31X-CC, 0-10	611.08	M	A					R											R	R							C			A									C	
32X-2, 132	616.42	M	A																C	R										C										
32X-CC, 43-53	619.11	P	A					F																						F					F				C	
33X-CC, 25-35	625.76	P	A																											F										Bad preservation

Table T5. Summary of nannofossil datums, age estimates, and references used at Site 1123.

Bioevent	Depth (mbsf)	Age (Ma)	Reference
Bottom acme *Emiliania huxleyi*	2.26	0.85	Berggren et al., 1995a
FO *Emiliania huxleyi*	5.60	0.24	Naish et al., 1998
LO *Pseudoemiliania lacunosa*	19.41	0.42	Naish et al., 1998
LO *Calcidiscus macintyrei*	67.58	1.60	Raffi et al., 1993
FO *Gephyrocapsa* (medium)	67.58	1.67	Raffi and Flores, 1995
LO *Discoaster brouweri*	67.58	1.96	Raffi and Flores, 1995
LO *Discoaster pentaradiatus*	87.10	2.30	Wei, 1993
LO *Discoaster surculus*	105.95	2.61	Raffi and Flores, 1995
LO *Reticulofenestra pseudoumbilicus*	124.65	3.82	Raffi and Flores, 1995
FO *Pseudoemiliania lacunosa*	134.60	4.00	Gartner, 1990
FO *Discoaster asymmetricus*	153.61	4.13	Shackleton et al., 1995
LO *Discoaster quinqueramus*	214.70	5.56	Raffi and Flores, 1995
FO *Amaurolithus primus*	273.84	7.39	Backman and Raffi, 1997
LO *Minylitha convallis*	282.77	7.73	Shackleton et al., 1995
FO *Minylitha convallis*	330.74	9.34	Raffi and Flores, 1995
LO *Coccolithus miopelagicus*	369.27	10.94	Backman and Raffi, 1997
LO *Calcidiscus premacintyrei*	403.92	12.65	Raffi and Flores, 1995
LO *Sphenolithus heteromorphus*	451.33	13.52	Backman and Raffi, 1997
FO *Calcidiscus premacintyrei*	504.48	17.40	Backman and Raffi, 1997
LO *Sphenolithus belemnos*	525.22	18.30	Berggren et al., 1995b
FO *Sphenolithus belemnos*	541.48	19.20	Berggren et al., 1995b
Acme *Clausicoccus subdistichus*	593.31	33.30	Berggren et al., 1995b
LO *Discoaster saipanensis*	613.75	~34.6	Berggren et al., 1995b

Table T6. Significant foraminiferal and bolboformid datum levels at Site 1123.

Foraminiferal and bolboformid events	Epoch	NZ stage	Age (Ma)	Core, section, interval (cm)	Depth (mbsf)
FO *Globorotalia hirsuta*	Pleistocene		~0.45	1123B-1H-1, 18-20cm	0.18
LO *Globorotalia puncticuloides*	Pleistocene	Wc	~0.6	1123B-2H-CC	15.60
LCO *Globorotalia puncticuloides*	Pleistocene	e Wc	~0.7	1123A-3H-CC	23.20
LO *Stilostomella* spp.	Pleistocene		~0.8	1123A-4H-CC	34.70
FO *Globorotalia truncatulinoides*	Pleistocene	e Wc	~0.8	1123A-5H-CC	44.20
FO *Globorotalia crassula*	late Pliocene	Wm/Wn	2.6	1123A-8H-CC	72.00
FO *Globorotalia tosaensis*	late Pliocene	Wm/Wn	3.2	1123A-8H-CC	72.80
LO *Globorotalia crassaformis* (dextral)	late Pliocene	Wn	2.1	1123A-9H-CC	82.40
FO *Globorotalia crassaformis* (dextral)	early Pliocene	Wp/Wm	3.0	1123A-10H-CC	91.90
FO *Globorotalia puncticuloides*	early Pliocene	Wp	3.4	1123A-11H-CC	101.10
LO *Globorotalia pliozea*	early Pliocene	Wp	3.4	1123A-11H-CC	101.10
LO *Globorotalia crassaconica*	early Pliocene	Wo	3.2	1123A-11H-CC	101.10
FO *Globorotalia inflata*	early Pliocene	e Wc	3.8	1123A-11H-CC	101.10
FO *Globorotalia inflata triangula*	early Pliocene	Wo/Wp	3.7	1123B-12H-CC	110.80
LCO *Globorotalia pliozea*	early Pliocene	Wo/Wp	3.7	1123A-12H-CC	110.80
LO *Globorotalia puncticulata*	early Pliocene	Wo/Wp	3.8	1123A-12H-CC	110.80
FO *Globorotalia crassaconica*	early Pliocene	Wo	4.7	1123B-18X-CC	163.70
LO *Globorotalia mons*	early Pliocene	Wo	4.8	1123B-18X-CC	163.70
FO *Sphaeroidinella dehiscens*	early Pliocene	Wo	4.8	1123B-18X-CC	163.70
FO *Globorotalia puncticulata*	basal Pliocene	Tk/Wo	5.2	1123B-19X-CC	172.30
LO *Globorotalia sphericomiozea*	Miocene/Pliocene	Tk/Wo	5.2	1123B-20X-4, 83-87 cm	177.65
LO *Globorotalia juanai*	Miocene/Pliocene	Tk/Wo	5.2	1123B-20X-CC	182.00
FO *Globorotalia pliozea*	late Miocene	Tk	5.4	1123B-20X-CC	182.00
LO *Globorotalia miotumida*	late Miocene	Tk	5.6	1123B-20X-CC	182.00
FO *Globorotalia mons*	late Miocene	Tk	5.5	1123B-21X-CC	191.40
FO *Globorotalia sphericomiozea*	late Miocene	Tk	5.6	1123B-21X-CC	191.40
FO *Sphaeroidinella paenedehiscens*	late Miocene	Tt	~8	1123B-27X-CC	249.30
LO *Bolboforma pentaspinosa*	late Miocene	Tt	7	1123B-27X-CC	249.30
LO *Globoquadrina dehiscens*	late Miocene	e Tt	9.9	1123B-35X-3, 132-136 cm	335.50
LO *Zeaglobigerina druryi*	late Miocene	Sw/Tt	11.3	1123B-39X-CC	364.50
FO *Neogloboquadrina pachyderma*	late Miocene	Sw/Tt	11.3	1123B-40X-CC	374.00
LO *Neogloboquadrina continuosa*	late Miocene	eTt	11	1123B-42X-CC	388.40
LO *Paragloborotalia mayeri*	late Miocene	e Tt	11.25	1123B-42X-CC	388.40
FO *Zeaglobigerina nepenthes*	middle Miocene	late Sw	11.8	1123B-42X-CC	388.40
LO *Globorotalia conica*	middle Miocene	Sw	~11.5	1123B-45X-CC	416.60
LO *Paragloborotalia partimlabiata*	late Miocene	Sl/Sw	13	1123B-46X-CC	428.36
FO *Paragloborotalia mayeri*	middle Miocene	Sl	13.2	1123B-46X-CC	428.40
FO *Globorotalia miotumida*	middle Miocene	Sl/Sw	13.2	1123B-46X-CC	428.40
LO *Globorotalia praemenardii*	middle Miocene	Sl/Sw	13.2	1123B-47X-CC	436.96
FO *Orbulina suturalis*	middle Miocene	Sc/Sl	15.1	1123B-46X-CC	428.40
FO *Globorotalia amuria*	middle Miocene		~16	1123B-48X-CC	445.60
FO *Globorotalia panda*	middle Miocene	Sc/Sl	15	1123B-48X-CC	445.60
FO *Cibicidoides wuellerstorfi*	early Miocene	Pl	16.4	1123B-49X-CC	457.10
FO *Globorotalia praemenardii*	middle Miocene	m Sc	15.8	1123B-50X-CC	468.60
LO *Globorotalia miozea*	middle Miocene	m Sc	15.8	1123B-51X-CC	479.60
LO *Catapsydrax stainforthi*	early Miocene	Pl	~16.4	1123B-51X-CC	479.60
LO *Paragloborotalia bella*	early Miocene	late Pl	16.3	1123C-19X-CC	498.10
FO *Globorotalia miozea*	early Miocene	late Pl	16.7	1123C-20X-CC	506.40
FO *Zeaglobigerina druryi*	early Miocene	Pl	17.4	1123B-52X-CC	488.60
LO *Catapsydrax dissimilis*	early Miocene	Pl	17.3	1123B-20X-CC	506.39
FO *Sphaeroidinellopsis disjuncta*	early Miocene	m Pl	18.5	1123C-21X-CC	517.00
LCO *Globorotalia zealandica*	early Miocene	m Pl	16.7	1123C-21X-CC	517.00
FO *Globorotalia zealandica*	early Miocene	m Pl	18.6	1123C-21X-CC	517.00
LO *Globorotalia incognita*	early Miocene	e Pl	18.6	1123C-23X-CC	536.70
FO *Globorotalia incognita*	early Miocene	Po	21.6	1123C-28X-CC	583.80
FO *Globoquadrina dehiscens*	late Oligocene	Lw	25	1123C-28X-CC	583.80
LO *Subbotina angiporoides*	early Oligocene	e Lwh	30	1123C-29X-CC	593.30
LCO *Paragloborotalia gemma*	early Oligocene	e Lwh	32	1123C-29X-CC	593.30
FO *Globigerinatheka index*	late Eocene	Ar	34.3	1123C-31X-CC	611.10
LO *Ponticulasphaera semiinvoluta*	late Eocene	Ar	34.8-35.3	1123C-31X-CC	611.10
FO *Paragloborotalia gemma*	late Eocene	late Ar	35	1123C-31X-CC	611.10
LO *Nuttallides truempyi*	late Eocene	Ar	?34.3	1123C-33X-CC	625.80

Note: New Zealand stages: Wc = Castlecliffian, Wm = Mangapanian, Wn = Nukumaruan, Wp = Waipipian, Wo = Opoitian, Tk = Kapitean, Tt = Tongaporutuan, Sw = Waiauan, Sl = Lillburnian, Pl = Altonian, Sc = Clifdenian, Po = Otaian, Lw = Waitakian, Lwh = Whaingaroan, Ar = Runangan, e = early, m = middle.

Table T7. Identification and abundance of planktonic foraminifers observed at Site 1123. (See table note. Continued on next page.)

Core, section interval (cm)	Depth	Preservation	Group abundance	*Globigerina bulloides*	*Globigerina quinqueloba*	*Globigerina umbilicata*	*Globigerinella aequilateralis*	*Globigerinita glutinata*	*Globigerinoides conglobatus*	*Globorotalia crassula*	*Globorotalia inflata*	*Globorotalia pseudopima*	*Globorotalia scitula*	*Globorotalia truncatulinoides*	*Neogloboquadrina pachyderma*	*Orbulina universa*	*Globigerina* spp.	*Globorotalia crassaformis hessi*	*Globorotalia crassaformis viola*	*Globorotalia puncticuloides*	*Globorotalia tumida*	*Globorotalia crassaformis*	*Globorotalia crassacarina*
181-1123B-																							
1H-1, 130-132	1.3	G	C							R	A		P	F									R
181-1123A-																							
1H-CC, 0-15	5.95	VG	A	F	D	F	R	P	R	P	F	P	R	F	A	R							
2H-CC, 16-26	15.61	VG	A	F	R	R				P	F		R	F	F	R	D	R	R	R	P		
3H-CC, 0-10	23.21	VG	A	F	R	R	P			R	F		P	P	F	R	D	R	P	F			R
4H-CC, 0-10	34.7	VG	A				P			R	F		P	P	F	P				F			R
5H-CC, 0-10	44.19	VG	A								F		P	P	F	P				F			R
6H-CC, 0-10	53.72										F				F	P							R
7H-CC, 11-21	63.15														F	P							
8H-CC, 11-16	72.02	G	C	F						P	F		R		F	R				A			
9H-CC, 17-27	82.33	G	C	F							R		R		F	P				A			
181-1123B-																							
10H-CC, 35-45	89.09	G	C	R	R						A		P				F			F			
181-1123A-																							
10H-CC, 15-20	91.88	G	C	F			P				F		P		F	R				A			
11H-CC, 11-21	101.14	G	C	R			P				R		P			P				A		R	
181-1123B-																							
12H-CC, 11-21	108.06	G	R								P		P							F		F	
181-1123A-																							
12H-CC, 13-23	110.76	G	C	F			P						R		R	R						P	
14H-CC, 12-22	129.66	G	C	R									P		R	R						P	
16H-CC, 21-26	148.66	G	F	F			P								F	P						R	
17H-CC, 22-27	158.57	G	F	P											F	P						R	
181-1123B-																							
18X-CC, 18-28	163.69	G	C	R	F								P		F	F						R	
19X-CC, 23-33	172.31	M	R	F				P					P		P	P						R	
20X-CC, 20-25	182	G	R	F									P		A	R						R	
21X-CC, 13-23	191.27	G	C	F	F			R					R		A	R							
22X-CC, 19-30	201.3			F				P					R			R							
22X-CC, 26-36	201.37	M	R	R	F										A								
23X-CC, 21-26	208.91	M	R												R	R							
25X-CC, 22-32	230	M	T												R	P							
181-1123C-																							
17X-CC, 29-39	236.29														R	F							
181-1123B-																							
27X-CC, 26-36	249.32	P	T	P											R								
28X-CC, 18-23	258.74	M	T					P								R	R						
29X-CC, 27-37	268.49	M	T												P	R							
30X-CC, 25-30	278	M	T	P												R							
31X-CC, 17-22	287.54	M	T	P												R							
32X-CC, 23-33	296.31	M	T					P							P	F							

Core, section interval (cm)	*Sphaeroidinella dehiscens*	*Globorotalia tosaensis*	*Globorotalia crassaformis* (dextral)	*Globigerina falconensis*	*Globigerinoides ruber*	*Globorotalia crassaconica*	*Globorotalia inflata triangula*	*Globorotalia pliozea*	*Zeaglobigerina woodi*	*Globorotalia puncticulata*	*Globigerinoides trilobus*	*Neogloboquadrina acostaensis*	*Globorotalia mons*	*Globorotalia juanai*	*Globorotalia miotumida*	*Globorotalia sphericomiozea*	*Globorotalia miotumida conoidea*	*Bolboforma pentaspinosa*	*Sphaeroidinellopsis paenedehiscens*	*Zeaglobigerina nepenthes*
181-1123B-																				
1H-1, 130-132																				
181-1123A-																				
1H-CC, 0-15																				
2H-CC, 16-26																				
3H-CC, 0-10																				
4H-CC, 0-10	P																			
5H-CC, 0-10																				
6H-CC, 0-10																				
7H-CC, 11-21																				
8H-CC, 11-16		P																		
9H-CC, 17-27			R																	
181-1123B-																				
10H-CC, 35-45		P	R																	
181-1123A-																				
10H-CC, 15-20			R	R	P															
11H-CC, 11-21						P	P	P	P											
181-1123B-																				
12H-CC, 11-21							P	P		F										
181-1123A-																				
12H-CC, 13-23					P	R		R	P	A										
14H-CC, 12-22					P	P		P	P	A	P									
16H-CC, 21-26	P				P	R		R	R	A		P								
17H-CC, 22-27					P	R		R	P	F		P								
181-1123B-																				
18X-CC, 18-28	P					R		R		A			R							
19X-CC, 23-33						R		R		R			R							
20X-CC, 20-25								R					R	R	P	R				
21X-CC, 13-23									A				P		F	F				
22X-CC, 19-30									F						F					
22X-CC, 26-36															F					
23X-CC, 21-26															F		F			
25X-CC, 22-32									F						F					
181-1123C-																				
17X-CC, 29-39															R		R			F
181-1123B-																				
27X-CC, 26-36															F			R	P	
28X-CC, 18-23									R						F					
29X-CC, 27-37									R						F					
30X-CC, 25-30									P						P			R		F
31X-CC, 17-22															F					F
32X-CC, 23-33									R						R			P		R

Core, section interval (cm)	*Globigerinoides bollii*	*Sphaeroidinellopsis seminulina*	*Globoquadrina dehiscens*	*Zeaglobigerina druryi*	*Catapsydrax parvulus*	*Neogloboquadrina continuosa*	*Paragloborotalia mayeri*	*Globorotalia conica*	*Sphaeroidinellopsis disjuncta*	*Globorotalia praemenardii*	*Orbulina suturalis*	*Globoquadrina praedehiscens*	*Globorotalia amuria*	*Globorotalia zealandica*	*Globoquadrina venzuelana*	*Globorotalia panda*	*Catapsydrax stainforthi*	*Globorotalia praescitula*	*Globorotalia miozea*	*Globigerina praebulloides*	*Globigerinoides bisphericus*	*Zeaglobigerina connecta*	*Globoquadrina baroemoenensis*	*Paragloborotalia bella*	*Catapsydrax dissimilis*	*Catapsydrax unicavus*	*Globorotalia incognita*	*Paragloborotalia opima nana*	*Subbotina angiporoides*	*Tenuitella gemma*	*Globigerinatheka index*	*Porticulosphaera semiinvoluta*	*Subbotina linaperta*
181-1123B-																																	
1H-1, 130-132																																	
181-1123A-																																	
1H-CC, 0-15																																	
2H-CC, 16-26																																	
3H-CC, 0-10																																	
4H-CC, 0-10																																	
5H-CC, 0-10																																	
6H-CC, 0-10																																	
7H-CC, 11-21																																	
8H-CC, 11-16																																	
9H-CC, 17-27																																	
181-1123B-																																	
10H-CC, 35-45																																	
181-1123A-																																	
10H-CC, 15-20																																	
11H-CC, 11-21																																	
181-1123B-																																	
12H-CC, 11-21																																	
181-1123A-																																	
12H-CC, 13-23																																	
14H-CC, 12-22																																	
16H-CC, 21-26																																	
17H-CC, 22-27																																	
181-1123B-																																	
18X-CC, 18-28																																	
19X-CC, 23-33																																	
20X-CC, 20-25																																	
21X-CC, 13-23																																	
22X-CC, 19-30																																	
22X-CC, 26-36																																	
23X-CC, 21-26																																	
25X-CC, 22-32																																	
181-1123C-																																	
17X-CC, 29-39															R					P			P										
181-1123B-																																	
27X-CC, 26-36																																	
28X-CC, 18-23																																	
29X-CC, 27-37																																	
30X-CC, 25-30																																	
31X-CC, 17-22																																	
32X-CC, 23-33	F	P																															

Table T7 (continued).

Core, section interval (cm)	Depth	Preservation	Group abundance	*Globigerina bulloides*	*Globigerina quinqueloba*	*Globigerina umbilicata*	*Globigerinella aequilateralis*	*Globigerinita glutinata*	*Globigerinoides conglobatus*	*Globorotalia crassula*	*Globorotalia inflata*	*Globorotalia pseudopima*	*Globorotalia scitula*	*Globorotalia truncatulinoides*	*Neogloboquadrina pachyderma*	*Orbulina universa*	*Globigerina* spp.	*Globorotalia crassaformis hessi*	*Globorotalia crassaformis viola*	*Globorotalia puncticuloides*	*Globorotalia tumida*	*Globorotalia crassaformis*	*Globorotalia crassacarina*	*Sphaeroidinella dehiscens*	*Globorotalia tosaensis*	*Globorotalia crassaformis* (dextral)	*Globigerina falconensis*	*Globigerinoides ruber*
34X-CC, 19-34	316.53	M	C													R												
35X-CC, 9-19	326.02	M	C													R												
36X-CC, 13-23	335.47	P	T																									
37X-CC, 22-32	345.2	M	R												R	P												
38X-CC, 31-41	354.79	M	R	R				P								P												
39X-CC, 29-39	364.48	M	R	P																								
40X-CC, 22-32	374.06	M	T												P													
41X-CC, 28-38	382.2	M	R																									
42X-CC, 24-34	388.44	M	T					P								R												
43X-CC, 14-24	399.52	M	T																									
44X-CC, 20-30	408.32	M	T																									
45X-CC, 18-28	416.56	M	F													P												
46X-CC, 20-25	428.36	M	T																									
47X-CC, 0-10	436.96	G	T																									
48X-CC, 0-15	445.6	G	T																									
49X-CC, 26-41	457.06	M	R	P																								
50X-CC, 39-54	468.6	M	T		R																							
51X-CC, 17-27	479.62	M	R		R																							
52X-CC, 26-36	488.56	M	C		R																							
181-1123C-																												
18X-CC, 35-45	488.85	M	C																									
19X-CC, 25-35	498.1	M	R																									
20X-CC, 0-15	506.39	M	R																									
21X-CC, 0-15	516.96	M	R														F											
22X-CC, 23-38	527.06	M	T																									
23X-CC, 28-38	536.71	M	R																									
25X-2, 32-34	548.02	M	C																									
27X-CC, 24-34	574.96	M	R																									
28X-CC, 5-15	583.78	M	T																									
29X-CC, 29-39	593.31	M	C																									
30X-CC, 15-25	599.64																											
31X-CC, 0-10	611.08	M	F																									
32X-CC, 43-53	619.11	P																										
33X-CC, 25-35	625.76	P	C																									

Core, section interval (cm)	*Globorotalia crassaconica*	*Globorotalia inflata triangula*	*Globorotalia pliozea*	*Zeaglobigerina woodi*	*Globorotalia puncticulata*	*Globigerinoides trilobus*	*Neogloboquadrina acostaensis*	*Globorotalia mons*	*Globorotalia juanai*	*Globorotalia miotumida*	*Globorotalia sphericomiozea*	*Globorotalia miotumida conoidea*	*Bolboforma pentaspinosa*	*Sphaeroidinellopsis paenedehiscens*	*Zeaglobigerina nepenthes*	*Globigerinoides bollii*	*Sphaeroidinellopsis seminulina*	*Globoquadrina dehiscens*	*Zeaglobigerina druryi*	*Catapsydrax parvulus*	*Neogloboquadrina continuosa*	*Paragloborotalia mayeri*	*Globorotalia conica*	*Sphaeroidinellopsis disjuncta*	*Globorotalia praemenardii*
34X-CC, 19-34												R			R										
35X-CC, 9-19												R			R										
36X-CC, 13-23												P						P							
37X-CC, 22-32										F		R		R	F			R							
38X-CC, 31-41										R		R		P	F			F							
39X-CC, 29-39												P						R	P						
40X-CC, 22-32										F		R					P	R	F	P					
41X-CC, 28-38												P						P	R						
42X-CC, 24-34										F					F			R	F		P	R			
43X-CC, 14-24										F							R	F	R		F	R			
44X-CC, 20-30										F							R	R			F	R			
45X-CC, 18-28												P					P						P	P	
46X-CC, 20-25										F								F			F	F	P		
47X-CC, 0-10																		F					P	F	R
48X-CC, 0-15																		P		P			P	F	F
49X-CC, 26-41				R		P												F					P	R	F
50X-CC, 39-54						R												R						R	F
51X-CC, 17-27				R		R												R						R	P
52X-CC, 26-36				R		P												F	P					R	
181-1123C-																									
18X-CC, 35-45				A														A						F	F
19X-CC, 25-35																		A						R	
20X-CC, 0-15																								F	
21X-CC, 0-15						R											P							P	
22X-CC, 23-38																									
23X-CC, 28-38																		R							
25X-2, 32-34				R														R							
27X-CC, 24-34				R														F							
28X-CC, 5-15																		P							
29X-CC, 29-39																									
30X-CC, 15-25																						R			
31X-CC, 0-10																									
32X-CC, 43-53																									
33X-CC, 25-35																									

Core, section interval (cm)	*Orbulina suturalis*	*Globoquadrina praedehiscens*	*Globorotalia amuria*	*Globorotalia zealandica*	*Globoquadrina venzuelana*	*Globorotalia panda*	*Catapsydrax stainforthi*	*Globorotalia praescitula*	*Globorotalia miozea*	*Globigerina praebulloides*	*Globigerinoides bisphericus*	*Zeaglobigerina connecta*	*Globoquadrina baroemoenensis*	*Paragloborotalia bella*	*Catapsydrax dissimilis*	*Catapsydrax unicavus*	*Globorotalia incognita*	*Paragloborotalia opima nana*	*Subbotina angiporoides*	*Tenuitella gemma*	*Globigerinatheka index*	*Porticulosphaera semiinvoluta*	*Subbotina linaperta*
34X-CC, 19-34																							
35X-CC, 9-19																							
36X-CC, 13-23																							
37X-CC, 22-32																							
38X-CC, 31-41																							
39X-CC, 29-39																							
40X-CC, 22-32																							
41X-CC, 28-38																							
42X-CC, 24-34																							
43X-CC, 14-24																							
44X-CC, 20-30																							
45X-CC, 18-28																							
46X-CC, 20-25	P																						
47X-CC, 0-10		R	P	R																			
48X-CC, 0-15		F	P	R	R	P																	
49X-CC, 26-41																							
50X-CC, 39-54							F																
51X-CC, 17-27							A	P	F														
52X-CC, 26-36							F	P	F	P	P	R											
181-1123C-																							
18X-CC, 35-45									F														
19X-CC, 25-35							R		F			P		R									
20X-CC, 0-15									P						R								
21X-CC, 0-15				A				P		R			P			R							
22X-CC, 23-38												P			F								
23X-CC, 28-38												P			D		R						
25X-2, 32-34												R			A		P	F					
27X-CC, 24-34												R			A		F						
28X-CC, 5-15												F			D		P						
29X-CC, 29-39															F				A	R			
30X-CC, 15-25																P			F				
31X-CC, 0-10																			R	R	F	R	R
32X-CC, 43-53																			F		F	R	
33X-CC, 25-35																			F	R	F	R	

Note: Preservation: VG = very good, G = good, M = moderate, and P = poor; total (group) abundance of planktonic foraminifers: A = abundant, C = common, F = few, R = rare, and T = trace; relative abundance of species: D = dominant, A = abundant, F = few/frequent, R = rare, and P = present.

Table T8. Identification and abundance of diatoms and silicoflagellates at Site 1123. (**See table note.** Continued on next seven pages.)

Core, section, interval (cm)	Depth	Diatom abundance	*Actinocyclus curvatulus*	*Actinocyclus ehrenbergii*	*Actinocyclus ellipticus*	*Actinocyclus ingens*	*Actinocyclus ingens* var. *nodus*	*Actinocyclus karstenii*	*Actinoptychus senarius*	*Asterolampra insignis*	*Asterolampra marylandica*	*Aulacoseira granulata*	*Azpeitia africana*	*Azpeitia nodulifer*	*Azpeitia tabularis*	*Cavitatus jouseanus*	*Cestodiscus convexus*	*Cestodiscus novozaelandicus*	*Cestodiscus* sp.	*Chaetoceros* resting spores	*Cocconeis* sp.	*Coscinodiscus descrescens*	*Coscinodiscus marginatus*	*Coscinodiscus radiatus*	*Coscinodiscus rhombicus*	*Craspedodiscus* sp.	*Cyclotella striata*	*Denticulopsis dimorpha*	*Denticulopsis hustedtii*	*Denticulopsis praedimorpha*	*Denticulopsis* sp.	*Diploneis* sp.	*Eucampia antarctica*	*Eunotia* sp.	*Gladius* sp.	*Grammatophora* sp.	*Hemiaulus caracteristicus*
181-1123A-																																					
?1H-CC, 0-15	5.95	R																						F													
2H-CC, 16-26	15.61	F																									T										
3H-CC, 0-10	23.21	C	R											F						R				R													
4H-CC, 0-10	34.7	C							T					R	R									R													
5H-5, 82-82	41.52	F												F										R													
5H-CC, 0-10	44.19	C	T			T																		F													
6H-CC, 0-10	53.72	F										T		R										R													
7H-CC, 11-21	63.15	C				T								T	R						T											T				
8H-CC, 11-16	72.02	C													R									T								T				
9H-CC, 17-27	82.33	C													R					R				R								T		T		
10H-CC, 15-20	91.88	C		R									T	R	R						T			R								F				T
11H-2, 59-59	93.97	C							T					F						F				R			T					R				
11H-2, 124-124	94.62	C				T								R	R																	R				
11H-CC, 11-21	101.14	C		R										F										R					T			R				
181-1123B-																																					
1H-1, 130-132	1.3	F							T			R			R					C				R													
1H-CC, 0-15	3.21	F							R						R									R									T				
2H-CC, 11-21	12.75	C							R					F										R								R	T				
3H-CC, 11-21	22.64	F																														T					
4H-CC, 10-20	32.1	C				T								F	R									R										R			
5H-CC, 7-17	41.57	C	T											F										R													
6H-CC	51.24	F										T		R										R													
7H-CC, 27-37	60.92	F	T											F														T									
9H-CC--	79.59	C			T									F										R													
10H-CC, 35-45	89.09	C		R	T				T					F	R									F		R						F					
11H-CC, 11-21	98.71	C		R	R	T			R					F										R				R				F					
12H-CC, 11-21	108.06	C			R	R								R										T			T					F				T	
13H-CC, 16-21	117.73	C		R					F					R														T				F					
20X-CC, 20-25	182	C			T	R			F					R									R	R				T				F					
21X-CC, 10-17	191.24	C			R	C			R														R	R													
24X-CC, 17-25	220.41	C			R	R		T	F					R																							
25X-CC, 22-32	230	C			R	R			R															R													
26X-CC, 22-32	234.08	C		R	R		T		R					R										R	T												
27X-CC, 26-36	249.32	C		R		R			F																							R					
28X-CC, 18-23	258.74	C		R					F		T			R	R								R	R							R	R					
29X-CC, 27-37	268.49	C			R	C			R														F	R							R	R					
30X-CC, 25-30	278	C				F									R								F					T			T	R					
31X-CC, 17-22	287.54	C			R	F									T								R					T			R	R					
32X-CC, 23-33	296.31	C			T	R																						R	R			R					

Table T8 (continued).

Core, section, interval (cm)	Depth	*Hemiaulus claviger*	*Hemiaulus incisus*	*Hemiaulus incurvus*	*Hemiaulus lyriformis*	*Hemiaulus polycystinorum*	*H. polycystinorum* var. *mesolepta*	*Hemiaulus polymorphus*	*Hemiaulus* sp.	*Hemiaulus subacutus*	*Hemidiscus cuneiformis*	*Hemidiscus karstenii*	*Hemidiscus karstenii* f. 1	*Hemidiscus ovalis*	*Hemidiscus triangularis*	*Hyalodiscus* sp.	*Liostephania* sp.	*Melosira architecturalis*	*Nitzschia barronii*	*Nitzschia cylindrica*	*Nitzschia denticuloides*	*Nitzschia fossilis*	*Nitzschia kerguelenis*	*Nitzschia kolackzeckii*	*Nitzschia marina*	*Nitzschia miocenica*	*Nitzschia panduriformis*	*Nitzschia reinholdii*	*Nitzschia ritscherii*	*Nitzschia weaveri*	*Paralia sulcata*	*Pseudeunotia doliolus*	*Pterotheca aculeifera*	*Pyxilla reticulata*	*Rhaphoneis amphiceros*	*Rhaphoneis surirelloides*
181-1123A-																																			
1H-CC, 0-15	5.95										T												R		F						T				
2H-CC, 16-26	15.61																						T	T	R			T			R				
3H-CC, 0-10	23.21								T		R												R		R			F	R		R		T		
4H-CC, 0-10	34.7								T													T	R		T			R			R				
5H-5, 82-82	41.52																								R			F			T				
5H-CC, 0-10	44.19										T											R			F			F		T	R				
6H-CC, 0-10	53.72																					R	R		R		T	F							
7H-CC, 11-21	63.15								T		F								T	T					R			F	R		T	R				
8H-CC, 11-16	72.02										F														F			F	T		R	R				
9H-CC, 17-27	82.33										F			R					R						R			F			R	R				
10H-CC, 15-20	91.88								R		R					T						T			R		R	R			T	R			
11H-2, 59-59	93.97										R					T						R			R		T	F		T		F		R	
11H-2, 124-124	94.62										R											R			R					R		R			
11H-CC, 11-21	101.14	T							R		R			R		T						R			R		R	F				R		T	
181-1123B-																																				
1H-1, 130-132	1.3																						R		F					R	R				
1H-CC, 0-15	3.21										R												F		F					F	F				R
2H-CC, 11-21	12.75										R	R										R	F		F				R		F	R			T
3H-CC, 11-21	22.64															T						R	F					R	R			T			
4H-CC, 10-20	32.1										R								R			T	R		F			F				T			
5H-CC, 7-17	41.57										F												T		F			F			R			T	T
6H-CC	51.24																								F			R			R	T			
7H-CC, 27-37	60.92										R								T			R			R			R				R			
9H-CC--	79.59										R								R			R			F			F			R	T			
10H-CC, 35-45	89.09										R											R			F		T	F				R			
11H-CC, 11-21	98.71										R	T				T						R			R			F		R	R		T	R	
12H-CC, 11-21	108.06								R		R	R													R		T	R		T	F			R	
13H-CC, 16-21	117.73								T		R														R	R		R			F		T		
20X-CC, 20-25	182								R		R			R							T				R			R			F		R	T	
21X-CC, 10-17	191.24								R		F			F				T				T									R		R	R	
24X-CC, 17-25	220.41										R			F		R		T				R			R			F			R		T		
25X-CC, 22-32	230			T					R		R			R	F	T				T		R				R		F			F		R	R	
26X-CC, 22-32	234.08										F			F								F			R			F			F			R	
27X-CC, 26-36	249.32								R		F		T		F					T		T				R			F			F		R		
28X-CC, 18-23	258.74								T		R															T			R			F			R	
29X-CC, 27-37	268.49								R		T			R															R			R		T		
30X-CC, 25-30	278										T			R				T																		
31X-CC, 17-22	287.54								R					R		R									T						R			T		
32X-CC, 23-33	296.31								R		T							T													R			T		

Table T8 (continued).

Core, section, interval (cm)	Depth	*Rhizosolenia bergonii*	*Rhizosolenia hebetata*	*Riedelia pacifica*	*Rocella gelida*	*Rocella praenitida*	*Rocella vigilans*	*Roperia tesselata*	*Simonseniella barboi*	*Skeletonemopsis barbarbadense*	*Stephanogonia* sp.	*Stephanopyxis grossecellulata*	*Stephanopyxis hyalinomarginata*	*Stephanopyxis marginata*	*Stephanopyxis turris*	*Thalassionema bacillaris*	*Thalassionema nitzschioides*	*Thalassionema nitzschioides* var. *parva*	*Thalassiosira convexa*	*Thalassiosira convexa* var. *aspinosa*	*Thalassiosira eccentrica*	*Thalassiosira insigna*	*Thalassiosira inura*	*Thalassiosira lentiginosa*	*Thalassiosira leptopus*	*Thalassiosira lineata*	*Thalassiosira miocenica*	*Thalassiosira oestrupii*	*Thalassiothrix longissima*	*Triceratium barbadense*	*Triceratium favus*	*Triceratium inconspicuum* var. *trilobata*	*Triceratium kanayae*	*Trinacria excavata*	*Trinacria simulacroides*	*Xanthiopyxis ovalis*
181-1123A-																																				
1H-CC, 0-15	5.95	R														T	T				R				T	R										R
2H-CC, 16-26	15.61	R	T												R		T				T				T		T		T							R
3H-CC, 0-10	23.21														R						T					R			R							R
4H-CC, 0-10	34.7							T									R				T								R							F
5H-5, 82-82	41.52		R												R	T	R		T		R				T				R							
5H-CC, 0-10	44.19														R		R				R							T	R							F
6H-CC, 0-10	53.72		T			T							R		R		R												R	T						R
7H-CC, 11-21	63.15														R						R				T			R	R							R
8H-CC, 11-16	72.02								F						R		F				T				R	T			R							R
9H-CC, 17-27	82.33								T						T		C		R		T			T	R	T			R	T						T
10H-CC, 15-20	91.88														R		C		R						R	T										R
11H-2, 59-59	93.97														R		C		R		R				R				R							
11H-2, 124-124	94.62		T						R						R		F		R		T				T	T			C							
11H-CC, 11-21	101.14																																				
181-1123B-																	R				R								F							C
1H-1, 130-132	1.3	T														F					R				R	T			R							C
1H-CC, 0-15	3.21							R							R		R				R				R	T		F	R							R
2H-CC, 11-21	12.75																R				R							T	R							
3H-CC, 11-21	22.64														T		F								R	T			F							
4H-CC, 10-20	32.1														R		R								R	T			F							R
5H-CC, 7-17	41.57								T								F												F							
6H-CC	51.24								R						T	R	F								T				F							
7H-CC, 27-37	60.92								R								F				R				R	T			F							R
9H-CC--	79.59																C		R			F			R				F							
10H-CC, 35-45	89.09	T				T							T		R		F		F		R	R			R	T			F		T					R
11H-CC, 11-21	98.71														R		F		T		T		T		R	T			C	T						
12H-CC, 11-21	108.06								R								F		R	R	R				R				F	T						
13H-CC, 16-21	117.73					T			R		T	T			R		C				T	T			R				R	R						F
20X-CC, 20-25	182					T	T		F	T	T						R				T		T						C					T		
21X-CC, 10-17	191.24								F								F				R			T	R		T			R			T			
24X-CC, 17-25	220.41			T					F						R		F				R				R				F	R						
25X-CC, 22-32	230								R			T					F	R			F				F											
26X-CC, 22-32	234.08								R								F				R				R				F							
27X-CC, 26-36	249.32								R								F								R				F							
28X-CC, 18-23	258.74								R						R		F								F				F							
29X-CC, 27-37	268.49								R						R		F								R				F							
30X-CC, 25-30	278				T				R						R		F												F				T			
32X-CC, 23-33	296.31								R						R		F	R											F							

Table T8 (continued).

Core, section, interval (cm)	Depth	Silicoflagellates	*Corbisema inermis inermis*	*Corbisema inermis minor* (Eoc.)	*Dictyocha neonautica*	*Dictyocha rhombica*	*Dictyocha spinosa* (Eoc.)	*Distephanus polyactis*	*Mesocena apiculata apiculata*	*Mesocena circulus*	*Mesocena diodon borderlandensis*	*Mesocena diodon diodon*	*Mesocena oamaruensis* (Eoc.-Olig.)	*Mesocena occidentalis* (Eoc.)	*Mesocena quadrangula*	*Mesocena triodon*	*Naviculopsis foliacea foliacea* (Eoc.)	*Paradictyocha apiculata*	*Valacerta tumidula* (Cretac.)
181-1123A-																			
1H-CC, 0-15	5.95																		
2H-CC, 16-26	15.61																		
3H-CC, 0-10	23.21																		
4H-CC, 0-10	34.7																		
5H-5, 82-82	41.52																		
5H-CC, 0-10	44.19																		
6H-CC, 0-10	53.72																		
7H-CC, 11-21	63.15																		
8H-CC, 11-16	72.02																		
9H-CC, 17-27	82.33																		
10H-CC, 15-20	91.88																		
11H-2, 59-59	93.97																		
11H-2, 124-124	94.62																		
11H-CC, 11-21	101.14																		
181-1123B-																			
1H-1, 130-132	1.3																		
1H-CC, 0-15	3.21																		
2H-CC, 11-21	12.75																		
3H-CC, 11-21	22.64																		
4H-CC, 10-20	32.1									T									
5H-CC, 7-17	41.57														R				
6H-CC	51.24																		
7H-CC, 27-37	60.92																		
9H-CC--	79.59																		
10H-CC, 35-45	89.09									T									
11H-CC, 11-21	98.71																		
12H-CC, 11-21	108.06			T		R													
13H-CC, 16-21	117.73					T													
20X-CC, 20-25	182				T	R					T								
21X-CC, 10-17	191.24																	R	T
24X-CC, 17-25	220.41						T							T					
25X-CC, 22-32	230					T					R							R	
26X-CC, 22-32	234.08					R													
27X-CC, 26-36	249.32					R													
28X-CC, 18-23	258.74																		
29X-CC, 27-37	268.49											R		T				T	
30X-CC, 25-30	278																	T	
31X-CC, 17-22	287.54																	T	
32X-CC, 23-33	296.31																	R	

Table T8 (continued).

Core, section, interval (cm)	Depth	Diatom abundance	*Actinocyclus curvatulus*	*Actinocyclus ehrenbergii*	*Actinocyclus ellipticus*	*Actinocyclus ingens*	*Actinocyclus ingens* var. *nodus*	*Actinocyclus karstenii*	*Actinoptychus senarius*	*Asterolampra insignis*	*Asterolampra marylandica*	*Aulacoseira granulata*	*Azpeitia africana*	*Azpeitia nodulifer*	*Azpeitia tabularis*	*Cavitatus jouseanus*	*Cestodiscus convexus*	*Cestodiscus novozaelandicus*	*Cestodiscus* sp.	*Chaetoceros* resting spores	*Cocconeis* sp.	*Coscinodiscus descrescens*	*Coscinodiscus marginatus*	*Coscinodiscus radiatus*	*Coscinodiscus rhombicus*	*Craspedodiscus* sp.	*Cyclotella striata*	*Denticulopsis dimorpha*	*Denticulopsis hustedtii*	*Denticulopsis praedimorpha*	*Denticulopsis* sp.	*Diploneis* sp.	*Eucampia antarctica*	*Eunotia* sp.	*Gladius* sp.	*Grammatophora* sp.	*Hemiaulus caracteristicus*
181-1123B-																																					
33X-CC, 15-25	306.85	F																					T														
34X-CC, 19-34	316.53	R																					T					T				T					
35X-CC, 9-19	326.02	R				T																										T					
36X-CC, 13-23	335.47	R																																			
37X-CC, 22-32	345.2	B																																			
38X-CC, 31-41	354.79	B																																			
39X-CC, 29-39	364.48	B																																			
40X-CC, 22-32	374.06	B																																			
41X-CC, 28-38	382.2	R																																			
42X-CC, 24-34	388.44	F				C	R																	R		T			R	R	R						
43X-CC, 14-24	399.52	F			R	F			T																	T						T					
44X-CC, 20-30	408.32	F			T	R			T							T								R							R	R					
45X-CC, 18-28	416.56	R																																			
46X-CC, 20-25	428.36	T				T																															
47X-CC, 0-10	436.96	R				T																													T		
48X-CC, 0-15	445.6	R																						R													
49X-CC, 26-41	457.06	R				R																	T								T	T					
50X-CC, 39-54	468.6	B																																			
51X-CC, 17-27	479.62	B																																			
52X-CC, 26-36	488.56	B																																			
181-1123C-																																					
18X-CC, 35-45	488.85	R																					T														
19X-CC, 25-35	498.1	T																					T														
20X-CC, 0-15	506.39	B																																			
21X-CC, 0-15	516.96	B																																			
22X-CC, 23-38	527.06	B																																			
23X-CC, 28-38	536.71	B																																			
24X-CC, 25-35	546.26	B																																			
25X-CC, 16-26	555.76	R														R							T			T											
26X-CC, 21-31	565.27	R			T											F			T			R	T														
27X-CC, 24-34	574.96	R														F							T												T		
29X-1, 115-115	584.93	R																																		T	
29X-2, 35-35	585.63	R														R																					
29X-4, 10-10	588.44	R																																			
29X-CC, 29-39	593.31	C								T								F	R																T		
30X-CC, 15-25	599.64	C																	R							T								T			
31X-CC, 0-10	611.08	C															T		R																		
32X-CC, 43-53	619.11	C							R										R																		R
33X-CC, 25-35	625.76	C																																			

Note: Total (group) abundance and relative abundance of diatoms: C = common, F = few, R = rare, and T = trace.

Table T8 (continued).

Core, section, interval (cm)	Depth	*Hemiaulus claviger*	*Hemiaulus incisus*	*Hemiaulus incurvus*	*Hemiaulus lyriformis*	*Hemiaulus polycystinorum*	*H. polycystinorum* var. *mesolepta*	*Hemiaulus polymorphus*	*Hemiaulus* sp.	*Hemiaulus subacutus*	*Hemidiscus cuneiformis*	*Hemidiscus karstenii*	*Hemidiscus karstenii* f. 1	*Hemidiscus ovalis*	*Hemidiscus triangularis*	*Hyalodiscus* sp.	*Liostephania* sp.	*Melosira architecturalis*	*Nitzschia barronii*	*Nitzschia cylindrica*	*Nitzschia denticuloides*	*Nitzschia fossilis*	*Nitzschia kergueleni*s	*Nitzschia kolackzeckii*	*Nitzschia marina*	*Nitzschia miocenica*	*Nitzschia panduriformis*	*Nitzschia reinholdii*	*Nitzschia ritscherii*	*Nitzschia weaveri*	*Paralia sulcata*	*Pseudeunotia doliolus*	*Pterotheca aculeifera*	*Pyxilla reticulata*	*Rhaphoneis amphiceros*	*Rhaphoneis surirelloides*
181-1123B-																																				
33X-CC, 15-25	306.85																													R						
34X-CC, 19-34	316.53								R							T													T			T			
35X-CC, 9-19	326.02																													T				T		
36X-CC, 13-23	335.47								T																								T			
37X-CC, 22-32	345.2																																			
38X-CC, 31-41	354.79																																			
39X-CC, 29-39	364.48																																			
40X-CC, 22-32	374.06																																			
41X-CC, 28-38	382.2								R																									T		
42X-CC, 24-34	388.44								T	T																				R						
43X-CC, 14-24	399.52																				T															
44X-CC, 20-30	408.32								R									R			T									R			R	T		
45X-CC, 18-28	416.56								T																								T			
46X-CC, 20-25	428.36																																			
47X-CC, 0-10	436.96																													T						
48X-CC, 0-15	445.6								T																									T		
49X-CC, 26-41	457.06								T																								T			
50X-CC, 39-54	468.6																																			
51X-CC, 17-27	479.62																																			
52X-CC, 26-36	488.56																																			
181-1123C-																																				
18X-CC, 35-45	488.85																													T						
19X-CC, 25-35	498.1																																			
20X-CC, 0-15	506.39																																			
21X-CC, 0-15	516.96																																			
22X-CC, 23-38	527.06																																			
23X-CC, 28-38	536.71																																			
24X-CC, 25-35	546.26																																			
25X-CC, 16-26	555.76																													T						
26X-CC, 21-31	565.27																													R				T	T	
27X-CC, 24-34	574.96																																			
29X-1, 115-115	584.93																																			
29X-2, 35-35	585.63																																			
29X-4, 10-10	588.44					T												T															T		
29X-CC, 29-39	593.31					F			F	T								R												F		T	F		
30X-CC, 15-25	599.64					R	T		F							T		R												F		T	F		
31X-CC, 0-10	611.08	T			T	R	R	R									T	R												R			F		
32X-CC, 43-53	619.11					R	T	R	T									R												R			F		
33X-CC, 25-35	625.76		T			R	R		F									R												R		T			

Table T8 (continued).

Core, section, interval (cm)	Depth	*Rhizosolenia bergonii*	*Rhizosolenia hebetata*	*Riedelia pacifica*	*Rocella gelida*	*Rocella praenitida*	*Rocella vigilans*	*Roperia tesselata*	*Simonseniella barboi*	*Skeletonemopsis barbarbadense*	*Stephanogonia* sp.	*Stephanopyxis grossecellulata*	*Stephanopyxis hyalinomarginata*	*Stephanopyxis marginata*	*Stephanopyxis turris*	*Thalassionema bacillaris*	*Thalassionema nitzschioides*	*Thalassionema nitzschioides* var. *parva*	*Thalassiosira convexa*	*Thalassiosira convexa* var. *aspinosa*	*Thalassiosira eccentrica*	*Thalassiosira insigna*	*Thalassiosira inura*	*Thalassiosira lentiginosa*	*Thalassiosira leptopus*	*Thalassiosira lineata*	*Thalassiosira miocenica*	*Thalassiosira oestrupii*	*Thalassiothrix longissima*	*Triceratium barbadense*	*Triceratium favus*	*T. inconspicuum* var. *trilobata*	*Triceratium kanayae*	*Trinacria excavata*	*Trinacria simulacroides*	*Xanthiopyxis ovalis*
181-1123B-																																			
33X-CC, 15-25	306.85																R											D							
34X-CC, 19-34	316.53								T						T		R											R							
35X-CC, 9-19	326.02								R						T		R											R							
36X-CC, 13-23	335.47																											T							
37X-CC, 22-32	345.2																																		
38X-CC, 31-41	354.79																																		
39X-CC, 29-39	364.48																																		
40X-CC, 22-32	374.06																																		
41X-CC, 28-38	382.2														T																				
42X-CC, 24-34	388.44																F	R										R							
43X-CC, 14-24	399.52																											R							
44X-CC, 20-30	408.32														R		R											F							R
45X-CC, 18-28	416.56														T																				
46X-CC, 20-25	428.36														T													T							
47X-CC, 0-10	436.96																																		
48X-CC, 0-15	445.6																											T							
49X-CC, 26-41	457.06																T											R							
50X-CC, 39-54	468.6																																		
51X-CC, 17-27	479.62																																	T	
52X-CC, 26-36	488.56																																		
181-1123C-																																			
18X-CC, 35-45	488.85														T																				
19X-CC, 25-35	498.1																																		
20X-CC, 0-15	506.39																																		
21X-CC, 0-15	516.96																																		
22X-CC, 23-38	527.06																																		
23X-CC, 28-38	536.71																																		
24X-CC, 25-35	546.26																																		
25X-CC, 16-26	555.76														R																				T
26X-CC, 21-31	565.27																																		T
27X-CC, 24-34	574.96																																		
29X-1, 115-115	584.93											T																							
29X-2, 35-35	585.63														T																				
29X-4, 10-10	588.44		T																																
29X-CC, 29-39	593.31		R			R	R					T		T	R															R			R		T
30X-CC, 15-25	599.64		R				R							T	R																				
31X-CC, 0-10	611.08					T									R																R				
32X-CC, 43-53	619.11					T									R																				
33X-CC, 25-35	625.76					R					T		R	R	R																	T				

Table T8 (continued).

Core, section, interval (cm)	Depth	Silicoflagellates	*Corbisema inermis inermis*	*Corbisema inermis minor* (Eoc.)	*Dictyocha neonautica*	*Dictyocha rhombica*	*Dictyocha spinosa* (Eoc.)	*Distephanus polyactis*	*Mesocena apiculata apiculata*	*Mesocena circulus*	*Mesocena diodon borderlandensis*	*Mesocena diodon diodon*	*Mesocena oamaruensis* (Eoc.-Olig.)	*Mesocena occidentalis* (Eoc.)	*Mesocena quadrangula*	*Mesocena triodon*	*Naviculopsis foliacea foliacea* (Eoc.)	*Paradictyocha apiculata*	*Valacerta tumidula* (Cretac.)
181-1123B-																			
33X-CC, 15-25	306.85																		
34X-CC, 19-34	316.53																		
35X-CC, 9-19	326.02								T									T	
36X-CC, 13-23	335.47																		
37X-CC, 22-32	345.2																		
38X-CC, 31-41	354.79																		
39X-CC, 29-39	364.48																		
40X-CC, 22-32	374.06																		
41X-CC, 28-38	382.2																		
42X-CC, 24-34	388.44															t			
43X-CC, 14-24	399.52																	T	
44X-CC, 20-30	408.32							T							T			T	
45X-CC, 18-28	416.56																		
46X-CC, 20-25	428.36																		
47X-CC, 0-10	436.96																		
48X-CC, 0-15	445.6																		
49X-CC, 26-41	457.06																		
50X-CC, 39-54	468.6																		
51X-CC, 17-27	479.62																		
52X-CC, 26-36	488.56																		
181-1123C-																			
18X-CC, 35-45	488.85																		
19X-CC, 25-35	498.1																		
20X-CC, 0-15	506.39																		
21X-CC, 0-15	516.96																		
22X-CC, 23-38	527.06																		
23X-CC, 28-38	536.71																		
24X-CC, 25-35	546.26																		
25X-CC, 16-26	555.76																		
26X-CC, 21-31	565.27																		
27X-CC, 24-34	574.96																		
29X-1, 115-115	584.93																		
29X-2, 35-35	585.63																		
29X-4, 10-10	588.44																		
29X-CC, 29-39	593.31			T													T		
30X-CC, 15-25	599.64			T													T		
31X-CC, 0-10	611.08								T										
32X-CC, 43-53	619.11												T						
33X-CC, 25-35	625.76								T										

Table T9. Identification and abundance of radiolarians observed at Site 1123. (**See table note.** Continued on next seven pages.)

Core, section, interval (cm)	Depth (mbsf)	Preservation	Group abundance	*Actinomma leptodermum*	*Actinomma* sp.	*Albatrossium* sp.	*Amphipyndax stocki*	*Amphirhopalum ypsilon*	*Amphistylus*(?) sp.	*Amphymenium amphistylium*	*Anthocyrtidium angulare*	*Anthocyrtidium ehrenbergi*	*Anthocyrtidium marieae*	*Aphetocyrtis gnomabox*	*Axoprunum angelinum*	*Axoprunum pierinae*	*Axoprunum* sp.	*Botryostrobus aquilonaris*	*Botryostrobus auritus/australis group*	*Botryostrobus miralestensis*	*Botryostrobus* sp.	*Buryella foremanae*	*Buryella* cf. *tetradica* (3 segments)	*Calocyclas*(?) *nakasekoi*	*Carpocanistrum* sp.	*Carpocanopsis bramlettei*	*Carpocanopsis cingulata*	*Calpocanopsis cristatum*	*Ceratocyrtis* sp.	*Collosphaera* sp.	*Cornutella profunda*	*Corythomelissa horrida*	*Cycladophora bicornis bicornis*	*Cycladophora davisiana cornutoides*	*Cycladophora davisiana davisiana*	*Cycladophora pliocenica*	*Cycladophora* sp.	*Cyrtocapsella cornuta*	*Cyrtocapsella japonica*	*Cyrtocapsella tetrapera*	*Dicolocapsa microcephala*	*Diartus hughesi*	*Dictyomitra multicostata*	*Dictyophimus hirundo*	*Dictyophimus* sp.	*Dictyophimus splendens*	*Dictyoprora mongolfieri*	*Didymocyrtis antepenultima*
181-1123A-																																															
1H-CC, 0-15	5.95	VG	VA		A																																										
2H-CC, 16-26	15.61	VG	VA		A			R				F							F						R					R					F	R					C				
3H-CC, 0-10	23.21	G	A	C				T											C																F	R					C				
4H-CC, 0-10	34.7	G	VA	C	A			R							R										R					R					A	R					C				
5H-CC, 0-10	44.19	G	VA	C	A			R				T							R												R					R	R					F				
6H-CC, 0-10	53.72	M	F					T							R				T										R						R	T					T				
7H-CC, 11-21	63.15	VG	A		A			R							T				R						R										T						R				
8H-CC, 11-16	72.02	G	A					T							T																										R				
9H-CC, 17-27	82.33	VG	A		A			T			T				R																				A						F				
10H-CC, 15-20	91.88	G	A					R				R			C				R						R										R						R				
11H-CC, 11-21	101.14	G	VA					F				F			C				F											F											R				
12H-CC, 13-23	110.76	VG	VA					T				R			F				F						R					F					R						R				
13H-CC, 14-19	119.69	M	A		C							R			R			R	R				T		R				R	F	R		T	R	R					R				
14H-CC, 12-22	129.66	M	A									R			R				C						R					F											R				
15H-CC, 21-26	139.54	M	A					T				R			F										R					R															
16H-CC, 21-26	148.66	G	VA		A		R					F			R				R						R					R	R													C	
17H-CC, 22-27	158.57	G	VA									R																												R					R	
181-1123B-																																															
16H-6, 123-126	145.13	VG	VA		C							R			F				R						R					R											R				
16H-CC, 0-10	145.76	VG	VA					T				F			F				R						R			R		R														
17H-2, 64-69	148.04	G	A									R			F										R			R	R	R	R										R			R	
17H-6, 127-133	154.67	M	A									R			F			T	R			T								R						R									
17H-CC, 35-40	155.63	VG	VA				T					R			R				F						R					R	R									T		R			R	
18X-CC, 18-28	163.69	VG	VA		F						T	F			F				R						R				R	R	R					R					R			R	
19X-CC, 23-33	172.31	G	A									R			R				R						R					R	R				T	T					R		T	T	
20X-CC, 20-25	182	M	A									R			R				T											T					R						R			R	
21X-CC, 13-23	191.27	G	VA		C		T			R		C			R			R	R				T		R					R	T											F	R	
22X-CC, 26-36	201.37	G	A		C							F			R							T							R	R	R									T		R	T	
23X-CC, 21-26	208.91	VG	VA		C							C			R				R						C				R	R	R				R				T			F	R	
24X-CC, 26-31	220.5	P	C									T			R				R												R					R									
25X-CC, 22-32	230	VG	VA							R		F			R				R										T		R	R				R						F	R	
26X-CC, 22-32	234.08	M	A												F				R						R					R		R					R					R			
27X-CC, 26-36	249.32	G	VA									C			F										F					C	R	T					R					R			
28X-CC, 18-23	258.74	G	A		C							F			R															F	R	R					R					R			
29X-CC, 27-37	268.49	VG	A									R							R						R					R		R					R					R			
30X-CC, 25-30	278	M	R		R							R																			R					T									
31X-CC, 17-22	287.54	M	C								R																																			
32X-CC, 23-33	296.31	G	VA																						F																			R			R

Table T9 (continued).

Core, section, interval (cm)	Depth (mbsf)	*Didymocyrtis laticonus*	*Didymocyrtis penultima*	*Didymocyrtis* sp.	*Didymocyrtis* sp. of Sakai	*Didymocyrtis tetrathalamus tetrathalamus*	*Dorcadospyris alata*	*Dorcadospyris mahurangi*	*Dorcadospirys tricelos*	*Druppatractus irregularis*	*Druppatractus* sp.	*Euchitonia* sp.	*Eucyrtidium acuminatum*	*Eucyrtidium antiquum*	*Eucyrtidium* sp. A	*Eucyrtidium spinosum*	*Eucyrtidium calvertense*	*Eucyrtidium cienkowskii group*	*Eucyrtidium matuyamai*	*Eucyrtidium punctatum*	*Eucyrtidium* sp.	*Eucyrtidium teuscheri teuscheri*	*Eucyrtidium yatsuoense*	*Eusyringium lagena*	*Gondwanaria dogieli*	*Gondwanaria* sp.	*Heliodiscus asteriscus*	*Hexacontium* sp.	*Lamprocyclas hannai*	*Lamprocyclas* sp.	*Lamprocyclas maritalis maritalis*	*Lamprocyrtis heteroporos*	*Lamprocyrtis nigriniae*	*Larcopyle* sp.	*Larcospira* sp.	*Liriospyris* sp.	*Lithelius* sp.	*Lithelius nautiloides*	*Lithopera bacca*	*Lithopera neotera*	*Lithopera renzae*	*Lophocyrtis aspera*	*Lophocyrtis longiventer*	*Lophocyrtis dumitricai*	*Lophophaena* spp.	*Lychnocanoma amphitrite*	*Lychnocanoma* cf. *babilonis*	*Lychnocanoma elongata*	*Lychnocanoma nipponica nipponica*	*Lychnocanoma nipponica Sakai*	*Lychnocanoma parallelipes*
181-1123A-																																																			
1H-CC, 0-15	5.95											R	F												R		F	C	C		R		R		R																
2H-CC, 16-26	15.61					R						F	A												R	R	R	C	C		F						T													
3H-CC, 0-10	23.21											R	C												R	T	F	C	C		C																				
4H-CC, 0-10	34.7					R						C	C												R		F	C	C		C						T	R												
5H-CC, 0-10	44.19					R						C	C														F	C	C		C																				
6H-CC, 0-10	53.72											F	R						T								R	C			R																				
7H-CC, 11-21	63.15											F	R				R					R					F		F		F																				
8H-CC, 11-16	72.02											F	C														R	A			F																				
9H-CC, 17-27	82.33									R		F					R					R					R		F		F																				
10H-CC, 15-20	91.88									F		C	R				F					R					F	A	C		F	C																		
11H-CC, 11-21	101.14									C		C					R					F					R	A	R		R	R																		
12H-CC, 13-23	110.76									R		C					F				R						F	C	C		F	C																		
13H-CC, 14-19	119.69											F					R				R				T		R	C	F		C	R																		
14H-CC, 12-22	129.66									R		R					F										C	F	R		R					T														
15H-CC, 21-26	139.54											R					F								T		R		R		F																		
16H-CC, 21-26	148.66			R						R		R					R				R						F	F	R		C																		
17H-CC, 22-27	158.57			R								F					C										R	R	R		R																		
181-1123B-																																																		
16H-6, 123-126	145.13											R					F					R					F	F	F		R							T												
16H-CC, 0-10	145.76			R								C					F					R			R		F	F	F		F	R				T												
17H-2, 64-69	148.04											C					C					R			R		R	C	R		R					T												
17H-6, 127-133	154.67			R								R					C										R	F	R		R														R				
17H-CC, 35-40	155.63											R					F					R					R	C			R																		
18X-CC, 18-28	163.69			R		R						F					F					F					R	C	R		F													R				
19X-CC, 23-33	172.31											F					F									T	F	C	R	R													R				
20X-CC, 20-25	182			R							R	F					F										R	F	R															R				
21X-CC, 13-23	191.27			R	R												F										R					R												R		F	T	
22X-CC, 26-36	201.37					T					F	F					R										F	C	R					C	R			R										
23X-CC, 21-26	208.91			R							C	R					F					R					R		R		A			R			T									R		
24X-CC, 26-31	220.5										F	R					F										T		T					R		T									T			
25X-CC, 22-32	230		R	F							C	F					F								T		R	R	R		R			C	R			T									R	
26X-CC, 22-32	234.08			R						R	R	C					R										F		R		R			R				T									T	
27X-CC, 26-36	249.32		F	F							C	R					R										C	R	R		F			R			T		T								F	
28X-CC, 18-23	258.74		T								C	F					R										F	F			F			R													R	
29X-CC, 27-37	268.49		F	F							C	F					C										F	R			C			R			T									R	
30X-CC, 25-30	278		T	C	C						F	R																R			R			C	T												
31X-CC, 17-22	287.54			F	C						F	R					R										C	R			R			F												T	
32X-CC, 23-33	296.31			F	F						A						F	R									F				T			R	R												

Table T9 (continued).

Core, section, interval (cm)	Depth (mbsf)	*Lychnocanoma* sp.	*Lychnocanoma* sp. A	*Lychnodictyum audax*	*Lophoconus biaurita* (Form C)	*Nassellaria* Form D	*Orodapis* sp.	*Periphaena decora*	*Periphaena heliastericus*	*Periphaena* sp.	*Peripyramis* sp.	*Phormocyrtis alexandrae*	*Phormocyrtis striata striata*	*Phormostichoartus corbula*	*Phormostichoartus fistula*	*Phorticium clevei*	*Prunopyle antarctica*	*Prunopyle hayesi*	*Prunopyle tetrapila*	*Prunopyle* sp.	*Pterocanium praetextum praetextum*	*Pterocanium prismatium*	*Pterocanium* sp.	*Pterocanium trilobum*	*Pterocorys zancleus*	*Pylospira* sp.	*Saturnalis circularis*	*Siphocampe* sp.	*Solenosphaera* spp.	*Sphaeropyle langii*	*Sphaeropyle robusta*	*Spongaster tetras tetras*	*Spongodiscus osculosus*	*Spongodiscus* sp.	*Spongoplegma antarcticum*	*Spongoplegma churchii*	*Spongotrochus glacialis*	*Stichocorys* sp.	*Stichocorys armata*	*Stichocorys delmontensis*	*Stichocorys johnsoni*	*Stichocorys peregrina*	*Stichocorys wolfii*	*Stylacontarium acquilonium*	*Stylacontarium bispiculum*	*Stylatractus neptunus*	*Stylatractus* sp.	*Stylatractus universus*	*Stylodictya* sp.	*Stylosphaera timmsi*	*Tetrapyle octacantha*
181-1123A-																																																		
1H-CC, 0-15	5.95						F				F					R	T				F												F	A			C									F			
2H-CC, 16-26	15.61						R				R					R					C			F	F	C	R	T					C	F		R									C	R			
3H-CC, 0-10	23.21										R					F	R				F			F	C		R					R	A	C		R									F	R		R	C	
4H-CC, 0-10	34.7										C					F	F	R			R			R	C	R						R	A	A		F									F	R		F	C	
5H-CC, 0-10	44.19										R					R	R								C		R	T				R	C												C	F		R	C	T
6H-CC, 0-10	53.72										R										R			R								R	A	R												R	R		R	C	T
7H-CC, 11-21	63.15										R							T						T								R	A												F	F		T	C	
8H-CC, 11-16	72.02										F												R	R									A												C	C			C	
9H-CC, 17-27	82.33										R												R	R			T			T		F	A			T									R	F		R	C	
10H-CC, 15-20	91.88										R					R																F	A												C	F			C	
11H-CC, 11-21	101.14										R											F		F			R			T		C	A												C	F			A	
12H-CC, 13-23	110.76				R						F					R	R					R					T			R		R	A				R								C	C			C	R
13H-CC, 14-19	119.69										R													R			R			R		F	A												C	R			C	T
14H-CC, 12-22	129.66										R						T													C		C	A				R								F	C			C		F
15H-CC, 21-26	139.54	R									R																			R			A				F							C	C			F		R
16H-CC, 21-26	148.66	F			C						R		R																	R		R	A				C		R				F	R	C			A		F
17H-CC, 22-27	158.57	T			C						R		R																	R			C						F				C		F			F		F
181-1123B-																																																			
16H-6, 123-126	145.13	R									F						T										R			F	T		R	C				C							C		C	C			F		R
16H-CC, 0-10	145.76										R													R						F			R	A				C		R				C	R	F	R			C		F
17H-2, 64-69	148.04				R						R																R			R			R	A			R	C		R				C		C	C			R		F
17H-6, 127-133	154.67	F			F						R		R														R			T			R	C				R		R				R	R	R	C			R		
17H-CC, 35-40	155.63	R		T	C						R		R																	R	R			A				C		R				C	R	R	R			A		
18X-CC, 18-28	163.69				R						F				T		T													R			C				C		R				C	R	R				C		F
19X-CC, 23-33	172.31	R			R						R										T									R	R		R	C			F		R				F	R	F	C			A		R
20X-CC, 20-25	182	R			R						R																			R			R	A				C		R				C		R	C			C		R
21X-CC, 13-23	191.27	F		R	R						R																			T				C			A		R				C		R	R			C		R
22X-CC, 26-36	201.37	R			R						R																R				R		R	A			R			R			R	T	F	C			C		R
23X-CC, 21-26	208.91	R		T	F	R					R																R				R		R	A									A			R			C	C	F
24X-CC, 26-31	220.5										R																R				R		R	R											R	R			A	R	
25X-CC, 22-32	230	R		R	R	T					R		R	R													R				R		R	C					R				C		R	R			F	R	R
26X-CC, 22-32	234.08	F			R						R			T			T										R				R		R	C				R		R				C		F		R	C	R	R
27X-CC, 26-36	249.32					R					R			R													R			R			F	A						R				C		R					R
28X-CC, 18-23	258.74	F		R							F			T				T												R			R	C						R				C		F		R		C	
29X-CC, 27-37	268.49	R		F		T					R						T						R							R			R	A						R				A		R		R		C		R
30X-CC, 25-30	278		T							R	T																			R			R	C										C		R	T			C		T
31X-CC, 17-22	287.54		R								T																						R	F										R		R	R			C		
32X-CC, 23-33	296.31	R			R						R																				T		C	A										C		R	R			F		

Table T9 (continued).

Core, section, interval (cm)	Depth (mbsf)	*Thecosphaera miocenica*	*Thecosphaera* sp.	*Theocorys redondoensis*	*Theocorys spongoconum*	*Theocorys* sp. A	*Theocorythium* sp.	*Theocorythium trachelium trachelium*	*Theocorythium vetulum*	*Theocyrtis* sp.	other *Spumellaria*
181-1123A-											
1H-CC, 0-15	5.95							F			
2H-CC, 16-26	15.61							C			
3H-CC, 0-10	23.21							R			
4H-CC, 0-10	34.7							C			
5H-CC, 0-10	44.19		C					C			
6H-CC, 0-10	53.72		F								
7H-CC, 11-21	63.15		A					R			
8H-CC, 11-16	72.02		C						F		
9H-CC, 17-27	82.33		C						F		
10H-CC, 15-20	91.88		F						F		
11H-CC, 11-21	101.14		C						R		
12H-CC, 13-23	110.76		C						R		
13H-CC, 14-19	119.69		C						C		
14H-CC, 12-22	129.66		C								
15H-CC, 21-26	139.54		C						R		
16H-CC, 21-26	148.66		R						C		
17H-CC, 22-27	158.57		F								
181-1123B-											
16H-6, 123-126	145.13		C			T					
16H-CC, 0-10	145.76		F						C		
17H-2, 64-69	148.04		C						F		
17H-6, 127-133	154.67								F		
17H-CC, 35-40	155.63		F	R		T			F		
18X-CC, 18-28	163.69		F	T					C		
19X-CC, 23-33	172.31		C						F		
20X-CC, 20-25	182		F	R		T			C		
21X-CC, 13-23	191.27		F	T					C		
22X-CC, 26-36	201.37		F						C		
23X-CC, 21-26	208.91		C			R			R		
24X-CC, 26-31	220.5								F		
25X-CC, 22-32	230		C	R		R			C		
26X-CC, 22-32	234.08								C		
27X-CC, 26-36	249.32		C						C		
28X-CC, 18-23	258.74		F						C		
29X-CC, 27-37	268.49		R						C		
30X-CC, 25-30	278		R								
31X-CC, 17-22	287.54		C								
32X-CC, 23-33	296.31		A								

Table T9 (continued).

Core, section, interval (cm)	Depth (mbsf)	Preservation	Group abundance	*Actinomma leptodermum*	*Actinomma* sp.	*Albatrossium* sp.	*Amphipyndax stocki*	*Amphirhopalum ypsilon*	*Amphistylus*(?) sp.	*Amphymenium amphistylium*	*Anthocyrtidium angulare*	*Anthocyrtidium ehrenbergi*	*Anthocyrtidium marieae*	*Aphetocyrtis gnomabox*	*Axoprunum angelinum*	*Axoprunum pierinae*	*Axoprunum* sp.	*Botryostrobus aquilonaris*	*Botryostrobus auritus/australis group*	*Botryostrobus miralestensis*	*Botryostrobus* sp.	*Buryella foremanae*	*Buryella* cf. *tetradica* (3 segments)	*Calocyclas*(?) *nakasekoi*	*Carpocanistrum* sp.	*Carpocanopsis bramlettei*	*Carpocanopsis cingulata*	*Calpocanopsis cristatum*	*Ceratocyrtis* sp.	*Collosphaera* sp.	*Cornutella profunda*	*Corythomelissa horrida*	*Cycladophora bicornis bicornis*	*Cycladophora davisiana cornutoides*	*Cycladophora davisiana davisiana*	*Cycladophora pliocenica*	*Cycladophora* sp.	*Cyrtocapsella cornuta*	*Cyrtocapsella japonica*	*Cyrtocapsella tetrapera*	*Dicolocapsa microcephala*	*Diartus hughesi*	*Dictyomitra multicostata*	*Dictyophimus hirundo*	*Dictyophimus* sp.	*Dictyophimus splendens*	*Dictyoprora mongolfieri*	*Didymocyrtis antepenultima*
33X-CC, 15-25	306.85	M	R																						T																			
34X-CC, 19-34	316.53	M	F								R														R																			
35X-CC, 9-19	326.02	VG	A		A							R							T								T													T				F
36X-CC, 13-23	335.47	G	R		R																						T																	
37X-CC, 22-32	345.2	M	T																																									
38X-CC, 31-41	354.79		B																																								
39X-CC, 29-39	364.48	G	T																																								
40X-CC, 22-32	374.06	M	R		R																																						T	
41X-CC, 28-38	382.2	M	VR																								T										T						
42X-CC, 24-34	388.44	G	A												R								T						T								A	R					
43X-CC, 14-24	399.52	G	R																						R												R	F					
44X-CC, 20-30	408.32	G	A												R										F					F	T						A				R		
45X-CC, 18-28	416.56	G	C		C																				R				R	R					R		A						
46X-CC, 20-25	428.36	M	R												R						F																F						
47X-CC, 0-10	436.96	G	VA																						C					F	R					R	A					
48X-CC, 0-15	445.6	P	R																	T										R							C					
49X-CC, 26-41	457.06	G	R																	F					R		R									T	F	C					
50X-CC, 39-54	468.6		B																																								
51X-CC, 17-27	479.62	G	VR																																T									
52X-CC, 26-36	488.56	G	R															R							R												R	R					
181-1123C-																																												
18X-CC, 35-45	488.85	G	R		F															R					R		R			T					R	R	C					
19X-CC, 25-35	498.1	G	C									T													F	R	T								R	C	C					
20X-CC, 0-15	506.39	G	T																																								
21X-CC, 0-15	516.96	M	T																																		T						
22X-CC, 23-38	527.06	M	T																																	T								
23X-CC, 28-38	536.71		B																																								
24X-CC, 25-35	546.26	P	VR																						C																			
25X-CC, 16-26	555.76	G	R																						F										T	R	C					
26X-CC, 21-31	565.27	M	R																						R												R						
27X-CC, 24-34	574.96	M	F		R								T												R												C						
28X-CC, 5-15	583.78	P	VR		R																																T						
29X-CC, 29-39	593.31	G	A		A				F					R																													
30X-CC, 15-25	599.64	M	A			T								C																													
31X-CC, 0-10	611.08	VG	VA		A	F										R															R	R							F				
32X-CC, 43-53	619.11	G	VA																																								
33X-CC, 25-35	625.76	M	VA																					R							R												

Note: Preservation: E = excellent, G = good, M = moderate, and P = poor; total abundance and relative abundance of radiolarians: A = abundant, C = common, F = few, R = rare, T = trace, and B = barren.

Table T9 (continued).

Core, section, interval (cm)	Depth (mbsf)	*Didymocyrtis laticonus*	*Didymocyrtis penultima*	*Didymocyrtis* sp.	*Didymocyrtis* sp. *D* of Sakai	*Didymocyrtis tetrathalamus tetrathalamus*	*Dorcadospyris alata*	*Dorcadospyris mahurangi*	*Dorcadospirys tricelos*	*Druppatractus irregularis*	*Druppatractus* sp.	*Euchitonia* sp.	*Eucyrtidium acuminatum*	*Eucyrtidium antiquum*	*Eucyrtidium* sp. A	*Eucyrtidium spinosum*	*Eucyrtidium calvertense*	*Eucyrtidium cienkowskii group*	*Eucyrtidium matuyamai*	*Eucyrtidium punctatum*	*Eucyrtidium* sp.	*Eucyrtidium teuscheri teuscheri*	*Eucyrtidium yatsuoense*	*Eusyringium lagena*	*Gondwanaria dogieli*	*Gondwanaria* sp.	*Heliodiscus asteriscus*	*Hexacontium* sp.	*Lamprocyclas hannai*	*Lamprocyclas* sp.	*Lamprocyclas maritalis maritalis*	*Lamprocyrtis heteroporos*	*Lamprocyrtis nigriniae*	*Larcopyle* sp.	*Larcospira* sp.	*Liriospyris* sp.	*Lithelius* sp.	*Lithelius nautiloides*	*Lithopera bacca*	*Lithopera neotera*	*Lithopera renzae*	*Lophocyrtis aspera*	*Lophocyrtis longiventer*	*Lophocyrtis dumitricai*	*Lophophaena* spp.	*Lychoncanoma amphitrite*	*Lychnocanoma* cf. *babilonis*	*Lychnocanoma elongata*	*Lychnocanoma nipponica nipponica*	*Lychnocanoma nipponica sakaii*	*Lychnocanoma parallelipes*
33X-CC, 15-25	306.85										F																							R															
34X-CC, 19-34	316.53			R	R												R										R						C	R														
35X-CC, 9-19	326.02			F	F					R		R					R										C		F		C		R														
36X-CC, 13-23	335.47			C						C																							R															
37X-CC, 22-32	345.2																																																
38X-CC, 31-41	354.79																																																
39X-CC, 29-39	364.48																																																
40X-CC, 22-32	374.06									R																																						
41X-CC, 28-38	382.2			R																											T		R														
42X-CC, 24-34	388.44	C		C						R	C	F					R	F										F			F		C				T		C								
43X-CC, 14-24	399.52	R		F								R																C		F		R		F					R								
44X-CC, 20-30	408.32	F		C						R	R	F					R	R				T	R				R	T		F		T						T								
45X-CC, 18-28	416.56	R		F						R	F							R					T							F		T						T								
46X-CC, 20-25	428.36										R																																					
47X-CC, 0-10	436.96			R						F	C	R						F						F				F			F		F													R	
48X-CC, 0-15	445.6										R																				T																
49X-CC, 26-41	457.06			R						R	R									R											R		R						R								
50X-CC, 39-54	468.6																																															
51X-CC, 17-27	479.62																																															
52X-CC, 26-36	488.56																																															
181-1123C-																																																
18X-CC, 35-45	488.85										R							R			R										T		R	T	R												
19X-CC, 25-35	498.1						R													F	R										R				R												
20X-CC, 0-15	506.39										R																								T													
21X-CC, 0-15	516.96																																															
22X-CC, 23-38	527.06																																															
23X-CC, 28-38	536.71																																															
24X-CC, 25-35	546.26						R				R																						F														
25X-CC, 16-26	555.76										R																																					
26X-CC, 21-31	565.27										T																				T																
27X-CC, 24-34	574.96							R			R																		T						T												
28X-CC, 5-15	583.78										T																																					
29X-CC, 29-39	593.31								R		R			T																														F				
30X-CC, 15-25	599.64								T		F																	F						F	R								R	R	R	T			
31X-CC, 0-10	611.08										F			R	F	C												C						R								F	A		R		F		
32X-CC, 43-53	619.11								R		R				T	T																											R				A		
33X-CC, 25-35	625.76								R		R				R									T						R														R		A	R	

Table T9 (continued).

Core, section, interval (cm)	Depth (mbsf)	*Lychnocanoma* sp.	*Lychnocanoma* sp. *A*	*Lychnodictyum audax*	*Lophoconus biaurita* (Form C)	*Nassellaria* Form D	*Orodapis* sp.	*Periphaena decora*	*Periphaena heliastericus*	*Periphaena* sp.	*Peripyramis* sp.	*Phormocyrtis alexandrae*	*Phormocyrtis striata striata*	*Phormostichoartus corbula*	*Phormostichoartus fistula*	*Phortidium clevei*	*Prunopyle antarctica*	*Prunopyle hayesi*	*Prunopyle tetrapila*	*Prunopyle* sp.	*Pterocanium praetextum praetextum*	*Pterocanium prismatium*	*Pterocanium* sp.	*Pterocanium trilobum*	*Pterocorys zancleus*	*Pylospira* sp.	*Saturnalis circularis*	*Siphocampe* sp.	*Solenosphaera* spp.	*Sphaeropyle langii*	*Sphaeropyle robusta*	*Spongaster tetras tetras*	*Spongodiscus osculosus*	*Spongodiscus* sp.	*Spongoplegma antarcticum*	*Spongoplegma churchii*	*Spongotrochus glacialis*	*Stichocorys* sp.	*Stichocorys armata*	*Stichocorys delmontensis*	*Stichocorys johnsoni*	*Stichocorys peregrina*	*Stichocorys wolfii*	*Stylacontarium acquilonium*	*Stylacontarium bispiculum*	*Stylatractus neptunus*
33X-CC, 15-25	306.85	T																															F							R				
34X-CC, 19-34	316.53	R																														R	C									R	R
35X-CC, 9-19	326.02	R									R																			R		R	C		C		R		R		R	C	C
36X-CC, 13-23	335.47				F																											R					T		T		R	C	
37X-CC, 22-32	345.2																															T											
38X-CC, 31-41	354.79																																										
39X-CC, 29-39	364.48																																										
40X-CC, 22-32	374.06	T																																							R	T
41X-CC, 28-38	382.2							R																								T									R	
42X-CC, 24-34	388.44	T						R			R						R													F		F	C						C		R	
43X-CC, 14-24	399.52							C						T																		C							R		F	
44X-CC, 20-30	408.32	R						R						T																R		A							A	R	R	R	
45X-CC, 18-28	416.56	T			R			R																						R		R									C	R	
46X-CC, 20-25	428.36																																									R	R	
47X-CC, 0-10	436.96	T									R																			R		A							C				
48X-CC, 0-15	445.6													T																		C									F		
49X-CC, 26-41	457.06					F					R						T															F					F		R		R		
50X-CC, 39-54	468.6																																										
51X-CC, 17-27	479.62																																									
52X-CC, 26-36	488.56																																								R		
181-1123C-																																											
18X-CC, 35-45	488.85							T																								R					T				R		
19X-CC, 25-35	498.1											F	R																F			R				T			R		F		
20X-CC, 0-15	506.39																												T														
21X-CC, 0-15	516.96																																										
22X-CC, 23-38	527.06																																										
23X-CC, 28-38	536.71																																										
24X-CC, 25-35	546.26	R			T						T	R	T																			R									F		
25X-CC, 16-26	555.76										T	R																															
26X-CC, 21-31	565.27											T																														T		
27X-CC, 24-34	574.96										R	R																				R							T			R		
28X-CC, 5-15	583.78																															R										R		
29X-CC, 29-39	593.31								T		T								T	R							R														A		
30X-CC, 15-25	599.64								R		R							T	R								R					R									F		
31X-CC, 0-10	611.08	R							R		F																					R	F									A		
32X-CC, 43-53	619.11	R									R								R																									
33X-CC, 25-35	625.76										R																															F		

Table T9 (continued).

Core, section, interval (cm)	Depth (mbsf)	*Thecosphaera miocenica*	*Thecosphaera* sp.	*Theocorys redondoensis*	*Theocorys spongoconum*	*Theocorys* sp. *A*	*Theocorythium* sp.	*Theocorythium trachelium trachelium*	*Theocorythium vetulum*	*Theocyrtis* sp.	other *Spumellaria*
33X-CC, 15-25	306.85		R								
34X-CC, 19-34	316.53										
35X-CC, 9-19	326.02		C						T		
36X-CC, 13-23	335.47										
37X-CC, 22-32	345.2										
38X-CC, 31-41	354.79										
39X-CC, 29-39	364.48										
40X-CC, 22-32	374.06										
41X-CC, 28-38	382.2		R								
42X-CC, 24-34	388.44		C								
43X-CC, 14-24	399.52										
44X-CC, 20-30	408.32	C	F	T							
45X-CC, 18-28	416.56		C								
46X-CC, 20-25	428.36										
47X-CC, 0-10	436.96			T	T						
48X-CC, 0-15	445.6										
49X-CC, 26-41	457.06			T	R						
50X-CC, 39-54	468.6										
51X-CC, 17-27	479.62										
52X-CC, 26-36	488.56										
181-1123C-											
18X-CC, 35-45	488.85		R								
19X-CC, 25-35	498.1		F		R						
20X-CC, 0-15	506.39										
21X-CC, 0-15	516.96										
22X-CC, 23-38	527.06										
23X-CC, 28-38	536.71										
24X-CC, 25-35	546.26				T						
25X-CC, 16-26	555.76										
26X-CC, 21-31	565.27										
27X-CC, 24-34	574.96										
28X-CC, 5-15	583.78										
29X-CC, 29-39	593.31									T	
30X-CC, 15-25	599.64		C							R	
31X-CC, 0-10	611.08		A								
32X-CC, 43-53	619.11										C
33X-CC, 25-35	625.76									R	C

Table T10. Significant radiolarian datum levels at Site 1123.

Events selected for Site 1123, Leg 181	Stage	Age (Ma)	Core, section, interval (cm)	Depth (mbsf)	Depth (mcd)	References
LO *Stylatractus universus*	Pleistocene	0.46	1123A-3H-CC	23.21	23.07	Caulet, 1991
LO *Axoprunum angelinum*	Pleistocene		1123A-4H-CC	34.7	32.26	
FO *Theocorythium trachelium*	early Pleistocene	1.6-1.7	1123A-7H-CC	63.15	65.85	Alexandrovich, 1989
LO *Eucyrtidium calvertense*	late Pliocene	1.92	1123A-7H-CC	63.15	65.85	Lazarus, 1992
LO *Theocorythium vetulum*	early Pleistocene	1.2-1.3	1123A-8H-CC	72.02	75.87	Alexandrovich, 1989
LO *Anthocyrtidium angulare*			1123A-9H-CC	82.33	86.82	
LO *Sphaeropyle langii*			1123A-9H-CC	82.23	86.82	
LO *Lamprocyrtis heteroporos*	Pliocene/Pleistocene	1.8	1123A-10H-CC	91.88	97.83	Morley and Nigrini, 1995
LO *Pterocanium prismatium*	early Pleistocene	1.7	1123A-11H-CC	101.1	107.32	Johnson, et al., 1989
LCO *Stichocorys* group	early Pleistocene	4.2	1123A-12H-CC	110.76	117.42	Motoyama and Maruyama, 1998
FO *Cycladophora davisiana davisiana*	late Pliocene	2.91-3.08	1123A-13H-CC	119.7	127.91	Morley and Nigrini, 1995
LO *Stichocorys peregrina*	late Pliocene	<3.0	1123A-15H-CC	139.5	149.38	Motoyama and Maruyama, 1998
LO *Sphaeropyle robusta*			1123B-16H-6, 123-126	145.13		
FO *Amphirhopalum ypsilon*	early Pliocene	3.9	1123B-16H-CC	145.76	157.78	Johnson, et al., 1989
LO *Lychnodictyum audax*	early Pliocene	3.7	1123B-17H-CC	155.63	167.57	Johnson, et al., 1989
LO *Dictyophimus splendens*	earliest Pliocene	5.0-5.2	1123B-19X-CC	172.31	184.25	Morley and Nigrini, 1995
FO *Sphaeropyle langii*	late Miocene	6.0-6.2	1123B-21X-CC	191.27	203.31	Morley and Nigrini, 1995
LO *Amphymenium amphistylium*			1123B-21X-CC	191.27	203.31	Morley and Nigrini, 1995
LO *Lychnocanoma parallelipes*	latest Miocene	5.6	1123B-21X-CC	191.27	203.31	Motoyama and Maruyama, 1998
FO *Stylacontarium aquilonium*	late Miocene	7.88	1123B-22X-CC	201.37	213.41	Morley and Nigrini, 1995
LO *Didymocyrtis penultima*			1123B-25X-CC	230		Motoyama and Maruyama, 1998
FO *Dictyophimus splendens*			1123B-27X-CC	249.32		
FO *Lychnocanoma parallelipes*	late Miocene	6.8-7.3	1123B-29X-CC	268.5	280.53	Motoyama and Maruyama, 1998
RI Acme *Stichocorys peregrina*	late Miocene	6.8-7.3	1123B-29X-CC	268.5	280.53	Motoyama and Maruyama, 1998
FO *Didymocyrtis penultima*			1123B-30X-CC	278	289.94	
Evolutionary transition *S. delmontensis* → *S. peregrina*	late Miocene	7.7	1123B-32X-CC	296.3	308.24	Morley and Nigrini, 1995
LO *Didymocyrtis antepenultima*	late Miocene	8.2	1123B-32X-CC	296.3	308.24	Motoyama and Maruyama, 1998
FO *Didymocyrtis antepenultima*	late Miocene	9.7	1123B-35X-CC	326	337.94	Johnson, et al., 1989
LO *Cyrtocapsella japonica*	late Miocene	9.9	1123B-41X-CC	382.2	394.14	Motoyama and Maruyama, 1998
RI Acme *Cyrtocapsella japonica*	late Miocene	10.2	1123B-42X-CC	388.4	400.34	Sakai and Aita, 1994
LO *Didymocyrtis laticonus*			1123B-42X-CC	388.4	400.34	
RD *Cyrtocapsella tetrapera*	middle Miocene	12.6	1123B-44X-CC	408.3	420.24	Motoyama and Maruyama, 1998
LO *Eucyrtidium yatsuoense*			1123B-44X-CC	408.3	420.24	
LO *Cyrtocapsella cornuta*	late middle Miocene	11.6-12.3	1123B-45X-CC	416.56		Motoyama and Maruyama, 1998
FO *Sphaeropyle robusta*			1123B-47X-CC	437		
LO *Theocorys spongoconum*			1123B-47X-CC	437		
LO *Eucyrtidium* sp. B of Sakai			1123C-19X-CC	498.1	507.42	
FO *Eucyrtidium punctatum*	early Miocene	17.02	1123C-19X-CC	498.1	507.42	Lazarus, 1992
FO *Cyrtocapsella tetrapera*	Miocene/Oligocene	23.62	1123C-27X-CC	574.96	584.28	Sanfilippo and Nigrini, 1998
LO *Eucyrtidium spinosum*	early Oligocene	31.7-31.9	1123C-31X-CC	611.1	620.51	Takemura and Ling, 1997
FO *Eucyrtidium antiquum*	early Oligocene	32.8-33.1	1123C-31X-CC	611.1	620.51	Takemura and Ling, 1997
FO *Eucyrtidium spinosum*	middle to late Eocene	36.7-38.1	1123C-32X-CC	619.65		Takemura and Ling, 1997

Table T11. Compilation of age data from magnetostratigraphic interpretation of Holes 1123B and 1123C.

Chron/Event (base)	Depth (mcd)	Age (Ma)
C1n	32.5	0.78
C1r.1r	37.25	0.99
C1r.1n	41.2	1.07
C1r.2ra	44.35	1.201
Cobb Mountain	45.1	1.211
C1r.2rb	69.65	1.77
C2n	73.25	1.95
C2r	93.75-100.30	2.581
C2An.1n	107.4	3.04
C2An.1r	111.85	3.11
C2An.2n	115.3	3.22
C2An.2r	120.45	3.33
C2An.3n	129.6	3.58
C2Ar	150.52	4.18
C3n.1n	153.8	4.29
C3n.1r	164.15	4.48
C3n.2n	166.75	4.62
C3n.2r	171.9	4.8
C3n.3n	173.2	4.89
C3n.3r	177.1	4.98
C3n.4n	184.9	5.23
New (y)	199.95	5.586
New (o)	201.55	5.623
C3r	213	5.894
C3An.1n	228.6	6.137
C3An.1r	233.05	6.269
C3An.2n	250.45	6.567
C3Ar	264.85	6.935
C3Bn	268.9	7.091
C3Br.1r	270.85	7.135
C3Br.1n	272	7.17
C3Br.2r	273.4	7.341
C3Br.2n	277.6	7.375
C3Br.3r	279.6	7.432
C4n.1n	282	7.562
C4n.1r	284.55	7.65
C4n.2n	300.2	8.072
C4r	318.7	8.699
C4An	328.1	9.025
C4Ar.1r	333.7	9.23
C4Ar.1n	337.85	9.308
C4Ar.2r	340.8	9.58
C4Ar.2n	346.2	9.642
C4Ar.3r	348	9.74
C5n.1n	349.95	9.88
C5n.1r	350.45	9.92
C5n.2n	380.6	10.949
C5r.1r	383.95	11.052
C5r.1n	384.6	11.099
C5r	404.4	11.935
C5An.1n	411.1	12.078
C5An.1r	414.75	12.184
C5An.2n	421.5	12.401
C5Ar.1r	432.6	12.678
New (y)	433.10	12.684
New (o)	434.10	12.795
C5Ar.1n	435.3	12.708
C5Ar.2r	437.5	12.775
C5Ar.2n	438.8	12.819
C5Ar.3r	444.05	12.991
C5AAn	449.9	13.139
C5AAr	457.2	13.302
C5ABn	462.95	13.51
C5ABr	465.4	13.703
C5ACn	469.3	14.076
C5ACr	471.6	14.178
new (y)	472.35	14.292
New (o)	473.10	14.406
C5ADn	474.45	14.612
C5ADr	477.65	14.8
C5Bn.1n	478.2	14.888
C5Bn.1r	481.1	15.034
C5Bn.2n	482.15	15.155
C5Br	499.15	16.014
C5Cn.1n	505.1	16.293
C5Cn.1r	507.5	16.327
C5Cn.2n	508.2	16.488
C5Cn.2r	511.4	16.556
C5Cn.3n	514	16.726
C5Cr	516.85	17.277
C5Dn	522.1	17.615
C5Dr	534.1	18.281
C5En	542.7	18.781
C5Er	546	19.048
C6n	579.3	20.131
Hiatus		21-33 Ma
C12r	600.4	33.058
C13n	609	33.545
C13r	625.35	34.655

Note: Ages are from Berggren et al. (1995), and ages of new intervals are from linear interpolation using adjacent points. y = youngest, o = oldest.

Table T12. Composite depth section, Site 1123. (See table note. Continued on next 10 pages.)

Leg	Site	Hole	Core	Type	Section	Section length	Depth (mbsf)	Offset	Composite depth (mcd)
181	1123	A	1	H	1	1.50	0.00	0.00	0.00
181	1123	A	1	H	2	1.50	1.50	0.00	1.50
181	1123	A	1	H	3	1.45	3.00	0.00	3.00
181	1123	A	1	H	4	1.50	4.45	0.00	4.45
181	1123	A	1	H	CC	0.15	5.95	0.00	5.95
181	1123	A	2	H	1	1.50	6.10	-1.80	4.30
181	1123	A	2	H	2	1.50	7.60	-1.80	5.80
181	1123	A	2	H	3	1.50	9.10	-1.80	7.30
181	1123	A	2	H	4	1.50	10.60	-1.80	8.80
181	1123	A	2	H	5	1.50	12.10	-1.80	10.30
181	1123	A	2	H	6	1.50	13.60	-1.80	11.80
181	1123	A	2	H	7	0.35	15.10	-1.80	13.30
181	1123	A	2	H	CC	0.26	15.45	-1.80	13.65
181	1123	A	3	H	1	1.50	15.60	-0.24	15.36
181	1123	A	3	H	2	1.50	17.10	-0.24	16.86
181	1123	A	3	H	3	1.50	18.60	-0.24	18.36
181	1123	A	3	H	4	1.50	20.10	-0.24	19.86
181	1123	A	3	H	5	1.30	21.60	-0.24	21.36
181	1123	A	3	H	6	0.31	22.90	-0.24	22.66
181	1123	A	3	H	CC	0.10	23.21	-0.24	22.97
181	1123	A	4	H	1	1.50	25.10	-2.44	22.66
181	1123	A	4	H	2	1.50	26.60	-2.44	24.16
181	1123	A	4	H	3	1.50	28.10	-2.44	25.66
181	1123	A	4	H	4	1.50	29.60	-2.44	27.16
181	1123	A	4	H	5	1.50	31.10	-2.44	28.66
181	1123	A	4	H	6	1.50	32.60	-2.44	30.16
181	1123	A	4	H	7	0.60	34.10	-2.44	31.66
181	1123	A	4	H	CC	0.10	34.70	-2.44	32.26
181	1123	A	5	H	1	1.50	34.60	1.04	35.64
181	1123	A	5	H	2	1.50	36.10	1.04	37.14
181	1123	A	5	H	3	1.50	37.60	1.04	38.64
181	1123	A	5	H	4	1.50	39.10	1.04	40.14
181	1123	A	5	H	5	1.50	40.60	1.04	41.64
181	1123	A	5	H	6	1.50	42.10	1.04	43.14
181	1123	A	5	H	7	0.59	43.60	1.04	44.64
181	1123	A	5	H	CC	0.10	44.19	1.04	45.23
181	1123	A	6	H	1	1.50	44.10	3.74	47.84
181	1123	A	6	H	2	1.50	45.60	3.74	49.34
181	1123	A	6	H	3	1.50	47.10	3.74	50.84
181	1123	A	6	H	4	1.50	48.60	3.74	52.34
181	1123	A	6	H	5	1.50	50.10	3.74	53.84
181	1123	A	6	H	6	1.50	51.60	3.74	55.34
181	1123	A	6	H	7	0.62	53.10	3.74	56.84
181	1123	A	6	H	CC	0.10	53.72	3.74	57.46
181	1123	A	7	H	1	1.50	53.60	3.88	57.48
181	1123	A	7	H	2	1.50	55.10	3.88	58.98
181	1123	A	7	H	3	1.50	56.60	3.88	60.48
181	1123	A	7	H	4	1.50	58.10	3.88	61.98
181	1123	A	7	H	5	1.50	59.60	3.88	63.48
181	1123	A	7	H	6	1.50	61.10	3.88	64.98
181	1123	A	7	H	7	0.44	62.60	3.88	66.48
181	1123	A	7	H	CC	0.21	63.04	3.88	66.92
181	1123	A	8	H	1	1.50	63.10	4.98	68.08
181	1123	A	8	H	2	1.50	64.60	4.98	69.58
181	1123	A	8	H	3	1.50	66.10	4.98	71.08
181	1123	A	8	H	4	1.50	67.60	4.98	72.58
181	1123	A	8	H	5	1.50	69.10	4.98	74.08
181	1123	A	8	H	6	1.31	70.60	4.98	75.58
181	1123	A	8	H	CC	0.16	71.91	4.98	76.89
181	1123	A	9	H	1	1.50	72.60	5.56	78.16
181	1123	A	9	H	2	1.50	74.10	5.56	79.66
181	1123	A	9	H	3	1.50	75.60	5.56	81.16
181	1123	A	9	H	4	1.50	77.10	5.56	82.66
181	1123	A	9	H	5	1.50	78.60	5.56	84.16
181	1123	A	9	H	6	1.50	80.10	5.56	85.66
181	1123	A	9	H	7	0.56	81.60	5.56	87.16
181	1123	A	9	H	CC	0.27	82.16	5.56	87.72

Table T12 (continued).

Leg	Site	Hole	Core	Type	Section	Section length	Depth (mbsf)	Offset	Composite depth (mcd)
181	1123	A	10	H	1	1.50	82.10	7.06	89.16
181	1123	A	10	H	2	1.50	83.60	7.06	90.66
181	1123	A	10	H	3	1.50	85.10	7.06	92.16
181	1123	A	10	H	4	1.50	86.60	7.06	93.66
181	1123	A	10	H	5	1.50	88.10	7.06	95.16
181	1123	A	10	H	6	1.50	89.60	7.06	96.66
181	1123	A	10	H	7	0.63	91.10	7.06	98.16
181	1123	A	10	H	CC	0.20	91.73	7.06	98.79
181	1123	A	11	H	1	1.50	91.60	7.26	98.86
181	1123	A	11	H	2	1.50	93.10	7.26	100.36
181	1123	A	11	H	3	1.50	94.60	7.26	101.86
181	1123	A	11	H	4	1.50	96.10	7.26	103.36
181	1123	A	11	H	5	1.50	97.60	7.26	104.86
181	1123	A	11	H	6	1.50	99.10	7.26	106.36
181	1123	A	11	H	7	0.43	100.60	7.26	107.86
181	1123	A	11	H	CC	0.21	101.03	7.26	108.29
181	1123	A	12	H	1	1.50	101.10	7.84	108.94
181	1123	A	12	H	2	1.50	102.60	7.84	110.44
181	1123	A	12	H	3	1.50	104.10	7.84	111.94
181	1123	A	12	H	4	1.50	105.60	7.84	113.44
181	1123	A	12	H	5	1.50	107.10	7.84	114.94
181	1123	A	12	H	6	1.50	108.60	7.84	116.44
181	1123	A	12	H	7	0.53	110.10	7.84	117.94
181	1123	A	12	H	CC	0.23	110.63	7.84	118.47
181	1123	A	13	H	1	1.50	110.60	9.39	119.99
181	1123	A	13	H	2	1.50	112.10	9.39	121.49
181	1123	A	13	H	3	1.05	113.60	9.39	122.99
181	1123	A	13	H	4	1.50	114.65	9.39	124.04
181	1123	A	13	H	5	1.50	116.15	9.39	125.54
181	1123	A	13	H	6	1.50	117.65	9.39	127.04
181	1123	A	13	H	7	0.40	119.15	9.39	128.54
181	1123	A	13	H	CC	0.19	119.55	9.39	128.94
181	1123	A	14	H	1	1.50	120.10	9.88	129.98
181	1123	A	14	H	2	1.50	121.60	9.88	131.48
181	1123	A	14	H	3	1.50	123.10	9.88	132.98
181	1123	A	14	H	4	1.50	124.60	9.88	134.48
181	1123	A	14	H	5	1.50	126.10	9.88	135.98
181	1123	A	14	H	6	1.50	127.60	9.88	137.48
181	1123	A	14	H	7	0.44	129.10	9.88	138.98
181	1123	A	14	H	CC	0.22	129.54	9.88	139.42
181	1123	A	15	H	1	1.50	129.60	11.34	140.94
181	1123	A	15	H	2	1.50	131.10	11.34	142.44
181	1123	A	15	H	3	1.50	132.60	11.34	143.94
181	1123	A	15	H	4	1.50	134.10	11.34	145.44
181	1123	A	15	H	5	1.50	135.60	11.34	146.94
181	1123	A	15	H	6	1.50	137.10	11.34	148.44
181	1123	A	15	H	7	0.73	138.60	11.34	149.94
181	1123	A	15	H	CC	0.26	139.33	11.34	150.67
181	1123	A	16	H	1	1.50	139.10	12.82	151.92
181	1123	A	16	H	2	1.50	140.60	12.82	153.42
181	1123	A	16	H	3	1.50	142.10	12.82	154.92
181	1123	A	16	H	4	1.50	143.60	12.82	156.42
181	1123	A	16	H	5	1.50	145.10	12.82	157.92
181	1123	A	16	H	6	1.50	146.60	12.82	159.42
181	1123	A	16	H	7	0.35	148.10	12.82	160.92
181	1123	A	16	H	CC	0.26	148.45	12.82	161.27
181	1123	B	1	H	1	1.50	0.00	0.00	0.00
181	1123	B	1	H	2	1.50	1.50	0.00	1.50
181	1123	B	1	H	3	0.21	3.00	0.00	3.00
181	1123	B	1	H	CC	0.15	3.21	0.00	3.21
181	1123	B	2	H	1	1.50	3.40	-0.74	2.66
181	1123	B	2	H	2	1.50	4.90	-0.74	4.16
181	1123	B	2	H	3	1.50	6.40	-0.74	5.66
181	1123	B	2	H	4	1.50	7.90	-0.74	7.16
181	1123	B	2	H	5	1.50	9.40	-0.74	8.66
181	1123	B	2	H	6	1.50	10.90	-0.74	10.16
181	1123	B	2	H	7	0.24	12.40	-0.74	11.66
181	1123	B	2	H	CC	0.21	12.64	-0.74	11.90

Table T12 (continued).

Leg	Site	Hole	Core	Type	Section	Section length	Depth (mbsf)	Offset	Composite depth (mcd)
181	1123	B	3	H	1	1.50	12.90	1.72	14.62
181	1123	B	3	H	2	1.50	14.40	1.72	16.12
181	1123	B	3	H	3	1.50	15.90	1.72	17.62
181	1123	B	3	H	4	1.50	17.40	1.72	19.12
181	1123	B	3	H	5	1.50	18.90	1.72	20.62
181	1123	B	3	H	6	1.50	20.40	1.72	22.12
181	1123	B	3	H	7	0.63	21.90	1.72	23.62
181	1123	B	3	H	CC	0.21	22.53	1.72	24.25
181	1123	B	4	H	1	1.50	22.40	0.72	23.12
181	1123	B	4	H	2	1.50	23.90	0.72	24.62
181	1123	B	4	H	3	1.50	25.40	0.72	26.12
181	1123	B	4	H	4	1.50	26.90	0.72	27.62
181	1123	B	4	H	5	1.50	28.40	0.72	29.12
181	1123	B	4	H	6	1.50	29.90	0.72	30.62
181	1123	B	4	H	7	0.60	31.40	0.72	32.12
181	1123	B	4	H	CC	0.20	32.00	0.72	32.72
181	1123	B	5	H	1	1.50	31.90	2.90	34.80
181	1123	B	5	H	2	1.50	33.40	2.90	36.30
181	1123	B	5	H	3	1.50	34.90	2.90	37.80
181	1123	B	5	H	4	1.50	36.40	2.90	39.30
181	1123	B	5	H	5	1.50	37.90	2.90	40.80
181	1123	B	5	H	6	1.50	39.40	2.90	42.30
181	1123	B	5	H	7	0.60	40.90	2.90	43.80
181	1123	B	5	H	CC	0.17	41.50	2.90	44.40
181	1123	B	6	H	1	1.50	41.40	1.60	43.00
181	1123	B	6	H	2	1.50	42.90	1.60	44.50
181	1123	B	6	H	3	1.50	44.40	1.60	46.00
181	1123	B	6	H	4	1.50	45.90	1.60	47.50
181	1123	B	6	H	5	1.50	47.40	1.60	49.00
181	1123	B	6	H	6	1.50	48.90	1.60	50.50
181	1123	B	6	H	7	0.53	50.40	1.60	52.00
181	1123	B	6	H	CC	0.25	50.93	1.60	52.53
181	1123	B	7	H	1	1.50	50.90	3.32	54.22
181	1123	B	7	H	2	1.50	52.40	3.32	55.72
181	1123	B	7	H	3	1.50	53.90	3.32	57.22
181	1123	B	7	H	4	1.50	55.40	3.32	58.72
181	1123	B	7	H	5	1.50	56.90	3.32	60.22
181	1123	B	7	H	6	1.50	58.40	3.32	61.72
181	1123	B	7	H	7	0.75	59.90	3.32	63.22
181	1123	B	7	H	CC	0.37	60.65	3.32	63.97
181	1123	B	8	H	1	1.50	60.40	3.10	63.50
181	1123	B	8	H	2	1.50	61.90	3.10	65.00
181	1123	B	8	H	3	1.50	63.40	3.10	66.50
181	1123	B	8	H	4	1.50	64.90	3.10	68.00
181	1123	B	8	H	5	1.50	66.40	3.10	69.50
181	1123	B	8	H	6	1.50	67.90	3.10	71.00
181	1123	B	8	H	7	0.59	69.40	3.10	72.50
181	1123	B	8	H	CC	0.20	69.99	3.10	73.09
181	1123	B	9	H	1	1.50	69.90	4.46	74.36
181	1123	B	9	H	2	1.50	71.40	4.46	75.86
181	1123	B	9	H	3	1.50	72.90	4.46	77.36
181	1123	B	9	H	4	1.50	74.40	4.46	78.86
181	1123	B	9	H	5	1.50	75.90	4.46	80.36
181	1123	B	9	H	6	1.50	77.40	4.46	81.86
181	1123	B	9	H	7	0.66	78.90	4.46	83.36
181	1123	B	9	H	CC	0.10	79.56	4.46	84.02
181	1123	B	10	H	1	1.50	79.40	4.82	84.22
181	1123	B	10	H	2	1.50	80.90	4.82	85.72
181	1123	B	10	H	3	1.50	82.40	4.82	87.22
181	1123	B	10	H	4	1.50	83.90	4.82	88.72
181	1123	B	10	H	5	1.50	85.40	4.82	90.22
181	1123	B	10	H	6	1.50	86.90	4.82	91.72
181	1123	B	10	H	7	0.34	88.40	4.82	93.22
181	1123	B	10	H	CC	0.45	88.74	4.82	93.56
181	1123	B	11	H	1	1.50	88.90	5.10	94.00
181	1123	B	11	H	2	1.50	90.40	5.10	95.50
181	1123	B	11	H	3	1.50	91.90	5.10	97.00
181	1123	B	11	H	4	1.50	93.40	5.10	98.50

Table T12 (continued).

Leg	Site	Hole	Core	Type	Section	Section length	Depth (mbsf)	Offset	Composite depth (mcd)
181	1123	B	11	H	5	1.50	94.90	5.10	100.00
181	1123	B	11	H	6	1.50	96.40	5.10	101.50
181	1123	B	11	H	7	0.70	97.90	5.10	103.00
181	1123	B	11	H	CC	0.21	98.60	5.10	103.70
181	1123	B	12	H	1	1.50	98.40	6.94	105.34
181	1123	B	12	H	2	1.50	99.90	6.94	106.84
181	1123	B	12	H	3	1.50	101.40	6.94	108.34
181	1123	B	12	H	4	1.50	102.90	6.94	109.84
181	1123	B	12	H	5	1.50	104.40	6.94	111.34
181	1123	B	12	H	6	1.50	105.90	6.94	112.84
181	1123	B	12	H	7	0.55	107.40	6.94	114.34
181	1123	B	12	H	CC	0.21	107.95	6.94	114.89
181	1123	B	13	H	1	1.50	107.90	7.16	115.06
181	1123	B	13	H	2	1.50	109.40	7.16	116.56
181	1123	B	13	H	3	1.50	110.90	7.16	118.06
181	1123	B	13	H	4	1.50	112.40	7.16	119.56
181	1123	B	13	H	5	1.50	113.90	7.16	121.06
181	1123	B	13	H	6	1.50	115.40	7.16	122.56
181	1123	B	13	H	7	0.67	116.90	7.16	124.06
181	1123	B	13	H	CC	0.21	117.57	7.16	124.73
181	1123	B	14	H	1	1.50	117.40	8.60	126.00
181	1123	B	14	H	2	1.50	118.90	8.60	127.50
181	1123	B	14	H	3	1.50	120.40	8.60	129.00
181	1123	B	14	H	4	1.50	121.90	8.60	130.50
181	1123	B	14	H	5	1.50	123.40	8.60	132.00
181	1123	B	14	H	6	1.50	124.90	8.60	133.50
181	1123	B	14	H	7	0.48	126.40	8.60	135.00
181	1123	B	14	H	CC	0.10	126.88	8.60	135.48
181	1123	B	15	H	1	1.50	126.90	9.88	136.78
181	1123	B	15	H	2	1.50	128.40	9.88	138.28
181	1123	B	15	H	3	1.53	129.90	9.88	139.78
181	1123	B	15	H	4	1.53	131.43	9.88	141.31
181	1123	B	15	H	5	1.50	132.96	9.88	142.84
181	1123	B	15	H	6	1.50	134.46	9.88	144.34
181	1123	B	15	H	7	0.62	135.96	9.88	145.84
181	1123	B	15	H	CC	0.23	136.58	9.88	146.46
181	1123	B	16	H	1	1.50	136.40	12.02	148.42
181	1123	B	16	H	2	1.50	137.90	12.02	149.92
181	1123	B	16	H	3	1.50	139.40	12.02	151.42
181	1123	B	16	H	4	1.50	140.90	12.02	152.92
181	1123	B	16	H	5	1.50	142.40	12.02	154.42
181	1123	B	16	H	6	1.50	143.90	12.02	155.92
181	1123	B	16	H	7	0.36	145.40	12.02	157.42
181	1123	B	16	H	CC	0.10	145.76	12.02	157.78
181	1123	B	17	H	1	1.50	145.90	11.94	157.84
181	1123	B	17	H	2	1.50	147.40	11.94	159.34
181	1123	B	17	H	3	1.50	148.90	11.94	160.84
181	1123	B	17	H	4	1.50	150.40	11.94	162.34
181	1123	B	17	H	5	1.50	151.90	11.94	163.84
181	1123	B	17	H	6	1.50	153.40	11.94	165.34
181	1123	B	17	H	7	0.38	154.90	11.94	166.84
181	1123	B	17	H	CC	0.40	155.28	11.94	167.22
181	1123	B	18	X	1	1.50	155.40	11.94	167.34
181	1123	B	18	X	2	1.50	156.90	11.94	168.84
181	1123	B	18	X	3	1.50	158.40	11.94	170.34
181	1123	B	18	X	4	1.50	159.90	11.94	171.84
181	1123	B	18	X	5	1.50	161.40	11.94	173.34
181	1123	B	18	X	6	0.61	162.90	11.94	174.84
181	1123	B	18	X	CC	0.28	163.51	11.94	175.45
181	1123	B	19	X	1	1.52	162.70	11.94	174.64
181	1123	B	19	X	2	1.52	164.22	11.94	176.16
181	1123	B	19	X	3	1.52	165.74	11.94	177.68
181	1123	B	19	X	4	1.52	167.26	11.94	179.20
181	1123	B	19	X	5	1.52	168.78	11.94	180.72
181	1123	B	19	X	6	1.52	170.30	11.94	182.24
181	1123	B	19	X	7	0.26	171.82	11.94	183.76
181	1123	B	19	X	CC	0.33	172.08	11.94	184.02
181	1123	B	20	X	1	1.52	172.30	11.94	184.24

Table T12 (continued).

Leg	Site	Hole	Core	Type	Section	Section length	Depth (mbsf)	Offset	Composite depth (mcd)
181	1123	B	20	X	2	1.52	173.82	11.94	185.76
181	1123	B	20	X	3	1.52	175.34	11.94	187.28
181	1123	B	20	X	4	1.50	176.86	11.94	188.80
181	1123	B	20	X	5	1.52	178.36	11.94	190.30
181	1123	B	20	X	6	1.52	179.88	11.94	191.82
181	1123	B	20	X	7	0.40	181.40	11.94	193.34
181	1123	B	20	X	CC	0.25	181.80	11.94	193.74
181	1123	B	21	X	1	1.50	181.90	11.94	193.84
181	1123	B	21	X	2	1.50	183.40	11.94	195.34
181	1123	B	21	X	3	1.50	184.90	11.94	196.84
181	1123	B	21	X	4	1.50	186.40	11.94	198.34
181	1123	B	21	X	5	1.50	187.90	11.94	199.84
181	1123	B	21	X	6	1.50	189.40	11.94	201.34
181	1123	B	21	X	7	0.24	190.90	11.94	202.84
181	1123	B	21	X	CC	0.23	191.14	11.94	203.08
181	1123	B	22	X	1	1.57	191.60	11.94	203.54
181	1123	B	22	X	2	1.50	193.17	11.94	205.11
181	1123	B	22	X	3	1.50	194.67	11.94	206.61
181	1123	B	22	X	4	1.50	196.17	11.94	208.11
181	1123	B	22	X	5	1.50	197.67	11.94	209.61
181	1123	B	22	X	6	1.50	199.17	11.94	211.11
181	1123	B	22	X	7	0.44	200.67	11.94	212.61
181	1123	B	22	X	CC	0.36	201.11	11.94	213.05
181	1123	B	23	X	1	1.50	201.20	11.94	213.14
181	1123	B	23	X	2	1.50	202.70	11.94	214.64
181	1123	B	23	X	3	1.50	204.20	11.94	216.14
181	1123	B	23	X	4	1.50	205.70	11.94	217.64
181	1123	B	23	X	5	1.50	207.20	11.94	219.14
181	1123	B	23	X	CC	0.26	208.70	11.94	220.64
181	1123	B	24	X	1	1.50	210.80	11.94	222.74
181	1123	B	24	X	2	1.50	212.30	11.94	224.24
181	1123	B	24	X	3	1.50	213.80	11.94	225.74
181	1123	B	24	X	4	1.50	215.30	11.94	227.24
181	1123	B	24	X	5	1.50	216.80	11.94	228.74
181	1123	B	24	X	6	1.50	218.30	11.94	230.24
181	1123	B	24	X	7	0.44	219.80	11.94	231.74
181	1123	B	24	X	CC	0.31	220.24	11.94	232.18
181	1123	B	25	X	1	1.50	220.40	11.94	232.34
181	1123	B	25	X	2	1.50	221.90	11.94	233.84
181	1123	B	25	X	3	1.50	223.40	11.94	235.34
181	1123	B	25	X	4	1.50	224.90	11.94	236.84
181	1123	B	25	X	5	1.50	226.40	11.94	238.34
181	1123	B	25	X	6	1.50	227.90	11.94	239.84
181	1123	B	25	X	7	0.38	229.40	11.94	241.34
181	1123	B	25	X	CC	0.32	229.78	11.94	241.72
181	1123	B	26	X	1	1.50	230.00	11.94	241.94
181	1123	B	26	X	2	1.50	231.50	11.94	243.44
181	1123	B	26	X	3	0.86	233.00	11.94	244.94
181	1123	B	26	X	CC	0.32	233.86	11.94	245.80
181	1123	B	27	X	1	1.50	239.60	11.94	251.54
181	1123	B	27	X	2	1.50	241.10	11.94	253.04
181	1123	B	27	X	3	1.50	242.60	11.94	254.54
181	1123	B	27	X	4	1.50	244.10	11.94	256.04
181	1123	B	27	X	5	1.50	245.60	11.94	257.54
181	1123	B	27	X	6	1.50	247.10	11.94	259.04
181	1123	B	27	X	7	0.46	248.60	11.94	260.54
181	1123	B	27	X	CC	0.36	249.06	11.94	261.00
181	1123	B	28	X	1	1.50	249.20	11.94	261.14
181	1123	B	28	X	2	1.50	250.70	11.94	262.64
181	1123	B	28	X	3	1.50	252.20	11.94	264.14
181	1123	B	28	X	4	1.50	253.70	11.94	265.64
181	1123	B	28	X	5	1.50	255.20	11.94	267.14
181	1123	B	28	X	6	1.50	256.70	11.94	268.64
181	1123	B	28	X	7	0.36	258.20	11.94	270.14
181	1123	B	28	X	CC	0.23	258.56	11.94	270.50
181	1123	B	29	X	1	1.50	258.80	11.94	270.74
181	1123	B	29	X	2	1.50	260.30	11.94	272.24
181	1123	B	29	X	3	1.50	261.80	11.94	273.74

Table T12 (continued).

Leg	Site	Hole	Core	Type	Section	Section length	Depth (mbsf)	Offset	Composite depth (mcd)
181	1123	B	29	X	4	1.50	263.30	11.94	275.24
181	1123	B	29	X	5	1.50	264.80	11.94	276.74
181	1123	B	29	X	6	1.50	266.30	11.94	278.24
181	1123	B	29	X	7	0.42	267.80	11.94	279.74
181	1123	B	29	X	CC	0.37	268.22	11.94	280.16
181	1123	B	30	X	1	1.50	268.40	11.94	280.34
181	1123	B	30	X	2	1.50	269.90	11.94	281.84
181	1123	B	30	X	3	1.50	271.40	11.94	283.34
181	1123	B	30	X	4	1.50	272.90	11.94	284.84
181	1123	B	30	X	5	1.50	274.40	11.94	286.34
181	1123	B	30	X	6	1.50	275.90	11.94	287.84
181	1123	B	30	X	7	0.35	277.40	11.94	289.34
181	1123	B	30	X	CC	0.30	277.75	11.94	289.69
181	1123	B	31	X	1	1.50	278.10	11.94	290.04
181	1123	B	31	X	2	1.50	279.60	11.94	291.54
181	1123	B	31	X	3	1.50	281.10	11.94	293.04
181	1123	B	31	X	4	1.50	282.60	11.94	294.54
181	1123	B	31	X	5	1.50	284.10	11.94	296.04
181	1123	B	31	X	6	1.50	285.60	11.94	297.54
181	1123	B	31	X	7	0.27	287.10	11.94	299.04
181	1123	B	31	X	CC	0.22	287.37	11.94	299.31
181	1123	B	32	X	1	1.50	287.70	11.94	299.64
181	1123	B	32	X	2	1.50	289.20	11.94	301.14
181	1123	B	32	X	3	1.50	290.70	11.94	302.64
181	1123	B	32	X	4	1.50	292.20	11.94	304.14
181	1123	B	32	X	5	1.50	293.70	11.94	305.64
181	1123	B	32	X	6	0.88	295.20	11.94	307.14
181	1123	B	32	X	CC	0.33	296.08	11.94	308.02
181	1123	B	33	X	1	1.50	297.30	11.94	309.24
181	1123	B	33	X	2	1.50	298.80	11.94	310.74
181	1123	B	33	X	3	1.50	300.30	11.94	312.24
181	1123	B	33	X	4	1.50	301.80	11.94	313.74
181	1123	B	33	X	5	1.50	303.30	11.94	315.24
181	1123	B	33	X	6	1.50	304.80	11.94	316.74
181	1123	B	33	X	7	0.40	306.30	11.94	318.24
181	1123	B	33	X	CC	0.25	306.70	11.94	318.64
181	1123	B	34	X	1	1.50	306.90	11.94	318.84
181	1123	B	34	X	2	1.50	308.40	11.94	320.34
181	1123	B	34	X	3	1.50	309.90	11.94	321.84
181	1123	B	34	X	4	1.50	311.40	11.94	323.34
181	1123	B	34	X	5	1.50	312.90	11.94	324.84
181	1123	B	34	X	6	1.50	314.40	11.94	326.34
181	1123	B	34	X	7	0.44	315.90	11.94	327.84
181	1123	B	34	X	CC	0.34	316.34	11.94	328.28
181	1123	B	35	X	1	1.50	316.50	11.94	328.44
181	1123	B	35	X	2	1.50	318.00	11.94	329.94
181	1123	B	35	X	3	1.50	319.50	11.94	331.44
181	1123	B	35	X	4	1.50	321.00	11.94	332.94
181	1123	B	35	X	5	1.50	322.50	11.94	334.44
181	1123	B	35	X	6	1.50	324.00	11.94	335.94
181	1123	B	35	X	7	0.43	325.50	11.94	337.44
181	1123	B	35	X	CC	0.19	325.93	11.94	337.87
181	1123	B	36	X	1	1.50	325.90	11.94	337.84
181	1123	B	36	X	2	1.50	327.40	11.94	339.34
181	1123	B	36	X	3	1.50	328.90	11.94	340.84
181	1123	B	36	X	4	1.50	330.40	11.94	342.34
181	1123	B	36	X	5	1.50	331.90	11.94	343.84
181	1123	B	36	X	6	1.50	333.40	11.94	345.34
181	1123	B	36	X	7	0.44	334.90	11.94	346.84
181	1123	B	36	X	CC	0.23	335.34	11.94	347.28
181	1123	B	37	X	1	1.50	335.50	11.94	347.44
181	1123	B	37	X	2	1.50	337.00	11.94	348.94
181	1123	B	37	X	3	1.50	338.50	11.94	350.44
181	1123	B	37	X	4	1.50	340.00	11.94	351.94
181	1123	B	37	X	5	1.50	341.50	11.94	353.44
181	1123	B	37	X	6	1.50	343.00	11.94	354.94
181	1123	B	37	X	7	0.48	344.50	11.94	356.44
181	1123	B	37	X	CC	0.32	344.98	11.94	356.92

Table T12 (continued).

Leg	Site	Hole	Core	Type	Section	Section length	Depth (mbsf)	Offset	Composite depth (mcd)
181	1123	B	38	X	1	1.50	345.10	11.94	357.04
181	1123	B	38	X	2	1.50	346.60	11.94	358.54
181	1123	B	38	X	3	1.50	348.10	11.94	360.04
181	1123	B	38	X	4	1.50	349.60	11.94	361.54
181	1123	B	38	X	5	1.50	351.10	11.94	363.04
181	1123	B	38	X	6	1.50	352.60	11.94	364.54
181	1123	B	38	X	7	0.38	354.10	11.94	366.04
181	1123	B	38	X	CC	0.41	354.48	11.94	366.42
181	1123	B	39	X	1	1.50	354.70	11.94	366.64
181	1123	B	39	X	2	1.50	356.20	11.94	368.14
181	1123	B	39	X	3	1.50	357.70	11.94	369.64
181	1123	B	39	X	4	1.50	359.20	11.94	371.14
181	1123	B	39	X	5	1.50	360.70	11.94	372.64
181	1123	B	39	X	6	1.50	362.20	11.94	374.14
181	1123	B	39	X	7	0.49	363.70	11.94	375.64
181	1123	B	39	X	CC	0.39	364.19	11.94	376.13
181	1123	B	40	X	1	1.50	364.40	11.94	376.34
181	1123	B	40	X	2	1.50	365.90	11.94	377.84
181	1123	B	40	X	3	1.50	367.40	11.94	379.34
181	1123	B	40	X	4	1.50	368.90	11.94	380.84
181	1123	B	40	X	5	1.50	370.40	11.94	382.34
181	1123	B	40	X	6	1.50	371.90	11.94	383.84
181	1123	B	40	X	7	0.44	373.40	11.94	385.34
181	1123	B	40	X	CC	0.32	373.84	11.94	385.78
181	1123	B	41	X	1	1.50	374.10	11.94	386.04
181	1123	B	41	X	2	1.50	375.60	11.94	387.54
181	1123	B	41	X	3	1.50	377.10	11.94	389.04
181	1123	B	41	X	4	1.50	378.60	11.94	390.54
181	1123	B	41	X	5	1.50	380.10	11.94	392.04
181	1123	B	41	X	6	0.32	381.60	11.94	393.54
181	1123	B	41	X	CC	0.38	381.92	11.94	393.86
181	1123	B	42	X	1	1.50	383.70	11.94	395.64
181	1123	B	42	X	2	1.50	385.20	11.94	397.14
181	1123	B	42	X	3	1.50	386.70	11.94	398.64
181	1123	B	42	X	CC	0.34	388.20	11.94	400.14
181	1123	B	43	X	1	1.50	393.40	11.94	405.34
181	1123	B	43	X	2	1.50	394.90	11.94	406.84
181	1123	B	43	X	3	1.50	396.40	11.94	408.34
181	1123	B	43	X	4	1.48	397.90	11.94	409.84
181	1123	B	43	X	CC	0.24	399.38	11.94	411.32
181	1123	B	44	X	1	1.50	403.00	11.94	414.94
181	1123	B	44	X	2	1.50	404.50	11.94	416.44
181	1123	B	44	X	3	1.50	406.00	11.94	417.94
181	1123	B	44	X	4	0.62	407.50	11.94	419.44
181	1123	B	44	X	CC	0.30	408.12	11.94	420.06
181	1123	B	45	X	1	1.50	412.60	11.94	424.54
181	1123	B	45	X	2	1.50	414.10	11.94	426.04
181	1123	B	45	X	3	0.78	415.60	11.94	427.54
181	1123	B	45	X	CC	0.28	416.38	11.94	428.32
181	1123	B	46	X	1	1.50	422.20	11.94	434.14
181	1123	B	46	X	2	1.50	423.70	11.94	435.64
181	1123	B	46	X	3	1.50	425.20	11.94	437.14
181	1123	B	46	X	4	1.46	426.70	11.94	438.64
181	1123	B	46	X	CC	0.25	428.16	11.94	440.10
181	1123	B	47	X	1	1.50	431.80	11.94	443.74
181	1123	B	47	X	2	1.50	433.30	11.94	445.24
181	1123	B	47	X	3	1.50	434.80	11.94	446.74
181	1123	B	47	X	4	0.66	436.30	11.94	448.24
181	1123	B	47	X	CC	0.10	436.96	11.94	448.90
181	1123	B	48	X	1	1.50	441.50	11.94	453.44
181	1123	B	48	X	2	1.50	443.00	11.94	454.94
181	1123	B	48	X	3	1.10	444.50	11.94	456.44
181	1123	B	48	X	CC	0.15	445.60	11.94	457.54
181	1123	B	49	X	1	1.50	450.80	11.94	462.74
181	1123	B	49	X	2	1.50	452.30	11.94	464.24
181	1123	B	49	X	3	1.50	453.80	11.94	465.74
181	1123	B	49	X	4	1.50	455.30	11.94	467.24
181	1123	B	49	X	CC	0.41	456.80	11.94	468.74

Table T12 (continued).

Leg	Site	Hole	Core	Type	Section	Section length	Depth (mbsf)	Offset	Composite depth (mcd)
181	1123	B	50	X	1	1.50	460.40	11.94	472.34
181	1123	B	50	X	2	1.50	461.90	11.94	473.84
181	1123	B	50	X	3	1.50	463.40	11.94	475.34
181	1123	B	50	X	4	1.50	464.90	11.94	476.84
181	1123	B	50	X	5	1.50	466.40	11.94	478.34
181	1123	B	50	X	6	0.31	467.90	11.94	479.84
181	1123	B	50	X	CC	0.54	468.21	11.94	480.15
181	1123	B	51	X	1	1.50	470.00	11.94	481.94
181	1123	B	51	X	2	1.50	471.50	11.94	483.44
181	1123	B	51	X	3	1.50	473.00	11.94	484.94
181	1123	B	51	X	4	1.50	474.50	11.94	486.44
181	1123	B	51	X	5	1.50	476.00	11.94	487.94
181	1123	B	51	X	6	1.50	477.50	11.94	489.44
181	1123	B	51	X	7	0.45	479.00	11.94	490.94
181	1123	B	51	X	CC	0.27	479.45	11.94	491.39
181	1123	B	52	X	1	1.50	479.30	11.94	491.24
181	1123	B	52	X	2	1.50	480.80	11.94	492.74
181	1123	B	52	X	3	1.50	482.30	11.94	494.24
181	1123	B	52	X	4	1.50	483.80	11.94	495.74
181	1123	B	52	X	5	1.50	485.30	11.94	497.24
181	1123	B	52	X	6	1.50	486.80	11.94	498.74
181	1123	B	52	X	CC	0.36	488.30	11.94	500.24
181	1123	C	1	H	1	1.50	0.00	0.00	0.00
181	1123	C	1	H	2	1.50	1.50	0.00	1.50
181	1123	C	1	H	3	1.50	3.00	0.00	3.00
181	1123	C	1	H	4	1.50	4.50	0.00	4.50
181	1123	C	1	H	5	1.50	6.00	0.00	6.00
181	1123	C	1	H	6	1.42	7.50	0.00	7.50
181	1123	C	1	H	CC	0.10	8.92	0.00	8.92
181	1123	C	2	H	1	1.50	9.00	-0.28	8.72
181	1123	C	2	H	2	1.50	10.50	-0.28	10.22
181	1123	C	2	H	3	1.50	12.00	-0.28	11.72
181	1123	C	2	H	4	1.50	13.50	-0.28	13.22
181	1123	C	2	H	5	1.50	15.00	-0.28	14.72
181	1123	C	2	H	6	1.50	16.50	-0.28	16.22
181	1123	C	2	H	7	0.43	18.00	-0.28	17.72
181	1123	C	2	H	CC	0.10	18.43	-0.28	18.15
181	1123	C	3	H	1	1.50	18.50	0.80	19.30
181	1123	C	3	H	2	1.50	20.00	0.80	20.80
181	1123	C	3	H	3	1.50	21.50	0.80	22.30
181	1123	C	3	H	4	1.50	23.00	0.80	23.80
181	1123	C	3	H	5	1.50	24.50	0.80	25.30
181	1123	C	3	H	6	1.50	26.00	0.80	26.80
181	1123	C	3	H	7	0.61	27.50	0.80	28.30
181	1123	C	3	H	CC	0.18	28.11	0.80	28.91
181	1123	C	4	H	1	1.50	28.00	0.72	28.72
181	1123	C	4	H	2	1.50	29.50	0.72	30.22
181	1123	C	4	H	3	1.50	31.00	0.72	31.72
181	1123	C	4	H	4	1.50	32.50	0.72	33.22
181	1123	C	4	H	5	1.50	34.00	0.72	34.72
181	1123	C	4	H	6	1.50	35.50	0.72	36.22
181	1123	C	4	H	7	0.43	37.00	0.72	37.72
181	1123	C	4	H	CC	0.16	37.43	0.72	38.15
181	1123	C	5	H	1	1.50	37.50	-0.86	36.64
181	1123	C	5	H	2	1.50	39.00	-0.86	38.14
181	1123	C	5	H	3	1.50	40.50	-0.86	39.64
181	1123	C	5	H	4	1.50	42.00	-0.86	41.14
181	1123	C	5	H	5	1.50	43.50	-0.86	42.64
181	1123	C	5	H	6	1.20	45.00	-0.86	44.14
181	1123	C	5	H	CC	0.15	46.20	-0.86	45.34
181	1123	C	6	H	1	1.50	47.00	-0.14	46.86
181	1123	C	6	H	2	1.50	48.50	-0.14	48.36
181	1123	C	6	H	3	1.50	50.00	-0.14	49.86
181	1123	C	6	H	4	1.50	51.50	-0.14	51.36
181	1123	C	6	H	5	1.50	53.00	-0.14	52.86
181	1123	C	6	H	6	1.50	54.50	-0.14	54.36
181	1123	C	6	H	7	0.67	56.00	-0.14	55.86
181	1123	C	6	H	CC	0.24	56.67	-0.14	56.53

Table T12 (continued).

Leg	Site	Hole	Core	Type	Section	Section length	Depth (mbsf)	Offset	Composite depth (mcd)
181	1123	C	7	H	1	1.50	56.50	0.98	57.48
181	1123	C	7	H	2	1.50	58.00	0.98	58.98
181	1123	C	7	H	3	1.50	59.50	0.98	60.48
181	1123	C	7	H	4	1.50	61.00	0.98	61.98
181	1123	C	7	H	5	1.50	62.50	0.98	63.48
181	1123	C	7	H	6	1.50	64.00	0.98	64.98
181	1123	C	7	H	7	0.65	65.50	0.98	66.48
181	1123	C	7	H	CC	0.20	66.15	0.98	67.13
181	1123	C	8	H	1	1.50	66.00	1.72	67.72
181	1123	C	8	H	2	1.50	67.50	1.72	69.22
181	1123	C	8	H	3	1.50	69.00	1.72	70.72
181	1123	C	8	H	4	1.50	70.50	1.72	72.22
181	1123	C	8	H	5	1.50	72.00	1.72	73.72
181	1123	C	8	H	6	1.50	73.50	1.72	75.22
181	1123	C	8	H	7	0.64	75.00	1.72	76.72
181	1123	C	8	H	CC	0.18	75.64	1.72	77.36
181	1123	C	9	H	1	1.50	75.50	2.72	78.22
181	1123	C	9	H	2	1.50	77.00	2.72	79.72
181	1123	C	9	H	3	1.50	78.50	2.72	81.22
181	1123	C	9	H	4	1.50	80.00	2.72	82.72
181	1123	C	9	H	5	1.50	81.50	2.72	84.22
181	1123	C	9	H	6	1.10	83.00	2.72	85.72
181	1123	C	9	H	CC	0.05	84.10	2.72	86.82
181	1123	C	10	H	1	1.50	85.00	3.48	88.48
181	1123	C	10	H	2	1.50	86.50	3.48	89.98
181	1123	C	10	H	3	1.50	88.00	3.48	91.48
181	1123	C	10	H	4	1.50	89.50	3.48	92.98
181	1123	C	10	H	5	1.50	91.00	3.48	94.48
181	1123	C	10	H	6	1.50	92.50	3.48	95.98
181	1123	C	10	H	7	0.79	94.00	3.48	97.48
181	1123	C	10	H	CC	0.15	94.79	3.48	98.27
181	1123	C	11	H	1	1.50	94.50	5.66	100.16
181	1123	C	11	H	2	1.50	96.00	5.66	101.66
181	1123	C	11	H	3	1.50	97.50	5.66	103.16
181	1123	C	11	H	4	1.50	99.00	5.66	104.66
181	1123	C	11	H	5	1.50	100.50	5.66	106.16
181	1123	C	11	H	6	1.50	102.00	5.66	107.66
181	1123	C	11	H	7	0.55	103.50	5.66	109.16
181	1123	C	11	H	CC	0.16	104.05	5.66	109.71
181	1123	C	12	H	1	1.50	104.00	5.04	109.04
181	1123	C	12	H	2	1.50	105.50	5.04	110.54
181	1123	C	12	H	3	1.50	107.00	5.04	112.04
181	1123	C	12	H	4	1.50	108.50	5.04	113.54
181	1123	C	12	H	5	1.50	110.00	5.04	115.04
181	1123	C	12	H	6	1.50	111.50	5.04	116.54
181	1123	C	12	H	7	0.63	113.00	5.04	118.04
181	1123	C	12	H	CC	0.24	113.63	5.04	118.67
181	1123	C	13	H	1	1.50	113.50	6.68	120.18
181	1123	C	13	H	2	1.50	115.00	6.68	121.68
181	1123	C	13	H	3	1.50	116.50	6.68	123.18
181	1123	C	13	H	4	1.50	118.00	6.68	124.68
181	1123	C	13	H	5	1.50	119.50	6.68	126.18
181	1123	C	13	H	6	1.50	121.00	6.68	127.68
181	1123	C	13	H	7	0.50	122.50	6.68	129.18
181	1123	C	13	H	CC	0.24	123.00	6.68	129.68
181	1123	C	14	H	1	1.50	123.00	7.78	130.78
181	1123	C	14	H	2	1.50	124.50	7.78	132.28
181	1123	C	14	H	3	1.50	126.00	7.78	133.78
181	1123	C	14	H	4	1.50	127.50	7.78	135.28
181	1123	C	14	H	5	1.50	129.00	7.78	136.78
181	1123	C	14	H	6	1.50	130.50	7.78	138.28
181	1123	C	14	H	7	0.73	132.00	7.78	139.78
181	1123	C	14	H	CC	0.32	132.73	7.78	140.51
181	1123	C	15	H	1	0.97	132.50	8.75	141.25
181	1123	C	15	H	2	1.50	133.47	8.75	142.22
181	1123	C	15	H	3	1.50	134.97	8.75	143.72
181	1123	C	15	H	4	1.50	136.47	8.75	145.22
181	1123	C	15	H	5	1.50	137.97	8.75	146.72

Table T12 (continued).

Leg	Site	Hole	Core	Type	Section	Section length	Depth (mbsf)	Offset	Composite depth (mcd)
181	1123	C	15	H	6	1.50	139.47	8.75	148.22
181	1123	C	15	H	7	0.78	140.97	8.75	149.72
181	1123	C	15	H	CC	0.34	141.75	8.75	150.50
181	1123	C	16	H	1	1.50	142.00	10.56	152.56
181	1123	C	16	H	2	1.50	143.50	10.56	154.06
181	1123	C	16	H	3	1.50	145.00	10.56	155.56
181	1123	C	16	H	4	1.50	146.50	10.56	157.06
181	1123	C	16	H	5	1.50	148.00	10.56	158.56
181	1123	C	16	H	6	1.50	149.50	10.56	160.06
181	1123	C	16	H	7	0.52	151.00	10.56	161.56
181	1123	C	16	H	CC	0.27	151.52	10.56	162.08
181	1123	C	17	X	1	1.50	230.00	10.56	240.56
181	1123	C	17	X	2	1.50	231.50	10.56	242.06
181	1123	C	17	X	3	1.50	233.00	10.56	243.56
181	1123	C	17	X	4	1.50	234.50	10.56	245.06
181	1123	C	17	X	CC	0.39	236.00	10.56	246.56
181	1123	C	18	X	1	1.50	484.00	8.70	492.70
181	1123	C	18	X	2	1.50	485.50	8.70	494.20
181	1123	C	18	X	3	1.50	487.00	8.70	495.70
181	1123	C	18	X	CC	0.45	488.50	8.70	497.20
181	1123	C	19	X	1	1.50	488.50	9.56	498.06
181	1123	C	19	X	2	1.50	490.00	9.56	499.56
181	1123	C	19	X	3	1.50	491.50	9.56	501.06
181	1123	C	19	X	4	1.50	493.00	9.56	502.56
181	1123	C	19	X	5	1.50	494.50	9.56	504.06
181	1123	C	19	X	6	1.50	496.00	9.56	505.56
181	1123	C	19	X	7	0.35	497.50	9.56	507.06
181	1123	C	19	X	CC	0.35	497.85	9.56	507.41
181	1123	C	20	X	1	1.50	498.10	9.56	507.66
181	1123	C	20	X	2	1.50	499.60	9.56	509.16
181	1123	C	20	X	3	1.50	501.10	9.56	510.66
181	1123	C	20	X	4	1.50	502.60	9.56	512.16
181	1123	C	20	X	5	1.50	504.10	9.56	513.66
181	1123	C	20	X	6	0.79	505.60	9.56	515.16
181	1123	C	20	X	CC	0.15	506.39	9.56	515.95
181	1123	C	21	X	1	1.50	507.70	9.56	517.26
181	1123	C	21	X	2	1.50	509.20	9.56	518.76
181	1123	C	21	X	3	1.50	510.70	9.56	520.26
181	1123	C	21	X	4	1.50	512.20	9.56	521.76
181	1123	C	21	X	5	1.50	513.70	9.56	523.26
181	1123	C	21	X	6	1.50	515.20	9.56	524.76
181	1123	C	21	X	7	0.26	516.70	9.56	526.26
181	1123	C	21	X	CC	0.15	516.96	9.56	526.52
181	1123	C	22	X	1	1.50	517.40	9.56	526.96
181	1123	C	22	X	2	1.50	518.90	9.56	528.46
181	1123	C	22	X	3	1.50	520.40	9.56	529.96
181	1123	C	22	X	4	1.50	521.90	9.56	531.46
181	1123	C	22	X	5	1.50	523.40	9.56	532.96
181	1123	C	22	X	6	1.50	524.90	9.56	534.46
181	1123	C	22	X	7	0.43	526.40	9.56	535.96
181	1123	C	22	X	CC	0.38	526.83	9.56	536.39
181	1123	C	23	X	1	1.50	527.00	9.56	536.56
181	1123	C	23	X	2	1.50	528.50	9.56	538.06
181	1123	C	23	X	3	1.50	530.00	9.56	539.56
181	1123	C	23	X	4	1.50	531.50	9.56	541.06
181	1123	C	23	X	5	1.50	533.00	9.56	542.56
181	1123	C	23	X	6	1.50	534.50	9.56	544.06
181	1123	C	23	X	7	0.43	536.00	9.56	545.56
181	1123	C	23	X	CC	0.38	536.43	9.56	545.99
181	1123	C	24	X	1	1.50	536.60	9.56	546.16
181	1123	C	24	X	2	1.50	538.10	9.56	547.66
181	1123	C	24	X	3	1.50	539.60	9.56	549.16
181	1123	C	24	X	4	1.50	541.10	9.56	550.66
181	1123	C	24	X	5	1.50	542.60	9.56	552.16
181	1123	C	24	X	6	1.50	544.10	9.56	553.66
181	1123	C	24	X	7	0.41	545.60	9.56	555.16
181	1123	C	24	X	CC	0.35	546.01	9.56	555.57
181	1123	C	25	X	1	1.50	546.20	9.56	555.76

Table T12 (continued).

Leg	Site	Hole	Core	Type	Section	Section length	Depth (mbsf)	Offset	Composite depth (mcd)
181	1123	C	25	X	2	1.50	547.70	9.56	557.26
181	1123	C	25	X	3	1.50	549.20	9.56	558.76
181	1123	C	25	X	4	1.50	550.70	9.56	560.26
181	1123	C	25	X	5	1.50	552.20	9.56	561.76
181	1123	C	25	X	6	1.50	553.70	9.56	563.26
181	1123	C	25	X	7	0.40	555.20	9.56	564.76
181	1123	C	25	X	CC	0.26	555.60	9.56	565.16
181	1123	C	26	X	1	1.50	555.70	9.56	565.26
181	1123	C	26	X	2	1.50	557.20	9.56	566.76
181	1123	C	26	X	3	1.50	558.70	9.56	568.26
181	1123	C	26	X	4	1.50	560.20	9.56	569.76
181	1123	C	26	X	5	1.50	561.70	9.56	571.26
181	1123	C	26	X	6	1.50	563.20	9.56	572.76
181	1123	C	26	X	7	0.36	564.70	9.56	574.26
181	1123	C	26	X	CC	0.31	565.06	9.56	574.62
181	1123	C	27	X	1	1.50	565.40	9.56	574.96
181	1123	C	27	X	2	1.50	566.90	9.56	576.46
181	1123	C	27	X	3	1.50	568.40	9.56	577.96
181	1123	C	27	X	4	1.50	569.90	9.56	579.46
181	1123	C	27	X	5	1.50	571.40	9.56	580.96
181	1123	C	27	X	6	1.50	572.90	9.56	582.46
181	1123	C	27	X	7	0.32	574.40	9.56	583.96
181	1123	C	27	X	CC	0.34	574.72	9.56	584.28
181	1123	C	28	X	1	1.50	575.10	9.56	584.66
181	1123	C	28	X	2	1.50	576.60	9.56	586.16
181	1123	C	28	X	3	1.50	578.10	9.56	587.66
181	1123	C	28	X	4	1.50	579.60	9.56	589.16
181	1123	C	28	X	5	1.50	581.10	9.56	590.66
181	1123	C	28	X	6	1.13	582.60	9.56	592.16
181	1123	C	28	X	CC	0.15	583.73	9.56	593.29
181	1123	C	29	X	1	1.50	584.70	9.56	594.26
181	1123	C	29	X	2	1.50	586.20	9.56	595.76
181	1123	C	29	X	3	1.50	587.70	9.56	597.26
181	1123	C	29	X	4	1.50	589.20	9.56	598.76
181	1123	C	29	X	5	1.50	590.70	9.56	600.26
181	1123	C	29	X	6	0.82	592.20	9.56	601.76
181	1123	C	29	X	CC	0.39	593.02	9.56	602.58
181	1123	C	30	X	1	1.50	594.30	9.56	603.86
181	1123	C	30	X	2	1.50	595.80	9.56	605.36
181	1123	C	30	X	3	1.50	597.30	9.56	606.86
181	1123	C	30	X	4	0.69	598.80	9.56	608.36
181	1123	C	30	X	CC	0.25	599.49	9.56	609.05
181	1123	C	31	X	1	1.50	603.90	9.56	613.46
181	1123	C	31	X	2	1.50	605.40	9.56	614.96
181	1123	C	31	X	3	1.50	606.90	9.56	616.46
181	1123	C	31	X	4	1.50	608.40	9.56	617.96
181	1123	C	31	X	5	1.18	609.90	9.56	619.46
181	1123	C	31	X	CC	0.10	611.08	9.56	620.64
181	1123	C	32	X	1	1.50	613.60	9.56	623.16
181	1123	C	32	X	2	1.50	615.10	9.56	624.66
181	1123	C	32	X	3	1.50	616.60	9.56	626.16
181	1123	C	32	X	4	0.58	618.10	9.56	627.66
181	1123	C	32	X	CC	0.53	618.68	9.56	628.24
181	1123	C	33	X	1	1.35	623.20	9.56	632.76
181	1123	C	33	X	2	0.96	624.55	9.56	634.11
181	1123	C	33	X	CC	0.35	625.51	9.56	635.07

Note: This table is also available in **ASCII format.**

Table T13. Splice tie points, Site 1123.

Site	Hole	Core	Type	Section	Depth in section (cm)	Depth (mbsf)	Depth (mcd)		Site	Hole	Core	Type	Section	Depth in section (cm)	Depth (mbsf)	Depth (mcd)
1123	C	1	H	5	112.0	7.12	7.12	Tie to	1123	B	2	H	3	146.0	7.86	7.12
1123	B	2	H	6	92.0	11.82	11.08	Tie to	1123	C	2	H	2	86.0	11.36	11.08
1123	C	2	H	5	100.0	16.00	15.72	Tie to	1123	B	3	H	1	109.0	14.00	15.72
1123	B	3	H	6	88.0	21.28	23.00	Tie to	1123	C	3	H	3	70.0	22.20	23.00
1123	C	3	H	6	36.0	26.36	27.16	Tie to	1123	B	4	H	3	104.0	26.44	27.16
1123	B	4	H	5	132.0	29.72	30.44	Tie to	1123	C	4	H	2	22.0	29.72	30.44
1123	C	4	H	6	120.0	36.70	37.42	Tie to	1123	B	5	H	1	144.0	33.34	37.42
1123	B	5	H	4	140.0	37.80	40.70	Tie to	1123	C	5	H	3	106.0	41.56	40.70
1123	C	5	H	6	20.0	45.20	44.34	Tie to	1123	B	6	H	1	134.0	42.74	44.34
1123	B	6	H	4	60.0	46.50	48.10	Tie to	1123	C	6	H	1	124.0	48.24	48.10
1123	C	6	H	6	144.0	55.94	55.80	Tie to	1123	B	7	H	2	8.0	52.48	55.80
1123	B	7	H	5	96.0	57.86	61.18	Tie to	1123	C	7	H	3	70.0	60.20	61.18
1123	C	7	H	6	68.0	64.68	65.66	Tie to	1123	B	8	H	2	65.0	62.56	65.66
1123	B	8	H	5	24.0	66.64	69.74	Tie to	1123	C	8	H	2	52.0	68.02	69.74
1123	C	8	H	6	144.0	74.94	76.66	Tie to	1123	B	9	H	2	80.0	72.20	76.66
1123	B	9	H	5	68.0	76.58	81.04	Tie to	1123	C	9	H	2	132.0	78.32	81.04
1123	C	9	H	6	12.0	83.12	85.84	Tie to	1123	B	10	H	2	12.0	81.02	85.84
1123	B	10	H	6	44.0	87.34	92.16	Tie to	1123	C	10	H	3	68.0	88.68	92.16
1123	C	10	H	7	4.0	94.04	97.52	Tie to	1123	B	11	H	3	52.0	92.42	97.52
1123	B	11	H	6	28.0	96.68	101.78	Tie to	1123	C	11	H	2	12.0	96.12	101.78
1123	C	11	H	5	124.0	101.74	107.40	Tie to	1123	B	12	H	2	56.0	100.46	107.40
1123	B	12	H	5	104.0	105.44	112.38	Tie to	1123	C	12	H	3	34.0	107.34	112.38
1123	C	12	H	5	134.0	111.34	116.38	Tie to	1123	B	13	H	1	132.0	109.22	116.38
1123	B	13	H	5	76.0	114.66	121.82	Tie to	1123	C	13	H	2	13.0	115.14	121.82
1123	C	13	H	6	68.0	121.68	128.36	Tie to	1123	B	14	H	2	86.0	119.76	128.36
1123	B	14	H	5	88.0	124.28	132.88	Tie to	1123	C	14	H	2	60.0	125.10	132.88
1123	C	14	H	6	104.0	131.54	139.32	Tie to	1123	B	15	H	2	104.0	129.44	139.32
1123	B	15	H	5	116.0	134.12	144.00	Tie to	1123	C	15	H	3	28.0	135.25	144.00
1123	C	15	H	7	20.0	141.17	149.92	Tie to	1123	B	16	H	1	150.0	137.90	149.92
1123	B	16	H	5	136.0	143.76	155.78	Tie to	1123	C	16	H	3	22.0	145.22	155.78
1123	C	16	H	5	70.0	148.70	159.26	Tie to	1123	B	17	H	1	142.0	147.32	159.26
1123	B	17	H	7	36.0	155.26	167.20									

Note: This table is also available in **ASCII format.**

Table T14. Translation to stretched mbsf and mcd scales.

181 Core	Slope (*m*)	Intercept (*b*)	Offset (*M*)
1123B-23X	1.2703	–54.40	11.94
1123B-26X	2.5000	–345.06	11.94
1123B-41X	1.2703	–101.13	11.94
1123B-42X	2.1364	–436.08	11.94
1123B-43X	1.5932	–233.39	11.94
1123B-44X	1.8725	–351.65	11.94
1123B-45X	2.5543	–641.37	11.94
1123B-46X	1.6041	–255.07	11.94
1123B-47X	1.8577	–370.39	11.94
1123B-48X	2.3737	–606.60	11.94
1123B-49X	1.6491	–292.78	11.94
1123B-50X	1.2208	–101.66	11.94
1123C-20X	1.1491	–74.27	9.56

Notes: For each core listed, this table gives a slope (*m*) and intercept (*b*) for a linear transformation from reported mbsf to stretched mbsf. Stretched mbsf = (*m* x mbsf) + *b*. For example, to translate a sample from 181-1123B-43X-4, 96 cm, at 398.86 mbsf onto stretched mbsf: (398.86 x 1.5932) – 233.39 = 402.07 stretched mbsf. To subsequently translate a sample to stretched mcd, add the offset in the last column of this table. Stretched mcd for the above example is 414.01 stretched mcd. Note that this table does not include a direct translation between mcd and stretched mcd.

Table T15. Biostratigraphic events identified at Site 1123, using shipboard analysis data. (See table note. Continued on next page.)

	Events	Group	Figure 29	Age (Ma)	Sample	Depth (mbsf)	Depth (mcd)
1	FO *Globorotalia hirsuta*	F		~0.45	1123B-1H-1, 18–20 cm	0.18	0.18
2	Bottom acme of *Emiliania huxleyi*	N		0.09	1123A-1H-2, 145 cm	1.57	1.57
3	FO *Emiliania huxleyi*	N		0.24	1123A-1H-4, 75 cm	5.25	5.25
4	Base of acme *Hemidiscus karstenii*	D	26	0.42	1123B-2H-CC	12.85	12.11
5	LO *Globorotalia puncticuloides*	F		~0.6	1123B-2H-CC	15.60	15.36
6	LCO *Globorotalia puncticuloides*	F		~0.7	1123A-3H-CC	23.31	23.07
7	LO *Stylatractus universus*	R		0.46	1123A-3H-CC	23.31	23.07
8	LO *Pseudoumbilica lacunosa*	N	31	0.42	1123A-3H-CC	23.31	23.07
9	LO *Nitzschia reinholdii*	D	27	0.65	1123B-3H-CC	22.74	24.46
10	FO *Globorotalia truncatulinoides*	F		~0.8	1123A-5H-CC	44.29	44.15
11	FO *Theocorythium trachelium*	R		1.6–1.7	1123A-7H-CC	63.15	65.85
12	LO *Eucyrtidium calvertense*	R		1.92	1123A-7H-CC	63.15	65.85
13	FO *Gephyrocapsa* (medium)	N		1.67	1123A-7H-CC	63.15	66.25
14	LO *Calcidiscus macintyrei*	N		1.6	1123A-8H-CC	72.07	75.87
15	FO *Globorotalia crassula*	F	1	2.6	1123A-9H-CC	72.00	75.80
16	LO *Globorotalia crassaformis* (dextral)	F	2	2.1	1123A-9H-CC	72.00	75.80
17	FO *Globorotalia tosaensis*	F		3.2	1123A-8H-CC	72.07	75.87
18	LO *Theocorythium vetulum*	R		1.2–1.3	1123A-8H-CC	72.07	75.87
19	LO *Thalassiosira convexa*	D		2.1	1123B-10H-CC	89.19	94.01
20	FO *Globorotalia crassaformis* (dextral)	F	3	3.0	1123A-10H-CC	91.93	97.83
21	LO *Lamprocyrtis heteroporos*	R		1.8	1123A-10H-CC	91.93	97.83
22	LO *Discoaster tamalis*	N	32	2.8	1123A-11H-CC	98.81	103.91
23	FO *Globorotalia puncticuloides*	F		3.4	1123A-11H-CC	101.24	107.32
24	LO *Globorotalia pliozea*	F		3.4	1123A-11H-CC	101.24	107.32
25	LO *Globorotalia crassaconica*	F	4	3.2	1123A-11H-CC	101.24	107.32
26	FO *Globorotalia inflata*	F		3.8	1123A-11H-CC	101.24	107.32
27	LO *Pterocanium prismatium*	R		1.7	1123A-11H-CC	101.24	107.32
28	FO *Globorotalia inflata triangula*	F		3.7	1123B-12H-CC	108.16	115.10
29	LCO *Stichocorys* group	R		4.2	1123A-12H-CC	110.76	117.42
30	LCO *Globorotalia pliozea*	F		3.7	1123A-12H-CC	110.86	117.52
31	LO *Globorotalia puncticulata*	F	5	3.8	1123A-12H-CC	110.86	117.52
32	FO *Cycladophora davisiana davisiana*	R		2.91–3.08	1123A-13H-CC	119.70	127.91
33	LO *Reticulofenestra pseudoumbilicus*	N	33	3.82	1123A-14H-CC	129.76	138.46
34	FO *Pseudoemiliania lacunosa*	N		4	1123A-14H-CC	129.76	139.15
35	LO *Stichocorys peregrina*	R		3.0	1123B-15H-CC	139.50	149.38
36	FO *Amphirhopalum ypsilon*	R		3.9	1123B-16H-CC	145.76	157.78
37	FO *Discoaster asymmetricus*	N	34	4.13	1123A-16H-CC	148.71	160.35
38	LO *Lychnodictyum audax*	R		3.7	1123B-17H-CC	155.63	167.57
39	FO *Globorotalia crassaconica*	F	6	4.7	1123B-18X-CC	163.79	175.73
40	FO *Sphaeroidinella dehiscens*	F		4.8	1123B-18X-CC	163.79	175.73
41	LO *Dictyophimus splendens*	R		5.0–5.2	1123B-19X-CC	172.31	184.25
42	FO *Globorotalia puncticulata*	F	8	5.2	1123B-19X-CC	172.31	184.25
43	LO *Globorotalia sphericomiozea*	F	9	5.2	1123B-20X-4, 83–87 cm	177.69	189.53
44	LO *Globorotalia juanai*	F		5.2	1123B-20X-CC	182.05	193.99
45	FO *Globorotalia pliozea*	F		5.4	1123B-20X-CC	182.05	193.99
46	LO *Globorotalia miotumida*	F		5.6	1123B-20X-CC	182.05	193.99
47	LO *Globorotalia mons*	F	7	4.8	1123B-21X-CC	191.37	203.31
48	FO *Globorotalia sphericomiozea*	F	10	5.6	1123B-21X-CC	191.37	203.31
49	LO *Lychnocanoma parallelipes*	R		5.6	1123B-21X-CC	191.37	203.31
50	FO *Sphaeropyle langii*	R		6.0–6.2	1123B-21X-CC	191.37	203.31
51	FO *Globorotalia juanai*	F		6.6	1123B-22X-CC	201.47	213.41
52	FO *Stylacontarium acquilonium*	R		7.88	1123B-22X-CC	201.47	213.41
53	LO *Discoaster quinqueramus*	N	35	5.56	1123B-24X-CC	220.55	232.49
54	FO *Sphaeroidinella paenedehiscens*	F		~8	1123B-27X-CC	249.42	261.36
55	LO *Bolboforma pentaspinosa*	F	11	7	1123B-27X-CC	249.42	261.36
56	FO *Lychnocanoma parallelipes*	R		6.8–7.3	1123B-29X-CC	268.50	280.53
57	Acme *Stichocorys peregrina*	R		6.8–7.3	1123B-29X-CC	268.50	280.53
58	FO *Nitzschia reinholdii*	D	28	7.2–7.3	1123B-29X-CC	268.59	280.53
59	FO *Discoaster quinqueramus*	N	36	8.3	1123B-30X-CC	278.05	289.99
60	LO *Minylitha convallis*	N		7.73	1123B-30X-CC	278.05	289.99
61	FO *Hemidiscus ovalis*	D	29	7.9	1123B-31X-CC	287.59	299.53
62	LO *Didymocyrtis antepenultima*	R		8.2	1123B-32X-CC	296.30	308.24
63	LO *Globoquadrina dehiscens*	F	14	9.9	1123B-35X-3, 132–134 cm	320.82	332.76
64	FO *Didymocyrtis antepenultima*	R		9.7	1123B-35X-CC	326.00	337.94
65	FO *Minylitha convallis*	N	37	9.34	1123B-35X-CC	330.74	342.68
66	FO *Neogloboquadrina pachyderma*	F	12	11.3	1123B-38X-CC	354.89	366.83
67	FO *Zeaglobigerina nepenthes*	F	13	11.8	1123B-38X-CC	354.89	366.83
68	LO *Zeaglobigerina druryi*	F	15	11.3	1123B-39X-CC	364.58	376.52

Table T15 (continued).

	Events	Group	Figure 29	Age (Ma)	Sample	Depth (mbsf)	Depth (mcd)
69	LO *Coccolithus miopelagicus*	N	38	10.9	1123B-40X-CC	374.16	386.10
70	LO *Cyrtocapsella japonica*	R		9.9	1123B-41X-CC	382.20	394.14
71	Acme *Cyrtocapsella japonica*	R		10.2	1123B-42X-CC	388.40	400.34
72	LO *Paragloborotalia mayeri*	F		11.25	1123B-43X-CC	399.62	411.56
73	LO *Neogloboquadrina continuosa*	F		11	1123B-43X-CC	399.62	411.56
74	*Nitzschia denticuloides*	D	30	11.3–13.5	1123B-43X-CC	399.62	411.56
75	LO *Calcidiscus premacintyrei*	N	39	12.65	1123B-43X-CC	399.62	411.56
76	LCO *Cyrtocapsella tetrapera*	R		12.6	1123B-44X-CC	408.30	420.24
77	LO *Globorotalia conica*	F		~ 11.5	1123B-45X-CC	416.66	428.60
78	FO *Paragloborotalia mayeri*	F		13.2	1123B-46X-CC	428.41	440.35
79	FO *Globorotalia miotumida*	F	16	13.2	1123B-46X-CC	428.41	440.35
80	FO *Orbulina suturalis*	F		15.1	1123B-46X-CC	428.41	440.35
81	LO *Globorotalia praemenardii*	F	17	13.2	1123B-47X-CC	437.06	449.00
82	FO *Globorotalia amuria*	F		~ 16	1123B-48X-CC	445.75	457.69
83	FO *Globorotalia panda*	F		15	1123B-48X-CC	445.75	457.69
84	FO *Cibicidoides wuellerstorfi*	F		16.4	1123B-49X-CC	457.21	469.15
85	LO *Sphenolithus heteromorphus*	N	40	13.57	1123B-49X-CC	457.21	469.15
86	FO *Globorotalia praemenardii*	F	18	15.8	1123B-50X-CC	468.60	480.54
87	LO *Globorotalia miozea*	F	19	15.8	1123B-51X-CC	479.72	491.66
88	LO *Catapsydrax stainforthi*	F	20	16.4	1123B-51X-CC	479.72	491.66
89	FO *Zeaglobigerina druryi*	F		17.4	1123B-52X-CC	488.60	500.54
90	FO *Eucyrtidium punctatum*	R		17.1	1123C-19X-CC	498.10	507.42
91	LO *Paragloborotalia bella*	F		16.3	1123C-19X-CC	498.10	507.42
92	FO *Calcidiscus premacintyrei*	N		17.4	1123C-20X-3, 147 cm	502.47	514.41
93	FO *Globorotalia miozea*	F		16.7	1123C-20X-CC	506.54	515.86
94	LO *Catapsydrax dissimilis*	F	23	17.3	1123C-20X-CC	506.39	515.86
95	FO *Sphaeroidinellopsis disjuncta*	F	21	18.5	1123C-21X-CC	517.11	526.43
96	FO *Globorotalia zealandica*	F	22	18.5	1123C-21X-CC	517.11	526.43
97	FO *Sphenolithus heteromorphus*	N	41	18.3	1123C-21X-CC	517.11	526.43
98	LO *Sphenolithus belemnos*	N	42	19.2	1123C-22X-6, 136 cm	526.26	538.20
99	LO *Globorotalia incognita*	F	24	18.6	1123C-23X-CC	536.70	546.02
100	FO *Cyrtocapsella tetrapera*	R		23.62	1123C-27X-CC	574.96	584.28
101	FO *Globorotalia incognita*	F	25	21.6	1123C-28X-CC	583.80	593.12
102	FO *Globoquadrina dehiscens*	F		25	1123C-28X-CC	583.80	593.12
103	LO *Subbotina angiporoides*	F		30	1123C-28X-CC	583.80	593.12
104	Acme *Clausicoccus subdistichus*	N	43	33.3	1123C-29X-CC	593.41	602.37
105	LCO *Paragloborotalia gemma*	F		32	1123C-29X-CC	593.41	602.37
106	LO *Globigerinatheka index*	F		34.3	1123C-31X-CC	611.18	620.50
107	LO *Globigerinatheka semiinvoluta*	F		~ 34.8	1123C-31X-CC	611.18	620.50
108	FO *Paragloborotalia gemma*	F		~ 35	1123C-31X-CC	611.18	620.50
109	LO *Eucyrtidium spinosum*	R		31.7–32.0	1123C-31X-CC	611.10	620.51
110	FO *Eucyrtidium antiquum*	R		32.8–33.1	1123C-31X-CC	611.10	620.44
111	LO *Discoaster saipanensis*	N	44	34.6	1123C-31X-CC	611.18	620.50
112	LO *Nuttallides truempyi*	F		? 34.8	1123C-33X-CC	625.80	635.12

Notes: F = foraminifer, N = nannofossils, D = diatoms, R = radiolarians. Most samples are from core catchers. Events numbered 1–44, under the column labeled "Figure 29," are plotted in the age-depth graph of Figure F29.

Table T16. Age-depth data, derived from the polarity chron depth estimates for the Neogene and from the biochronostratigraphy for the Paleogene, used for the calculation of the average rates of restored sedimentation in Figure F30.

Age (m.y.)	Depth (mcd)
0.00	0.00
0.78	32.50
1.07	41.20
1.77	69.65
1.95	73.25
3.05	107.40
3.58	129.60
4.18	150.52
4.48	164.15
4.98	177.10
5.32	184.90
6.14	228.60
6.57	250.50
7.10	268.90
7.65	284.60
8.10	300.20
9.00	328.10
9.74	348.00
10.95	380.60
11.94	404.40
12.18	414.75
12.71	435.30
13.14	449.90
14.08	469.30
14.80	477.65
16.01	499.15
16.73	514.00
17.60	522.10
18.78	542.70
20.13	579.30
21.60	596.70
30.00	597.00
34.00	620.00
36.00	635.12

Table T17. Composition of interstitial waters at Site 1123.

Core, section, interval (cm)	Depth (mbsf)	Depth (mcd)	Salinity	Cl^- (mM)	pH	Alkalinity (mM)	Na^+ (mM)	Mg^{2+} (mM)	Ca^{2+} (mM)	SO_4^{2-} (mM)	HPO_4^{2-} (µM)	NH^{4+} (µM)	H_4SiO_4 (µM)	K^+ (mM)	Li^+ (µM)	Sr^{2+} (µM)
181-1123A-																
1H-1, 140-150	1.40	1.40	34.5	555	7.45	4.22	471	53.3	10.8	27.9	15.2	88	546	11.8	26	100
1H-3, 135-145	4.35	4.35	34.5	556	7.52	4.30	468	54.3	10.9	27.2	15.0	151	577	11.9	26	111
2H-1, 140-150	7.50	5.70	34.5	556	7.52	4.74	472	52.4	10.1	26.6	14.8	190	576	11.7	27	118
2H-3, 140-150	10.50	8.70	34.5	557	7.56	5.25	472	52.4	9.9	26.1	15.1	223	599	11.7	28	131
2H-5, 140-150	13.50	11.70	34.5	558	7.58	5.61	472	52.4	9.6	25.4	16.4	277	605	11.6	28	141
3H-1, 140-150	17.00	16.76	34.5	559	7.65	6.33	473	52.1	9.3	24.5	12.1	345	615	11.6	31	177
3H-3, 140-150	20.00	19.76	34.5	561	7.60	6.73	475	51.2	9.1	23.3	12.5	391	638	11.7	33	199
3H-5, 120-130	22.80	22.56	34.5	561	7.66	6.85	474	51.1	9.1	22.9	10.8	404	692	12.2	34	208
4H-1, 140-150	26.50	24.06	34.5	562	7.66	6.99	475	51.1	8.8	22.4	11.2	419	674	11.8	35	223
4H-3, 140-150	29.50	27.06	34.5	563	7.63	7.03	474	51.5	9.0	22.4	12.0	418	684	12.0	34	224
4H-5, 140-150	32.50	30.06	34.0	563	7.68	7.14	479	49.8	8.6	22.9	11.1	437	728	12.4	36	241
5H-1, 140-150	36.00	35.86	34.0	562	7.65	6.60	479	50.3	8.4	23.7	9.9	424	661	11.9	36	240
5H-3, 140-150	39.00	38.86	34.0	562	7.65	7.50	476	50.2	8.2	21.5	10.5	447	684	11.5	37	257
5H-5, 140-150	42.00	41.86	34.0	562	7.92	8.35	475	49.9	8.3	21.2	10.1	477	695	11.7	39	264
6H-1, 140-150	45.50	48.06	34.0	562	7.66	7.63	478	48.5	7.7	20.2	8.8	495	693	11.6	40	290
6H-3, 140-150	48.50	51.06	34.0	562	7.63	7.76	476	49.0	8.1	20.6	9.4	565	679	11.8	42	303
6H-5, 140-150	51.50	54.06	34.0	563	7.56	7.86	479	48.2	7.7	20.2	7.8	573	700	11.7	42	314
7H-4, 140-150	59.50	62.20	34.0	563	7.75	7.42	478	47.7	7.7	19.6	9.0	597	694	11.8	45	352
8H-4, 140-150	69.00	72.80	34.0	564	7.64	8.14	478	47.1	7.6	18.1	7.8	620	706	11.7	47	390
9H-4, 140-150	78.50	82.88	34.0	563	7.65	8.26	478	46.6	7.6	17.7	6.5	663	716	11.4	49	416
10H-4, 140-150	88.00	93.88	34.0	563	7.65	8.44	476	46.0	7.6	16.5	6.8	683	789	11.5	52	450
11H-4, 140-150	97.50	103.58	34.0	564	7.64	8.37	477	45.2	7.6	16.1	4.6	717	772	11.2	55	487
12H-4, 140-150	107.00	113.66	34.0	564	7.46	8.53	475	45.4	7.9	15.4	4.3	716	772	11.5	56	520
13H-4, 140-150	116.50	124.26	34.0	564	7.32	8.21	475	45.0	8.3	15.0	4.7	720	756	11.3	67	551
14H-4, 140-150	126.00	134.70	34.0	564	7.32	8.21	478	43.1	8.1	14.4	4.6	695	762	11.1	71	587
15H-4, 140-150	135.50	145.66	34.0	564	7.19	8.24	479	42.2	8.1	14.5	3.8	722	802	11.4	76	635
16H-3, 140-150	143.50	155.14	34.0	564	7.56	7.95	478	42.0	8.5	13.9	4.0	738	808	11.1	79	645
17H-4, 140-150	154.50	164.64	34.0	563	7.22	8.22	475	42.0	9.1	13.5	4.3	711	842	11.2	88	688
181-1123B-																
17H-4, 140-150	151.80	163.74	33.5	564	7.25	8.37	474	43.6	9.2	13.8	4.1	779	850	11.3	101	—
20X-4, 140-150	178.20	190.20	33.5	565	7.25	7.38	472	42.7	10.5	13.5	3.4	732	899	11.3	120	852
23X-3, 140-150	205.60	217.54	33.5	564	7.22	7.10	474	39.2	11.2	12.4	3.2	747	945	11.0	143	934
26X-2, 140-150	232.90	244.84	33.5	567	7.22	6.15	480	36.9	12.7	12.8	1.7	708	965	10.3	172	1112
29X-4, 140-150	264.70	276.64	33.5	565	7.24	5.61	477	35.9	14.0	12.7	1.7	760	999	10.4	192	1250
32X-4, 140-150	293.60	305.54	33.5	566	7.51	4.79	476	34.4	16.3	12.9	1.4	679	1014	10.3	229	1367
35X-4, 140-150	322.40	334.34	33.5	563	7.19	4.68	473	32.6	18.3	13.0	3.2	677	1012	9.8	257	1481
38X-4, 140-150	351.00	362.94	33.5	565	7.23	3.91	474	31.2	19.6	12.1	1.4	620	541	9.9	296	1488
41X-4, 140-150	380.00	391.94	33.5	564	7.33	2.95	478	28.2	20.0	11.9	1.7	633	886	9.7	325	1643
44X-3, 135-150	407.35	419.29	33.5	565	7.23	3.30	480	28.9	21.0	13.9	1.9	589	1002	9.1	331	1614
47X-3, 135-150	436.15	448.09	34.0	565	7.24	3.64	476	26.6	23.5	11.9	1.7	579	1056	8.8	374	1663
50X-4, 135-150	466.25	478.19	33.0	559	7.47	1.66	468	25.9	25.4	11.2	2.2	436	632	7.1	396	1702
52X-3, 135-150	483.65	495.59	33.5	561	7.57	1.22	472	24.9	25.4	11.9	1.7	544	660	8.0	427	1678
181-1123C-																
19X-4, 135-150	494.35	503.91	33.5	573	7.33	1.73	480	24.8	27.7	11.9	1.9	493	978	7.1	444	1772
22X-4, 135-150	532.85	532.81	33.5	574	7.47	1.64	480	24.2	28.5	11.4	1.4	415	274	6.7	462	1734
25X-4, 135-150	552.05	561.61	33.5	576	7.32	2.06	485	24.6	27.3	12.1	1.9	467	838	7.3	451	1578
28X-4, 135-150	580.95	590.51	33.5	578	7.35	1.91	486	22.5	28.8	11.1	2.2	468	902	7.2	482	1652
31X-4, 135-150	609.75	619.31	33.5	573	—	—	—	22.6	31.6	11.7	—	—	1062	6.3	—	—
33X-1, 123-135	624.43	633.99	—	—	—	—	—	—	—	—	—	—	—	—	—	—

Notes: — = not available. This table is also available in **ASCII format.**

Table T18. Inorganic carbon, carbonate, total carbon, total organic carbon, total nitrogen, total sulfur, and atomic organic carbon/nitrogen values for sediments from Holes 1123A, 1123B, and 1123C. (**See table note.** Continued on next two pages.)

Core, section, interval (cm)	Depth (mbsf)	IC (%)	$CaCO_3$ (%)	TC (%)	TOC (%)	TN (%)	TS (%)	$[C/N]_a$
181-1123A-								5.8
1H-1, 10-11	0.1	6.69	55.7	7.33	0.64	0.13	ND	9
1H-1, 86-87	0.86	4.51	37.6	5.67	1.15	0.15	0.08	
1H-4, 58-59	5.03	6.92	57.6					
2H-3, 39-40	9.49	3.05	25.4					10.1
2H-4, 39-40	10.99	7.28	60.6	8.03	0.75	0.09	ND	
3H-2, 76-77	17.86	8.65	72.1					
3H-5, 100-102	22.6	5.39	44.9					9.4
4H-1, 67-69	25.77	4.25	35.4	5.32	1.07	0.13	ND	
4H-1, 110-112	26.2	6.89	57.4					
5H-3, 103-104	38.63	8.97	74.7					13.1
5H-4, 65-66	39.75	7.81	65.1	8.7	0.88	0.08	0.06	
6H-2, 66-67	46.26	8.6	71.7					
6H-4, 104-105	49.64	6.37	53.1					8.8
7H-4, 64-65	58.74	1.31	10.9	2.07	0.76	0.1	0.09	13.4
7H-6, 64-65	61.74	8.24	68.6	8.97	0.73	0.06	ND	8.8
8H-2, 60-61	65.2	4.39	36.6	5.15	0.76	0.1	ND	
8H-4, 60-61	68.2	8.41	70					
9H-4, 83-84	77.93	6.72	56					
9H-4, 108-110	78.18	8.61	71.7					9.1
11H-2, 50-51	93.6	6.18	51.4	6.74	0.57	0.07	ND	
11H-5, 50-51	98.1	9.57	79.7					
12H-3, 35-36	104.45	8.46	70.5					9.6
12H-4, 35-36	105.95	7.03	58.6	7.77	0.73	0.09	0.06	
13H-2, 119-120	113.29	9.29	77.4					
13H-4, 139-139	116.04	8.17	68					13.6
14H-2, 123-124	122.83	8.25	68.7	8.89	0.64	0.06	ND	
14H-4, 123-124	125.83	7.4	61.7					
15H-3, 138-139	133.98	7.82	65.2					8.5
16H-1, 50-51	139.6	5.82	48.5	6.44	0.62	0.09	ND	
16H-2, 88-89	141.48	7.15	59.6					
17H-3, 36-37	151.96	7.94	66.1					17.6
17H-3, 133-134	152.93	8.94	74.4	9.57	0.63	0.04	0.3	
181-1123B-								
14H-1, 52-52	117.92	8.61	71.7					
15H-1, 52-53	127.42	8.55	71.3					15.7
17H-3, 63-64	149.53	8.55	71.2	9.33	0.78	0.06	ND	
17H-5, 89-90	152.79	7.82	65.1					
17H-7, 11-12	155.01	8.31	69.2					
18X-1, 39-40	155.79	8.77	73.1					4.6
18X-4, 130-131	161.2	4.4	36.6	4.73	0.33	0.08	0.22	
18X-5, 92-93	162.32	6.93	57.7					
19X-1, 48-49	163.18	6.64	55.3					11.7
19X-3, 52-53	166.26	7.32	61	7.95	0.62	0.06	0.26	
19X-7, 15-16	171.97	7.29	60.7					5.3
20X-1, 60-61	172.9	1.85	15.4	2.25	0.4	0.09	0.12	
20X-3, 60-61	175.94	6.93	57.8					
20X-6, 60-61	180.48	6.37	53.1					12.1
21X-1, 66-67	182.56	6.61	55	7.34	0.73	0.07	ND	
21X-2, 66-67	184.06	5.19	43.2					
21X-3, 66-67	185.56	6.37	53.1					8.4
22X-2, 66-67	193.83	5.36	44.7	5.85	0.49	0.07	ND	
22X-4, 116-117	197.33	5.53	46.1					
22X-6, 93-94	200.1	7.31	60.9					
23X-1, 73-74	201.93	5.01	41.7					7.9
23X-3, 73-74	204.93	8.25	67.9	8.63	0.48	0.07	ND	
23X-5, 84-85	208.04	8.55	71.2					
24X-2, 48-49	212.78	8.13	67.7					11.8
24X-5, 39-40	217.19	6.29	52.4	7.06	0.77	0.08	ND	
25X-3, 90-91	224.3	6.36	53					
25X-4, 35-36	225.25	8	66.6					14
26X-1, 28-29	230.28	8.06	67.2	8.72	0.66	0.06	0.1	

Table T18 (continued).

Core, section, interval (cm)	Depth (mbsf)	IC (%)	$CaCO_3$ (%)	TC (%)	TOC (%)	TN (%)	TS (%)	$[C/N]_a$
26X-2, 87-88	232.37	7.53	62.8					
27X-1, 146-147	241.06	6.44	53.7					6.3
27X-4, 47-48	244.57	3.98	33.1	4.48	0.5	0.09	ND	
28X-2, 77-78	251.47	5.92	49.3					
28X-4, 77-78	254.47	6.73	56					11.4
29X-2, 49-50	260.79	6.73	56	7.47	0.74	0.08	0.1	
29X-5, 42-43	265.22	6.72	55.9					
30X-1, 33-34	268.73	7.05	58.7					4.4
30X-4, 36-37	273.26	5.4	45	5.68	0.28	0.07	ND	
30X-6, 5-6	275.95	5.09	42.4					
31X-1, 115-116	279.25	6.84	57					9.1
31X-3, 125-126	282.35	6.19	51.5	6.86	0.67	0.09	ND	
32X-1, 85-87	288.55	6.21	51.8					
32X-1, 115-117	288.85	5.12	42.6					
33X-1, 24-25	297.54	7.48	62.3					10
33X-2, 118-119	299.98	5.82	48.5	6.5	0.68	0.08	ND	
33X-3, 131-132	301.61	5.43	45.2					
34X-3, 4-5	309.94	7.02	58.5					10
34X-5, 47-48	313.37	6.58	54.8	7.18	0.59	0.07	ND	
34X-5, 55-56	313.45	6.64	55.3					
35X-1, 117-117	317.67	6.85	57					13.4
35X-5, 27-28	322.77	6.12	51	6.73	0.61	0.05	ND	
35X-6, 88-89	324.88	7.2	60					
36X-1, 42-43	326.32	8.24	68.6					25.9
36X-5, 41-42	332.31	8.51	70.9	8.96	0.44	0.02	ND	
37X-3, 135-136	339.85	7.96	66.3					
37X-5, 42-43	341.92	7.94	66.1					17.2
38X-2, 81-82	347.41	8.01	66.7	8.6	0.59	0.04	ND	
38X-4, 81-82	350.41	7.87	65.5					
39X-1, 55-56	355.25	7.88	65.7					
39X-4, 84-85	360.04	6.47	53.9					14.2
40X-2, 61-62	366.51	7.93	66	8.42	0.49	0.04	ND	
40X-5, 61-62	371.01	8.62	71.8					
41X-2, 42-43	376.02	7.7	64.1					
41X-5, 44-45	380.54	7.74	64.5					
42X-1, 92-93	384.62	8.32	69.3					
43X-1, 67-68	394.07	6.53	54.4					
43X-4, 15-16	398.05	8.03	66.9					12.7
44X-1, 112-113	404.12	7.08	59	7.65	0.57	0.05	ND	
44X-4, 37-38	407.87	7.94	66.1					
45X-1, 110-111	413.7	7.96	66.3					
45X-3, 43-44	416.03	8.22	68.5					11
46X-1, 94-95	423.14	8.63	71.9	9.09	0.47	0.05	ND	
46X-4, 82-83	427.52	6.99	58.3					
47X-1, 111-112	432.91	8.26	68.8					14.7
47X-2, 88-89	434.18	8.25	68.7	8.88	0.63	0.05	ND	
47X-4, 13-14	436.43	7.68	64					
48X-1, 14-15	441.64	8.59	71.5					14.7
48X-1, 59-60	442.09	8.59	71.6	9.22	0.63	0.05	ND	
49X-1, 39-40	451.19	8.21	68.4					9.4
49X-3, 118-119	454.98	5.81	48.4	6.33	0.52	0.06	0.04	
49X-4, 95-96	456.25	8.42	70.1					
50X-1, 31-32	460.71	5.23	43.5					10.8
50X-2, 112-113	463.02	7.71	64.2	8.17	0.46	0.05	ND	
50X-6, 20-21	468.1	4.92	41					
51X-4, 46-47	474.96	6.6	55					6.3
51X-6, 100-101	478.5	2.39	19.9	2.74	0.35	0.07	ND	
52X-1, 42-43	479.72	4.92	41					3.2
52X-5, 49-50	485.79	7.25	60.4	7.42	0.16	0.06	ND	
181-1123C-								
19X-2, 95-96	490.95	7.14	59.5					3.7
19X-3, 44-45	491.94	3.38	28.2	3.6	0.16	0.07	0.08	
20X-1, 110-111	499.2	5.68	47.3					9.5
20X-2, 53-54	500.13	2.66	22.2	3.1	0.43	0.05	ND	
20X-6, 16-17	505.76	7.62	63.5					10.7
21X-1, 30-31	508	6.56	54.6	6.99	0.43	0.05	ND	
21X-6, 68-69	515.88	5.01	41.7					
22X-1, 67-68	518.07	5.46	45.5					10.4

Table T18 (continued).

Core, section, interval (cm)	Depth (mbsf)	IC (%)	$CaCO_3$ (%)	TC (%)	TOC (%)	TN (%)	TS (%)	$[C/N]_a$
22X-3, 75-77	521.15	5.98	49.8	6.51	0.52	0.06	ND	
22X-7, 18-19	526.58	6.06	50.5					4
23X-2, 56-57	529.06	3.34	27.8	3.59	0.25	0.07	ND	
23X-4, 60-61	532.1	4.48	37.3					
23X-6, 60-61	535.1	4.64	38.7					
24X-1, 57-58	537.17	6.25	52					13.2
24X-4, 57-58	541.67	6.51	54.3	7.08	0.57	0.05	ND	
25X-2, 38-39	548.08	10.12	84.3					
25X-5, 46-47	552.66	6.3	52.5					
26X-2, 56-57	557.76	6.11	50.9					14.4
26X-4, 78-79	560.98	6.64	55.3	7.09	0.46	0.04	ND	
27X-2, 48-49	567.38	5.27	43.9					
27X-3, 46-48	568.86	8.67	72.2					18.6
27X-5, 46-48	571.86	8.27	68.9	8.89	0.62	0.04	ND	
28X-1, 57-58	575.67	8.05	67					
28X-2, 87-88	577.47	8.01	66.8					15.2
28X-5, 53-54	581.63	8.11	67.6	8.75	0.64	0.05	ND	
29X-1, 78-79	585.48	8.35	69.5					
29X-3, 73-74	588.43	9.72	81					8.3
32X-1, 104-105	614.64	7.7	64.1	8.12	0.42	0.06	ND	
32X-4, 49-50	618.59	9.19	76.6					

Notes: Carbonate is calculated assuming that all inorganic carbon is calcite. ND = not detected. This table is also available in **ASCII format.**

Table T19. Result of Rock-Eval pyrolysis of selected samples from Site 1123.

Core, section, interval (cm)	Depth (mbsf)	Tmax (°C)	S_1	S_2	S_3	PI	PC	S_2/S_3	HI	OI	TOC
181-1123A-											
1H-1, 86-87	0.10	413	0.14	0.87	2.08	0.86	0.08	0.42	76	181	1.15
4H-1, 67-68	25.77	394	0.10	0.38	1.85	0.79	0.04	0.21	36	173	1.07
8H-2, 60-61	68.20	384	0.13	0.27	1.82	0.68	0.03	0.15	36	239	0.76
12H-4, 35-36	105.95	379	0.10	0.16	1.39	0.62	0.02	0.12	22	190	0.73
181-1123B-											
17H-3, 63-64	149.53	384	0.11	0.11	1.27	0.50	0.02	0.09	14	161	0.79
24X-5, 39-40	217.19	367	0.08	0.10	1.24	0.56	0.01	0.08	13	161	0.77
31X-3, 125-126	282.35	341	0.15	0.04	1.40	0.21	0.02	0.03	6	209	0.67
47X-2, 88-89	434.18	NA	0.13	0.06	0.92	0.32	0.02	0.07	9	137	0.67
181-1123C-											
22X-3, 75-76	526.58	NA	0.10	0.02	1.20	0.17	0.01	0.02	4	231	0.52
28X-5, 53-54	581.63	346	0.16	0.09	1.23	0.36	0.02	0.07	14	192	0.64

Notes: Units of the various Rock-Eval parameters are given in "Organic Geochemistry," p. 22, in the "Explanatory Notes" chapter. NA = data not available.

Table T20. List of index properties measured from Holes 1123A, 1123B, and 1123C. (See table note. Continued on next three pages.)

Leg	Hole	Core	Section	Interval (cm)	Depth (mbsf)	Wet-water content (%)	Dry-water content (%)	Wet-bulk density (g/cm^3)	Dry density (g/cm^3)	Grain density (g/cm^3)	Porosity (%)	Void ratio
181	1123A	1H	1	119-121	1.19	49.8	99.3	1.467	0.736	2.574	71.4	2.50
181	1123A	1H	3	126-128	4.26	49.3	97.2	1.501	0.761	2.742	72.2	2.60
181	1123A	2H	2	145-147	9.05	52.8	112.0	1.448	0.683	2.699	74.7	2.95
181	1123A	2H	4	140-142	12.00	49.2	96.7	1.495	0.760	2.692	71.8	2.54
181	1123A	2H	6	139-141	14.99	46.4	86.5	1.529	0.820	2.668	69.3	2.25
181	1123A	3H	2	129-131	18.39	43.4	76.7	1.587	0.898	2.742	67.2	2.05
181	1123A	3H	4	36-38	20.46	43.6	77.4	1.582	0.892	2.736	67.4	2.07
181	1123A	3H	5	33-35	21.93	45.0	81.7	1.555	0.856	2.696	68.3	2.15
181	1123A	4H	1	69-71	25.79	47.2	89.2	1.520	0.803	2.678	70.0	2.33
181	1123A	4H	3	73-75	28.83	47.5	90.5	1.522	0.799	2.716	70.6	2.40
181	1123A	4H	6	135-137	33.95	48.0	92.4	1.511	0.785	2.698	70.9	2.44
181	1123A	5H	2	74-76	36.84	43.5	77.1	1.568	0.885	2.655	66.6	2.00
181	1123A	5H	4	98-100	40.08	42.7	74.7	1.592	0.911	2.715	66.4	1.98
181	1123A	5H	6	123-125	43.33	43.4	76.8	1.591	0.900	2.769	67.5	2.08
181	1123A	6H	2	63-65	46.23	36.6	57.8	1.698	1.076	2.740	60.7	1.55
181	1123A	6H	3	109-111	48.19	37.6	60.1	1.660	1.037	2.650	60.9	1.56
181	1123A	6H	6	138-140	52.98	38.0	61.2	1.661	1.030	2.680	61.6	1.60
181	1123A	7H	1	108-110	54.68	44.0	78.7	1.577	0.882	2.743	67.8	2.11
181	1123A	7H	4	54-56	58.64	41.6	71.2	1.601	0.935	2.673	65.0	1.86
181	1123A	7H	6	97-99	62.07	40.3	67.5	1.631	0.974	2.717	64.2	1.79
181	1123A	8H	2	59-61	65.19	42.5	74.0	1.600	0.919	2.741	66.5	1.98
181	1123A	8H	3	31-33	66.41	42.5	73.8	1.599	0.920	2.729	66.3	1.97
181	1123A	8H	5	70-72	69.80	39.3	64.9	1.645	0.998	2.713	63.2	1.72
181	1123A	9H	2	40-42	74.50	40.9	69.1	1.618	0.957	2.699	64.6	1.82
181	1123A	9H	4	69-71	77.79	37.7	60.4	1.674	1.044	2.716	61.6	1.60
181	1123A	9H	6	7-9	80.17	41.6	71.2	1.613	0.942	2.732	65.5	1.90
181	1123A	10H	1	91-93	83.01	44.0	78.6	1.568	0.878	2.689	67.3	2.06
181	1123A	10H	3	54-56	85.64	36.5	57.6	1.690	1.073	2.702	60.3	1.52
181	1123A	10H	6	39-41	89.99	37.3	59.5	1.673	1.049	2.686	60.9	1.56
181	1123A	11H	2	65-67	93.75	40.9	69.3	1.616	0.954	2.694	64.6	1.82
181	1123A	11H	4	97-99	97.07	38.7	63.2	1.654	1.013	2.706	62.6	1.67
181	1123A	11H	6	111-113	100.21	39.0	64.0	1.648	1.005	2.700	62.8	1.69
181	1123A	12H	3	135-137	105.45	38.2	61.9	1.659	1.024	2.692	61.9	1.63
181	1123A	12H	4	55-57	106.15	40.1	66.8	1.625	0.974	2.673	63.6	1.74
181	1123A	12H	6	111-113	109.71	36.8	58.1	1.692	1.070	2.724	60.7	1.55
181	1123A	13H	2	130-132	113.40	36.0	56.2	1.706	1.092	2.728	60.0	1.50
181	1123A	13H	4	130-132	115.95	34.6	53.0	1.730	1.131	2.726	58.5	1.41
181	1123A	13H	6	137-139	119.02	36.2	56.8	1.695	1.081	2.699	59.9	1.50
181	1123A	14H	2	139-141	122.99	35.1	54.2	1.719	1.115	2.718	59.0	1.44
181	1123A	14H	4	132-134	125.92	36.2	56.7	1.696	1.083	2.702	59.9	1.50
181	1123A	14H	6	135-137	128.95	35.6	55.2	1.707	1.100	2.703	59.3	1.46
181	1123A	15H	1	139-141	130.99	39.4	65.1	1.641	0.994	2.698	63.2	1.72
181	1123A	15H	3	135-137	133.95	36.4	57.1	1.694	1.078	2.705	60.1	1.51
181	1123A	15H	6	140-142	138.50	37.0	58.8	1.688	1.063	2.727	61.0	1.57
181	1123A	16H	1	140-142	140.50	37.5	60.1	1.673	1.045	2.703	61.3	1.59
181	1123A	16H	3	128-130	143.38	36.2	56.6	1.695	1.082	2.694	59.8	1.49
181	1123A	16H	5	143-145	146.53	35.2	54.2	1.709	1.108	2.681	58.7	1.42
181	1123A	16H	7	30-32	148.40	34.0	51.5	1.734	1.144	2.696	57.6	1.36
181	1123A	17H	1	145-146	150.05	32.2	47.6	1.766	1.197	2.694	55.6	1.25
181	1123A	17H	3	141-143	153.01	32.2	47.5	1.780	1.207	2.743	56.0	1.27
181	1123A	17H	5	139-141	155.99	30.9	44.8	1.787	1.235	2.683	54.0	1.17
181	1123B	1H	2	141-143	2.91	50.4	101.6	1.477	0.732	2.683	72.7	2.66
181	1123B	2H	1	140-142	4.80	50.7	102.8	1.475	0.727	2.699	73.0	2.71
181	1123B	2H	3	140-142	7.80	51.3	105.3	1.466	0.714	2.686	73.4	2.76
181	1123B	2H	5	136-138	10.76	47.3	89.7	1.520	0.801	2.685	70.2	2.35
181	1123B	3H	1	139-141	14.29	46.5	86.9	1.537	0.822	2.724	69.8	2.31
181	1123B	3H	3	139-141	17.29	43.8	78.1	1.574	0.884	2.711	67.4	2.07
181	1123B	3H	5	144-146	20.34	43.3	76.4	1.583	0.898	2.717	67.0	2.03
181	1123B	4H	5	128-130	29.68	46.3	86.4	1.532	0.822	2.682	69.3	2.26
181	1123B	5H	3	71-73	35.61	44.2	79.3	1.561	0.870	2.671	67.4	2.07
181	1123B	6H	4	66-68	46.56	35.5	55.0	1.701	1.097	2.674	59.0	1.44
181	1123B	7H	3	93-95	54.83	41.0	69.6	1.616	0.953	2.702	64.7	1.84
181	1123B	8H	4	95-97	65.85	41.8	71.9	1.604	0.933	2.707	65.5	1.90
181	1123B	9H	4	7-9	74.47	44.0	78.4	1.563	0.876	2.663	67.1	2.04
181	1123B	10H	2	68-70	81.58	39.8	66.1	1.642	0.989	2.731	63.8	1.76
181	1123B	11H	4	119-121	94.59	40.6	68.4	1.616	0.959	2.674	64.1	1.79

Table T20 (continued).

Leg	Hole	Core	Section	Interval (cm)	Depth (mbsf)	Wet-water content (%)	Dry-water content (%)	Wet-bulk density (g/cm^3)	Dry density (g/cm^3)	Grain density (g/cm^3)	Porosity (%)	Void ratio
181	1123B	12H	5	92-94	105.32	37.7	60.4	1.672	1.042	2.708	61.5	1.60
181	1123B	13H	6	130-132	116.70	35.9	55.9	1.702	1.092	2.704	59.6	1.48
181	1123B	14H	6	139-141	126.29	35.2	54.2	1.715	1.112	2.704	58.9	1.43
181	1123B	15H	7	55-57	136.51	37.6	60.4	1.670	1.041	2.699	61.4	1.59
181	1123B	16H	2	137-139	139.27	35.4	54.8	1.716	1.109	2.727	59.3	1.46
181	1123B	17H	2	145-147	148.85	33.2	49.8	1.742	1.163	2.676	56.5	1.30
181	1123B	17H	4	128-130	151.68	32.2	47.5	1.765	1.197	2.690	55.5	1.25
181	1123B	17H	6	139-141	154.79	29.9	42.6	1.819	1.276	2.720	53.1	1.13
181	1123B	18X	1	124-126	156.64	31.6	46.2	1.782	1.219	2.709	55.0	1.22
181	1123B	18X	3	131-133	159.71	31.8	46.6	1.783	1.216	2.723	55.3	1.24
181	1123B	18X	5	113-115	162.53	37.2	59.3	1.676	1.052	2.691	60.9	1.56
181	1123B	19X	1	117-119	163.87	37.8	60.7	1.667	1.038	2.694	61.5	1.60
181	1123B	19X	3	137-139	167.11	33.4	50.1	1.745	1.162	2.695	56.9	1.32
181	1123B	19X	5	139-141	170.17	31.7	46.5	1.770	1.208	2.676	54.9	1.22
181	1123B	20X	1	142-144	173.72	38.2	61.8	1.665	1.029	2.714	62.1	1.64
181	1123B	20X	3	143-145	176.77	36.7	57.9	1.689	1.070	2.707	60.5	1.53
181	1123B	20X	5	124-126	179.60	36.4	57.2	1.695	1.078	2.713	60.2	1.52
181	1123B	20X	7	33-35	181.73	34.0	51.4	1.730	1.143	2.682	57.4	1.35
181	1123B	21X	2	36-38	183.76	36.9	58.4	1.692	1.068	2.734	60.9	1.56
181	1123B	21X	4	34-36	186.74	34.8	53.4	1.722	1.123	2.705	58.5	1.41
181	1123B	21X	6	12-14	189.52	28.1	39.1	1.850	1.330	2.703	50.8	1.03
181	1123B	22X	1	129-131	192.89	33.1	49.4	1.757	1.176	2.718	56.7	1.31
181	1123B	22X	3	42-44	195.09	34.5	52.6	1.721	1.128	2.680	57.9	1.38
181	1123B	22X	5	24-26	197.91	33.9	51.3	1.734	1.146	2.691	57.4	1.35
181	1123B	23X	1	61-63	201.81	35.0	53.8	1.714	1.114	2.690	58.6	1.41
181	1123B	23X	3	54-56	204.74	30.1	43.0	1.794	1.255	2.649	52.6	1.11
181	1123B	23X	5	49-51	207.69	29.3	41.5	1.815	1.282	2.671	52.0	1.08
181	1123B	24X	2	63-65	212.93	29.1	41.1	1.815	1.287	2.659	51.6	1.07
181	1123B	24X	4	65-67	215.95	34.2	52.0	1.734	1.141	2.712	57.9	1.38
181	1123B	24X	6	69-71	218.99	34.5	52.6	1.725	1.130	2.695	58.1	1.39
181	1123B	25X	2	33-35	222.23	34.1	51.7	1.738	1.146	2.717	57.8	1.37
181	1123B	25X	5	61-63	227.01	32.8	48.8	1.754	1.178	2.689	56.2	1.28
181	1123B	25X	6	77-79	228.67	33.8	51.0	1.736	1.149	2.690	57.3	1.34
181	1123B	26X	1	19-21	230.19	32.1	47.2	1.776	1.206	2.721	55.7	1.26
181	1123B	26X	3	21-23	233.21	33.6	50.7	1.754	1.164	2.748	57.6	1.36
181	1123B	27X	1	27-29	239.87	37.1	59.1	1.680	1.056	2.704	60.9	1.56
181	1123B	27X	4	55-57	244.65	35.9	55.9	1.712	1.098	2.743	60.0	1.50
181	1123B	27X	6	107-109	248.17	34.2	52.0	1.733	1.140	2.707	57.9	1.37
181	1123B	28X	1	36-38	249.56	32.5	48.1	1.773	1.197	2.734	56.2	1.28
181	1123B	28X	3	28-30	252.48	33.0	49.2	1.755	1.176	2.706	56.5	1.30
181	1123B	28X	5	59-61	255.79	35.9	56.0	1.705	1.093	2.717	59.8	1.49
181	1123B	29X	2	54-56	260.84	31.1	45.1	1.801	1.241	2.737	54.7	1.21
181	1123B	29X	4	48-50	263.78	33.0	49.3	1.757	1.177	2.716	56.7	1.31
181	1123B	29X	6	112-114	267.42	32.5	48.1	1.766	1.193	2.712	56.0	1.27
181	1123B	30X	1	109-111	269.49	32.7	48.5	1.766	1.189	2.723	56.3	1.29
181	1123B	30X	3	128-130	272.68	34.8	53.3	1.724	1.125	2.714	58.6	1.41
181	1123B	30X	5	130-132	275.70	34.0	51.5	1.739	1.147	2.715	57.7	1.37
181	1123B	30X	7	29-31	277.69	33.7	50.8	1.750	1.160	2.734	57.6	1.36
181	1123B	31X	1	135-137	279.45	32.8	48.9	1.754	1.178	2.691	56.2	1.29
181	1123B	31X	3	57-59	281.67	34.1	51.7	1.736	1.144	2.708	57.7	1.37
181	1123B	31X	5	127-129	285.37	34.0	51.5	1.737	1.147	2.710	57.7	1.36
181	1123B	31X	7	20-22	287.30	31.4	45.8	1.781	1.221	2.692	54.6	1.20
181	1123B	32X	1	134-136	289.04	32.9	49.0	1.754	1.177	2.694	56.3	1.29
181	1123B	32X	3	143-145	292.13	32.9	49.0	1.762	1.182	2.724	56.6	1.30
181	1123B	32X	5	134-136	295.04	32.6	48.4	1.759	1.185	2.696	56.0	1.28
181	1123B	32X	6	57-59	295.77	35.3	54.5	1.714	1.109	2.711	59.1	1.44
181	1123B	33X	2	143-145	300.23	31.3	45.7	1.789	1.228	2.714	54.8	1.21
181	1123B	33X	3	121-123	301.51	31.5	46.0	1.788	1.224	2.721	55.0	1.22
181	1123B	33X	6	147-149	306.27	30.4	43.7	1.808	1.258	2.718	53.7	1.16
181	1123B	34X	1	147-149	308.37	32.3	47.8	1.765	1.194	2.698	55.7	1.26
181	1123B	34X	4	62-64	312.02	35.0	53.9	1.724	1.120	2.733	59.0	1.44
181	1123B	34X	6	149-150	315.89	31.7	46.5	1.784	1.218	2.724	55.3	1.24
181	1123B	35X	1	138-140	317.88	34.0	51.6	1.737	1.146	2.712	57.7	1.37
181	1123B	35X	3	137-139	320.87	34.0	51.4	1.741	1.150	2.719	57.7	1.37
181	1123B	35X	5	141-143	323.91	33.7	50.8	1.742	1.155	2.708	57.3	1.35
181	1123B	36X	2	138-140	328.78	32.4	48.0	1.770	1.196	2.722	56.0	1.28
181	1123B	36X	4	144-146	331.84	31.0	45.0	1.797	1.240	2.722	54.4	1.20
181	1123B	36X	6	148-150	334.88	30.9	44.7	1.809	1.250	2.753	54.6	1.20

Table T20 (continued).

Leg	Hole	Core	Section	Interval (cm)	Depth (mbsf)	Wet-water content (%)	Dry-water content (%)	Wet-bulk density (g/cm^3)	Dry density (g/cm^3)	Grain density (g/cm^3)	Porosity (%)	Void ratio
181	1123B	37X	1	138-140	336.88	30.7	44.4	1.799	1.246	2.709	54.0	1.17
181	1123B	37X	3	112-114	339.62	28.5	39.8	1.849	1.322	2.721	51.4	1.06
181	1123B	37X	5	126-128	342.76	29.4	41.7	1.826	1.289	2.710	52.4	1.10
181	1123B	38X	1	71-73	345.81	29.9	42.6	1.819	1.275	2.720	53.1	1.13
181	1123B	38X	3	112-114	349.22	28.0	38.8	1.865	1.343	2.737	50.9	1.04
181	1123B	38X	5	124-126	352.34	26.7	36.4	1.888	1.384	2.727	49.2	0.97
181	1123B	39X	1	65-67	355.35	27.5	38.0	1.867	1.353	2.717	50.2	1.01
181	1123B	39X	3	65-67	358.35	28.7	40.3	1.844	1.315	2.722	51.7	1.07
181	1123B	39X	5	17-19	360.87	26.7	36.5	1.880	1.378	2.705	49.1	0.96
181	1123B	40X	1	66-68	365.06	27.7	38.3	1.861	1.346	2.709	50.3	1.01
181	1123B	40X	3	56-58	367.96	27.4	37.8	1.867	1.355	2.708	50.0	1.00
181	1123B	40X	6	93-95	372.83	28.1	39.0	1.863	1.340	2.740	51.1	1.05
181	1123B	41X	2	46-48	376.06	28.8	40.4	1.837	1.308	2.705	51.6	1.07
181	1123B	41X	4	79-81	379.39	28.5	39.8	1.838	1.314	2.688	51.1	1.05
181	1123B	41X	5	60-62	380.70	29.6	42.1	1.822	1.282	2.713	52.7	1.12
181	1123B	42X	1	129-131	384.99	27.1	37.3	1.875	1.366	2.716	49.7	0.99
181	1123B	42X	3	70-72	387.40	30.7	44.3	1.801	1.248	2.710	53.9	1.17
181	1123B	43X	2	76-78	395.66	28.6	40.2	1.858	1.326	2.761	52.0	1.08
181	1123B	43X	4	112-114	399.02	26.8	36.7	1.886	1.380	2.729	49.4	0.98
181	1123B	44X	1	112-114	404.12	28.1	39.1	1.863	1.339	2.743	51.2	1.05
181	1123B	44X	3	23-25	406.23	32.9	49.1	1.753	1.176	2.696	56.4	1.29
181	1123B	45X	2	96-98	415.06	27.3	37.5	1.875	1.364	2.726	50.0	1.00
181	1123B	46X	1	31-33	422.51	27.7	38.4	1.861	1.344	2.712	50.4	1.02
181	1123B	46X	4	100-102	427.70	26.6	36.2	1.885	1.384	2.709	48.9	0.96
181	1123B	47X	1	143-145	433.23	28.7	40.2	1.846	1.317	2.725	51.7	1.07
181	1123B	47X	3	127-129	436.07	29.7	42.2	1.825	1.284	2.722	52.8	1.12
181	1123B	48X	1	133-135	442.83	25.9	34.9	1.903	1.411	2.717	48.1	0.93
181	1123B	48X	3	54-56	445.04	25.8	34.7	1.906	1.415	2.718	47.9	0.92
181	1123B	49X	3	127-129	455.07	21.8	27.9	2.014	1.574	2.760	43.0	0.75
181	1123B	50X	1	142-144	461.82	25.8	34.7	1.900	1.410	2.703	47.8	0.92
181	1123B	50X	3	144-146	464.84	27.3	37.6	1.881	1.367	2.748	50.3	1.01
181	1123B	50X	5	117-119	467.57	19.4	24.0	2.061	1.661	2.723	39.0	0.64
181	1123B	51X	1	138-140	471.38	21.6	27.6	2.002	1.568	2.719	42.3	0.73
181	1123B	51X	3	142-144	474.42	19.7	24.5	2.062	1.656	2.743	39.6	0.66
181	1123B	51X	5	145-147	477.45	19.9	24.9	2.050	1.641	2.732	39.9	0.67
181	1123B	51X	7	43-45	479.43	19.3	23.8	2.076	1.676	2.749	39.0	0.64
181	1123B	52X	2	115-117	481.95	21.0	26.6	2.031	1.603	2.751	41.7	0.72
181	1123B	52X	4	130-132	485.10	22.8	29.6	2.070	1.597	2.750	46.2	0.86
181	1123B	52X	6	130-132	488.10	23.3	30.3	1.978	1.517	2.756	44.9	0.82
181	1123C	18X	1	112-114	485.12	18.3	22.4	2.085	1.704	2.716	37.3	0.59
181	1123C	18X	3	119-121	488.19	20.9	26.5	2.028	1.604	2.739	41.5	0.71
181	1123C	19X	1	123-125	489.73	23.1	30.1	1.974	1.517	2.738	44.6	0.81
181	1123C	19X	3	132-134	492.82	22.1	28.4	2.005	1.562	2.753	43.3	0.76
181	1123C	19X	5	142-144	495.92	25.2	33.7	1.920	1.436	2.724	47.3	0.90
181	1123C	20X	1	121-123	499.31	20.2	25.3	2.051	1.636	2.749	40.5	0.68
181	1123C	20X	3	133-135	502.43	18.4	22.5	2.098	1.713	2.746	37.6	0.60
181	1123C	21X	1	143-145	509.13	18.1	22.1	2.107	1.726	2.748	37.2	0.59
181	1123C	21X	3	145-147	512.15	18.0	21.9	2.107	1.729	2.743	37.0	0.59
181	1123C	21X	5	144-146	515.14	20.1	25.1	2.051	1.639	2.743	40.2	0.67
181	1123C	21X	7	20-22	516.90	18.0	21.9	2.105	1.726	2.738	37.0	0.59
181	1123C	22X	1	133-135	518.73	19.4	24.1	2.077	1.673	2.761	39.4	0.65
181	1123C	22X	3	142-144	521.82	18.5	22.6	2.095	1.708	2.746	37.8	0.61
181	1123C	22X	5	127-129	524.67	17.8	21.7	2.110	1.734	2.738	36.7	0.58
181	1123C	22X	7	36-38	526.76	19.5	24.2	2.078	1.673	2.768	39.6	0.66
181	1123C	23X	1	137-139	528.37	20.3	25.4	2.055	1.638	2.763	40.7	0.69
181	1123C	23X	3	135-137	531.35	18.5	22.7	2.096	1.709	2.748	37.8	0.61
181	1123C	23X	5	131-133	534.31	19.7	24.5	2.068	1.660	2.758	39.8	0.66
181	1123C	24X	1	38-40	536.98	18.9	23.4	2.091	1.695	2.764	38.7	0.63
181	1123C	24X	3	38-40	539.98	19.7	24.6	2.066	1.658	2.756	39.8	0.66
181	1123C	24X	5	82-84	543.42	20.1	25.2	2.043	1.632	2.724	40.1	0.67
181	1123C	25X	1	110-112	547.30	22.5	29.0	1.993	1.545	2.745	43.7	0.78
181	1123C	25X	2	39-41	548.09	24.5	32.5	1.932	1.457	2.714	46.3	0.86
181	1123C	25X	3	59-61	549.79	24.8	32.9	1.932	1.454	2.729	46.7	0.88
181	1123C	26X	1	72-74	556.42	28.5	39.9	1.847	1.320	2.720	51.5	1.06
181	1123C	26X	3	76-78	559.46	26.2	35.5	1.891	1.396	2.702	48.3	0.94
181	1123C	26X	5	90-92	562.60	23.1	30.0	1.970	1.515	2.727	44.4	0.80
181	1123C	27X	1	58-60	565.98	26.0	35.1	1.900	1.407	2.716	48.2	0.93
181	1123C	27X	3	119-121	569.59	21.6	27.6	1.997	1.565	2.707	42.2	0.73

Table T20 (continued).

Leg	Hole	Core	Section	Interval (cm)	Depth (mbsf)	Wet-water content (%)	Dry-water content (%)	Wet-bulk density (g/cm^3)	Dry density (g/cm^3)	Grain density (g/cm^3)	Porosity (%)	Void ratio
181	1123C	27X	5	75-77	572.15	20.2	25.3	2.049	1.636	2.743	40.4	0.68
181	1123C	28X	1	99-101	576.09	19.6	24.4	2.050	1.648	2.713	39.3	0.65
181	1123C	28X	3	93-95	579.03	20.6	25.9	2.011	1.597	2.681	40.4	0.68
181	1123C	28X	5	77-79	581.87	20.9	26.4	2.012	1.591	2.700	41.1	0.70
181	1123C	29X	1	82-84	585.52	19.4	24.1	2.078	1.675	2.763	39.4	0.65
181	1123C	29X	3	70-72	588.40	20.1	25.2	2.043	1.631	2.726	40.2	0.67
181	1123C	29X	5	63-65	591.33	17.7	21.4	2.118	1.744	2.748	36.5	0.58
181	1123C	30X	1	64-66	594.94	20.7	26.1	2.036	1.614	2.744	41.2	0.70
181	1123C	30X	4	33-35	599.13	17.1	20.7	2.108	1.747	2.698	35.2	0.54
181	1123C	31X	3	134-136	608.24	17.2	20.8	2.102	1.740	2.693	35.4	0.55
181	1123C	31X	5	85-87	610.75	16.6	19.9	2.120	1.768	2.695	34.4	0.53
181	1123C	32X	1	54-56	614.14	17.8	21.6	2.073	1.704	2.662	36.0	0.56
181	1123C	32X	3	131-133	617.91	14.1	16.5	2.188	1.878	2.691	30.2	0.43
181	1123C	33X	1	83-85	624.03	15.7	18.6	2.154	1.816	2.711	33.0	0.49

Note: This table is also available in **ASCII format.**